

The role of 4E-T in translational regulation and mRNA decay

Dissertation

der Mathematisch-Naturwissenschaftlichen Fakultät
der Eberhard Karls Universität Tübingen
zur Erlangung des Grades eines
Doktors der Naturwissenschaften
(Dr. rer. nat.)

vorgelegt von
Felix Alexander Paul Räsch
aus Hermeskeil

Tübingen
2020

Gedruckt mit Genehmigung der Mathematisch-Naturwissenschaftlichen Fakultät der
Eberhard Karls Universität Tübingen.

Tag der mündlichen Qualifikation:

05.08.2020

Dekan:

Prof. Dr. Wolfgang Rosenstiel

1. Berichterstatter:

Prof. Dr. Ralf-Peter Jansen

2. Berichterstatter:

Prof. Dr. Patrick Müller

This thesis describes work conducted in the laboratory of Prof. Dr. Elisa Izaurralde in the Department of Biochemistry at the Max Planck Institute for Developmental Biology, Tübingen, Germany, from February 2015 to May 2020. The work was supervised by Prof. Dr. Ralf-Peter Jansen at the Eberhard Karls University Tübingen, Germany, and was supported by a fellowship from the International PhD program of the MPI for Developmental Biology. I declare that this thesis is the product of my own work. The parts that have been published or where other sources have been used were cited accordingly. Work carried out by my colleagues was also indicated accordingly.

Acknowledgements

This thesis would not have been possible without all the support I received during the last years for which I will be forever grateful.

I would like to express my deepest gratitude to Prof. Dr. Elisa Izaurralde for giving me the opportunity to work in her lab and giving me support and guidance that shaped my understanding of science more than anything. She was a great mentor who cared deeply about the growth of her PhD students and her devotion to science was truly inspiring for me. Thank you for everything.

I also want to say my most sincere gratitude to Dr. Cátia Igreja who closely supervised me throughout all my PhD studies. Her infinite patience to explain and discuss science was essential for me to grow as a scientist and without her none of this work would have been possible.

I want to thank Dr. Eugene Valkov for filling some of the void that Elisa left by giving invaluable guidance to me and other PhD students and making sure we stay focused on our next steps.

I want to thank our interim director Prof. Dr. Ralf Sommer for making it possible that I could finish my PhD studies as good as possible.

I want to thank my TAC members and examiners Prof. Dr. Ralf-Peter Jansen and Prof. Dr. Patrick Müller for their continuous support throughout the years and my committee members Prof. Dr. Thorsten Stafforst and Prof. Dr. Dirk Schwarzer for evaluating me in these complicated times.

I want to thank my colleagues from department II for a pleasant and stimulating work atmosphere. There was always someone willing to discuss any ideas and teach me new methods. I am especially grateful to Ramona Weber, Dr. Vincenzo Ruscica, Dr. Csilla Keskeny, Michelle Noble, Dr. Aoife Hanet and Simone Larivera for their friendship inside and outside the lab. You made the last years a time I will look fondly back upon.

Und zuletzt möchte ich meiner Familie danken, meiner Mutter Elisabeth, meinem Vater Hubert und meiner Schwester Anna, auf deren unbedingte Unterstützung ich mich immer verlassen konnte und ohne die ich wohl nie diesen Weg eingeschlagen hätte.

Contents

Abbreviations	1
Summary	3
Zusammenfassung	4
List of Publications and Contributions	5
1 Introduction	6
1.1 Eukaryotic gene expression.....	6
1.2 Translation of mRNA.....	7
1.2.1 Regulation of translation by 4E-binding proteins	7
1.3 The poly(A) tail.....	8
1.4 mRNA surveillance	9
1.5 mRNA decay	10
1.6 The CCR4-NOT complex	11
1.7 mRNA decay triggered by AU-rich elements and microRNAs.....	12
1.8 The decapping complex	13
1.8.1 PatL1	14
1.8.2 LSM14A.....	14
1.8.3 DDX6	14
1.9 Processing (P)-bodies	15
1.10 eIF4E-transporter (4E-T).....	16
1.10.1 4E-T is a 4E-BP involved in mRNA decay.....	16
1.10.2 4E-T is important for development	17
2 Aims and Objectives	19
2.1 4E-T.....	19
2.2 HELZ.....	20
3 Results and discussion I: 4E-T	21
3.1 4E-T promotes deadenylation and blocks decapping of bound mRNAs	21
3.1.1 4E-T bound mRNAs are deadenylated and not degraded	22
3.2 4E-T is a binding platform for RNA-associated proteins	23
3.2.1 P-body formation is mediated by 4E-T's interaction network.....	24
3.2.2 Recruitment of CCR4-NOT is mediated by the mid region of 4E-T	25
3.3 Binding of eIF4E/4EHP is essential for blocking decapping by 4E-T	26
3.4 4E-T is involved in TRNC6B mediated mRNA decay	27
3.4.1 miRNAs and 4E-T.....	28
3.5 4E-T can block decapping of ARE containing mRNA	29

Contents

3.6	4E-T can modulate the fate of an mRNA from decay to storage.....	30
3.7	mRNA storage and 4E-T.....	32
3.7.1	P-bodies as sites of mRNA storage.....	32
3.8	Translational activation of stored mRNAs.....	33
3.9	The 4E-T associated transcriptome.....	35
3.10	Conclusions.....	35
4	Results and discussion II: HELZ.....	36
5	References.....	37
6	Original manuscripts discussed in this thesis.....	50

Abbreviations

4E-BP	4E-binding protein
4EHP	eIF4E homologous protein
4E-T	Eukaryotic translation initiation factor 4E transporter
AGO	Argonaute protein
ARE	AU-rich element
BGG	Beta globin gene
CAF1/NOT7	CCR4-NOT transcription complex subunit 7
CAF40/NOT9	CCR4-NOT transcription complex subunit 9
cap	5' mRNA 7-methyl-guanosine
CCR4/NOT6	CCR4-NOT transcription complex subunit 6
CCR4-NOT	Carbon catabolite repressor 4; Negative on TATA-less
CPE	Cytoplasmic polyadenylation element
CPEB	Cytoplasmic polyadenylation element binding protein
CUP	Protein cup
DCP1	mRNA decapping enzyme 1
DCP2	mRNA decapping enzyme 2
DDX6	DEAD-box helicase 6
DNA	Deoxyribonucleic acid
EDC1-4	Enhancer of decapping protein 1-4
eIF4A	Eukaryotic translation initiation factor 4A
eIF4E	Eukaryotic translation initiation factor 4E
EIF4ENIF	eIF4E nuclear import factor (gene of 4E-T)
eIF4F	Eukaryotic translation initiation factor 4F
eIF4G	Eukaryotic translation initiation factor 4G
EJC	Exon junction complex
ELAVL1/HuR	ELAV-like protein 1
GIGYF	GRB10-interacting GYF protein
HEK293T	Human embryonic kidney 293T cells
HeLa	Henrietta Lacks, cell line derived from cervical cancer cells
HELZ	Putative RNA Helicase with Zinc-finger
kDa	Kilodalton

Abbreviations

LSM14A	Protein LSM14 homolog A
LSM1-7	Like Sm protein 1-7
miRISC	microRNA-induced silencing complex
miRNA	microRNA
mRNA	Messenger RNA
mRNP	Messenger ribonucleoprotein
NGD	No-go decay
NMD	Nonsense-mediated decay
NOT1	CCR4-NOT transcription complex subunit 1
NPC	Nuclear pore complex
NSD	Nonstop mediated decay
PABP	Poly(A)-binding protein
PABPC	Cytoplasmic poly(A)-binding protein
PAN2	PAN2-PAN3 deadenylation complex catalytic subunit PAN2
PAN3	PAN2-PAN3 deadenylation complex catalytic subunit PAN2
PatL1	Protein PAT1 homolog 1
P-body	Processing body
poly(A)	Poly-adenosine
PTC	Premature termination codon
Pum2	Pumilio homolog 2
RBP	RNA binding protein
RISC	RNA-induced silencing complex
RNA	Ribonucleic acid
SCD6	Yeast homolog of LSM14A
Smaug2	Protein Smaug homolog 2
TNRC6B	Trinucleotide repeat-containing gene 6B protein
TTP	Tristetraprolin
UNR/CSDE1	Cold shock domain-containing protein E1
UTR	Untranslated region
XRN1	5'-3' exoribonuclease 1

Summary

The eukaryotic initiation factor 4E (eIF4E) binds the cap structure of an mRNA as the first step of cap dependent translation. Together with the RNA helicase eIF4A and the scaffolding protein eIF4G, eIF4E forms the eIF4F complex, which recruits the 43S pre-initiation complex to initiate translation. The eIF4E-transporter (4E-T) is an eIF4E-binding protein (4E-BP) responsible for the nucleocytoplasmic shuttling of eIF4E. Additionally, 4E-T prevents translation initiation by competing with eIF4G for binding to eIF4E. 4E-T is also a P-body protein that contributes to mRNA decay triggered by AU-rich elements (ARE) and microRNAs (miRNAs).

The work described in this thesis focuses on the molecular mechanisms and protein interaction partners used by 4E-T in the regulation of mRNA decay. To study the effects of 4E-T on mRNA stability and translation, tethering assays with reporter transcripts coupled to northern blotting were performed in human cells. Binding of 4E-T to a reporter promoted CCR4-NOT dependent mRNA deadenylation. Unlike typical 5'-3' mRNA decay, the 4E-T bound mRNA was not decapped and degraded but remained stable as a deadenylated decay intermediate. Binding assays indicated that recruitment of the CCR4-NOT complex to an mRNA by 4E-T is mediated by the so far uncharacterized middle region of 4E-T and independent of the interaction partners described to date.

The studies reported here also indicate that the interaction of 4E-T with the cap binding proteins eIF4E or 4EHP prevented decapping of the deadenylated mRNA. Furthermore, we found that inhibition of decapping by 4E-T participates in the regulation of gene expression by the microRNA effector protein TNRC6B, the CCR4-NOT scaffolding protein NOT1 and in the turnover of ARE containing reporter mRNAs. These results show that 4E-T can potentially stabilize mRNAs targeted for decay in a wide range of biological processes, including microRNA-mediated gene silencing.

This work highlights that inhibition of decapping by 4E-T allows the storage of deadenylated and silenced mRNAs. To date, this is the first insight into the molecular mechanism of mRNA storage in human cells, which plays important yet poorly understood functions in oocyte and neuronal development.

Zusammenfassung

Der eukaryotic initiation factor 4E (eIF4E) bindet die Cap-Struktur einer mRNA im ersten Schritt der Cap abhängigen Translation. Zusammen mit der Helikase eIF4A und dem verbindenden Protein eIF4G, bildet eIF4E den eIF4F Komplex, welcher den 43S Präinitiationskomplex zu einer mRNA rekrutiert, um die Translation zu initiieren. eIF4E-transporter (4E-T) ist ein eIF4E-binding protein (4E-BP), dass eIF4E zwischen dem Zytoplasma und dem Nukleus transferiert. Darüber hinaus verhindert 4E-T die Initiierung der Translation, indem es mit eIF4G um die Binding von eIF4E konkurriert. 4E-T ist ein P-body Protein und wirkt bei mRNA Abbau, ausgelöst durch AU-reiche Elemente (ARE) und microRNAs (miRNAs), mit.

Diese Arbeit konzentriert sich auf die molekularen Mechanismen und Interaktionspartner, die von 4E-T verwendet werden, um den mRNA Abbau zu regulieren. Zur Untersuchung welchen Effekt 4E-T auf die Stabilität und die Translation von mRNA hat, wurden Tethering assays mit Reporter-Transkripten zusammen mit Northern blots verwendet. Das Binden von 4E-T an die Reporter mRNA löste CCR4-NOT abhängige Deadenylierung aus. Im Gegensatz zu typischem 5' zu 3' mRNA Abbau, wurde von der 4E-T gebundenen mRNA nicht die Cap-Struktur entfernt. Daher blieb die mRNA stabil als ein deadenyliertes Abbauzwischenprodukt erhalten. Anhand von Bindungstests fanden wir heraus, dass 4E-T den CCR4-NOT Komplex mittels eines bisher nicht charakterisierten Bereichs in der mittleren Domäne zu einer mRNA bringt, unabhängig von bekannten Interaktionspartnern.

Wir fanden heraus, dass 4E-T Decapping durch seine Interaktion mit den Cap-bindenden Proteinen eIF4E oder 4EHP (eIF4E homologous protein) blockiert. Des Weiteren konnten wir beobachten, dass das Blockieren von Decapping durch 4E-T in der Regulierung der Genexpression durch das miRNA Effektor Protein TNRC6B, das CCR4-NOT Verbindungsprotein NOT1 und bei ARE-enthaltenden Reporter mRNAs, eine Rolle spielt. Daher kann 4E-T wahrscheinlich mRNA vor Abbau beschützen, die in einer Vielzahl von biologischen Prozessen beteiligt ist.

Diese Arbeit zeigt, dass das Blockieren von Decapping durch 4E-T es ermöglicht deadenylierte und stillgelegte mRNA zu lagern. Dies ist bisher der erste Einblick in den molekularen Mechanismus von mRNA Lagerung in menschlichen Zellen, ein wichtiger Mechanismus der kaum verstanden aber essenziell für Oozyten und neuronale Entwicklung ist.

List of Publications and Contributions

1. 4E-T-bound mRNAs are stored in a silenced and deadenylated form.

Felix Räscher, Ramona Weber, Elisa Izaurralde and Cátia Igreja (2020)

Genes and Development, 34 (11-12)

I performed all the experiments, apart from creating and characterizing the 4EHP-null cells in Supplemental Figure S7D, E. I designed and cloned most of the constructs and contributed to planning the project. I prepared all the figures and wrote the manuscript together with Cátia Igreja.

2. HELZ directly interacts with CCR4–NOT and causes decay of bound mRNAs.

Aoife Hanet, Felix Räscher, Ramona Weber, Vincenzo Ruscica, Maria Fauser, Tobias Raisch, Duygu Kuzuoğlu-Öztürk, Chung-Te Chang, Dipankar Bhandari, Cátia Igreja, Lara Wohlbold (2019)

Life Science Alliance, Volume 2 (5)

I performed and contributed to designing some of the experiments and commented on the manuscript. In detail these experiments are the western blots shown in Figure 3C, 3G, 3J, 3M, 5D, 5H, S2F, the RNase H experiment in Figure S1A and the tethering assay in S2E.

1 Introduction

1.1 Eukaryotic gene expression

Protein synthesis is a fundamental process of all living beings. The information to combine amino acids in the right order is coded in genes in the DNA. In eukaryotic cells, reading of this information starts in the nucleus with the transcription of the DNA into pre-messenger RNA (pre-mRNA) (Figure 1). The newly transcribed RNA gets modified at the 5' end by the addition of the cap structure, a 7-methylguanosine linked to the RNA with a triphosphate bridge. This cap is important for nuclear export of the mRNA, translation initiation and protection from exonucleases, among others (Varani, 1997). At the 3' end the transcribed RNA gets cleaved and polyadenylated, which is directed by specific sequence elements close to the cleavage site (Mandel et al., 2008). This poly(A) tail consists of usually more than 100 adenosines and protects the RNA from degradation from the 3' end, promotes translation and is required for export to the cytoplasm (Munroe and Jacobson, 1990). From the pre-mRNA

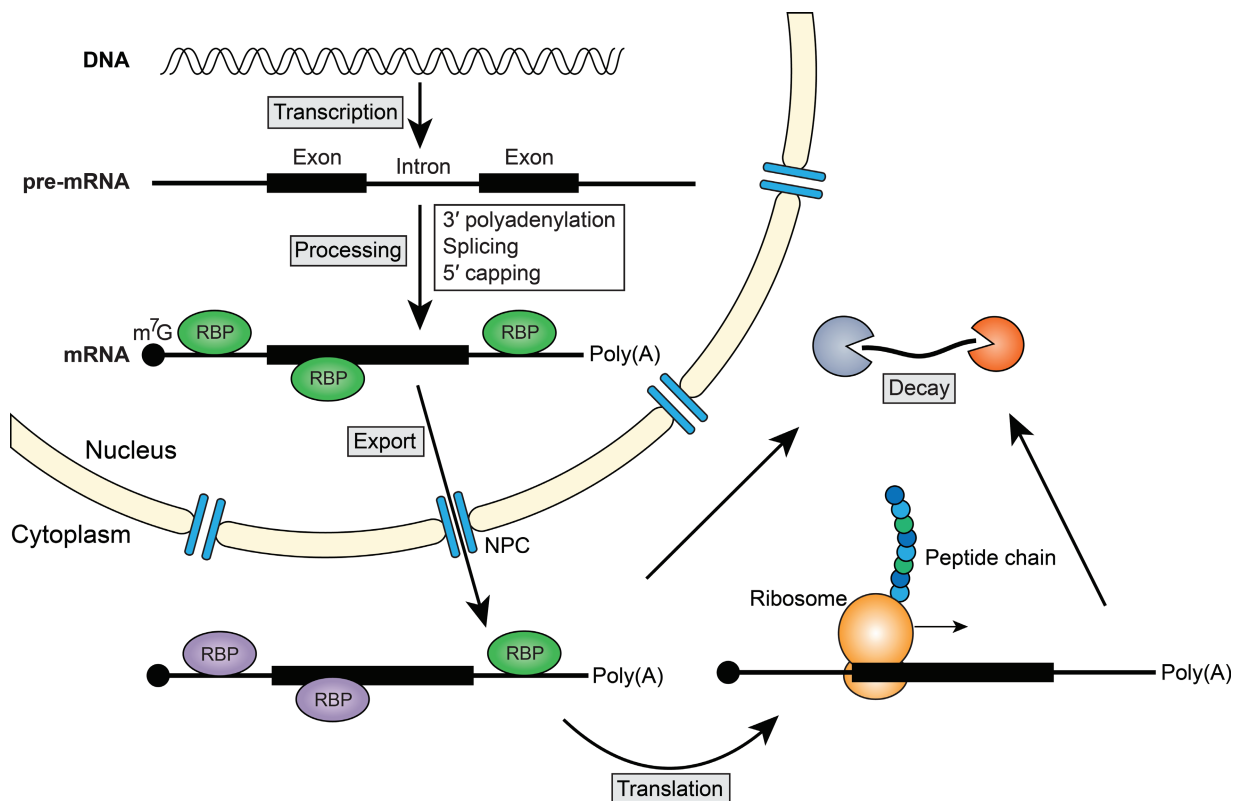


Figure 1 Overview of eukaryotic gene expression. The DNA is first transcribed into a pre-mRNA by RNA polymerase II. Subsequent pre-mRNA processing includes 3' poly(A) tail and a 5' cap structure addition and splicing out of introns. The mature mRNA, bound by several RNA binding proteins (RBP), forms a messenger ribonucleoprotein (mRNP). This complex is exported out of the nucleus and into the cytoplasm through the nuclear pore complex (NPC). In the cytoplasm, different RBPs associate with the mRNA to promote recruitment of the ribosome and protein synthesis. At any step of its lifetime the mRNA can be degraded by several mRNA decay factors.

noncoding regions, named introns, get removed by splicing, a process performed by the large spliceosome complex, yielding the mature messenger RNA (mRNA).

The mRNA, bound by several proteins forming a messenger ribonucleoprotein (mRNP), is then exported into the cytoplasm through the nuclear pore complex (NPC) (Stutz and Izaurralde, 2003). In the cytoplasm, upon remodeling of the mRNP and ribosome recruitment, the mRNA can be translated into proteins (Maquat et al., 2010; Rissland, 2017).

1.2 Translation of mRNA

Translation is the process of creating peptide chains by decoding the sequence information stored in an mRNA, which is facilitated by the ribosome. The first step of cap-dependent translation is the assembly of the eukaryotic initiation factor 4F (eIF4F) complex on the cap structure of an mRNA. The eIF4F complex consists of the cap binding protein eIF4E, the RNA-Helicase eIF4A and the scaffolding protein eIF4G. This complex mediates the recruitment of the 43S pre-initiation complex, composed of the small ribosomal subunit, several initiation factors and the initiator Met-tRNA (methionine transfer RNA) to the mRNA. The pre-initiation complex moves along the mRNA until it recognizes a start codon which leads to the joining of the large ribosomal subunit and thus the assembly of the full ribosome (Jackson et al., 2010). The ribosome catalyzes stepwise the formation of peptide bonds between amino acids brought to the ribosome by tRNAs, which recognize nucleotide triplets (codons) on the mRNA by base pairing. The nascent peptide chain gets thus extended until the ribosome encounters a termination codon, which triggers the hydrolysis and release of the peptide chain by several release factors (Schuller and Green, 2018).

Translation must be precisely controlled to guarantee that the right amount of proteins is produced and to protect against faulty, potentially harmful products. Therefore, translational control mechanisms operate in eukaryotic cells on many stages of translation (Kozak, 1992).

1.2.1 Regulation of translation by 4E-binding proteins

Ribosome recruitment is tightly regulated by mechanisms that target different steps of translation initiation (Sonenberg and Hinnebusch, 2009). The eIF4E-binding proteins (4E-BPs), for instance, block translation initiation by disrupting the assembly of the eIF4F complex. They mimic the binding of eIF4G with eIF4E by using the same binding motifs, the so-called eIF4E-binding motifs, to compete with eIF4G for the same surface on eIF4E (Haghighat et al., 1995). The canonical eIF4E-binding motif is characterized by Tyr-X₄-Leu-Φ (where X is any amino

acid and Φ a hydrophobic residue) (Haghighat et al., 1995) whereas the non-canonical motifs, located 15-20 residues downstream of the canonical ones, show little conservation but greatly enhance eIF4E binding and thus competition with eIF4G (Igreja et al., 2014; Peter et al., 2015a, 2015b).

4E-BPs are important for synaptic plasticity and memory (Banko, 2005) and as a major effector of the mammalian target of rapamycin (mTOR) pathway 4E-BP1 controls a wide variety of processes like cell proliferation and cell cycle progression (Ma and Blenis, 2009). Due to their activity as translational repressors, 4E-BPs also act as tumor suppressors (Dowling et al., 2010; Martineau et al., 2013).

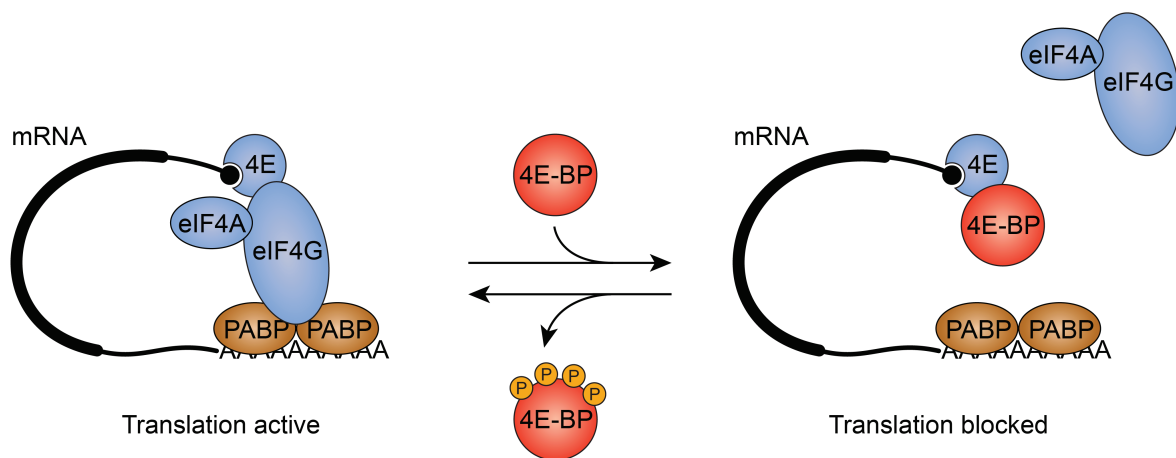


Figure 2 Mechanism of translational repression by 4E-binding proteins (4E-BP). The eIF4F complex consisting of eIF(4G), eIF(4A) and the cap binding protein eIF(4E), is required for translation initiation. 4E-BPs compete with 4G for binding to 4E and thus prevent the assembly of the complex. This activity can be regulated by phosphorylation (P) of 4E-BP (Gingras et al., 1999).

1.3 The poly(A) tail

With the exception of most histone mRNAs, all eukaryotic mRNAs are 3' end polyadenylated (Davila Lopez and Samuelsson, 2007). The poly(A) tail facilitates export of the mRNA to the cytoplasm where it gets shortened to roughly 60 to 100 adenosines, in humans (Chang et al., 2014b; Eisen et al., 2020a). The tail length has long been associated with the translational status of an mRNA because in *Xenopus laevis* oocytes the extension of the poly(A) tail by cytoplasmic polyadenylation was found to be necessary for the translation of specific maternal mRNAs (Richter, 1999). Furthermore, synthetic poly(A) tails facilitated translation of *c-mos* mRNA, which is required for meiotic maturation (Barkoff, 1998). The poly(A) tail is bound by the poly(A) binding protein (PABP), which interacts with eIF4G and facilitates translation initiation, supposedly by promoting the circularization of mRNA (Weill et al., 2012). In several organisms a correlation of poly(A) tail length with translation efficiency was

found in early development (Munroe and Jacobson, 1990). These observations have recently been confirmed by poly(A) tail sequencing coupled to ribosome profiling, which allows measuring the translation efficiency by calculating the ribosomes bound per mRNA (Subtelny et al., 2014). However, this correlation is lost in somatic cells, where translation efficiency only changes for mRNAs with poly(A) tail length below 20 adenosines (Park et al., 2016; Subtelny et al., 2014). Interestingly, this poly(A) tail length limit is roughly the number of adenosines required to bind a single PABP (~27) (Baer and Kornberg, 1983). This data suggests that the poly(A) tail length is in somatic cells not important for regulation of translation. However, it determines the stability of an mRNA by protecting it from decay. This assumption is based on the observation that removal of the poly(A) tail by deadenylases commits an mRNA to complete degradation (Chen and Shyu, 2011). Recently it was shown that the poly(A) tail is crucial for the decay rate of an mRNA, which is determined by its deadenylation rate (Eisen et al., 2020a).

1.4 mRNA surveillance

Cells have evolved surveillance mechanisms that sense and degrade faulty mRNAs. In eukaryotes, three pathways execute selective degradation of aberrant mRNAs: nonsense mediated decay (NMD), nonstop mediated decay (NSD) and no-go decay (NGD).

NMD specifically promotes the degradation of mRNAs containing a premature termination/stop codon (PTC) upstream of an exon junction complex (EJC) (Maquat and Li, 2001). The EJC and the NMD machinery form a complex with translation termination factors present at the PTC. This complex triggers the recruitment of the CCR4-NOT deadenylase complex to cause 5'-3' mRNA decay (Loh et al., 2013) or the endonuclease SMG6 which cleaves the mRNA, exposing it to decay by exonucleases (Eberle et al., 2009; Huntzinger et al., 2008). Alternatively, NMD has been suggested to be triggered by an increase in length of the 3' UTR due to a PTC (Shoemaker and Green, 2012).

NSD targets mRNAs without a stop codon, such as truncated transcripts, transcripts shortened by alternative polyadenylation beyond the stop codon, or ones with a mutated stop codon. Stalling of the ribosome due to reaching the end of the mRNA or reading into the poly(A) tail leads to mRNA decay by recruiting the exosome followed by exonucleolytic or first endonucleolytic degradation (Hoof et al., 2002; Klauer and van Hoof, 2012; Schaeffer and van Hoof, 2011).

NGD, another control mechanism that targets stalled ribosomes, has been found in yeast (Doma and Parker, 2006). Here, mRNAs with stalled ribosomes, due to strong secondary

structures in the coding sequence, get endonucleolytically cleaved and then degraded mainly by the activity of XRN1 (D'Orazio et al., 2019).

1.5 mRNA decay

mRNA degradation is a key step in the control of gene expression. It can occur at any step of an mRNA lifetime and it not only allows the destruction of faulty mRNAs but also influences the dynamics of mRNA abundance. The turnover rate is a major contributor to the steady state level of an mRNA (Wu and Brewer, 2012) and specific degradation of a subset of mRNA plays an essential role in many processes like the cell cycle dependent degradation of histone mRNA and inflammatory response (Schoenberg and Maquat, 2012).

mRNAs can be actively cleared from cells by specific recruitment of the decay machineries. For example, RNA quality control mechanisms trigger the decay of faulty RNAs as described above. Moreover, mRNAs can also contain destabilization motifs, such as microRNA binding sites or AU-rich elements (ARE) in the 3' UTR, recognized by specific RNA binding proteins (RBPs) which induce degradation of the bound transcript by recruiting decay factors (Garneau et al., 2007).

mRNA degradation in the cytoplasm is executed by exonucleases such as XRN1 (5'-3' decay) or the RNA exosome (3'-5' decay) (Figure 3) (Chen and Shyu, 2011). Since the mRNA is protected from both ends by the cap structure and the poly(A) tail, one of these features must be removed to expose the mRNA to exonucleolytic cleavage. Alternatively, endonucleolytic cleavage by endonucleases also creates unprotected ends susceptible to exonucleases (Garneau et al., 2007). At the 3' end of the mRNA, removal of the poly(A) tail is accomplished by the consecutive actions of two deadenylase complexes, Pan2-Pan3 and CCR4-NOT (Yamashita et al., 2005). Pan2-Pan3 preferably removes poly(A) bound by oligomers of the cytoplasmic poly(A) binding protein (PABPC) and trims the poly(A) tail before the CCR4-NOT complex takes over to further shorten it (Schäfer et al., 2019). In the absence of a poly(A) tail, the mRNA is exposed to decay in the 3'-5' direction by the RNA exosome, or to decapping followed by 5'-3' decay by XRN1 (Chen and Shyu, 2011; Schmid and Jensen, 2008).

The RNA exosome is a multisubunit complex consisting of nine conserved core proteins and one active exonuclease, DIS3 (Dziembowski et al., 2007). It can be found in the nucleus and the cytoplasm where it is involved in several steps of RNA metabolism including rRNA processing and mRNA turnover (Schmid and Jensen, 2008).

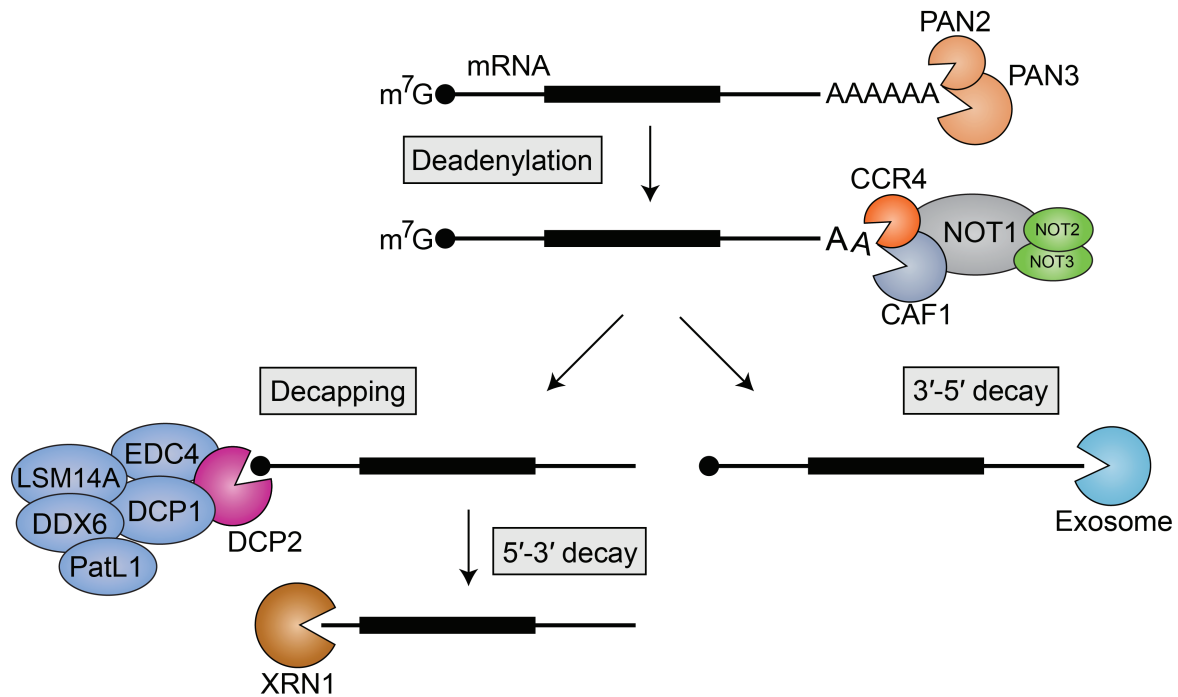


Figure 3: Deadenylation dependent mRNA decay. The poly(A) tail of an mRNA gets shortened in the cytoplasm by the action of two deadenylase complexes: The PAN2-PAN3 and the CCR4-NOT complex. Recruitment of the CCR4-NOT complex to an mRNA leads to the rapid removal of the poly(A) tail by the deadenylase subunits. Subsequently, the mRNA can be degraded from 3' to the 5' end by the exosome complex or the m⁷G cap of the mRNA can be removed by the decapping enzyme DCP2 and its cofactors. The unprotected mRNA is then degraded from 5' to 3' by the exonuclease XRN1.

For the vast majority of transcripts, cytoplasmic turnover depends on deadenylation followed by decapping, which has been concluded based on the accumulation of adenylated or deadenylated intermediates upon compromising the CCR4-NOT complex or DCP2, respectively (Chen et al., 2009; Yamashita et al., 2005; Zheng et al., 2008). The 5'-3' mRNA decay pathway is usually triggered by recruiting the CCR4-NOT complex to an mRNA via specific RNA binding proteins (RBP). These RBP can interact with the various subunits of the complex (Miller and Reese, 2012).

1.6 The CCR4-NOT complex

The CCR4-NOT complex is a conserved multi protein assembly involved in several cellular processes. In the nucleus, it regulates transcription, histone modifications, mRNA quality control and export (Miller and Reese, 2012). In the cytoplasm, when recruited to an mRNA by various RNA binding proteins, it rapidly deadenylates the mRNA by the activity of various combinations of the deadenylases CCR4 (NOT6), NOT6L, NOT7 and NOT8 (Lau et al., 2009). The deadenylated mRNA gets subsequently decapped by DCP2 and exonucleolytically degraded by XRN1 from 5'-3' (Figure 3) (Chen and Shyu, 2011). When

recruited, the complex also represses translation independently of deadenylation. DDX6 and 4E-T (in *Xenopus*) have been shown to be at least partly responsible for this repression (Kuzuoğlu-Öztürk et al., 2016; Waghray et al., 2015).

The CCR4-NOT complex is assembled around the scaffolding subunit NOT1. The N-terminus of NOT1 binds to NOT10 and NOT11 which contribute to RNA binding and deadenylation (Bawankar et al., 2013; Raisch et al., 2019). The middle region of NOT1 binds the deadenylase subunits, the RNA helicase DDX6 (Chen et al., 2014; Mathys et al., 2014) and CAF40 (also known as NOT9), a binding platform for multiple RBPs (Bulbrook et al., 2018; Chen et al., 2014; Mathys et al., 2014; Sgromo et al., 2017, 2018) and the not-core subunit and E3 ubiquitin ligase NOT4 (Keskeny et al., 2019). The C-terminus of NOT1 forms together with NOT2 and NOT3 the NOT module which mediates the interaction with several RBP, stabilizes the complex and also contributes to deadenylation (Bhaskar et al., 2013; Boland et al., 2013; Raisch et al., 2019; Sgromo et al., 2017).

Known RBPs that recruit the CCR4-NOT complex to specific mRNAs are the Nanos 1-3 proteins (Bhandari et al., 2014; Raisch et al., 2016), Roquin (Sgromo et al., 2017, 2018), Bicaudal-C (Chicoine et al., 2007), Smaug (Semotok et al., 2005), (Rambout et al., 2016), HELZ (Hanet et al., 2019), the AU-rich element binding protein TTP (Bulbrook et al., 2018) and the miRNA-induced silencing complex-associated TNRC6 proteins (Chen et al., 2009, 2014; Zipprich et al., 2009).

1.7 mRNA decay triggered by AU-rich elements and microRNAs

Two examples of mRNA sequence features that trigger deadenylation-dependent decay are adenosine/uridine-rich elements (ARE) and miRNA binding sites. ARE are motifs in the 3' UTR with a high frequency of adenosines and uridines found in mRNAs encoding proteins critical for cell growth and immune response (LaMarre et al., 2004). They have been first described as destabilizing sequence motifs that reduce mRNA half-lives (Treisman, 1985). These sequences are recognized by RBPs which recruit factors of the mRNA decay machinery. One prominent ARE binding protein is tristetraprolin (TTP). Direct binding of TTP to the MIF4G domain of CNOT1 (Fabian et al., 2013) or NOT9 (Bulbrook et al., 2018) causes degradation of the bound mRNA. Alternatively, TTP can also recruit the exosome to degrade ARE containing mRNAs (Chen et al., 2001). The effect of ARE motifs on mRNA stability depends on which RBP binds it. So does ELAVL1 (also known as HuR), in contrast to TTP, inhibit decay of deadenylated mRNAs (Peng, 1998).

microRNAs (miRNA) are typically ~22 nucleotides long non-coding RNAs that upon binding to 3' UTR motifs trigger translational repression and 5'-3' mRNA decay (Izaurre, 2015). miRNAs are processed from a transcribed RNA by the microprocessor complex and Dicer. The processed miRNA is loaded into an Argonaute (AGO) protein and directs the miRNA-induced silencing complex (miRISC) to a target sequence (Bartel, 2004). In animals, they bind target sequences only with partial complementary and thus can have a broad range of targets involved in all biological processes (Bartel, 2009). The miRISC consists of AGO, the associated miRNA and a tri-nucleotide repeat-containing protein (TNRC6). The latter interacts via multiple tryptophan residues with NOT9 or directly with NOT1 to recruit the CCR4-NOT complex (Chekulaeva et al., 2011; Chen et al., 2014; Fabian and Sonenberg, 2012; Fabian et al., 2011). As a consequence, miRNA-mediated gene silencing elicits translational repression and 5'-3' mRNA decay (Chen et al., 2014; Fabian and Sonenberg, 2012).

1.8 The decapping complex

The removal of the 7-methyl-guanosine (m^7G) cap structure commits an mRNA irreversibly to exonucleolytic degradation by XRN1 which is why this process has to be tightly regulated. The major decapping enzyme in human cells is DCP2. It hydrolyses the 5' cap structure and releases m^7GDP and 5'-monophosphorylated mRNA by the activity of its Nudix domain (Wang et al., 2002). The conserved core of the decapping complex is formed by DCP2 and DCP1, which enhances the enzymatic activity of DCP2 greatly by improving binding of the mRNA substrate (Steiger et al., 2003; Valkov et al., 2016). Several other factors also enhance DCP2 decapping activity. Known decapping activators include the enhancer of decapping (EDC)1-4 proteins, the LSM1-7 complex, DDX6, LSM14A, and PatL1 (Arribas-Layton et al., 2013).

EDC1 and 2 have not been found in eukaryotes other than budding yeast, while EDC3 is highly conserved in eukaryotes and EDC4 only in metazoan (Arribas-Layton et al., 2013). EDC3 can stimulate decapping *in vitro* by binding the decapping complex via its LS domain (Fromm et al., 2012). EDC4 provides a scaffold for assembling DCP1 and DCP2 and furthermore binds XRN1, thus also potentially stimulating degradation of decapped mRNA (Chang et al., 2014a, 2019). The LSM1-7 complex forms a heptameric ring which binds preferably deadenylated mRNA close to the 3' end and promotes in conjunction with Pat1p decapping, which has been shown in yeast (Bouveret et al., 2000; Chowdhury et al., 2007; Tharun and Parker).

1.8.1 PatL1

PatL1 has been identified as a decapping activator due to the accumulation of deadenylated and capped reporter mRNA upon depletion of the homologous Pat1p protein in yeast (Bouveret et al., 2000). In human cells, PatL1 localizes to P-bodies and promotes deadenylation and decapping of bound mRNA, as a result of its interaction with the CCR4-NOT complex (Braun et al., 2010; Ozgur et al., 2010). PatL1 also interacts with the LSM1-7 ring, which facilitates binding to deadenylated 3' ends of an mRNA (Chowdhury et al., 2007), with the decapping enzyme DCP2 and the decapping factors DDX6 and EDC4. These protein-protein interactions place PatL1 at the interface between deadenylation and decapping, i.e. it forms a bridge between the CCR4-NOT and the decapping complex (Braun et al., 2010; Ozgur et al., 2010). Lack of PatL1 leads in yeast to reduced growth and viability and is lethal in *C. elegans* early development (Boag et al., 2008; Wang et al., 2002). Apart from its cytoplasmic role, PatL1 also shuttles to the nucleus where it interacts with the LSM2-8 complex and regulates splicing (Vindry et al., 2017).

1.8.2 LSM14A

LSM14A (also known as RAP55) shares with the LSM1-7 complex and EDC3 the conserved LSm domain. Similar to EDC3 but in contrast to LSM1-7, this domain in LSM14A does not mediate RNA binding but protein-protein interactions (Brandmann et al., 2018). In yeast, the LSM14A homolog SCD6 binds to DCP2 and enhances its decapping activity. Binding to DCP2 is mutually exclusive with EDC3 (Fromm et al., 2012). In addition, LSM14A also competes with EDC3 for binding to DDX6. Due to a strong overlap in interaction partners EDC3 and LSM14A have been suggested to be redundant (Decourty et al., 2008). However, LSM14A has distinct interaction partners like the translational repressor eIF4E-transporter (4E-T) (Brandmann et al., 2018) and eIF4G. SCD6 interacts with eIF4G through its RGG domain which causes translation repression presumably by preventing eIF4F dependent 43S pre-initiation complex recruitment (Rajyaguru et al., 2012). Furthermore, LSM14A is essential for P-body formation and its P-body localization is presumably directed via arginine methylation by PRMT1 (Matsumoto et al., 2012; Yang, 2006).

1.8.3 DDX6

DDX6 (Me31B in *D. melanogaster*, Dhh1 in budding yeast) is an RNA helicase which has been identified as a decapping activator in *S. cerevisiae* due to the accumulation of capped

mRNA decay intermediates upon its depletion (Coller et al., 2001). DDX6 consists of two RecA-like domains and contains RNA binding elements conserved between DEAD-box helicases. However, its helicase activity seems to be more relevant for controlling RNA-protein complexes than for helicase typical RNA unwinding (Presnyak and Coller, 2013). Interestingly, DDX6 has mutually exclusive interactions with multiple decapping activators (EDC3, LSM14A and PatL1) and the translational repressors eIF4E-transporter (4E-T). All these proteins bind to a conserved surface on the RecA2 domain of the RNA helicase (Ozgun et al., 2015; Sharif et al., 2013; Tritschler et al., 2009). In addition, DDX6 is able to bind the MIF4G domain of NOT1, which stimulates the DDX6 RNA helicase ATPase activity and is important for miRNA mediated translational repression (Mathys et al., 2014; Rouya et al., 2014). The interaction of NOT1 with DDX6 can occur simultaneously with 4E-T, but not with EDC3 or PatL1 (Chen et al., 2014; Ozgun et al., 2015). These observations, together with its high abundance in cells and on mRNA, suggests that DDX6 might be central to decision making over the fate of an mRNA (Ernoul-Lange et al., 2012). When recruited to an mRNA it promotes decapping, deadenylation dependent mRNA decay and translational repression independently of decay (Chen et al., 2014; Mathys et al., 2014; Rouya et al., 2014).

1.9 Processing (P)-bodies

Many of the 5'-3' mRNA decay factors can be found in membraneless cytoplasmic foci called processing bodies (P-bodies) (Luo et al., 2018). This observation, together with the accumulation of polyadenylated mRNAs in P-bodies upon knockdown of XRN1, led to the initial description of P-bodies as sites of mRNA decay (Cougot et al., 2004; Sheth, 2003). However, more recent evidences indicate that P-bodies have a role in mRNA storage. For instance, some mRNAs can exit P-bodies and reenter translation (Bregues et al., 2005). In addition, recent analysis of purified P-bodies revealed the accumulation of repressed mRNAs without significant changes in mRNA abundance (Hubstenberger et al., 2017).

Several factors are crucial for P-body formation. These include DDX6, LSM14A, mRNA and 4E-T (Andrei et al., 2005; Marnef et al., 2012; Standart and Weil, 2018). Together, these factors presumably form a scaffold where other factors assemble to and leading to liquid-liquid phase separation (Andrei et al., 2005; Banani et al., 2016, 2017). Phase separation might allow the sequestering of components or the compartmentalization of biochemical processes without the need of separating structures (Banani et al., 2016). However, it is so far still unknown if the aggregation and phase separation leading to P-bodies has an actual function, since it has been

shown that P-bodies are not required for mRNA decay, but are a consequence of it (Eulalio et al., 2007; Wilbertz et al., 2019).

1.10 eIF4E-transporter (4E-T)

1.10.1 4E-T is a 4E-BP involved in mRNA decay

4E-T was first described as a 4E-BP and a shuttling protein that mediates the nuclear import of eIF4E (Dostie et al., 2000). Subsequent studies revealed that it is also involved in the decay of mRNAs containing AREs and in the decay and translational repression of miRNA targets (Ferraiuolo et al., 2005; Jafarnejad et al., 2018; Kamenska et al., 2014a, 2016; Nishimura et al., 2015). When tethered to a reporter mRNA, 4E-T elicits translational repression without affecting mRNA stability (Kamenska et al., 2014a, 2016). 4E-T localizes to P-bodies, is essential for their formation and also brings eIF4E to P-bodies (Ferraiuolo et al., 2005).

4E-T is predicted to be mostly unstructured (Kamenska et al., 2014b) with evolutionary conserved regions that mediate protein-protein interactions. These conserved regions represent short linear sequence motifs (SLiMs) embedded in disordered low-complexity sequence (Figure 4). This protein architecture is typically found in translational repressors and decapping activators, and is thought to facilitate the assembly of RNP-granules (Jonas and Izaurralde, 2013). These SLiMs mediate specific interactions with specific decay factors, including DDX6, the CCR4-NOT complex subunits NOT1 and NOT4, as well as the decapping factors PatL1 and LSM14A (Kamenska et al., 2014a, 2016). A structure of a 4E-T fragment in complex with DDX6 and NOT1 demonstrates a physical link of 4E-T with the 5'-3' mRNA decay machinery (Ozgur et al., 2015). The assembly of NOT1, DDX6 and 4E-T is in *Xenopus laevis* responsible for translational repression by the CCR4-NOT complex (Waghray et al., 2015).

The 4E-binding region contains the canonical 4E-binding motif which mediates binding to eIF4E as well as the eIF4E homologous protein (4EHP) (Chapat et al., 2017; Dostie et al., 2000). 4EHP competes with eIF4E for binding to the cap structure but does not interact with eIF4G, thus repressing translation (Joshi et al., 2004; Rom et al., 1998). Translational repression by 4EHP is important for *Drosophila* development (Cho et al., 2005, 2006) and together with the GIGYF proteins it controls mouse embryonal development (Morita et al., 2012) and the expression of ARE containing mRNAs (Peter et al., 2019). 4EHP binding by 4E-T increases its affinity to the cap structure and contributes to miRNA dependent translational repression (Chapat et al., 2017).

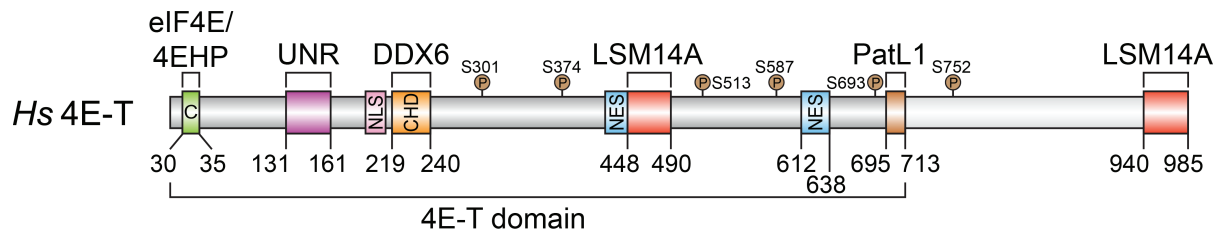


Figure 4 Schematic overview of 4E-T. The binding regions for eIF4E/4EHP, UNR, DDX6 and LSM14A have been described before (Kamenska et al., 2016; Nishimura et al., 2015). The PatL1 binding region and the refined LSM14A region is described in this work. The identified phosphorylation sites according to Cargnello et al. (2012) are indicated with a P. The 4E-T domain is similar to other 4E-T proteins. NLS: nuclear localization signal, NES: nuclear export signal, CHD: Cup homology domain, C: canonical eIF4E binding motif.

Another described interaction motif in 4E-T binds to the cold shock domain protein upstream of N-Ras (CSDE1, UNR) (Kamenska et al., 2016). This protein has diverse roles in translational regulation and is essential for mouse embryonic development, among others (Ray et al., 2015). Together with DDX6 it contributes to translational repression caused by 4E-T (Kamenska et al., 2016).

4E-T is hyperphosphorylated by the c-Jun N-terminal Kinase during arsenite-induced stress, which leads to increased P-body size (Cargnello et al. 2012). Six phosphorylation sites have been identified in the middle region of 4E-T (Figure 4) (Cargnello et al., 2012) but their functional consequences apart from P-body assembly are still unknown.

1.10.2 4E-T is important for development

4E-T is essential for proper neuronal development during mouse embryogenesis. Together with the RBPs Smaug2 and Pum2, 4E-T forms a translational repressor complex that specifically controls the expression of pro-neurogenic transcription factors regulating neuronal differentiation and specification (Amadei et al., 2015; Zahr et al., 2018). 4E-T is important for angiogenesis by promoting turnover of regulatory mRNAs, a process that is controlled by alternative splicing regulated by the ARE-binding protein ELAVL1.

Furthermore, 4E-T is also highly expressed in developing oocytes and plays an important role in oogenesis as it is required for the release from prophase arrest (Pfender et al., 2015; Villaescusa et al., 2006). In human, a nonsense and missense mutation in the *EIF4ENIF* gene are associated with premature ovarian failure (Kasippillai et al., 2013) and diminished ovarian reserve (Zhao et al., 2019), respectively. Further evidence for the importance of 4E-T in germ cell development was given in *C. elegans* where it is required for normal gonad organization (Sengupta et al., 2013).

D. melanogaster (*Dm*) expresses two 4E-T domain containing proteins: CG32016 (4E-T) and the 4E-T related protein CUP. Although the function of *Dm* 4E-T is currently unknown, CUP is required for proper ovary development and oocyte growth (Keyes and Spradling, 1997). CUP represses *oskar* and *nanos* mRNA during transport in the oocyte to prevent premature translation by binding the RBPs Bruno and Smaug, respectively (Nakamura et al., 2004; Nelson et al., 2004). At the molecular level, CUP represses translation and induces deadenylation of a target mRNA. The deadenylated mRNA is protected from decapping so that it can be translated at a specific location in the oocyte (Igreja and Izaurralde, 2011).

Taken together, 4E-T is an important regulator of translation and mRNA stability in developmental processes such as neuronal and ovary development. Nevertheless, 4E-T is constitutively expressed in all cells in the human body hinting at a general role in post-transcriptional regulation. The mechanisms employed by 4E-T in the control of gene expression are so far poorly understood.

2 Aims and Objectives

2.1 4E-T

Past observations point to an important role of 4E-T in oocyte and neuronal development and an extensive integration of 4E-T in the 5'-3' mRNA decay pathway. Although 4E-T is involved in mRNA decay triggered by AU-rich elements and microRNAs, recruitment of 4E-T to an mRNA reporter does not affect its stability.

First, in order to resolve these contradicting observations on the role of 4E-T in mRNA decay, I wanted to study in detail the molecular events occurring upon the recruitment of 4E-T to an mRNA. Therefore, I tethered a MS2-4E-T fusion protein to a luciferase reporter mRNA containing specific MS2-binding sequences in the 3' UTR. Changes in luciferase activity and reporter mRNA levels thus depict 4E-T dependent effects on translation and mRNA turnover. Visualization of the transcript via northern blotting furthermore allows the identification of changes in poly(A) tail length upon binding of 4E-T to the mRNA.

Second, as 4E-T interacts with several members of the 5'-3' mRNA decay pathway, I investigated the relevance of these protein-protein interactions in 4E-T dependent regulation of gene expression. To this end, 4E-T deletion mutants that specifically abolish the binding to each protein partner individually were created and compared in tethering assays to wild type 4E-T for their ability to repress translation, promote deadenylation, and block decapping.

Finally, I aimed at characterizing the contribution of 4E-T to mRNA decay triggered by AU-rich elements and microRNAs, which control the turnover of a plethora of mRNAs and influence multiple biological processes. Therefore, I tested how depletion and overexpression of 4E-T affected the stability of reporter transcripts mimicking miRNA or AU-rich elements dependent mRNA turnover.

Taken together, the goal of my studies was to understand the role of 4E-T in mRNA metabolism and which protein partners are required for its function. This knowledge will further our molecular understanding of the functions of an essential P-body component and important factor in development. Because 4E-T is closely associated with deadenylation and decapping factors as well as cap binding proteins, these studies will also help to unravel the communication between the poly(A) tail and the cap structure.

2.2 HELZ

RNA helicases are involved in all steps of RNA metabolism. HELZ is putative RNA helicase that interacts with the CCR4-NOT deadenylase complex and PABPC1. However, the role of HELZ in mRNA turnover has remained elusive. The aim of this project was to characterize the interaction of HELZ with the deadenylase complex and its role in RNA metabolism. *In vivo* and *in vitro* pulldown experiments were used to study the interaction of HELZ with the CCR4-NOT complex and associated factors. By employing tethering assays coupled to luciferase measurements and northern blotting we tested the influence of HELZ in translation and mRNA stability.

In summary, these experiments will contribute to the understanding of the role of RNA helicases in mRNA decay and translational regulation and highlight the integration of RNA helicases with the CCR4-NOT complex.

3 Results and discussion I: 4E-T

This part describes and discusses the first manuscript attached to this thesis, titled: “**4E-T-bound mRNAs are stored in a silenced and deadenylated form**”. References to figures in this publication start with “P1”.

3.1 4E-T promotes deadenylation and blocks decapping of bound mRNAs

Deadenylation is the first step of 5'-3' mRNA decay and is carried out by the coordinated action of the deadenylase complexes Pan2-Pan3 and CCR4-NOT (Chen and Shyu, 2011). Once the poly(A) tail is mostly removed the mRNA gets decapped and subsequently degraded from the 5' end by XRN1 (Yamashita et al., 2005).

We found that recruitment of 4E-T to a reporter mRNA induces the shortening of its poly(A) tail. However, the deadenylated mRNA in the presence of 4E-T remains capped and protected from degradation (P1 Figure 1). This observation stands in contrast to other proteins known to initiate deadenylation, which mostly lead to mRNA decay (Bawankar et al., 2013; Bhandari et al., 2014; Chen et al., 2009; Hanet et al., 2019; Loh et al., 2013; Raisch et al., 2016; Ruscica et al., 2019; Sgromo et al., 2017, 2018). Thus, 4E-T tethering initiates an incomplete version of the 5'-3' mRNA decay pathway. After deadenylation, the reporter mRNA bound to 4E-T is kept in an intermediated decay state, where it is translationally repressed and protected from further degradation (P1 Figure 1B, C and P1 Figure S1).

In a previous report, it was shown that 4E-T wild type does not change mRNA abundance upon tethering but that the canonical eIF4E binding mutant reduces reporter mRNA levels strongly (Kamenska et al., 2014a). These observations are in accordance with our findings. However, in this study the authors did not observe the accumulation of deadenylated mRNA in the presence of 4E-T. Since the decay caused by the canonical mutant is deadenylation dependent (P1 Figure 4), we assume that in this study 4E-T also promotes deadenylation but the resolution of the northern blot was merely not high enough to resolve the deadenylated band from the polyadenylated one.

We furthermore noticed that upon tethering of 4E-T some mRNA is not stabilized in a deadenylated state but degraded, which varied slightly between reporter systems used (P1 Figure 1C, P1 Figure S1B, F, H, K) and 4E-T/reporter mRNA ratios (data not shown). This concentration-dependent effect of 4E-T may indicate that blocking of decapping requires higher concentrations of the protein compared to deadenylation. Alternatively, poly(A) tail shortening could occur even upon transient and low binding rates of 4E-T to the reporter, whereas blocking

decapping requires constant binding of 4E-T to the mRNA, which is more likely at a higher 4E-T to reporter ratio.

3.1.1 4E-T bound mRNAs are deadenylated and not degraded

RNase H cleavage assays confirmed that the 4E-T bound mRNA is deadenylated. In this assay, DNA-RNA duplexes formed by oligo(dT) and the poly(A) tail are digested by RNase H. The cleaved mRNA can be visualized by northern blotting as a fast migrating band compared to uncleaved mRNA. Treatment of the 4E-T bound reporter with RNase H and oligo(dT) had almost no effect on the migration of the mRNA compared to the control mRNA. Moreover, the size of the 4E-T bound reporter was very similar to the unbound mRNA upon RNase H cleavage. These observations indicate that 4E-T promoted the shortening of the poly(A) tail of a bound reporter mRNA (P1 Figure 1E).

The accumulation of deadenylated mRNA raises the question why the mRNA is not degraded from 3' to 5' by the RNA exosome since the lack of poly(A) tail would make the mRNA susceptible to this mode of decay (Garneau et al., 2007). One possibility would be that unspecific degradation by the exosome happens so slowly that it allows accumulation of the deadenylated reporter mRNA. Alternatively, 3' decay could be actively inhibited. Closer inspection of the migration pattern of the 4E-T bound mRNA suggests that the reporter is not fully deadenylated. In the presence of 4E-T, the reporter migrates not as fast as the cleaved one (P1 Figure 1E lanes 3 vs 4). This indicates that the poly(A) tail is not completely removed but instead a few adenosines remain, which could be enough to protect the mRNA from 3'-5' decay. In order to determine the precise length of the remaining poly(A) tail of 4E-T bound mRNA, a more sensitive method would be required like poly(A) tail sequencing or endogenously cleaving the 3' end of the reporter coupled with high resolution northern blotting (Bartel, 2009; Chang et al., 2014b; Stoeckle and Guan, 1993).

Decapping can take place before the poly(A) tail is completely removed (Yamashita et al., 2005). Recent evidence suggests that decapping starts at a poly(A) tail length of less than 50 and increases in likelihood to a length of less than 20 nucleotides (Eisen et al., 2020a). This length coincides with the binding of one or two PABPC molecules (Schäfer et al., 2019). Thus, it is tempting to speculate that 4E-T binding protects, in addition to the cap from decapping, a short stretch of adenosines from deadenylation which would protect the mRNA from 3' decay.

In vitro, fully assembled CCR4-NOT complex removes the complete poly(A) tail (Raisch et al., 2019). Together with the finding of fully deadenylated transcripts in cells (Eisen et al., 2020a), this suggests that preventing full deadenylation of an mRNA is an active process. One

possibility could be the protection of the 3' end by adding non-adenosine nucleotides, especially guanylation and uridylation, which has been observed for a large number of transcripts (Chang et al., 2014b).

Guanylation correlates with increased mRNA stability and blocks deadenylation but is almost exclusively found in mRNAs with long poly(A) tails (Chang et al., 2014b; Lim et al., 2018). On the contrary, uridylation can be found mainly in poly(A) tails shorter than ~25 nucleotides. Uridylation correlates with decreased mRNA stability and is suggested to stimulate decapping (Chang et al., 2014b; Eisen et al., 2020a; Rissland and Norbury, 2009).

Thus, neither guanylation nor uridylation seem to be involved in 4E-T mediated storage of deadenylated mRNA. However, terminal Us are known to inhibit deadenylation in *Arabidopsis thaliana* and the *in vitro* activity of the fully assembled human CCR4-NOT complex (Raisch et al., 2019; Sement et al., 2013). Therefore, while adding Us to the end of a short poly(A) tail does not usually stabilize the transcript, it will prevent complete deadenylation and might thus protect the mRNA from exosome dependent decay, steering the mRNA towards the decapping dependent 5'-3' decay pathway (Sement et al., 2013). This would subject the mRNA to means of regulations associated with the 5'-3' decay pathway and consequently would also allow storage by 4E-T. A comprehensive characterization of the 3' ends of 4E-T bound transcripts with deep sequencing is necessary to further understand 4E-T dependent mRNA storage.

3.2 4E-T is a binding platform for RNA-associated proteins

4E-T is a mostly unstructured protein. Its interactions with other proteins are mainly mediated by short linear motifs (SLiMs). SLiMs-mediated interactions are typical in decapping associated proteins (Jonas and Izaurralde, 2013; Kamenska et al., 2014a). The disordered architecture of 4E-T is compatible with the assembly of dynamic RNPs and the formation of mesh like structures characteristic of RNA granules like P-bodies (Jonas and Izaurralde, 2013). On a technical note, the disordered structure allows the convenient deletion of protein regions usually without affecting its folding and thus allows the straightforward mapping of protein-protein interaction sites.

The 4E-T binding surfaces for the cap binding protein eIF4E, the translational regulator UNR, the RNA helicase DDX6 and the decapping factor LSM14A have been described before (Dostie et al., 2000; Kamenska et al., 2016; Nishimura et al., 2015). Here, we refined the region essential for interaction with the decapping factor PatL1 to a short stretch of 19 amino acids in the C-terminal part of 4E-T (Figure 4, P1 Figure S2B). This short region has been implicated

in P-body localization, however, its deletion has no effect on 4E-T localization as other C-terminal sequences are additionally required for P-body localization (P1 Figure S3) (Kamenska et al., 2014a). Therefore, the interaction of 4E-T with PatL1 probably contributes to localizing 4E-T to P-bodies but only in conjunction with a so far little characterized C-terminal region (Kamenska et al., 2014a).

The multiple interactions of 4E-T with decapping factors and RNA associated proteins indicate that 4E-T has an important role in the assembly of RNPs and P-bodies. 4E-T might act as a scaffolding protein where translational repressors, decay machinery and transport factors assemble to regulate mRNA fate. Post transcriptional modifications have been implicated in regulating these assemblies. 4E-T is strongly phosphorylated by the c-Jun N-terminal kinase (JNK) under oxidative stress conditions, which promotes self-oligomerization and P-body assembly (Figure 4) (Cargnello et al., 2012). This observation indicates that phosphorylation enhanced binding of 4E-T with its partners, stimulating the assembly of the mesh like network underlying P-body formation. Interestingly, the phosphorylation sites are mainly in the middle region of 4E-T, which we found to mediate binding to the CCR4-NOT complex (Figure 4, P1 Figure 2D and P1 Figure 3).

Further evidence for the relevance of phosphorylation in 4E-BP-RNP assembly is given by the mTOR (mammalian target of rapamycin) kinase dependent phosphorylation of 4E-BP1-3. Phosphorylation of 4E-BP1-3 decreases binding to eIF4E which makes them unable to repress translation (Gingras et al., 1999; Laplante and Sabatini, 2012). To date, it remains unclear if the interaction of 4E-T with eIF4E is also subjected to regulation by phosphorylation. Future experiments are required to determine the effect of phosphorylation on the interactions of 4E-T with its partners and the regulation of mRNA fate.

3.2.1 P-body formation is mediated by 4E-T's interaction network

P-bodies are formed by phase separation caused by RNA-protein aggregates (Banani et al., 2016, 2017). So far, DDX6, LSM14A, 4E-T and mRNA have been found to be essential for P-body formation (Andrei et al., 2005; Marnef et al., 2012; Standart and Weil, 2018). DDX6 and LSM14A have intrinsic RNA binding ability and 4E-T can simultaneously interact with both of them. Thus, in the presence of 4E-T, a chain of protein-protein and protein-RNA interactions is established that promote P-body formation. A single 4E-T can interact with several mRNA molecules simultaneously, via DDX6 and LSM14A, which in turn can link to additional 4E-T/DDX6/LSM14A complexes forming an interconnected mesh of RNA and proteins. The assembly of this network is supported by the observations that RNA mediates 4E-

T dimerization and the interaction of 4E-T with DDX6 is required for P-body assembly (Cargnello et al., 2012; Kamenska et al., 2016).

The work described in this thesis further shows that LSM14A contributes to recruiting 4E-T into P-bodies. The deletion of the LSM14A binding sites on 4E-T compromises 4E-T localization to P-bodies (P1 Figure S3). These findings support the role of 4E-T in bridging the network of interactions that fuel P-body formation.

3.2.2 Recruitment of CCR4-NOT is mediated by the mid region of 4E-T

The structure of the ternary 4E-T-DDX6-NOT1 complex shows that the CHD region of 4E-T binds to the RecA2 domain of full length DDX6 in complex with the MIF4G domain of NOT1, therefore revealing a physical link between NOT1 MIF4G and 4E-T CHD. Interestingly, other DDX6 binding partners that bind mutually exclusive with 4E-T, such as PatL1 and EDC3, block binding of NOT1 to DDX6, due to electrostatic repulsion (Ozgun et al., 2015).

The results presented in this thesis suggest that in the absence of an interaction with DDX6, 4E-T is still able to interact with the CCR4-NOT complex. This was confirmed in cells depleted of DDX6, in which 4E-T was still able to interact with NOT1 (P1 Figure S5A). Furthermore, deletion of the conserved DDX6 interacting region CHD (CUP homology domain) did neither affect the interaction of 4E-T with NOT1 nor 4E-T's ability to promote deadenylation, even though binding to DDX6 is mostly abolished (P1 Figure 2C, S2, S4). Thus, 4E-T recruits the CCR4-NOT complex via multiple and possibly redundant binding regions.

To define the minimal CCR4-NOT interacting region in 4E-T, we first tested 4E-T mutants with deletions that disrupt binding to protein partners individually or in combination. Binding assays with these mutants indicated that 4E-T interaction with NOT1 is independent of UNR, DDX6, LSM14A, PatL1 and eIF4E/4EHP (P1 Figure 2C, S2). We found that the middle (mid) region of 4E-T, ranging from the nuclear localization signal to the second nuclear export signal and encompassing the DDX6 and one of the LSM14A binding regions, was sufficient to bind NOT1 and promote deadenylation of the tethered reporter (P1 Figure 2D, P1 Figure 3). Of note, the mid region of 4E-T contains most of the phosphorylation sites described in the protein (Figure 4), which thus might regulate the recruitment of the CCR4-NOT complex. Attempts to narrow down the binding region revealed multiple small fragments of the mid region that induced the degradation of a bound reporter (data not shown). Therefore, recruitment of the CCR4-NOT complex by 4E-T appears to be mediated by multiple and redundant short linear motifs (SLiMs). It is thus tempting to speculate that 4E-T recruits the

CCR4-NOT complex in a manner similar to TNRC6, which wraps around CNOT9 binding with low specificity to redundant binding sites (Chekulaeva et al., 2011; Chen et al., 2014).

We also observed that 4E-T binds mainly to the C-terminal region of NOT1 consisting of a MIF4G domain and the NOT module (P1 Figure S5B, C). The latter associates with the NOT2 and NOT3 subunits of the CCR4-NOT complex (Boland et al., 2013). This module has been described before as a binding platform for multiple proteins that recruit the CCR4-NOT complex to target mRNAs (Boland et al., 2013). Among these are the Nanos proteins (Bhandari et al., 2014; Raisch et al., 2016), Bicaudal-C (Chicoine et al., 2007) and HELZ (Hanet et al., 2019). The interaction with the C-term of NOT1 further corroborates that 4E-T binds to the CCR4-NOT complex independently of DDX6, which binds the central region of NOT1 (Chen et al., 2014).

3.3 Binding of eIF4E/4EHP is essential for blocking decapping by 4E-T

4E-T is so far the only 4E-BP that has been shown to be able to bind both eIF4E and the translational repressor eIF4E-homologous protein (4EHP or eIF4E-2, P1 Figure S6) (Chapat et al., 2017; Dostie et al., 2000). This stands in contrast to eIF4G and 4E-BP1-3, which only associate with eIF4E and the Grb10-interacting GYF (glycine-tyrosine-phenylalanine) domain protein which specifically interacts with 4EHP and not with eIF4E (Joshi et al., 2004; Peter et al., 2017, 2019; Ruscica et al., 2019). We observed that in order to block decapping, 4E-T requires an intact canonical 4E binding motif (P1 Figure 4, P1 Figure S6). This motif mediates binding to eIF4E as well as 4EHP (P1 Figure S6) (Chapat et al., 2017; Dostie et al., 2000; Kamenska et al., 2014a).

In order to dissect the contributions of the eIF4E and 4EHP, we tested the ability of 4E-T to block decapping upon knockdown eIF4E and in 4EHP-null cells, created via CRISPR-Cas9 gene editing. In both conditions 4E-T was still able to block decapping, suggesting that both proteins can be used to block decapping (P1 Figure S7). However, the knockdown of eIF4E was not complete, which is probably not possible due to eIF4E being an essential protein for growth (Altmann et al., 1987). Therefore, we cannot exclude that a complete depletion of eIF4E might abolish the block of decapping and thus that eIF4E is solely responsible, which could be indicated by the modest, but not significant reduction of accumulated mRNA upon eIF4E knockdown (P1 Figure S7A-C). We furthermore noticed that the loss of 4EHP seems to reduce 4E-Ts ability to promote deadenylation, evidenced by the more polyadenylated reporter mRNA upon 4E-T tethering than in control cells (P1 Figure S7F). This might hint towards a role of 4EHP in promoting deadenylation while eIF4E might inhibit it, which coincides with

reports that eIF4E binding reduces the interaction of 4E-T with the CCR4-NOT complex (Kamenska et al., 2014a).

Although eIF4E and/or 4EHP binding is important to protect a 4E-T bound mRNA from decay, the underlying mechanism is still unclear. It has been shown that N-terminal peptides of 4E-T comprising the 4E-binding motif increase the binding affinity of 4EHP but not eIF4E to the cap structure (Chapat et al., 2017). While the affinity of 4EHP in complex with 4E-T to the cap was still much weaker than the affinity of eIF4E to the cap, this nonetheless demonstrates how 4E-T could protect the cap from decapping by increasing the affinity of cap binding proteins to the cap.

Apart from increasing the affinity, 4E-T could also stabilize the interaction of eIF4E/4EHP with the cap structure by binding the mRNA close to the cap and forming a stable complex. While 4E-T has not been shown to have any RNA binding activity itself, several of its interaction partners can bind RNA directly. Most intriguingly, the yeast homolog of LSM14A, SCD6, forms a repressive complex with eIF4G and cap-bound eIF4E (Rajyaguru et al., 2012). It is thus compelling to speculate that LSM14A could stabilize 4E-T with eIF4E/4EHP at the cap in a similar manner. LSM14A has been identified as an RNA binding protein, although its LS_m domain, a domain generally associated with RNA binding, is used for protein binding (Baltz et al., 2012; Brandmann et al., 2018; Castello et al., 2012). In support of this possibility is the observation that relative to wild type protein, tethering of the 4E-T mutant lacking the LSM14A binding regions reduces the amount of protected and deadenylated reporter mRNA, and thus more transcript is degraded (P1 Figure S4A lane 5 vs 2, B).

Interestingly, in the absence of an interaction with DDX6 and PatL1 (4E-T Δ DDX6 or Δ PatL1) the amount of deadenylated reporter accumulating in the presence of 4E-T increased (P1 Figure S4A lane 4,6 vs 2, B). This result is in agreement with the fact that DDX6 and PatL1 have been described as decapping activators (Nissan et al., 2010). Binding of these factors to mRNA should thus enhance DCP2 activity. Because of these antagonistic contributions of the different binding partners, we speculate that 4E-T acts as a scaffold for factors whose compilation determines the efficiency of decapping. While eIF4E, 4EHP and LSM14A block mRNA decapping, DDX6 and PatL1 enhance it.

3.4 4E-T is involved in TRNC6B mediated mRNA decay

TNRC6 proteins (also called GW182) are essential for miRNA mediated gene silencing by recruiting the CCR4-NOT complex to miRISC-bound mRNAs (Braun et al., 2011; Chekulaeva et al., 2011; Chen et al., 2009, 2014; Fabian et al., 2011). Previous work from the

Izaurrealde laboratory has shown that recruitment of TNRC6B to a reporter mRNA promotes deadenylation and leads to the accumulation of deadenylated reporter transcript (Lazzaretti et al., 2009). We further found that the accumulation of deadenylated mRNA intermediates when tethering TNRC6B, only occurs if 4E-T is present in cells (P1 Figure 5). Due to their similarity, we assume that TNRC6A and TNRC6C can also employ 4E-T in a similar manner to TNRC6B. In the initial study there were slight variations in the amount of the deadenylated reporter bound to the different TNRC6 proteins (Lazzaretti et al., 2009). Differences in 4E-T recruitment, regulation or binding of additional protein partners among TNRC6A, B and C might control the amount of mRNA that is decapped.

We furthermore noticed that 4E-T was not required for TNRC6B mediated mRNA deadenylation (P1 Figure 5A lane 2 vs 4). This is in agreement with the observations that TNRC6B can bind NOT1 and NOT9 directly (Chekulaeva et al., 2011; Chen et al., 2014). 4E-T instead was crucial to block decapping following TNRC6B dependent mRNA deadenylation. In the absence of 4E-T, the deadenylated mRNA gets decapped and degraded, while in the presence of 4E-T decapping is inhibited, and the deadenylated mRNA accumulates in cells. It remains unclear how 4E-T, TNRC6B and the CCR4-NOT complex coordinate the repression and storage of a miRNA targeted mRNA. As both 4E-T and TNRC6B bind to the deadenylase complex, multiple protein interactions might be established upon recruitment of the silencing complex to the mRNA. Defining the regions in TNRC6B required to bind 4E-T and to protect the mRNA from decapping might help to understand how miRNA targets are stored in cells.

3.4.1 miRNAs and 4E-T

Silencing of miRNA targets is characterized by translational repression, deadenylation, decapping and mRNA degradation (Izaurrealde, 2015). Most of the repression elicited by miRNAs can be attributed to mRNA destabilization (Eichhorn et al., 2014) and also the dominant miRNA dependent translational repression observed in early embryos can be attributed to deadenylation (Subtelny et al., 2014). miRNA triggered deadenylation depends on TNRC6/GW182 proteins (Behm-Ansmant, 2006; Chekulaeva et al., 2011; Rehwinkel, 2005).

The data presented here indicates that 4E-T can block decapping of TNRC6B targeted mRNAs, and thus suggests that 4E-T is able to protect miRNA targets from degradation. This would implicate 4E-T in a multitude of pathways influencing virtually all cellular processes (Bartel, 2009).

Recent experiments showed that when sequencing the poly(A) tails of miR-1 and miR-155 targets no major accumulation of deadenylated mRNA was observed (Eisen et al., 2020b).

Furthermore, 4E-T has been shown to be an enhancer of miRNA mediated silencing. Depletion of cellular 4E-T reduced the decay rate of *HMGA2*, a let7 miRNA target mRNA, in an eIF4E/4EHP-dependent manner (Nishimura et al., 2015) and relieved some of the translational repression of an R-Luc-let-7 reporter (Kamenska et al., 2014a, 2016) as well as an F-Luc reporter with the miRNA targeted DUSP6 3' UTR (Jafarnejad et al., 2018).

These seemingly contradicting observations on the role of 4E-T during miRNA-mediated gene silencing might be associated with distinct contributions of the protein during the silencing process. The multitude of protein interactions established by 4E-T permit the regulation of all the silencing steps, i.e. translational repression, deadenylation and decapping. Distinct 4E-T-based RNPs may therefore differentially control translation and mRNA stability. For example, 4E-T could contribute to repression while at the same time inhibiting mRNA decay. Deadenylated mRNA is translationally repressed and thus blocking decapping does not change the amount of translated mRNA, which would make this stabilization virtually undetectable when only looking at translation.

The ability of 4E-T to either enhance or inhibit miRNA dependent mRNA decay further demonstrates how 4E-T could affect mRNA turnover differently depending on its mode of recruitment and mRNP composition. We would speculate that, for example, when recruited via eIF4E to an mRNA 4E-T enhances decay, while when recruited downstream of deadenylation factors it stabilizes the mRNA. Similarly, in complex with eIF4E/4EHP, 4E-T would inhibit and in the absence of this interaction enhance mRNA decay. Variations in miRNA induced RISCs composition could therefore also explain why different miRNAs can have varying effects on mRNA levels even with similar effects on translation (Behm-Ansmant, 2006).

Thus, exploring the composition of miRISCs and characterizing the individual interactions is crucial for understanding 4E-T's contribution to miRNA silencing.

3.5 4E-T can block decapping of ARE containing mRNA

The results described so far indicate that 4E-T can interfere with decapping following mRNA deadenylation by the CCR4-NOT complex. To further confirm this, we tested if 4E-T can block decapping of mRNAs with AU-rich elements (ARE). ARE can lead to mRNA destabilization by recruiting the CCR4-NOT complex (Bulbrook et al., 2018; Fabian et al., 2013) and 4E-T has been shown to contribute to decay caused by ARE (Ferraiuolo et al., 2005). Therefore, we used a BGG reporter containing the ARE of the *FOS* gene in its 3' UTR. Expression of the ARE binding protein tristetraprolin (TTP) induced degradation of the reporter (P1 Figure 6B, C). In cells overexpressing TTP and 4E-T simultaneously, decay of the reporter

was blocked and the transcript accumulated as a deadenylated intermediate. Thus, 4E-T can block decapping of ARE-mediated mRNA decay.

We also observed that in cells overexpressing 4E-T but not TTP, the abundance of polyadenylated BGG-ARE mRNA increased (P1 Figure 6B lane 1 vs 2, C). This result suggests that in the absence of TTP, 4E-T also inhibits turnover of the BGG-ARE reporter either in a deadenylation-independent manner or by inhibiting deadenylation. Apart from recruiting the CCR4-NOT complex, ARE can also promote exosome-dependent mRNA decay (Chen et al., 2001). Therefore, it could be that overexpression of TTP in HEK293T cells might steer decay of the reporter to deadenylation-dependent mRNA decapping, since TTP binds directly to the CCR4-NOT complex (Bulbrook et al., 2018; Fabian et al., 2013).

For TTP independent decay, 4E-T could thus either interfere with recruiting deadenylases or the exosome to the ARE containing mRNA, or 4E-T could block deadenylation independent decapping, which, however, has only been observed in yeast before (Badis et al., 2004). Alternatively, 4E-T could also control ARE mediated turnover indirectly by affecting the transcription of the mRNA.

We conclude that 4E-T is important for ARE mediated mRNA turnover and can block decapping triggered by TTP. Interestingly, it has been shown that a reporter containing the ARE of CSF2 accumulates partly in a deadenylated form (Chen et al., 1995) and that binding of the ARE-binding protein ELAVL1 (also known as HuR) to an ARE containing mRNA protects the deadenylated mRNA from further degradation (Peng, 1998). ELAVL1, furthermore has been found by mass spectrometry to co-purify with 4E-T (Kamenska et al., 2016). It would thus be worth testing if 4E-T is involved in these processes.

3.6 4E-T can modulate the fate of an mRNA from decay to storage

Following up on the observation that 4E-T can block decapping of mRNAs targeted by CCR4-NOT dependent processes, we wanted to test if 4E-T can affect decapping of an mRNA targeted directly by the CCR4-NOT complex. Overexpression of 4E-T led to the accumulation of deadenylated reporter mRNA upon tethering NOT1 (P1 Figure 6E, F). These results suggest that 4E-T can potentially block decapping of any mRNA targeted for deadenylation by the CCR4-NOT complex. Since NOT1 is six times more abundant than 4E-T in HeLa cells (Hein et al., 2015), the majority of CCR4-NOT targeted mRNAs will be deadenylated and further degraded in these cells, explaining why no deadenylated mRNA accumulates when tethering NOT1 but keeping endogenous levels of 4E-T (P1 Figure 6E, F). Increased local concentration (e.g. P-bodies) or high tissue abundance of 4E-T (e.g. oocytes (Villaescusa et al., 2006).) and

specific mRNA recruitment of the protein would then inhibit decapping of deadenylated transcripts.

In conclusion, our data shows that in principle 4E-T can interfere with decapping of any mRNA upon CCR4-NOT dependent deadenylation and that 4E-T expression levels could globally inhibit deadenylation dependent mRNA decapping. Specific recruitment of 4E-T to an mRNA or upregulating the expression of 4E-T might thus prevent decay of an mRNA otherwise targeted for decay, storing it in a silenced state. It remains unclear how and if 4E-T targets specific mRNAs. So far, we know that in HEK293T cells, 4E-T cellular levels are sufficient to prevent decapping and subsequent decay of a reporter mRNA tethered to TNRC6B, suggesting a specific recruitment of 4E-T by TNRC6B.

In order to protect an mRNA from decapping, it is most likely necessary that 4E-T is stably associated with the transcript. Once 4E-T is bound to an mRNA, the interactions with eIF4E/4EHP, and to a minor extent with DDX6/LSM14A and PatL1 will determine if the mRNA is stored in a deadenylated form or decapped and degraded (Figure 5, discussed in 3.3). The interaction with eIF4E/4EHP might be regulated as has been shown for 4E-BP1. Phosphorylation of 4E-BP1 by mTOR disrupts binding to eIF4E and thus releases translational repression (Gingras et al., 1999). Alternatively, dissociation of 4E-T from the mRNP would irreversibly commit the deadenylated mRNA to decay.

Studying how 4E-T is recruited to an mRNA and how the binding to its interaction partners is modulated by post-translational modifications will greatly improve the understanding of mRNA storage.

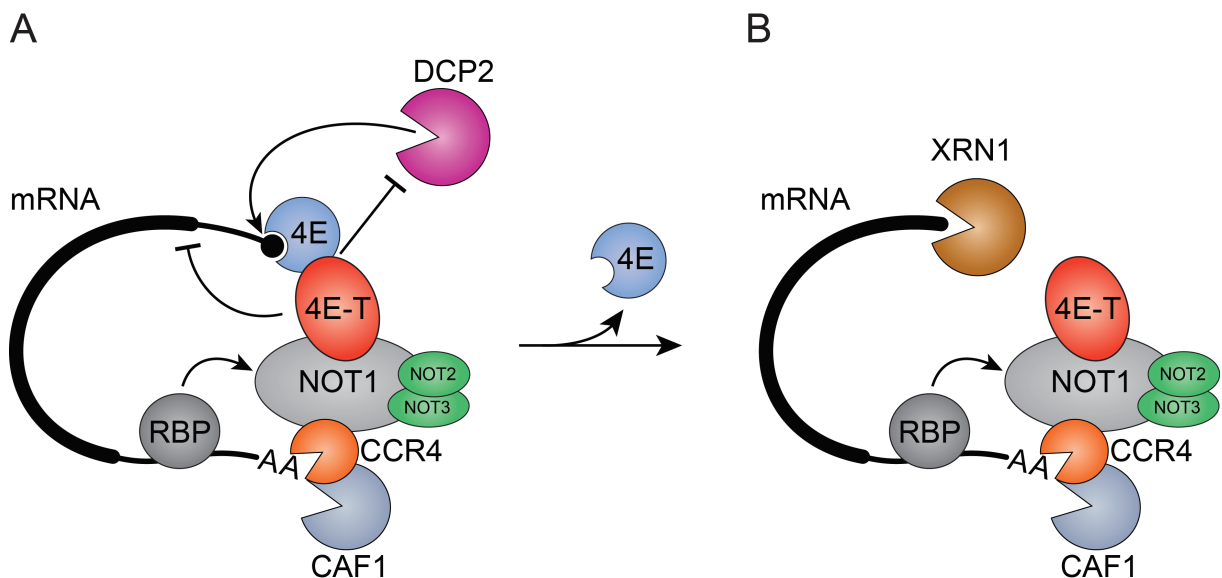


Figure 5 Model for the role of 4E-T as a determinant of mRNA storage or decay. When bound to the mRNA and eIF4E (4E), 4E-T stores the mRNA in a deadenylated and silenced state by blocking decapping (A). When eIF4E binding is relieved or 4E-T removed from the mRNA, decapping and decay from the 5' end can take place (B).

3.7 mRNA storage and 4E-T

The mechanism of keeping mRNA in a silenced state with short poly(A) tails has been first observed for maternal mRNAs during oogenesis where protein abundance is mainly regulated on a translational and not a transcriptional level (Huarte et al., 1992; Piccioni et al., 2005). Here, mRNAs are kept in a deadenylated and silenced state until activated for translation by cytoplasmic polyadenylation (Richter, 1999).

4E-T is expressed at high levels in developing oocytes and has been associated with premature ovarian failure in humans (Kasippillai et al., 2013; Minshall et al., 2007; Villaescusa et al., 2006). Furthermore, the 4E-T related and *Drosophila*-specific protein CUP has been shown to deadenylate and block decapping of *oskar* mRNA, repressing its expression during localization in early embryogenesis (Igreja and Izaurralde, 2011; Nakamura et al., 2004). It is thus intriguing to speculate that human 4E-T might be involved in maintaining maternal mRNAs also in a deadenylated and silenced state. Apart from long term storage, deadenylation without decay would also provide an additional way to selectively and temporarily regulate mRNA expression during phases in development where poly(A) tail length determines translation efficiency (Eichhorn et al., 2016; Subtelny et al., 2014).

Storage of deadenylated mRNAs has also important implications for localized translation in neurons and synaptic plasticity (Poon et al., 2006). Localized translation at the synapses requires mRNA silencing during transport from the nucleus to prevent premature translation (Sahoo et al., 2018). Synaptic mRNAs are translationally activated by the action of cytoplasmic polyadenylation element binding protein (CPEB) and the polyadenylase Gld2, suggesting that they are transported to the synapses in a deadenylated state (Udagawa et al., 2012; Wu et al., 1998). 4E-T is crucial for neuronal development by regulating differentiation and specification (Amadei et al., 2015; Yang et al., 2014; Zahr et al., 2018). Therefore, it might be possible that 4E-T participates in the control of localized translation in neurons and represses neuronal mRNAs in a manner similar to the eIF4E-binding protein Neuroguidin. Neuroguidin controls neuronal development in *Xenopus* by repressing mRNAs in a CPE dependent manner via binding CPEB, which could thus facilitate the specific repression of mRNAs targeted for deadenylated storage (Jung et al., 2006).

3.7.1 P-bodies as sites of mRNA storage

P-bodies are sites of mRNA storage (Hubstenberger et al., 2017). As these granules are present in all cell types, storage of mRNA might play significant yet undiscovered cellular

functions. mRNAs enriched in P-bodies were found to be repressed, protected from the 5' end and to have a high variation of poly(A) tail length, which was noticed when comparing the enriched mRNAs to a poly(A) tail sequencing dataset (Hubstenberger et al., 2017). Furthermore, FISH analysis was unable to detect poly(A) tails in P-bodies (Aizer et al., 2014) and P-bodies lack PABP (Kedersha et al., 2005). These observations point towards a deadenylated storage of mRNA in P-bodies. As an essential component of these granules, blocking of decapping by 4E-T might be crucial for the storage of mRNA in P-bodies. Additional studies measuring the length of the poly(A) tail of transcripts associated with 4E-T and P-bodies would increase our understanding of the mechanistic details of mRNA storage.

Transcriptome wide measurements of poly(A) tail length via TAIL-seq and Pal-seq did not reveal any specific mRNA stored in a deadenylated state under normal growth conditions (Chang et al., 2014b; Subtelny et al., 2014) but it was shown that during S phase some specific mRNAs are deadenylated and not degraded (Park et al., 2016). This data suggests that storage of deadenylated transcripts might be mainly a short-term mechanism facilitating efficient but temporary silencing of mRNAs without degradation.

In order to find out if 4E-T bound mRNAs are kept in a stable state to facilitate re-using or if their decay is just delayed, it would be important to find out if 4E-T bound mRNAs can be readenylated and returned to the translation pool.

3.8 Translational activation of stored mRNAs

Temporary mRNA storage has been observed during stress response and the cell cycle. (Bhattacharyya et al., 2006; Brengues et al., 2005; Park et al., 2016). Silenced mRNAs present in P-bodies can return to the translation pool following miRNA-mediated repression upon stress relief (Bhattacharyya et al., 2006; Brengues et al., 2005). Activation of a repressed and deadenylated mRNA would require the remodeling of the mRNP particle, i.e. the dissociation of repressor proteins and elongation of the poly(A) tail. Cytoplasmic polyadenylation is crucial for oocyte maturation in frogs, *Drosophila* and mice, where it activates maternal mRNAs (Richter, 1999). Here, a specific sequence in an mRNA, the cytoplasmic polyadenylation signal (CPE), targets an mRNA for polyadenylation leading to its translational activation (Fox et al., 1989). The CPE is bound by CPE-binding protein (CPEB), which then recruits a cytoplasmic poly(A) polymerase (Mendez and Richter, 2001). This mode of translational activation is crucial during early development, promotes translation of specific mRNAs in cycling somatic cells and is required for localized translation involved in synaptic plasticity (Groisman et al., 2002; Udagawa et al., 2012).

In the absence of a CPE, cytoplasmic polyadenylation of repressed transcripts is much less documented or understood. *bicoid* mRNA, which lacks a clear CPE, is subject to cytoplasmic polyadenylation during embryogenesis (Verrotti et al., 1996). However, the underlying processes are not clear yet. Possible mechanisms of polyadenylation and translation activation include the recruitment of CPEB and/or polyadenylases by RNA-binding or associated proteins. This has been demonstrated for the RNA binding protein Pumilio in *Xenopus*, which represses bound mRNA and also interacts with CPEB. Upon removal of Pumilio the mRNA gets readenylated and translated (Nakahata et al., 2001; Padmanabhan and Richter, 2006). Interestingly, human Pumilio forms a repressive complex with 4E-T that controls differentiation in neurogenesis (Etten et al., 2012). Furthermore, *Xenopus* 4E-T forms a translational repressor complex with CPEB together with DDX6, LSM14A and PatL1, that inhibits translation during early oogenesis (Minshall et al., 2007). It could thus be possible that 4E-T employs a similar mechanism to Pumilio in *Xenopus* and gets recruited to an mRNA via an RBP to initiate storage. 4E-T dissociation from the repressed transcript and/or post-translational modifications of the protein might then permit mRNA re-adenylation and translation.

Another mechanism relevant for reactivation of stored mRNAs might be 3' end modifications. Inhibition of decapping or 5' decay leads to a strong accumulation of uridylated, short tailed mRNA (Lim et al., 2018). It is not clear yet if uridylation takes place in order to enhance decapping or as a consequence of inhibited decay. However, if uridine tails are added to the deadenylated 4E-T bound mRNAs, reactivation of the stored mRNA for translation would require removal of the modified tails. So far, the reversibility of uridylation has not been addressed. Uridine nucleotides can be removed by the 3'-5' endonuclease DIS3L2, which degrades uridylated mRNAs in yeast and is also active in human cells (Lubas et al., 2013; Malecki et al., 2013). Additionally, the CCR4-NOT complex is also able to remove uridine nucleotides to some extent depending on its subunit composition (Niinuma et al., 2016; Raisch et al., 2019; Tang et al., 2019).

Alternatively, the short poly(A) tails of a 4E-T bound mRNA might be protected from 3' end modifications such as uridylation, for example by keeping the CCR4-NOT complex bound to the 3' end. Studies that address the RNP and the nature of the 3' end of 4E-T bound mRNAs are therefore critical to understand the role of the 3' end in mRNA storage and reactivation.

3.9 The 4E-T associated transcriptome

A central challenge to understanding the biological relevance of 4E-T and the processes that are controlled by its ability to block decapping, is the identification of the transcripts regulated by this 4E-T.

Target mRNA binding is most likely directed by RNA binding proteins (RBP) like Pumilio2 or Smaug2, which have been found to form a complex with 4E-T to repress mRNAs important for neurogenesis during mouse embryogenesis (Amadei et al., 2015; Zahr et al., 2018). We tested if 4E-T controls the RNA levels or poly(A) tail length of some of the human homologues of the target mRNAs identified in these studies but found no effect in HEK293T and HeLa 4E-T knockout cells via northern blotting (data not shown). Since 4E-T's target binding is probably controlled by its protein partners, these interactions must be tightly controlled and are probably specific to cell types and developmental processes. Therefore, the 4E-T bound transcriptome might vary between different cell types. RNA immunoprecipitation coupled with RNA sequencing would uncover the identity of 4E-T bound mRNAs and provide endogenous mRNAs targets to test how 4E-T affects their poly(A) tail. Interesting biological contexts to determine the 4E-T associated transcriptome include oogenesis, neuronal development and cells under transitory conditions, like stress, growth or differentiation.

3.10 Conclusions

In summary, we describe for the first time 4E-T as a protein that promotes deadenylation by recruiting the CCR4-NOT complex to a target mRNA. In addition, 4E-T blocks decapping and further decay of the deadenylated mRNA by its interaction with the cap-binding proteins eIF4E/4EHP. Moreover, 4E-T interferes with decapping triggered by the miRNA associated factor TNRC6B, AU-rich elements and potentially any mRNA targeted by the CCR4-NOT complex. The regulatory mechanisms of 4E-T controlled stabilization and the cellular processes targeted by this mechanism remain yet to be explored.

4 Results and discussion II: HELZ

This part describes and discusses briefly the second manuscript attached to this thesis, titled: “HELZ directly interacts with CCR4-NOT and causes decay of bound mRNA”. References to figures in this publication start with “P2”.

The putative RNA Helicase with Zinc-finger (HELZ) interacts with the CCR4-NOT complex and PABPC1 (Hasgall et al., 2011; Mathys et al., 2014). However, a putative role of HELZ in deadenylation and mRNA turnover has not been addressed before. The work presented in this manuscript shows that recruitment of HELZ to a reporter mRNA induces 5'-3' mRNA decay. The interaction between HELZ and the CCR4-NOT complex is direct, as shown using *in vitro* pulldown experiments, and depends on at least two redundant short linear motifs (SLiMs) in the unstructured C-terminus of HELZ (P2 Figure 2). SLiM-mediated interaction with CCR4-NOT is a binding mechanism commonly used by interactors of the deadenylase complex and, as described in this thesis, applies also for 4E-T (Bhandari et al., 2014; Chen et al., 2014; Fabian et al., 2013; Keskeny et al., 2019). Furthermore, HELZ-mediated deadenylation-dependent mRNA decay is conserved in Metazoa (P2 Figure 3 and 4).

We also describe that HELZ can repress translation in the absence of mRNA decay. This is also mediated by the CCR4-NOT complex and does not depend on binding to PABPC1 (P2 Figure 5). However, it is unlikely that HELZ acts as a general translational repressor because it has been shown to promote translation (Hasgall et al., 2011). Based on our results, this is probably done indirectly by controlling the expression of mRNAs relevant for translational regulation. Thus, HELZ probably controls the expression of specific mRNAs by recruiting the CCR4-NOT complex to them. The specificity of HELZ could be based on the recognition of specific RNA sequences by its Zinc-finger domain in a manner similar to the Zinc-finger protein TTP which binds specifically to AU-rich elements in an mRNA (Fabian et al., 2013).

Transcriptome analysis using RNA-Seq of HEK293T *HELZ*-knock out cells revealed that HELZ regulates the expression of a great number of genes involved in processes such as neurogenesis, nervous system development, cell adhesion or signaling (P2 Figure 6). While these results do not allow to differentiate changes on mRNA stability from effects on transcription, they still highlight the broad influence that HELZ has on mRNA abundance and provide targets for future studies.

In summary, we describe HELZ as a protein that has the ability to directly recruit the CCR4-NOT complex to specific transcripts in order to promote mRNA decay and repress translation.

5 References

- Aizer, A., Kalo, A., Kafri, P., Shraga, A., Ben-Yishay, R., Jacob, A., Kinor, N., and Shav-Tal, Y. (2014). Quantifying mRNA targeting to P-bodies in living human cells reveals their dual role in mRNA decay and storage. *J. Cell Sci.* *127*, 4443–4456.
- Altmann, M., Handschin, C., and Trachsel, H. (1987). mRNA cap-binding protein: cloning of the gene encoding protein synthesis initiation factor eIF-4E from *Saccharomyces cerevisiae*. *Mol. Cell. Biol.* *7*, 998–1003.
- Amadei, G., Zander, M.A., Yang, G., Dumelie, J.G., Vessey, J.P., Lipshitz, H.D., Smibert, C.A., Kaplan, D.R., and Miller, F.D. (2015). A Smaug2-Based Translational Repression Complex Determines the Balance between Precursor Maintenance versus Differentiation during Mammalian Neurogenesis. *J. Neurosci.* *35*, 15666–15681.
- Andrei, M.A., Ingelfinger, D., Heintzmann, R., Achsel, T., Rivera-Pomar, R., and Lührmann, R. (2005). A role for eIF4E and eIF4E-transporter in targeting mRNPs to mammalian processing bodies. *RNA N. Y. N* *11*, 717–727.
- Arribas-Layton, M., Wu, D., Lykke-Andersen, J., and Song, H. (2013). Structural and functional control of the eukaryotic mRNA decapping machinery. *Biochim. Biophys. Acta* *1829*, 580–589.
- Badis, G., Saveanu, C., Fromont-Racine, M., and Jacquier, A. (2004). Targeted mRNA Degradation by Deadenylation-Independent Decapping. *Mol. Cell* *15*, 5–15.
- Baer, B., and Kornberg, R. (1983). The protein responsible for the repeating structure of cytoplasmic poly(A)-ribonucleoprotein. *J. Cell Biol.* *96*, 717–721.
- Baltz, A.G., Munschauer, M., Schwanhäusser, B., Vasile, A., Murakawa, Y., Schueler, M., Youngs, N., Penfold-Brown, D., Drew, K., Milek, M., et al. (2012). The mRNA-Bound Proteome and Its Global Occupancy Profile on Protein-Coding Transcripts. *Mol. Cell* *46*, 674–690.
- Banani, S.F., Rice, A.M., Peeples, W.B., Lin, Y., Jain, S., Parker, R., and Rosen, M.K. (2016). Compositional Control of Phase-Separated Cellular Bodies. *Cell* *166*, 651–663.
- Banani, S.F., Lee, H.O., Hyman, A.A., and Rosen, M.K. (2017). Biomolecular condensates: organizers of cellular biochemistry. *Nat. Rev. Mol. Cell Biol.* *18*, 285–298.
- Banko, J.L. (2005). The Translation Repressor 4E-BP2 Is Critical for eIF4F Complex Formation, Synaptic Plasticity, and Memory in the Hippocampus. *J. Neurosci.* *25*, 9581–9590.
- Barkoff, A. (1998). Meiotic maturation in *Xenopus* requires polyadenylation of multiple mRNAs. *EMBO J.* *17*, 3168–3175.
- Bartel, D.P. (2004). MicroRNAs: Genomics, Biogenesis, Mechanism, and Function. *Cell* *116*, 281–297.
- Bartel, D.P. (2009). MicroRNAs: Target Recognition and Regulatory Functions. *Cell* *136*, 215–233.
- Bawankar, P., Loh, B., Wohlbold, L., Schmidt, S., and Izaurralde, E. (2013). NOT10 and C2orf29/NOT11 form a conserved module of the CCR4-NOT complex that docks onto the NOT1 N-terminal domain. *RNA Biol.* *10*, 228–244.
- Behm-Ansmant, I. (2006). mRNA degradation by miRNAs and GW182 requires both CCR4:NOT deadenylase and DCP1:DCP2 decapping complexes. *Genes Dev.* *20*, 1885–1898.

- Bhandari, D., Raisch, T., Weichenrieder, O., Jonas, S., and Izaurralde, E. (2014). Structural basis for the Nanos-mediated recruitment of the CCR4-NOT complex and translational repression. *Genes Dev.* *28*, 888–901.
- Bhaskar, V., Roudko, V., Basquin, J., Sharma, K., Urlaub, H., Séraphin, B., and Conti, E. (2013). Structure and RNA-binding properties of the Not1–Not2–Not5 module of the yeast Ccr4–Not complex. *Nat. Struct. Mol. Biol.* *20*, 1281–1288.
- Bhattacharyya, S.N., Habermacher, R., Martine, U., Closs, E.I., and Filipowicz, W. (2006). Relief of microRNA-Mediated Translational Repression in Human Cells Subjected to Stress. *Cell* *125*, 1111–1124.
- Boag, P.R., Atalay, A., Robida, S., Reinke, V., and Blackwell, T.K. (2008). Protection of specific maternal messenger RNAs by the P body protein CGH-1 (Dhh1/RCK) during *Caenorhabditis elegans* oogenesis. *J. Cell Biol.* *182*, 543–557.
- Boland, A., Chen, Y., Raisch, T., Jonas, S., Kuzuoğlu-Öztürk, D., Wohlbold, L., Weichenrieder, O., and Izaurralde, E. (2013). Structure and assembly of the NOT module of the human CCR4–NOT complex. *Nat. Struct. Mol. Biol.* *20*, 1289–1297.
- Bouveret, E., Rigaut, G., Shevchenko, A., Wilm, M., and Séraphin, B. (2000). A Sm-like protein complex that participates in mRNA degradation. *EMBO J.* *19*, 1661–1671.
- Brandmann, T., Fakim, H., Padamsi, Z., Youn, J., Gingras, A., Fabian, M.R., and Jinek, M. (2018). Molecular architecture of LSM14 interactions involved in the assembly of mRNA silencing complexes. *EMBO J.* *37*, e97869.
- Braun, J.E., Tritschler, F., Haas, G., Igreja, C., Truffault, V., Weichenrieder, O., and Izaurralde, E. (2010). The C-terminal α – α superhelix of Pat is required for mRNA decapping in metazoa. *EMBO J.* *29*, 2368–2380.
- Braun, J.E., Huntzinger, E., Fauser, M., and Izaurralde, E. (2011). GW182 Proteins Directly Recruit Cytoplasmic Deadenylation Complexes to miRNA Targets. *Mol. Cell* *44*, 120–133.
- Bregues, M., Teixeira, D., and Parker, R. (2005). Movement of Eukaryotic mRNAs Between Polysomes and Cytoplasmic Processing Bodies. *Science* *310*, 486–489.
- Bulbrook, D., Brazier, H., Mahajan, P., Kliszczak, M., Fedorov, O., Marchese, F.P., Aubareda, A., Chalk, R., Picaud, S., Strain-Damerell, C., et al. (2018). Tryptophan-Mediated Interactions between Tristetraprolin and the CNOT9 Subunit Are Required for CCR4-NOT Deadenylation Complex Recruitment. *J. Mol. Biol.* *430*, 722–736.
- Cargnello, M., Tcherkezian, J., Dorn, J.F., Huttlin, E.L., Maddox, P.S., Gygi, S.P., and Roux, P.P. (2012). Phosphorylation of the Eukaryotic Translation Initiation Factor 4E-Transporter (4E-T) by c-Jun N-Terminal Kinase Promotes Stress-Dependent P-Body Assembly. *Mol. Cell Biol.* *32*, 4572–4584.
- Castello, A., Fischer, B., Eichelbaum, K., Horos, R., Beckmann, B.M., Strein, C., Davey, N.E., Humphreys, D.T., Preiss, T., Steinmetz, L.M., et al. (2012). Insights into RNA Biology from an Atlas of Mammalian mRNA-Binding Proteins. *Cell* *149*, 1393–1406.
- Chang, C.-T., Bercovich, N., Loh, B., Jonas, S., and Izaurralde, E. (2014a). The activation of the decapping enzyme DCP2 by DCP1 occurs on the EDC4 scaffold and involves a conserved loop in DCP1. *Nucleic Acids Res.* *42*, 5217–5233.
- Chang, C.-T., Muthukumar, S., Weber, R., Levdansky, Y., Chen, Y., Bhandari, D., Igreja, C., Wohlbold, L., Valkov, E., and Izaurralde, E. (2019). A low-complexity region in human

- XRN1 directly recruits deadenylation and decapping factors in 5'–3' messenger RNA decay. *Nucleic Acids Res.* *47*, 9282–9295.
- Chang, H., Lim, J., Ha, M., and Kim, V.N. (2014b). TAIL-seq: Genome-wide Determination of Poly(A) Tail Length and 3' End Modifications. *Mol. Cell* *53*, 1044–1052.
- Chapat, C., Jafarnejad, S.M., Matta-Camacho, E., Hesketh, G.G., Gelbart, I.A., Attig, J., Gkogkas, C.G., Alain, T., Stern-Ginossar, N., Fabian, M.R., et al. (2017). Cap-binding protein 4EHP effects translation silencing by microRNAs. *Proc. Natl. Acad. Sci.* *114*, 5425–5430.
- Chekulaeva, M., Mathys, H., Zipprich, J.T., Attig, J., Colic, M., Parker, R., and Filipowicz, W. (2011). miRNA repression involves GW182-mediated recruitment of CCR4–NOT through conserved W-containing motifs. *Nat. Struct. Mol. Biol.* *18*, 1218–1226.
- Chen, C.-Y.A., and Shyu, A.-B. (2011). Mechanisms of deadenylation-dependent decay. *Wiley Interdiscip. Rev. RNA* *2*, 167–183.
- Chen, C.Y., Xu, N., and Shyu, A.B. (1995). mRNA decay mediated by two distinct AU-rich elements from c-fos and granulocyte-macrophage colony-stimulating factor transcripts: different deadenylation kinetics and uncoupling from translation. *Mol. Cell. Biol.* *15*, 5777–5788.
- Chen, C.-Y., Gherzi, R., Ong, S.-E., Chan, E.L., Raijmakers, R., Pruijn, G.J.M., Stoecklin, G., Moroni, C., Mann, M., and Karin, M. (2001). AU Binding Proteins Recruit the Exosome to Degrade ARE-Containing mRNAs. *Cell* *107*, 451–464.
- Chen, C.-Y.A., Zheng, D., Xia, Z., and Shyu, A.-B. (2009). Ago–TNRC6 triggers microRNA-mediated decay by promoting two deadenylation steps. *Nat. Struct. Mol. Biol.* *16*, 1160–1166.
- Chen, Y., Boland, A., Kuzuoğlu-Öztürk, D., Bawankar, P., Loh, B., Chang, C.-T., Weichenrieder, O., and Izaurralde, E. (2014). A DDX6–CNOT1 Complex and W-Binding Pockets in CNOT9 Reveal Direct Links between miRNA Target Recognition and Silencing. *Mol. Cell* *54*, 737–750.
- Chicoine, J., Benoit, P., Gamberi, C., Paliouras, M., Simonelig, M., and Lasko, P. (2007). Bicardal-C Recruits CCR4–NOT Deadenylase to Target mRNAs and Regulates Oogenesis, Cytoskeletal Organization, and Its Own Expression. *Dev. Cell* *13*, 691–704.
- Cho, P.F., Poulin, F., Cho-Park, Y.A., Cho-Park, I.B., Chicoine, J.D., Lasko, P., and Sonenberg, N. (2005). A New Paradigm for Translational Control: Inhibition via 5'–3' mRNA Tethering by Bicoid and the eIF4E Cognate 4EHP. *Cell* *121*, 411–423.
- Cho, P.F., Gamberi, C., Cho-Park, Y.A., Cho-Park, I.B., Lasko, P., and Sonenberg, N. (2006). Cap-Dependent Translational Inhibition Establishes Two Opposing Morphogen Gradients in *Drosophila* Embryos. *Curr. Biol.* *16*, 2035–2041.
- Chowdhury, A., Mukhopadhyay, J., and Tharun, S. (2007). The decapping activator Lsm1p–7p–Pat1p complex has the intrinsic ability to distinguish between oligoadenylated and polyadenylated RNAs. *RNA* *13*, 998–1016.
- Coller, J.M., Tucker, M., Sheth, U., Valencia-Sanchez, M.A., and Parker, R. (2001). The DEAD box helicase, Dhh1p, functions in mRNA decapping and interacts with both the decapping and deadenylase complexes. *RNA* *7*, 1717–1727.
- Cougot, N., Babajko, S., and Séraphin, B. (2004). Cytoplasmic foci are sites of mRNA decay in human cells. *J. Cell Biol.* *165*, 31–40.

- Davila Lopez, M., and Samuelsson, T. (2007). Early evolution of histone mRNA 3' end processing. *RNA* *14*, 1–10.
- Decourty, L., Saveanu, C., Zemam, K., Hantraye, F., Frachon, E., Rousselle, J.-C., Fromont-Racine, M., and Jacquier, A. (2008). Linking functionally related genes by sensitive and quantitative characterization of genetic interaction profiles. *Proc. Natl. Acad. Sci.* *105*, 5821–5826.
- Doma, M.K., and Parker, R. (2006). Endonucleolytic cleavage of eukaryotic mRNAs with stalls in translation elongation. *Nature* *440*, 561–564.
- D’Orazio, K.N., Wu, C.C.-C., Sinha, N., Loll-Krippelber, R., Brown, G.W., and Green, R. (2019). The endonuclease Cue2 cleaves mRNAs at stalled ribosomes during No Go Decay. *ELife* *8*, e49117.
- Dostie, J., Ferraiuolo, M., Pause, A., Adam, S.A., and Sonenberg, N. (2000). A novel shuttling protein, 4E-T, mediates the nuclear import of the mRNA 5' cap-binding protein, eIF4E. *EMBO J.* *19*, 3142–3156.
- Dowling, R.J.O., Topisirovic, I., Alain, T., Bidinosti, M., Fonseca, B.D., Petroulakis, E., Wang, X., Larsson, O., Selvaraj, A., Liu, Y., et al. (2010). mTORC1-Mediated Cell Proliferation, But Not Cell Growth, Controlled by the 4E-BPs. *Science* *328*, 1172–1176.
- Dziembowski, A., Lorentzen, E., Conti, E., and Séraphin, B. (2007). A single subunit, Dis3, is essentially responsible for yeast exosome core activity. *Nat. Struct. Mol. Biol.* *14*, 15–22.
- Eberle, A.B., Lykke-Andersen, S., Mühlemann, O., and Jensen, T.H. (2009). SMG6 promotes endonucleolytic cleavage of nonsense mRNA in human cells. *Nat. Struct. Mol. Biol.* *16*, 49–55.
- Eichhorn, S.W., Guo, H., McGeary, S.E., Rodriguez-Mias, R.A., Shin, C., Baek, D., Hsu, S., Ghoshal, K., Villén, J., and Bartel, D.P. (2014). mRNA Destabilization Is the Dominant Effect of Mammalian MicroRNAs by the Time Substantial Repression Ensues. *Mol. Cell* *56*, 104–115.
- Eichhorn, S.W., Subtelny, A.O., Kronja, I., Kwasnieski, J.C., Orr-Weaver, T.L., and Bartel, D.P. (2016). mRNA poly(A)-tail changes specified by deadenylation broadly reshape translation in *Drosophila* oocytes and early embryos. *ELife* *5*, e16955.
- Eisen, T.J., Eichhorn, S.W., Subtelny, A.O., Lin, K.S., McGeary, S.E., Gupta, S., and Bartel, D.P. (2020a). The Dynamics of Cytoplasmic mRNA Metabolism. *Mol. Cell* S1097276519308962.
- Eisen, T.J., Eichhorn, S.W., Subtelny, A.O., and Bartel, D.P. (2020b). MicroRNAs Cause Accelerated Decay of Short-Tailed Target mRNAs. *Mol. Cell* S1097276519308950.
- Ernault-Lange, M., Baconnais, S., Harper, M., Minshall, N., Souquere, S., Boudier, T., Bénard, M., Andrey, P., Pierron, G., Kress, M., et al. (2012). Multiple binding of repressed mRNAs by the P-body protein Rck/p54. *RNA N. Y. N* *18*, 1702–1715.
- Etten, J.V., Schagat, T.L., Hrit, J., Weidmann, C.A., Brumbaugh, J., Coon, J.J., and Goldstrohm, A.C. (2012). Human Pumilio Proteins Recruit Multiple Deadenylation Factors to Efficiently Repress Messenger RNAs. *J. Biol. Chem.* *287*, 36370–36383.
- Eulalio, A., Behm-Ansmant, I., Schweizer, D., and Izaurralde, E. (2007). P-Body Formation Is a Consequence, Not the Cause, of RNA-Mediated Gene Silencing. *Mol. Cell. Biol.* *27*, 3970–3981.

- Fabian, M.R., and Sonenberg, N. (2012). The mechanics of miRNA-mediated gene silencing: a look under the hood of miRISC. *Nat. Struct. Mol. Biol.* *19*, 586–593.
- Fabian, M.R., Cieplak, M.K., Frank, F., Morita, M., Green, J., Srikumar, T., Nagar, B., Yamamoto, T., Raught, B., Duchaine, T.F., et al. (2011). miRNA-mediated deadenylation is orchestrated by GW182 through two conserved motifs that interact with CCR4–NOT. *Nat. Struct. Mol. Biol.* *18*, 1211–1217.
- Fabian, M.R., Frank, F., Rouya, C., Siddiqui, N., Lai, W.S., Karetnikov, A., Blackshear, P.J., Nagar, B., and Sonenberg, N. (2013). Structural basis for the recruitment of the human CCR4–NOT deadenylase complex by tristetraprolin. *Nat. Struct. Mol. Biol.* *20*, 735–739.
- Ferraiuolo, M.A., Basak, S., Dostie, J., Murray, E.L., Schoenberg, D.R., and Sonenberg, N. (2005). A role for the eIF4E-binding protein 4E-T in P-body formation and mRNA decay. *J. Cell Biol.* *170*, 913–924.
- Fox, C.A., Sheet, M.D., and Wickens, M.P. (1989). Poly(A) addition during maturation of frog oocytes: distinct nuclear and cytoplasmic activities and regulation by tile sequence UUUUUAU. *Genes Dev.* *3*, 2151–2162.
- Fromm, S.A., Truffault, V., Kamenz, J., Braun, J.E., Hoffmann, N.A., Izaurrealde, E., and Sprangers, R. (2012). The structural basis of Edc3- and Scd6-mediated activation of the Dcp1:Dcp2 mRNA decapping complex: Structure of the Edc3-Dcp2 complex. *EMBO J.* *31*, 279–290.
- Garneau, N.L., Wilusz, J., and Wilusz, C.J. (2007). The highways and byways of mRNA decay. *Nat. Rev. Mol. Cell Biol.* *8*, 113–126.
- Gingras, A.-C., Gygi, S.P., Raught, B., Polakiewicz, R.D., Abraham, R.T., Hoekstra, M.F., Aebersold, R., and Sonenberg, N. (1999). Regulation of 4E-BP1 phosphorylation: a novel two-step mechanism. *Genes Dev.* *13*, 1422–1437.
- Groisman, I., Jung, M.-Y., Sarkissian, M., Cao, Q., and Richter, J.D. (2002). Translational Control of the Embryonic Cell Cycle. *Cell* *109*, 473–483.
- Haghighat, A., Mader, S., Pause, A., and Sonenberg, N. (1995). Repression of cap-dependent translation by 4E-binding protein 1: competition with p220 for binding to eukaryotic initiation factor-4E. *EMBO J.* *14*, 5701–5709.
- Hanet, A., Räsch, F., Weber, R., Ruscica, V., Fauser, M., Raisch, T., Kuzuoğlu-Öztürk, D., Chang, C.-T., Bhandari, D., Igreja, C., et al. (2019). HELZ directly interacts with CCR4–NOT and causes decay of bound mRNAs. *Life Sci. Alliance* *2*.
- Hasgall, P.A., Hoogewijs, D., Faza, M.B., Panse, V.G., Wenger, R.H., and Camenisch, G. (2011). The Putative RNA Helicase HELZ Promotes Cell Proliferation, Translation Initiation and Ribosomal Protein S6 Phosphorylation. *PLOS ONE* *6*, e22107.
- Hein, M.Y., Hubner, N.C., Poser, I., Cox, J., Nagaraj, N., Toyoda, Y., Gak, I.A., Weisswange, I., Mansfeld, J., Buchholz, F., et al. (2015). A Human Interactome in Three Quantitative Dimensions Organized by Stoichiometries and Abundances. *Cell* *163*, 712–723.
- Hoof, A. van, Frischmeyer, P.A., Dietz, H.C., and Parker, R. (2002). Exosome-Mediated Recognition and Degradation of mRNAs Lacking a Termination Codon. *Science* *295*, 2262–2264.
- Huarte, J., Stutz, A., O’Connell, M.L., Gubler, P., Belin, D., Darrow, A.L., Strickland, S., and Vassalli, J.-D. (1992). Transient translational silencing by reversible mRNA deadenylation. *Cell* *69*, 1021–1030.

- Hubstenberger, A., Courel, M., Bénard, M., Souquere, S., Ernoult-Lange, M., Chouaib, R., Yi, Z., Morlot, J.-B., Munier, A., Fradet, M., et al. (2017). P-Body Purification Reveals the Condensation of Repressed mRNA Regulons. *Mol. Cell* 68, 144-157.e5.
- Huntzinger, E., Kashima, I., Fauser, M., Sauliere, J., and Izaurralde, E. (2008). SMG6 is the catalytic endonuclease that cleaves mRNAs containing nonsense codons in metazoan. *RNA* 14, 2609–2617.
- Igreja, C., and Izaurralde, E. (2011). CUP promotes deadenylation and inhibits decapping of mRNA targets. *Genes Dev.* 25, 1955–1967.
- Igreja, C., Peter, D., Weiler, C., and Izaurralde, E. (2014). 4E-BPs require non-canonical 4E-binding motifs and a lateral surface of eIF4E to repress translation. *Nat. Commun.* 5, 4790.
- Izaurralde, E. (2015). Breakers and blockers--miRNAs at work. *Science* 349, 380–382.
- Jackson, R.J., Hellen, C.U.T., and Pestova, T.V. (2010). The mechanism of eukaryotic translation initiation and principles of its regulation. *Nat. Rev. Mol. Cell Biol.* 11, 113–127.
- Jafarnejad, S.M., Chapat, C., Matta-Camacho, E., Gelbart, I.A., Hesketh, G.G., Arguello, M., Garzia, A., Kim, S.-H., Attig, J., Shapiro, M., et al. (2018). Translational control of ERK signaling through miRNA/4EHP-directed silencing. *ELife* 7, e35034.
- Jonas, S., and Izaurralde, E. (2013). The role of disordered protein regions in the assembly of decapping complexes and RNP granules. *Genes Dev.* 27, 2628–2641.
- Joshi, B., Cameron, A., and Jagus, R. (2004). Characterization of mammalian eIF4E-family members. *Eur. J. Biochem.* 271, 2189–2203.
- Jung, M.-Y., Lorenz, L., and Richter, J.D. (2006). Translational Control by Neuroguidin, a Eukaryotic Initiation Factor 4E and CPEB Binding Protein. *Mol. Cell. Biol.* 26, 4277–4287.
- Kamenska, A., Lu, W.-T., Kubacka, D., Broomhead, H., Minshall, N., Bushell, M., and Standart, N. (2014a). Human 4E-T represses translation of bound mRNAs and enhances microRNA-mediated silencing. *Nucleic Acids Res.* 42, 3298–3313.
- Kamenska, A., Simpson, C., and Standart, N. (2014b). eIF4E-binding proteins: new factors, new locations, new roles. *Biochem. Soc. Trans.* 42, 1238–1245.
- Kamenska, A., Simpson, C., Vindry, C., Broomhead, H., Bénard, M., Ernoult-Lange, M., Lee, B.P., Harries, L.W., Weil, D., and Standart, N. (2016). The DDX6–4E-T interaction mediates translational repression and P-body assembly. *Nucleic Acids Res.* 44, 6318–6334.
- Kasipillai, T., MacArthur, D.G., Kirby, A., Thomas, B., Lambalk, C.B., Daly, M.J., and Welt, C.K. (2013). Mutations in *eIF4ENIF1* Are Associated With Primary Ovarian Insufficiency. *J. Clin. Endocrinol. Metab.* 98, E1534–E1539.
- Kedersha, N., Stoecklin, G., Ayodele, M., Yacono, P., Lykke-Andersen, J., Fritzler, M.J., Scheuner, D., Kaufman, R.J., Golan, D.E., and Anderson, P. (2005). Stress granules and processing bodies are dynamically linked sites of mRNP remodeling. *J. Cell Biol.* 169, 871–884.
- Keskeny, C., Raisch, T., Sgromo, A., Igreja, C., Bhandari, D., Weichenrieder, O., and Izaurralde, E. (2019). A conserved CAF40-binding motif in metazoan NOT4 mediates association with the CCR4–NOT complex. *Genes Dev.* 33, 236–252.

- Keyes, L.N., and Spradling, A.C. (1997). The *Drosophila* gene *fs(2)cup* interacts with *otu* to define a cytoplasmic pathway required for the structure and function of germ-line chromosomes. *Dev. Camb. Engl.* *124*, 1419–1431.
- Klauer, A.A., and van Hoof, A. (2012). Degradation of mRNAs that lack a stop codon: a decade of nonstop progress: Degradation of mRNAs that lack a stop codon. *Wiley Interdiscip. Rev. RNA* *3*, 649–660.
- Kozak, M. (1992). Regulation of Translation in Eukaryotic Systems. *Annu. Rev. Cell Biol.* *8*, 197–225.
- Kuzuoğlu-Öztürk, D., Bhandari, D., Huntzinger, E., Fauser, M., Helms, S., and Izaurralde, E. (2016). miRISC and the CCR4–NOT complex silence mRNA targets independently of 43S ribosomal scanning. *EMBO J.* *35*, 1186–1203.
- LaMarre, J., Gingerich, T.J., Feige, J.-J., and LaMarre, J. (2004). AU-rich elements and the control of gene expression through regulated mRNA stability. *Anim. Health Res. Rev.* *5*, 49–63.
- Laplante, M., and Sabatini, D.M. (2012). mTOR Signaling in Growth Control and Disease. *Cell* *149*, 274–293.
- Lau, N.-C., Kolkman, A., van Schaik, F.M.A., Mulder, K.W., Pijnappel, W.W.M.P., Heck, A.J.R., and Timmers, H.Th.M. (2009). Human Ccr4–Not complexes contain variable deadenylase subunits. *Biochem. J.* *422*, 443–453.
- Lazzaretti, D., Tournier, I., and Izaurralde, E. (2009). The C-terminal domains of human TNRC6A, TNRC6B, and TNRC6C silence bound transcripts independently of Argonaute proteins. *RNA* *15*, 1059–1066.
- Lim, J., Kim, D., Lee, Y., Ha, M., Lee, M., Yeo, J., Chang, H., Song, J., Ahn, K., and Kim, V.N. (2018). Mixed tailing by TENT4A and TENT4B shields mRNA from rapid deadenylation. *Science* *361*, 701–704.
- Loh, B., Jonas, S., and Izaurralde, E. (2013). The SMG5-SMG7 heterodimer directly recruits the CCR4-NOT deadenylase complex to mRNAs containing nonsense codons via interaction with POP2. *Genes Dev.* *27*, 2125–2138.
- Lubas, M., Damgaard, C.K., Tomecki, R., Cysewski, D., Jensen, T.H., and Dziembowski, A. (2013). Exonuclease hDIS3L2 specifies an exosome-independent 3'-5' degradation pathway of human cytoplasmic mRNA. *EMBO J.* *32*, 1855–1868.
- Luo, Y., Na, Z., and Slavoff, S.A. (2018). P-Bodies: Composition, Properties, and Functions. *Biochemistry* *57*, 2424–2431.
- Ma, X.M., and Blenis, J. (2009). Molecular mechanisms of mTOR-mediated translational control. *Nat. Rev. Mol. Cell Biol.* *10*, 307–318.
- Malecki, M., Viegas, S.C., Carneiro, T., Golik, P., Dressaire, C., Ferreira, M.G., and Arraiano, C.M. (2013). The exoribonuclease Dis3L2 defines a novel eukaryotic RNA degradation pathway. *EMBO J.* *32*, 1842–1854.
- Mandel, C.R., Bai, Y., and Tong, L. (2008). Protein factors in pre-mRNA 3'-end processing. *Cell. Mol. Life Sci.* *65*, 1099–1122.
- Maquat, L.E., and Li, X. (2001). Mammalian heat shock p70 and histone H4 transcripts, which derive from naturally intronless genes, are immune to nonsense-mediated decay. *RNA* *7*, 445–456.

- Maquat, L.E., Tarn, W.-Y., and Isken, O. (2010). The Pioneer Round of Translation: Features and Functions. *Cell* 142, 368–374.
- Marnef, A., Weil, D., and Standart, N. (2012). RNA-related nuclear functions of human Pat1b, the P-body mRNA decay factor. *Mol. Biol. Cell* 23, 213–224.
- Martineau, Y., Azar, R., Bousquet, C., and Pyronnet, S. (2013). Anti-oncogenic potential of the eIF4E-binding proteins. *Oncogene* 32, 671–677.
- Mathys, H., Basquin, J., Ozgur, S., Czarnocki-Cieciura, M., Bonneau, F., Aartse, A., Dziembowski, A., Nowotny, M., Conti, E., and Filipowicz, W. (2014). Structural and Biochemical Insights to the Role of the CCR4-NOT Complex and DDX6 ATPase in MicroRNA Repression. *Mol. Cell* 54, 751–765.
- Matsumoto, K., Nakayama, H., Yoshimura, M., Masuda, A., Dohmae, N., Matsumoto, S., and Tsujimoto, M. (2012). PRMT1 is required for RAP55 to localize to processing bodies. *RNA Biol.* 9, 610–623.
- Mendez, R., and Richter, J.D. (2001). Translational control by CPEB: a means to the end. *Nat. Rev. Mol. Cell Biol.* 2, 521–529.
- Miller, J.E., and Reese, J.C. (2012). Ccr4-Not complex: the control freak of eukaryotic cells. *Crit. Rev. Biochem. Mol. Biol.* 47, 315–333.
- Minshall, N., Reiter, M.H., Weil, D., and Standart, N. (2007). CPEB Interacts with an Ovary-specific eIF4E and 4E-T in Early *Xenopus* Oocytes. *J. Biol. Chem.* 282, 37389–37401.
- Morita, M., Ler, L.W., Fabian, M.R., Siddiqui, N., Mullin, M., Henderson, V.C., Alain, T., Fonseca, B.D., Karashchuk, G., Bennett, C.F., et al. (2012). A Novel 4EHP-GIGYF2 Translational Repressor Complex Is Essential for Mammalian Development. *Mol. Cell Biol.* 32, 3585–3593.
- Munroe, D., and Jacobson, A. (1990). Tales of poly(A): a review. *Gene* 91, 151–158.
- Nakahata, S., Katsu, Y., Mita, K., Inoue, K., Nagahama, Y., and Yamashita, M. (2001). Biochemical Identification of *Xenopus* Pumilio as a Sequence-specific Cyclin B1 mRNA-binding Protein That Physically Interacts with a Nanos Homolog, Xcat-2, and a Cytoplasmic Polyadenylation Element-binding Protein. *J. Biol. Chem.* 276, 20945–20953.
- Nakamura, A., Sato, K., and Hanyu-Nakamura, K. (2004). *Drosophila* Cup Is an eIF4E Binding Protein that Associates with Bruno and Regulates oskar mRNA Translation in Oogenesis. *Dev. Cell* 6, 69–78.
- Nelson, M.R., Leidal, A.M., and Smibert, C.A. (2004). *Drosophila* Cup is an eIF4E-binding protein that functions in Smaug-mediated translational repression. *EMBO J.* 23, 150–159.
- Niinuma, S., Fukaya, T., and Tomari, Y. (2016). CCR4 and CAF1 deadenylases have an intrinsic activity to remove the post-poly(A) sequence. *RNA* 22, 1550–1559.
- Nishimura, T., Padamsi, Z., Fakim, H., Milette, S., Dunham, W.H., Gingras, A.-C., and Fabian, M.R. (2015). The eIF4E-Binding Protein 4E-T Is a Component of the mRNA Decay Machinery that Bridges the 5' and 3' Termini of Target mRNAs. *Cell Rep.* 11, 1425–1436.
- Nissan, T., Rajyaguru, P., She, M., Song, H., and Parker, R. (2010). Decapping Activators in *Saccharomyces cerevisiae* Act by Multiple Mechanisms. *Mol. Cell* 39, 773–783.

- Ozgur, S., Chekulaeva, M., and Stoecklin, G. (2010). Human Pat1b Connects Deadenylation with mRNA Decapping and Controls the Assembly of Processing Bodies. *Mol. Cell Biol.* *30*, 4308–4323.
- Ozgur, S., Basquin, J., Kamenska, A., Filipowicz, W., Standart, N., and Conti, E. (2015). Structure of a Human 4E-T/DDX6/CNOT1 Complex Reveals the Different Interplay of DDX6-Binding Proteins with the CCR4-NOT Complex. *Cell Rep.* *13*, 703–711.
- Padmanabhan, K., and Richter, J.D. (2006). Regulated Pumilio-2 binding controls RINGO/Spy mRNA translation and CPEB activation. *Genes Dev.* *20*, 199–209.
- Park, J.-E., Yi, H., Kim, Y., Chang, H., and Kim, V.N. (2016). Regulation of Poly(A) Tail and Translation during the Somatic Cell Cycle. *Mol. Cell* *62*, 462–471.
- Peng, S.S.-Y. (1998). RNA stabilization by the AU-rich element binding protein, HuR, an ELAV protein. *EMBO J.* *17*, 3461–3470.
- Peter, D., Weber, R., Köne, C., Chung, M.-Y., Ebertsch, L., Truffault, V., Weichenrieder, O., Igreja, C., and Izaurralde, E. (2015a). Mex1 proteins use both canonical bipartite and novel tripartite binding modes to form eIF4E complexes that display differential sensitivity to 4E-BP regulation. *Genes Dev.* *29*, 1835–1849.
- Peter, D., Igreja, C., Weber, R., Wohlbold, L., Weiler, C., Ebertsch, L., Weichenrieder, O., and Izaurralde, E. (2015b). Molecular Architecture of 4E-BP Translational Inhibitors Bound to eIF4E. *Mol. Cell* *57*, 1074–1087.
- Peter, D., Weber, R., Sandmeir, F., Wohlbold, L., Helms, S., Bawankar, P., Valkov, E., Igreja, C., and Izaurralde, E. (2017). GIGYF1/2 proteins use auxiliary sequences to selectively bind to 4EHP and repress target mRNA expression. *Genes Dev.* *31*, 1147–1161.
- Peter, D., Ruscica, V., Bawankar, P., Weber, R., Helms, S., Valkov, E., Igreja, C., and Izaurralde, E. (2019). Molecular basis for GIGYF–Me31B complex assembly in 4EHP-mediated translational repression. *Genes Dev.*
- Pfender, S., Kuznetsov, V., Pasternak, M., Tischer, T., Santhanam, B., and Schuh, M. (2015). Live imaging RNAi screen reveals genes essential for meiosis in mammalian oocytes. *Nature* *524*, 239–242.
- Piccioni, F., Zappavigna, V., and Verrotti, A.C. (2005). Translational regulation during oogenesis and early development: The cap-poly(A) tail relationship. *C. R. Biol.* *328*, 863–881.
- Poon, M.M., Choi, S.-H., Jamieson, C.A.M., Geschwind, D.H., and Martin, K.C. (2006). Identification of Process-Localized mRNAs from Cultured Rodent Hippocampal Neurons. *J. Neurosci.* *10*.
- Presnyak, V., and Collier, J. (2013). The DHH1/RCKp54 family of helicases: An ancient family of proteins that promote translational silencing. *Biochim. Biophys. Acta BBA - Gene Regul. Mech.* *1829*, 817–823.
- Raisch, T., Bhandari, D., Sabath, K., Helms, S., Valkov, E., Weichenrieder, O., and Izaurralde, E. (2016). Distinct modes of recruitment of the CCR4–NOT complex by *Drosophila* and vertebrate Nanos. *EMBO J.* *35*, 974–990.
- Raisch, T., Chang, C.-T., Leviansky, Y., Muthukumar, S., Raunser, S., and Valkov, E. (2019). Reconstitution of recombinant human CCR4-NOT reveals molecular insights into regulated deadenylation. *Nat. Commun.* *10*, 1–14.
- Rajyaguru, P., She, M., and Parker, R. (2012). Scd6 Targets eIF4G to Repress Translation: RGG Motif Proteins as a Class of eIF4G-Binding Proteins. *Mol. Cell* *45*, 244–254.

- Rambout, X., Detiffe, C., Bruyr, J., Mariavelle, E., Cherkaoui, M., Brohée, S., Demoitie, P., Lebrun, M., Soin, R., Lesage, B., et al. (2016). The transcription factor ERG recruits CCR4–NOT to control mRNA decay and mitotic progression. *Nat. Struct. Mol. Biol.* *23*, 663–672.
- Ray, S., Catnaigh, P.Ó., and Anderson, E.C. (2015). Post-transcriptional regulation of gene expression by Unr. *Biochem. Soc. Trans.* *43*, 323–327.
- Rehwinkel, J. (2005). A crucial role for GW182 and the DCP1:DCP2 decapping complex in miRNA-mediated gene silencing. *RNA* *11*, 1640–1647.
- Richter, J.D. (1999). Cytoplasmic Polyadenylation in Development and Beyond. *MICROBIOL MOL BIOL REV* *63*, 11.
- Rissland, O.S. (2017). The organization and regulation of mRNA-protein complexes: mRNP organization and regulation. *Wiley Interdiscip. Rev. RNA* *8*, e1369.
- Rissland, O.S., and Norbury, C.J. (2009). Decapping is preceded by 3' uridylation in a novel pathway of bulk mRNA turnover. *Nat. Struct. Mol. Biol.* *16*, 616–623.
- Rom, E., Kim, H.C., Gingras, A.-C., Marcotrigiano, J., Favre, D., Olsen, H., Burley, S.K., and Sonenberg, N. (1998). Cloning and Characterization of 4EHP, a Novel Mammalian eIF4E-related Cap-binding Protein. *J. Biol. Chem.* *273*, 13104–13109.
- Rouya, C., Siddiqui, N., Morita, M., Duchaine, T.F., Fabian, M.R., and Sonenberg, N. (2014). Human DDX6 effects miRNA-mediated gene silencing via direct binding to CNOT1. *RNA* *20*, 1398–1409.
- Ruscica, V., Bawankar, P., Peter, D., Helms, S., Igreja, C., and Izaurralde, E. (2019). Direct role for the Drosophila GIGYF protein in 4EHP-mediated mRNA repression. *Nucleic Acids Res.* *47*, 7035–7048.
- Sahoo, P.K., Smith, D.S., Perrone-Bizzozero, N., and Twiss, J.L. (2018). Axonal mRNA transport and translation at a glance. *J. Cell Sci.* *8*.
- Schaeffer, D., and van Hoof, A. (2011). Different nuclease requirements for exosome-mediated degradation of normal and nonstop mRNAs. *Proc. Natl. Acad. Sci.* *108*, 2366–2371.
- Schäfer, I.B., Yamashita, M., Schuller, J.M., Schüssler, S., Reichelt, P., Strauss, M., and Conti, E. (2019). Molecular Basis for poly(A) RNP Architecture and Recognition by the Pan2-Pan3 Deadenylation. *Cell* *177*, 1619-1631.e21.
- Schmid, M., and Jensen, T.H. (2008). The exosome: a multipurpose RNA-decay machine. *Trends Biochem. Sci.* *33*, 501–510.
- Schoenberg, D.R., and Maquat, L.E. (2012). Regulation of cytoplasmic mRNA decay. *Nat. Rev. Genet.* *13*, 246–259.
- Schuller, A.P., and Green, R. (2018). Roadblocks and resolutions in eukaryotic translation. *Nat. Rev. Mol. Cell Biol.* *19*, 526–541.
- Sement, F.M., Ferrier, E., Zuber, H., Merret, R., Alioua, M., Deragon, J.-M., Bousquet-Antonelli, C., Lange, H., and Gagliardi, D. (2013). Uridylation prevents 3' trimming of oligoadenylated mRNAs. *Nucleic Acids Res.* *41*, 7115–7127.
- Semotok, J.L., Cooperstock, R.L., Pinder, B.D., Vari, H.K., Lipshitz, H.D., and Smibert, C.A. (2005). Smaug Recruits the CCR4/POP2/NOT Deadenylation Complex to Trigger Maternal Transcript Localization in the Early Drosophila Embryo. *Curr. Biol.* *15*, 284–294.

- Sengupta, M.S., Low, W.Y., Patterson, J.R., Kim, H.-M., Traven, A., Beilharz, T.H., Colaiacovo, M.P., Schisa, J.A., and Boag, P.R. (2013). ifet-1 is a broad-scale translational repressor required for normal P granule formation in *C. elegans*. *J. Cell Sci.* *126*, 850–859.
- Sgromo, A., Raisch, T., Bawankar, P., Bhandari, D., Chen, Y., Kuzuoğlu-Öztürk, D., Weichenrieder, O., and Izaurralde, E. (2017). A CAF40-binding motif facilitates recruitment of the CCR4-NOT complex to mRNAs targeted by *Drosophila* Roquin. *Nat. Commun.* *8*, 14307.
- Sgromo, A., Raisch, T., Backhaus, C., Keskeny, C., Alva, V., Weichenrieder, O., and Izaurralde, E. (2018). *Drosophila* Bag-of-marbles directly interacts with the CAF40 subunit of the CCR4–NOT complex to elicit repression of mRNA targets. *RNA* *24*, 381–395.
- Sharif, H., Ozgur, S., Sharma, K., Basquin, C., Urlaub, H., and Conti, E. (2013). Structural analysis of the yeast Dhh1–Pat1 complex reveals how Dhh1 engages Pat1, Edc3 and RNA in mutually exclusive interactions. *Nucleic Acids Res.* *41*, 8377–8390.
- Sheth, U. (2003). Decapping and Decay of Messenger RNA Occur in Cytoplasmic Processing Bodies. *Science* *300*, 805–808.
- Shoemaker, C.J., and Green, R. (2012). Translation drives mRNA quality control. *Nat. Struct. Mol. Biol.* *19*, 594–601.
- Sonenberg, N., and Hinnebusch, A.G. (2009). Regulation of Translation Initiation in Eukaryotes: Mechanisms and Biological Targets. *Cell* *136*, 731–745.
- Standart, N., and Weil, D. (2018). P-Bodies: Cytosolic Droplets for Coordinated mRNA Storage. *Trends Genet.* *34*, 612–626.
- Steiger, M., Carr-Schmid, A., Schwartz, D.C., Kiledjian, M., and Parker, R. (2003). Analysis of recombinant yeast decapping enzyme. *RNA N. Y. N* *9*, 231–238.
- Stoeckle, M.Y., and Guan, L. (1993). High-resolution analysis of gro α mRNA poly(A) shortening: regulation by interleukin-1 β . *Nucleic Acids Res.* *21*, 1613–1617.
- Stutz, F., and Izaurralde, E. (2003). The interplay of nuclear mRNP assembly, mRNA surveillance and export. *Trends Cell Biol.* *13*, 319–327.
- Subtelny, A.O., Eichhorn, S.W., Chen, G.R., Sive, H., and Bartel, D.P. (2014). Poly(A)-tail profiling reveals an embryonic switch in translational control. *Nature* *508*, 66–71.
- Tang, T.T.L., Stowell, J.A.W., Hill, C.H., and Passmore, L.A. (2019). The intrinsic structure of poly(A) RNA determines the specificity of Pan2 and Caf1 deadenylases. *Nat. Struct. Mol. Biol.* *26*, 433–442.
- Tharun, S., and Parker, R. Targeting an mRNA for Decapping: Displacement of Translation Factors and Association of the Lsm1p–7p Complex on Deadenylated Yeast mRNAs. *Mol. Cell* *9*.
- Treisman, R. (1985). Transient accumulation of c-fos RNA following serum stimulation requires a conserved 5' element and c-fos 3' sequences. *Cell* *42*, 889–902.
- Tritschler, F., Braun, J.E., Eulalio, A., Truffault, V., Izaurralde, E., and Weichenrieder, O. (2009). Structural Basis for the Mutually Exclusive Anchoring of P Body Components EDC3 and Tral to the DEAD Box Protein DDX6/Me31B. *Mol. Cell* *33*, 661–668.
- Udagawa, T., Swanger, S.A., Takeuchi, K., Kim, J.H., Nalavadi, V., Shin, J., Lorenz, L.J., Zukin, R.S., Bassell, G.J., and Richter, J.D. (2012). Bidirectional Control of mRNA

- Translation and Synaptic Plasticity by the Cytoplasmic Polyadenylation Complex. *Mol. Cell* 47, 253–266.
- Valkov, E., Muthukumar, S., Chang, C.-T., Jonas, S., Weichenrieder, O., and Izaurralde, E. (2016). Structure of the Dcp2–Dcp1 mRNA-decapping complex in the activated conformation. *Nat. Struct. Mol. Biol.* 23, 574–579.
- Varani, G. (1997). A cap for all occasions. *Structure* 5, 855–858.
- Verrotti, A.C., Thompson, S.R., Wreden, C., Strickland, S., and Wickens, M. (1996). Evolutionary conservation of sequence elements controlling cytoplasmic polyadenylation. *Proc. Natl. Acad. Sci.* 93, 9027–9032.
- Villaescusa, J.C., Allard, P., Carminati, E., Kontogiannea, M., Talarico, D., Blasi, F., Farookhi, R., and Verrotti, A.C. (2006). Clast4, the murine homologue of human eIF4E-Transporter, is highly expressed in developing oocytes and post-translationally modified at meiotic maturation. *Gene* 367, 101–109.
- Vindry, C., Marnef, A., Broomhead, H., Twyffels, L., Ozgur, S., Stoecklin, G., Llorian, M., Smith, C.W., Mata, J., Weil, D., et al. (2017). Dual RNA Processing Roles of Pat1b via Cytoplasmic Lsm1-7 and Nuclear Lsm2-8 Complexes. *Cell Rep.* 20, 1187–1200.
- Waghray, S., Williams, C., Coon, J.J., and Wickens, M. (2015). *Xenopus* CAF1 requires NOT1-mediated interaction with 4E-T to repress translation in vivo. *RNA* 21, 1335–1345.
- Wang, Z., Jiao, X., Carr-Schmid, A., and Kiledjian, M. (2002). The hDcp2 protein is a mammalian mRNA decapping enzyme. *Proc. Natl. Acad. Sci.* 99, 12663–12668.
- Weill, L., Belloc, E., Bava, F.-A., and Méndez, R. (2012). Translational control by changes in poly(A) tail length: recycling mRNAs. *Nat. Struct. Mol. Biol.* 19, 577–585.
- Wilbertz, J.H., Voigt, F., Horvathova, I., Roth, G., Zhan, Y., and Chao, J.A. (2019). Single-Molecule Imaging of mRNA Localization and Regulation during the Integrated Stress Response. *Mol. Cell* 73, 946-958.e7.
- Wu, X., and Brewer, G. (2012). The regulation of mRNA stability in mammalian cells: 2.0. *Gene* 500, 10–21.
- Wu, L., Wells, D., Tay, J., Mendis, D., Abbott, M.-A., Barnitt, A., Quinlan, E., Heynen, A., Fallon, J.R., and Richter, J.D. (1998). CPEB-Mediated Cytoplasmic Polyadenylation and the Regulation of Experience-Dependent Translation of α -CaMKII mRNA at Synapses. *Neuron* 11.
- Yamashita, A., Chang, T.-C., Yamashita, Y., Zhu, W., Zhong, Z., Chen, C.-Y.A., and Shyu, A.-B. (2005). Concerted action of poly(A) nucleases and decapping enzyme in mammalian mRNA turnover. *Nat. Struct. Mol. Biol.* 12, 1054–1063.
- Yang, W.-H. (2006). RNA-associated protein 55 (RAP55) localizes to mRNA processing bodies and stress granules. *RNA* 12, 547–554.
- Yang, G., Smibert, C.A., Kaplan, D.R., and Miller, F.D. (2014). An eIF4E1/4E-T Complex Determines the Genesis of Neurons from Precursors by Translationally Repressing a Proneurogenic Transcription Program. *Neuron* 84, 723–739.
- Zahr, S.K., Yang, G., Kazan, H., Borrett, M.J., Yuzwa, S.A., Voronova, A., Kaplan, D.R., and Miller, F.D. (2018). A Translational Repression Complex in Developing Mammalian Neural Stem Cells that Regulates Neuronal Specification. *Neuron* 97, 520-537.e6.

-
- Zhao, M., Feng, F., Chu, C., Yue, W., and Li, L. (2019). A novel EIF4ENIF1 mutation associated with a diminished ovarian reserve and premature ovarian insufficiency identified by whole-exome sequencing. *J. Ovarian Res.* *12*, 119.
- Zheng, D., Ezzeddine, N., Chen, C.-Y.A., Zhu, W., He, X., and Shyu, A.-B. (2008). Deadenylation is prerequisite for P-body formation and mRNA decay in mammalian cells. *J. Cell Biol.* *182*, 89–101.
- Zipprich, J.T., Bhattacharyya, S., Mathys, H., and Filipowicz, W. (2009). Importance of the C-terminal domain of the human GW182 protein TNRC6C for translational repression. *RNA* *15*, 781–793.

6 Original manuscripts discussed in this thesis

Attached are the original manuscripts of the following publications:

1. 4E-T-bound mRNAs are stored in a silenced and deadenylated form.

Felix Räscher, Ramona Weber, Elisa Izaurralde and Cátia Igreja (2020)

Genes and Development, 34 (11-12)

2. HELZ directly interacts with CCR4–NOT and causes decay of bound mRNAs.

Aoife Hanet, Felix Räscher, Ramona Weber, Vincenzo Ruscica, Maria Fauser, Tobias Raisch, Duygu Kuzuoğlu-Öztürk, Chung-Te Chang, Dipankar Bhandari, Cátia Igreja, Lara Wohlbold (2019)

Life Science Alliance, Volume 2 (5)

4E-T-bound mRNAs are stored in a silenced and deadenylated form

Felix Räsch, Ramona Weber, Elisa Izaurrealde,¹ and Cátia Igreja

Department of Biochemistry, Max Planck Institute for Developmental Biology, D-72076 Tübingen, Germany

Human 4E-T is an eIF4E-binding protein (4E-BP) present in processing (P)-bodies that represses translation and regulates decay of mRNAs destabilized by AU-rich elements and microRNAs (miRNAs). However, the underlying regulatory mechanisms are still unclear. Here, we show that upon mRNA binding 4E-T represses translation and promotes deadenylation via the recruitment of the CCR4–NOT deadenylase complex. The interaction with CCR4–NOT is mediated by previously uncharacterized sites in the middle region of 4E-T. Importantly, mRNA decapping and decay are inhibited by 4E-T and the deadenylated target is stored in a repressed form. Inhibition of mRNA decapping requires the interaction of 4E-T with the cap-binding proteins eIF4E/4EHP. We further show that regulation of decapping by 4E-T participates in mRNA repression by the miRNA effector protein TNRC6B and that 4E-T overexpression interferes with tristetraprolin (TTP)- and NOT1-mediated mRNA decay. Thus, we postulate that 4E-T modulates 5'-to-3' decay by swapping the fate of a deadenylated mRNA from complete degradation to storage. Our results provide insight into the mechanism of mRNA storage that controls localized translation and mRNA stability in P-bodies.

[*Keywords*: deadenylation; decapping; eIF4E-binding proteins; P-bodies]

Supplemental material is available for this article.

Received December 27, 2019; revised version accepted April 2, 2020.

Ribosome recruitment in eukaryotes requires the assembly of the eukaryotic initiation factor (eIF)4F complex at the 5' cap structure of the messenger (m)RNA (Topisirovic et al. 2011). This heterotrimeric complex is formed through the interaction of the scaffold eIF4G with the cap-binding protein eIF4E and the RNA helicase eIF4A. Together, these proteins trigger a series of events that result in the recruitment of the preinitiation complex, composed of the 40S ribosomal subunit and associated factors, and in the initiation of translation (Hashem and Frank 2018; Merrick and Pavitt 2018).

The function of eIF4F in translation initiation is tightly regulated by the eIF4E-binding proteins (4E-BPs). This group of translational repressors share with eIF4G canonical and noncanonical binding motifs that recognize a common surface on eIF4E (Peter et al. 2015; Grüner et al. 2016, 2018). Consequently, 4E-BPs compete with eIF4G for eIF4E binding, disrupting eIF4F assembly and blocking translation (Haghighat et al. 1995; Mader et al. 1995).

The eIF4E-transporter protein (4E-T), or eukaryotic translation initiation factor 4E nuclear import factor 1 (EIF4ENIF1), is a nucleocytoplasmic shuttling 4E-BP required for the localization of eIF4E to the nucleus (Dostie

et al. 2000). However, in cells, 4E-T is predominantly located to processing (P)-bodies (Andrei et al. 2005; Ferraiuolo et al. 2005). P-bodies are dynamic cytoplasmic granules that form by the phase separation of RNA decay-associated proteins bound to translationally inactive transcripts (Standart and Weil 2018; Ivanov et al. 2019). These granules are thought to buffer the proteome through translational control and storage of mRNAs coding for regulatory proteins (Hubstenberger et al. 2017; Standart and Weil 2018).

In P-bodies, 4E-T establishes multiple interactions with proteins involved in mRNA turnover. In addition to the cap-binding proteins eIF4E and eIF4E homologous protein (4EHP), known 4E-T-binding partners include the cold-shock domain protein upstream of N-Ras (UNR), the RNA-dependent ATPase DDX6, the decapping factors LSM14A and PatL1, and the CCR4–NOT deadenylase complex (Kubacka et al. 2013; Kamenska et al. 2014; Ozgur et al. 2015; Brandmann et al. 2018). Several of these interactions are thought to be essential for P-body formation and to contribute to the control of translation and turnover of adenine and uracil (AU)-rich mRNAs destabilized by tristetraprolin (TTP) or transcripts repressed by micro (mi)RNAs (Ferraiuolo et al. 2005; Kamenska et al. 2014, 2016; Nishimura et al. 2015; Chapat et al. 2017; Jafarnejad et al. 2018).

¹Deceased April 30, 2018.

Corresponding author: catia.igreja@tuebingen.mpg.de

Article published online ahead of print. Article and publication date are online at <http://www.genesdev.org/cgi/doi/10.1101/gad.336073.119>. Freely available online through the *Genes & Development* Open Access option.

© 2020 Räsch et al. This article, published in *Genes & Development*, is available under a Creative Commons License (Attribution-NonCommercial 4.0 International), as described at <http://creativecommons.org/licenses/by-nc/4.0/>.

In mammals, 4E-T is an important component of repressor complexes that regulate the expression of pro-neurogenic factors during neurogenesis (Yang et al. 2014; Amadei et al. 2015; Zahr et al. 2018). In addition, 4E-T is essential for meiosis in oocytes (Pfender et al. 2015), and mutations in the gene have been associated with female infertility (Kasippillai et al. 2013; Zhao et al. 2019). However, the mechanism by which 4E-T affects these developmental processes is unclear.

In this study, we examined the molecular effects of 4E-T in gene expression. Our work demonstrates that 4E-T coordinates deadenylation with the suppression of decapping to store mRNAs targeted by the CCR4–NOT complex in silenced messenger ribonucleoprotein particles (mRNPs).

Results

4E-T represses translation and promotes mRNA deadenylation

To study the mechanism by which 4E-T represses mRNA expression, we used a reporter assay in human cells. 4E-T fused to the bacteriophage MS2 coat protein and an HA (hemagglutinin) tag (MS2-HA-4E-T) was tethered to a *Renilla* (R-Luc) luciferase reporter containing six MS2-binding sites in the 3' untranslated region (UTR; R-Luc-6xMS2bs) (Supplemental Fig. S1A). A plasmid encoding firefly luciferase (F-Luc-GFP) served as a transfection and normalization control. In HEK293T cells, MS2-HA-4E-T strongly reduced R-Luc activity compared with MS2-HA-GFP (Supplemental Fig. S1B, protein, black bars), as observed previously (Ferraiuolo et al. 2005; Kubacka et al. 2013; Kamenska et al. 2014). The abundance of the R-Luc mRNA did not significantly vary in the presence of 4E-T, as determined by Northern blotting (Supplemental Fig. S1B, mRNA, blue bars and S1C and D), indicating that 4E-T represses translation in the absence of mRNA decay. Furthermore, in cells expressing MS2-HA-4E-T the R-Luc mRNA migrated faster, resembling the transcript lacking the poly(A) tail (Supplemental Fig. S1C, lane 2, A₀). Deadenylation, or removal of the poly(A) tail, by the multisubunit CCR4–NOT complex (acting often in combination with PAN2/3) is the first step in cytoplasmic mRNA turnover (Wahle and Winkler 2013). Importantly, 4E-T had no effect on the F-Luc-GFP control or an R-Luc reporter lacking the MS2 binding sites (Supplemental Fig. S1E–G).

We also tethered 4E-T to reporter mRNAs containing distinct coding sequences, F-Luc and β -GLOBIN (Fig. 1A; Supplemental Fig. S1H), or five BoxB elements in the 3' UTR (R-Luc-5xBoxB) (Supplemental Fig. S1K; Lykke-Andersen et al. 2000; Pillai et al. 2004). We observed that independently of the reporter mRNA 4E-T induced translational repression and deadenylation without major changes in transcript abundance (Fig. 1B–D; Supplemental Fig. S1I,J,L–N).

We then performed an oligo(dT)-targeted ribonuclease H (RNase H) cleavage assay to verify that the 4E-T-bound mRNAs are in fact deadenylated. In cells expressing MS2-

HA-GFP, the BGG-6xMS2bs and BGG-GAP (control lacking the MS2bs) transcripts migrated faster after poly(A) tail cleavage (Fig. 1E, lanes 2 vs. 1, A₀). In contrast, the 4E-T-bound BGG-6xMS2bs mRNA migrated like the deadenylated transcript before and after cleavage by RNase H (Fig. 1E, lanes 3,4). Moreover, in cells expressing MS2-HA-4E-T, the poly(A) tail of the control BGG-GAP mRNA was only removed after RNase H and oligo(dT) addition (Fig. 1E, lanes 4 vs. 3). Thus, we conclude that human 4E-T induces deadenylation of a bound mRNA.

4E-T-mediated mRNA deadenylation requires the CCR4–NOT complex

To determine whether the CCR4–NOT complex is involved in 4E-T-mediated mRNA deadenylation, we inhibited the deadenylase activity of the complex by overexpressing a catalytically inactive form of the NOT8 enzyme (NOT8*; D40A, E42A) in human cells. The mutant enzyme impedes CCR4–NOT-dependent mRNA deadenylation in a dominant-negative manner (Piao et al. 2010). The inactive NOT8, but not HA-MBP, blocked mRNA deadenylation targeted by 4E-T as the BGG-6xMS2bs reporter accumulated as a polyadenylated (A_n) mRNA (Fig. 1F [lanes 4 vs. 2], G,H). Our results show that mRNA deadenylation induced by 4E-T requires the CCR4–NOT complex.

4E-T blocks decapping of bound mRNA

In the 5'–3' mRNA degradation pathway, removal of the poly(A) tail is followed by decapping and ultimately 5'–3' exonucleolytic degradation by XRN1 (Franks and Lykke-Andersen 2008). The unusual accumulation of deadenylated mRNA in the presence of 4E-T could result from inhibition of decapping or, alternatively, inhibition of XRN1 activity after decapping. To investigate whether the deadenylated BGG-6xMS2bs mRNA was capped, we used the Terminator nuclease, a 5'–3' exonuclease that degrades uncapped monophosphorylated RNA (Braun et al. 2012). The Terminator nuclease did not degrade the BGG-6xMS2bs reporter bound to MS2-HA-GFP or MS2-HA-4E-T (Fig. 1I), nor the BGG-GAP mRNA, indicating that these are capped transcripts. In contrast, the uncapped 18S rRNA was fully degraded upon addition of the Terminator nuclease (Fig. 1I, lanes 2,4). Our data suggest that 4E-T protects the deadenylated target mRNA from degradation by blocking decapping.

4E-T-dependent mRNA repression is independent of UNR, DDX6, PatL1, and LSM14A

4E-T is a largely disordered protein with well-characterized short linear motifs (SLiMs) that mediate binding to DDX6, UNR, LSM14A, and PatL1 (Fig. 2A). To understand whether the interactions of 4E-T with these proteins are important to deadenylate and prevent decapping of a bound transcript, we made use of mutant proteins lacking each of the binding sites (Δ DDX6, Δ UNR, and Δ LSM14A) (Supplemental Table S1; Kamenska et al. 2014, 2016;

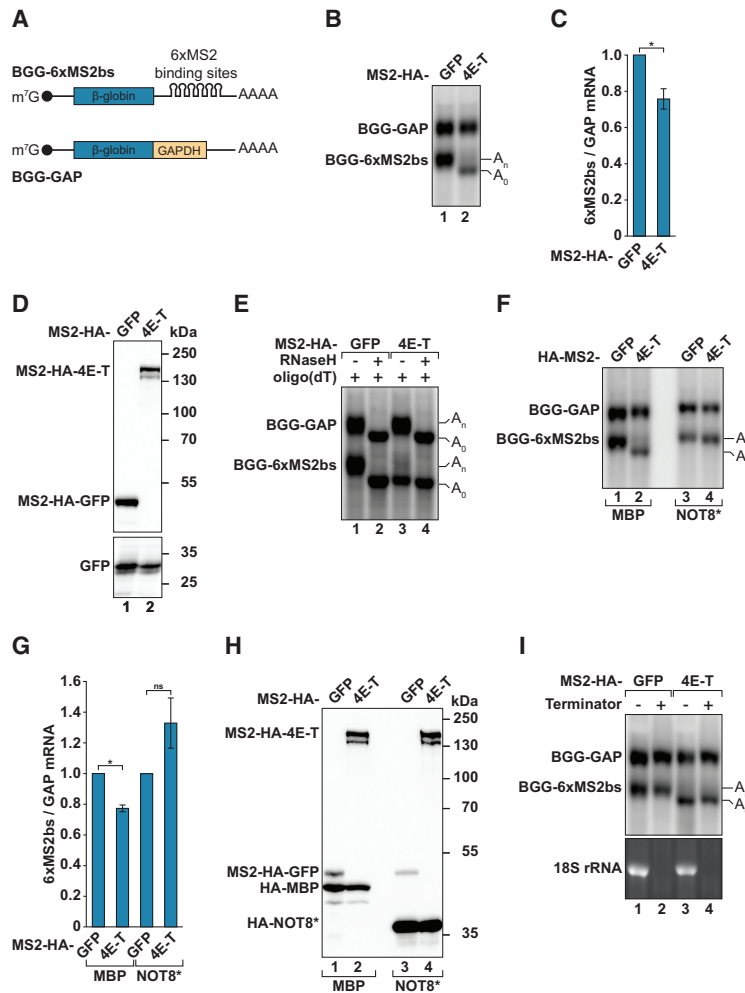


Figure 1. 4E-T promotes mRNA deadenylation and blocks decapping of a bound mRNA. (A) β -GLOBIN reporters used in this study. (BGG) β -GLOBIN. The BGG-GAP reporter contains a truncated version of the *GAPDH* (GAP) gene to distinguish it from the BGG-6xMS2bs reporter by size (Lykke-Andersen et al. 2000). The BGG-6xMS2bs reporter contains six MS2 binding sites in the 3' UTR. (B) Northern blot analysis of a tethering assay using the BGG-6xMS2bs reporter and MS2-HA-4E-T in HEK293T cells. A plasmid expressing BGG-GAP served as a transfection control and lacks the MS2-binding sites. The position of the deadenylated BGG-6xMS2bs reporter mRNA is marked with A₀, whereas the position of the reporter mRNA with an intact poly(A) is indicated as A_n. (C) BGG-6xMS2bs mRNA levels determined by Northern blotting were normalized to those of BGG-GAP and set to 1 in cells expressing MS2-HA-GFP. Mean values \pm standard deviation (SD) are shown ($n=3$). (* $P < 0.05$, paired t -test. (D) Western blot showing the expression levels of the tethered proteins. (E) RNA samples isolated from cells expressing MS2-HA-GFP or MS2-HA-4E-T, BGG-6xMS2bs and BGG-GAP were treated with oligo(dT)₁₅ in the presence (+) or absence (–) of RNase H and analyzed by Northern blot. Note that upon RNase H treatment the poly(A) tails of the BGG reporters are removed in the presence of oligo(dT). A₀, deadenylated and A_n, polyadenylated reporter mRNAs. (F–H) Tethering assay with the BGG-6xMS2bs, BGG-GAP and MS2-HA-GFP, or MS2-HA-4E-T performed in cells expressing HA-MBP or the catalytic inactive mutant of NOT8 (HA-NOT8*). In the Northern blot depicted in F, A₀ indicates the position of the deadenylated BGG-6xMS2bs mRNA while A_n indicates the position of the adenylated reporter mRNA. The graph in G depicts the relative quantification of the BGG-6xMS2bs mRNA levels, as described in B ($n=3$). (* $P < 0.05$; (ns) not significant, paired t -test. A representative Western blot showing the expression of all the proteins used in the assay is present in H. (I) RNA samples

isolated from cells expressing MS2-HA-GFP or MS2-HA-4E-T, the BGG-6xMS2bs and the BGG-GAP reporters were incubated with Terminator 5'-phosphate-dependent exonuclease and analyzed by Northern blotting. 18S ribosomal RNA (rRNA) served as uncapped RNA control. (A₀) Deadenylated reporter mRNAs; (A_n) polyadenylated reporter mRNAs.

Nishimura et al. 2015; Brandmann et al. 2018). The interaction of 4E-T with DDX6, UNR, and LSM14A was specifically abolished upon the deletion of the corresponding SLiMs, as assessed in pull-down assays following transient expression of the mutant proteins in human cells (Supplemental Fig. S2). In detail, deletion of the UNR binding site (Δ UNR, residues 131–161) prevented the interaction with UNR without affecting binding of 4E-T to eIF4E, DDX6, PatL1, and LSM14A (Supplemental Fig. S2A,B). Removal of the CUP homology domain (CHD, Δ DDX6, residues 219–240) only abrogated the association of 4E-T with DDX6 (Supplemental Fig. S2A,B). On the other hand, the interaction with LSM14A was strongly reduced upon the simultaneous deletion of two LSM14A binding sites present in 4E-T (residues 448–490 and 940–985, Δ LSM14A), whereas single deletion mutants (Δ 448–490 or 1–939) had decreased binding to LSM14A (Supplemental Fig. S2B,C). The Δ LSM14A 4E-T protein still copurified with UNR, DDX6, PatL1, and eIF4E (Supplemental Fig. S2A,B).

PatL1 has been shown to interact with the C-terminal region of 4E-T (Fig. 2A; Kamenska et al. 2014, 2016). To define more precisely the binding site of PatL1, we tested whether a region of 4E-T spanning amino acids 695–713 was required for the interaction. This region is conserved in 4E-T proteins and contributes to P-body localization (Supplemental Fig. S2D; Kamenska et al. 2014). Indeed, its deletion (Δ PatL1) abolished 4E-T binding to PatL1 without affecting the interaction with other protein partners (Supplemental Fig. S2A,B).

We then examined the subcellular localization of the 4E-T mutant proteins in HeLa cells. GFP-4E-T colocalized with the P-body marker and decapping factor EDC4, as judged by antibody staining (Supplemental Fig. S3A; Kedersha and Anderson 2007). Since none of the amino acid deletions altered the nuclear localization (NLS) or the nuclear export signals (NES) in 4E-T, the mutant proteins were mainly cytoplasmic (Fig. 2A; Supplemental Fig. S3B–H). However, while the Δ UNR,

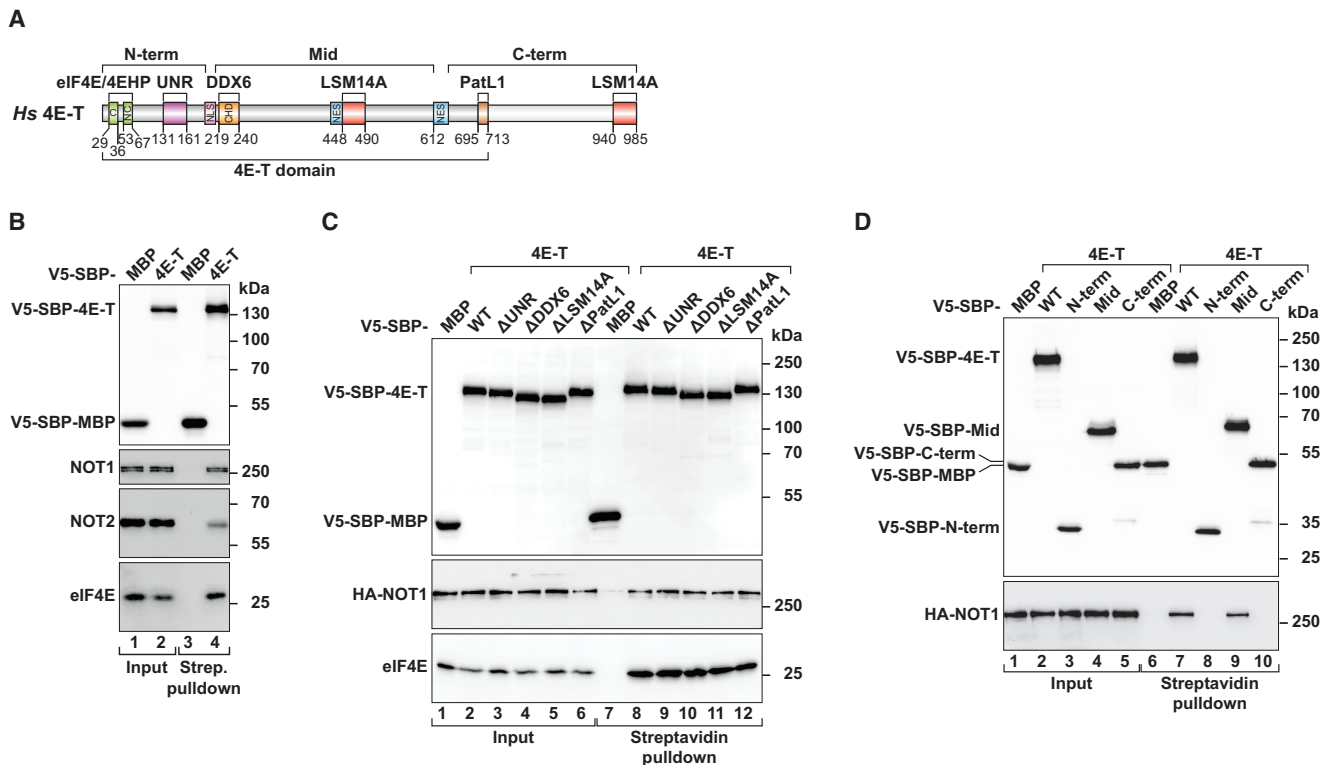


Figure 2. 4E-T interacts with the CCR4–NOT complex via its Mid region. (A) Schematic overview of the domain architecture and binding regions of 4E-T. The N-terminal (N-term) region of 4E-T contains two eIF4E-binding motifs ([C] canonical eIF4E-binding motif, [NC] noncanonical eIF4E-binding motif) and the UNR-interacting region. The middle (Mid) region of 4E-T includes the CUP homology domain (CHD) that mediates interaction with DDX6, and one of the LSM14A-interacting regions. The C-term of 4E-T interacts with PatL1 and LSM14A. (NLS) Nuclear localization signal; (NES) nuclear export signal. The amino acid positions at the domain/motif boundaries are indicated *below* the protein. (B–D) Analysis of the interaction of V5-SBP-4E-T wild type (WT), deletion mutants (Δ), or fragments (N-, Mid, and C-) with endogenous NOT1 and NOT2 (B) or HA-NOT1 (C,D). SBP-tagged proteins were pulled down using streptavidin-coated beads. V5-SBP-MBP served as a negative control. eIF4E was used as a positive binding control. The inputs were 20% for V5-SBP-proteins, 2% for NOT1 and NOT2, 20% for eIF4E, or 2% for HA-NOT1, whereas bound fractions corresponded to 10% for V5-SBP-proteins, 40% for NOT1 and NOT2, 10% for eIF4E or 40% for HA-NOT1. Samples were analyzed by Western blotting using anti-NOT1, anti-NOT2, anti-V5, anti-eIF4E, and anti-HA antibodies.

Δ DDX6 and Δ PatL1 4E-T proteins also localized to P-bodies, the Δ LSM14A mutant (and thus the 4E-T 4x Δ protein that lacks the binding sites for UNR, DDX6, PatL1, and LSM14A) was dispersed throughout the cytoplasm and the nucleus (Supplemental Fig. S3B–H). These results indicate that LSM14A binding regulates 4E-T P-body localization.

We also observed that in the absence of single or combined (4x Δ mutant) interactions with UNR, DDX6, LSM14A, or PatL1, 4E-T still retained the ability to induce deadenylation and protect mRNA from decay upon tethering to the BGG-6xMS2bs reporter (Supplemental Fig. S4A–F). Moreover, all mutants still repressed the translation of the R-Luc-6xMS2bs reporter (Supplemental Fig. S4G,H).

The Mid region of 4E-T interacts with CCR4–NOT

As our results highlighted mRNA deadenylation as a key event in the control of gene expression by 4E-T, we studied its interaction with the CCR4–NOT complex. In hu-

man cells, streptavidin-binding protein (SBP)-V5-4E-T copurified with the NOT1 and NOT2 subunits of CCR4–NOT, suggesting an association with the fully assembled complex (Fig. 2B). This interaction was not mediated by UNR, DDX6, LSM14A, and PatL1, as the corresponding 4E-T deletion mutants still associated with HA-NOT1 in pull-down assays (Fig. 2C).

Experimental evidence reported in the literature suggests that DDX6 bridges the interaction of 4E-T with NOT1 (Ozgun et al. 2015; Waghay et al. 2015). Our results indicate that 4E-T can also bind to the CCR4–NOT complex in the absence of an interaction with DDX6 (Fig. 2C). To confirm that 4E-T has additional interactions with the CCR4–NOT complex, we performed binding assays in DDX6-null HEK293T cells (Hanet et al. 2019). In cells depleted of DDX6, SBP-V5-4E-T still interacted with HA-NOT1 (Supplemental Fig. S5A). Thus, 4E-T establishes multiple and possibly redundant interactions with CCR4–NOT.

To delineate the region of 4E-T critical for the interaction with CCR4–NOT, we divided the protein into an

N-terminal (N-term) fragment comprising the eIF4E and the UNR binding sites (residues 1–194), a middle fragment (Mid) containing the DDX6 and the first LSM14A-binding sites (residues 212–612), and a C-term fragment encompassing the PatL1 and the second LSM14A-binding sites (residues 639–985) (Fig. 2A; Supplemental Table S1). These 4E-T fragments were then tested for the ability to bind to HA-NOT1. We observed that the interaction of 4E-T with HA-NOT1 is mediated by its Mid fragment (Fig. 2D, lane 9).

To obtain additional insight into this interaction, we investigated the region of NOT1 responsible for binding to 4E-T. Using a similar approach, we tested in coimmunoprecipitation assays the binding of 4E-T to N-term (residues 1–1089), Central (residues 1085–1605), and C-term (residues 1595–2376) (Supplemental Table S1; Supplemental Fig. S5B) fragments of NOT1 known to assemble in discrete CCR4–NOT subcomplexes (Raisch et al. 2019). The NOT1 C-term, which associates with the NOT2 and NOT3 subunits of the deadenylase complex (Bhaskar et al. 2013; Boland et al. 2013), was sufficient to bind to 4E-T. The NOT1 N-term and Central fragments did not or only weakly interacted with 4E-T (Supplemental Fig. S5C, lanes 6–8).

The Mid region of 4E-T represses the expression of target mRNAs

We then separately used each 4E-T fragment in tethering assays. Remarkably, binding of 4E-T Mid to the BGG-6xMS2bs transcript triggered efficient mRNA degradation

(Fig. 3A [lane 4], B,C). In contrast, the N-term had no effect on the reporter while the C-term partially reduced mRNA levels (Fig. 3A [lanes 2,3,5], B,C). All 4E-T fragments were dispersed in the cytoplasm and in the nucleus and compromised P-body integrity (Supplemental Fig. S3I–K). Consistent with the ability to bind CCR4–NOT, we observed that inhibition of decapping in cells overexpressing a catalytically inactive form of DCP2 (DCP2*, E148Q) (Wang et al. 2002; Chang et al. 2014) blocked decay induced by 4E-T Mid and resulted in the accumulation of the deadenylated reporter mRNA (Fig. 3A [lanes 7,9], B, C). Thus, the Mid region alone is able to trigger the decay of 4E-T-bound mRNAs through recruitment of CCR4–NOT. The reduction in reporter mRNA levels caused by the C-term was blocked in the presence of DCP2*. However, the C-term-bound mRNA was not deadenylated (Fig. 3A [lane 10], B).

Binding of 4E-T to eIF4E/4EHP inhibits decapping of deadenylated mRNA targets

In the context of full-length 4E-T, mRNA decay is blocked so that bound mRNAs are only deadenylated and not decapped and degraded by XRN1. In contrast, when in isolation, the 4E-T Mid region elicits the decay of a bound transcript. These observations indicate that the ability of 4E-T to protect an mRNA from decapping resides outside of its Mid region. As binding of cap-binding proteins to the cap protects the mRNA from 5'–3' decay (Schwartz and Parker 2000), we addressed whether 4E-T interaction

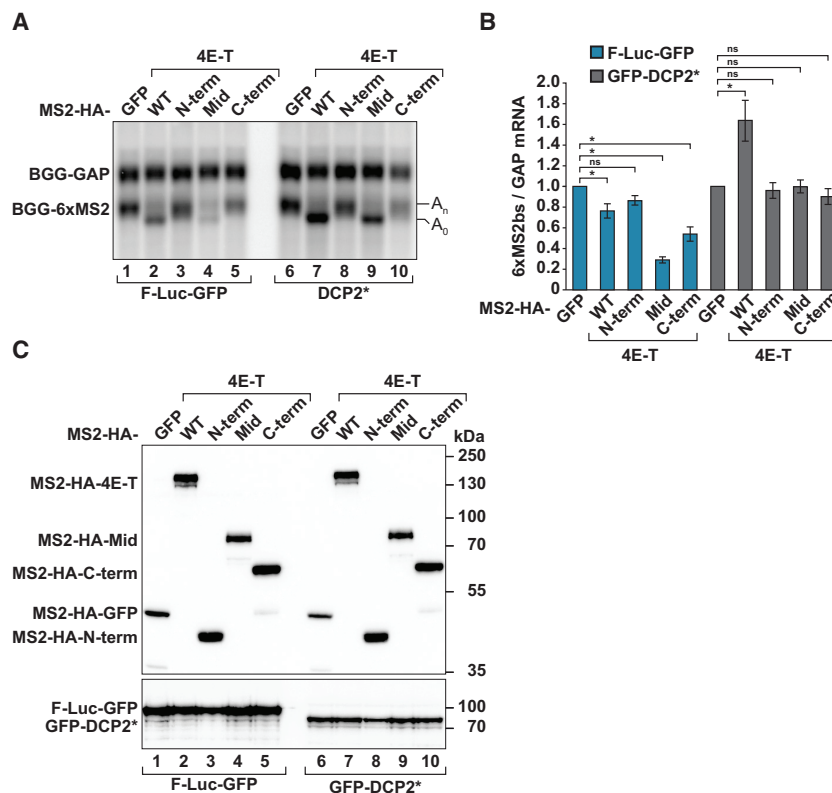


Figure 3. The Mid region of 4E-T promotes mRNA deadenylation. (A,B) HEK293T cells were transfected with plasmids coding for BGG-6xMS2bs, BGG-GAP, MS2-HA-GFP or MS2-HA-4E-T (WT or fragments) and F-Luc-GFP as a control or the catalytic inactive mutant of the decapping enzyme DCP2 (GFP-DCP2*). Northern blot analysis of representative RNA samples is shown in A. A₀, deadenylated and A_n, polyadenylated reporter mRNAs. Quantification of reporter mRNA levels was performed as described in Figure 1C and is depicted in B ($n=3$). (*) $P < 0.05$; (ns) not significant, paired t -test. (C) Expression levels of the proteins used in the tethering assay as analyzed by Western blotting.

with eIF4E/4EHP regulates the stability of its target mRNAs. To this end, we generated 4E-T mutants carrying alanine substitutions in the canonical eIF4E-binding motif (C; Y30A, L35A) (Supplemental Table S1; Supplemental Fig. S6A; Dostie et al. 2000). These amino acid substitutions disrupted binding of 4E-T to eIF4E and 4EHP but not to NOT1, DDX6, PatL1, HA-UNR, or LSM14A (Fig. 4A; Supplemental Fig. S6B–D). 4E-T P-body localization was also independent of eIF4E and 4EHP binding (Supplemental Fig. S3L; Ferraiuolo et al. 2005; Kamenska et al. 2014).

We next examined whether 4E-T was still able to promote deadenylation and protect the BGG-6xMS2bs

mRNA from decapping when impaired in eIF4E/4EHP binding. In contrast to wild-type protein, tethering of the 4E-T C mutant severely reduced the abundance of the BGG-6xMS2bs reporter (Fig. 4B [lane 3 vs. 2], C,D). The 4E-T C mutant induced 5'–3' decay as indicated by the accumulation of deadenylated mRNA upon inhibition of decapping in cells coexpressing catalytically inactive DCP2 (DCP2*) (Fig. 4B [lanes 5,6], C,D). Thus, binding of 4E-T to eIF4E/4EHP blocks decapping of deadenylated mRNA. These observations also indicate that 4E-T can promote deadenylation and degradation of the reporter mRNA in the absence of an interaction with eIF4E/4EHP. This function is then mediated by 4E-T's Mid region.

CUP is a *Drosophila*-specific 4E-BP that promotes deadenylation and inhibits decapping of its target mRNAs. The mRNA protective function of CUP requires its non-canonical eIF4E-binding motif (Igreja and Izaurralde 2011). In contrast to CUP, the canonical motif of 4E-T is indispensable to protect the deadenylated mRNA from decay (Fig. 4B,C). To determine whether the noncanonical motif of 4E-T is also necessary to protect associated mRNAs from decapping, we introduced aspartate substitutions in two conserved tryptophans located C-terminal to the canonical motif (NC; W61D, W66D) (Supplemental Table S1; Supplemental Fig. S6A). The NC mutant had reduced binding to eIF4E (Supplemental Fig. S6E), indicating that human 4E-T also uses a bipartite binding mode to interact with the cap-binding protein. Moreover, the BGG-6xMS2 mRNA was degraded upon binding to the NC mutant of 4E-T (Supplemental Fig. S6F–H). We conclude that both the canonical and noncanonical eIF4E-binding motifs of human 4E-T are required to protect the deadenylated mRNA from degradation.

Distinct roles for the cap-binding proteins in the regulation of deadenylation and decapping by 4E-T

To understand which of the cap-binding proteins is used by 4E-T to inhibit mRNA decapping, we tethered 4E-T to the BGG-6xMS2 reporter in the absence of eIF4E or 4EHP. eIF4E partial depletion using short RNA (shRNA)-mediated knockdown (Supplemental Fig. S7A) increased the degradation of the 4E-T-bound reporter; however, relative to cells treated with a scramble (Scr) shRNA, the reduction in mRNA levels was not significant ($P = 0.054$) (Supplemental Fig. S7B,C). As complete depletion of the cap-binding protein results in decreased cellular viability, these results suggest that eIF4E binding most likely contributes to the protection of deadenylated transcripts associated with 4E-T. Moreover, since 4E-T may still associate with 4EHP in the absence of eIF4E, destabilization of the 4E-T-bound mRNA is less prominent than upon disruption of its interaction with both cap-binding proteins (eIF4E-binding mutants of 4E-T) (Fig. 4; Supplemental Fig. S6).

To address the importance of 4EHP binding, we generated a 4EHP-null HEK293T cell line using CRISPR-Cas9 gene editing (Supplemental Fig. S7D). 4EHP-null cells proliferated slower compared with control (Ctrl) cells but had no obvious changes in general translation, as assessed by

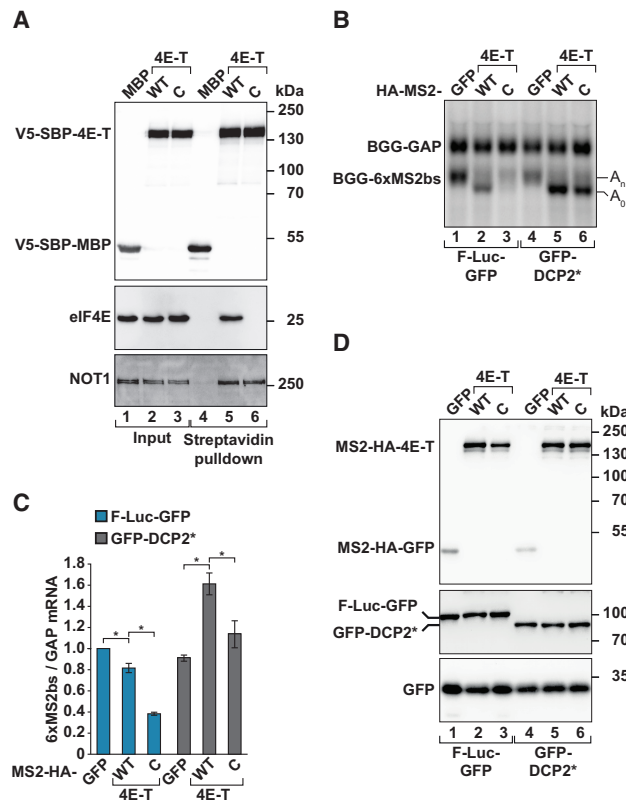


Figure 4. The 4E-T-eIF4E/4EHP interaction protects deadenylated mRNAs from degradation. (A) Streptavidin-based pull-down assays showing the association of V5-SBP-4E-T WT or canonical mutant (C) with eIF4E and NOT1. V5-SBP-MBP served as a negative control. The input (20% for the V5-SBP-tagged proteins and eIF4E, 2% for NOT1) and bound fractions (10% for the V5-SBP-tagged proteins and eIF4E, 40% for NOT1) were analyzed by Western blotting using the indicated antibodies. (B–D) Tethering assay using the plasmids coding for BGG-6xMS2bs, BGG-GAP, MS2-HA-GFP, or MS2-HA-4E-T (WT or the canonical eIF4E-binding motif mutant, C) in cells expressing F-Luc-GFP or mutant GFP-DCP2*. Northern blot analysis of representative RNA samples is shown in B. A₀, deadenylated and A_n, polyadenylated reporter mRNAs. Quantification of mRNA levels was performed as described in Figure 1C and is represented in the graph depicted in C ($n = 3$). (*) $P < 0.05$, paired t -test. (D) Western blot analysis demonstrating the expression of the proteins used in the tethering assay.

polysome profiling analysis (Supplemental Fig. S7E). In the absence of 4EHP, tethered 4E-T was still able to deadenylate and protect the reporter mRNA from further degradation (Supplemental Fig. S7F,G). In contrast to eIF4E depletion, the 4E-T-bound mRNA had a heterogeneous poly(A) tail in 4EHP-null cells, with a large fraction of the mRNA remaining polyadenylated (Supplemental Fig. S7F, lane 4 vs. 2). This observation suggests that deadenylation of the 4E-T-bound mRNA is lessened in the absence of 4EHP.

Overall, these results indicate that 4E-T protects a bound and deadenylated mRNA from degradation when in the presence of eIF4E or 4EHP.

Involvement of 4E-T in TNRC6B-mediated mRNA repression

Our results indicate that 4E-T protects deadenylated and repressed mRNAs from degradation. As 4E-T contributes

to miRNA-mediated gene silencing (Kamenska et al. 2014, 2016; Nishimura et al. 2015; Jafarnejad et al. 2018), we explored the possibility that 4E-T could influence the fate of deadenylated miRNA targets from decay to storage. Interestingly, the miRISC-associated TNRC6B protein regulates gene expression using a combination of translation repression, deadenylation, and mRNA degradation (Lazzaretti et al. 2009). In fact, upon tethering of TNRC6B to an R-Luc reporter, about 40% of the bound transcripts are not degraded and remain silenced in the deadenylated form (Lazzaretti et al. 2009). To investigate whether stabilization of the TNRC6B-bound reporter requires 4E-T, we tethered MS2-HA-TNRC6B to the BGG-6xMS2bs reporter in the presence or absence of 4E-T. Relative to MS2-HA-GFP, 50% of the BGG-6xMS2bs reporter was degraded upon TNRC6B binding (Fig. 5A,B). As observed before, a fraction of the transcripts also accumulated in the deadenylated form in cells expressing TNRC6B

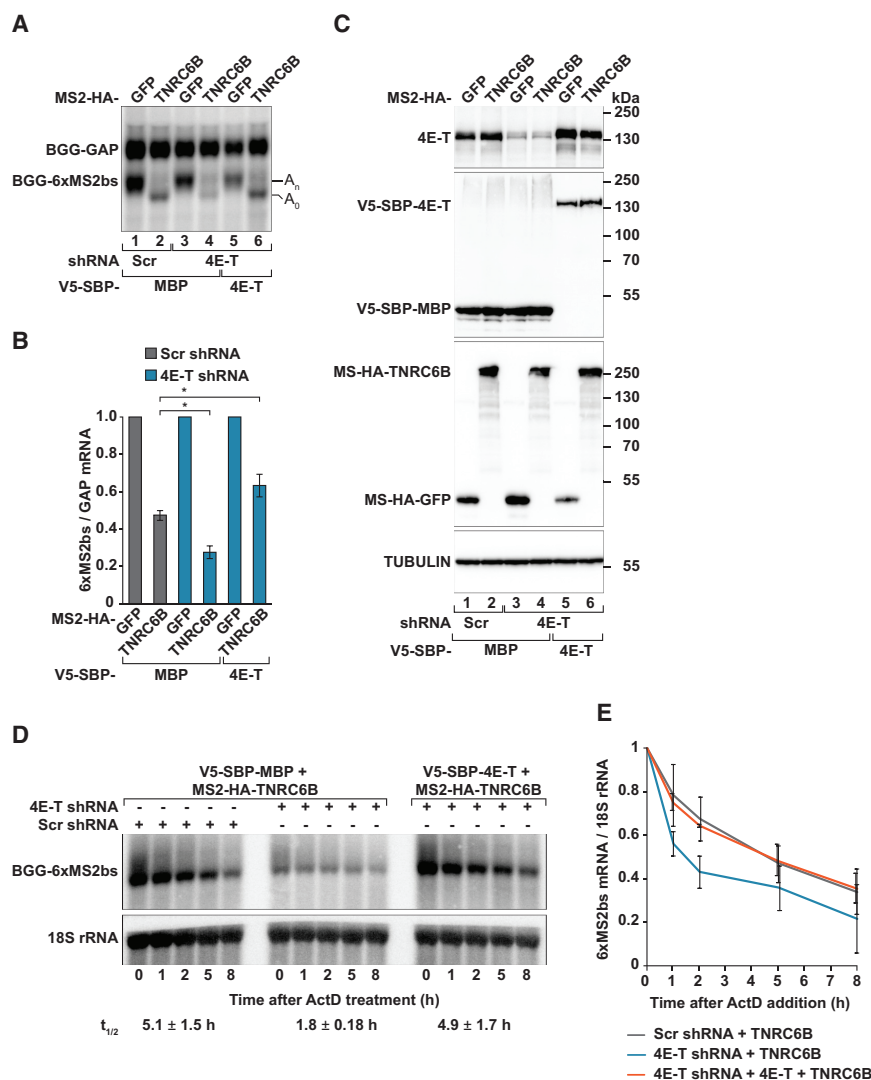


Figure 5. Inhibition of decapping by 4E-T participates in TNRC6B-mediated mRNA repression. (A,B) Tethering of MS2-HA-TNRC6B or MS2-HA-GFP to the BGG-6xMS2bs reporter in control, scramble (Scr) shRNA, and 4E-T-depleted (4E-T shRNA) HEK293T cells expressing V5-SBP-MBP or shRNA resistant V5-SBP-4E-T. BGG-GAP was used as a transfection control. A representative Northern blot analysis is shown in A. (A_0) Deadenylated reporter mRNAs; (A_n) polyadenylated reporter mRNAs. (B) BGG-6xMS2bs mRNA levels were normalized to that of BGG-GAP and set to 1 in the experimental conditions using MS2-HA-GFP. Mean values \pm SD are shown ($n=3$). (*) $P < 0.05$, paired t -test. (C) Western blot analysis showing the expression of V5-SBP-MBP, V5-SBP-4E-T, MS2-HA-GFP, and MS2-HA-TNRC6B proteins used in the assay described in A. (Top panel) The samples were also analyzed with anti-4E-T antibodies to show the decrease in endogenous 4E-T expression upon shRNA-mediated depletion. (Bottom panel) TUBULIN was used as a loading control. (D,E) Scramble shRNA and 4E-T shRNA-treated cells were treated with actinomycin D (ActD) and harvested at the indicated time points. (D) RNA samples were analyzed by Northern blotting. The same membrane was incubated with 32 P-labeled probes specific for the BGG mRNA and the 18S rRNA. Band intensities were quantified by PhosphorImager. (E) BGG-6xMS2bs mRNA levels were normalized to that of 18S rRNA and set to 1 for time point zero. The values at the remaining time points were calculated relative to time point zero and plotted as a function of time after ActD addition. Error bars represent the SD from three independent experiments.

The half-lives of the BGG-6xMS2bs mRNA in the different experimental conditions are shown below the Northern blot panels and are represented as the mean \pm SD.

(Fig. 5A [lanes 2 vs. 1], B). shRNA-mediated knockdown (KD) led to a pronounced decrease of 4E-T protein levels without affecting MS2-HA-TNRC6B expression (Fig. 5C). 4E-T depletion compromised the accumulation of the deadenylated TNRC6B-bound reporter, which was then mostly degraded (Fig. 5A [lane 4], B). The levels of the deadenylated TNRC6B-bound reporter were restored upon coexpression of a V5-SBP-tagged and shRNA-resistant version of 4E-T (Fig. 5A [lane 6], B,C).

To determine the decay rate of the reporter bound to TNRC6B in the presence and absence of 4E-T, we blocked transcription with actinomycin D. Reporter mRNA levels were determined in Scr shRNA and 4E-T shRNA-treated cells at different time points upon actinomycin D addition. We observed that BGG-6xMS2bs mRNA was destabilized in the absence of 4E-T. The half-life of the reporter mRNA decreased to 1.8 ± 0.18 h in 4E-T depleted cells compared with 5.1 ± 1.5 h in Scr shRNA-treated cells (Fig. 5D,E). Moreover, the stability of the BGG-6xMS2bs reporter bound to TNRC6B was restored to 4.9 ± 1.7 h upon re-expression of V5-SBP-4E-T (Fig. 5D,E).

Collectively, these data support the role of 4E-T in protecting TNRC6B-targeted mRNAs from decapping and further decay.

4E-T overexpression blocks decay of transcripts destabilized by TTP and NOT1

To broaden its role as a decapping inhibitory factor, we addressed the consequences of 4E-T overexpression in human cells, a condition that could mimic the localized and enriched presence of the protein in P-bodies (Hubstenberger et al. 2017) or the high expression levels observed in oocytes (Villaescusa et al. 2006; Minshall et al. 2007). In this context, we investigated steady-state levels of a β -GLOBIN (BGG) reporter mRNA targeted to degradation by TTP due to the presence of the FOS AU-rich element (ARE) in the 3' UTR (BGG-ARE) (Fig. 6A; Ferraiuolo et al. 2005). Overexpression of TTP in HEK293T cells resulted in a reduction of the BGG-ARE mRNA levels to 50% relative to cells expressing MBP (Fig. 6B [lane 3 vs. 1], C). Coexpression of 4E-T inhibited TTP-mediated decay of the BGG-ARE reporter, which accumulated as a deadenylated decay intermediate (Fig. 6B [lane 4], C,D). These results are consistent with a role of 4E-T in blocking deadenylation-dependent mRNA decapping. In control cells, the abundance of the polyadenylated BGG-ARE reporter increased in the presence of 4E-T (Fig. 6B [lanes 2 vs. 1], C), indicating that 4E-T also inhibits TTP-independent degradation of an mRNA destabilized by the FOS ARE.

We also tested the effect of 4E-T overexpression on the decay of mRNAs directly targeted by the CCR4-NOT complex. Therefore, we tethered MS2-HA-NOT1 to the BGG-6xMS2bs reporter in the presence or absence of V5-SBP-4E-T. Relative to MS2-HA-GFP, this reporter is degraded to 30% when bound by NOT1 (Fig. 6E [lanes 3 vs. 1], F,G). Overexpression of 4E-T blocked NOT1-dependent decapping and the deadenylated reporter accumulated in cells (Fig. 6F,G, lanes 4 vs. 3).

In conclusion, our data supports the notion that 4E-T, in complex with eIF4E or 4EHP, stabilizes deadenylated mRNAs by interfering with decapping.

Discussion

Just as germ cell granules, neuronal granules or stress granules, P-bodies coordinate the storage of translationally inactive mRNAs in the cell cytoplasm (Bhattacharyya et al. 2006; Voronina et al. 2011; Hutten et al. 2014; Hubstenberger et al. 2017; Schütz et al. 2017; Ivanov et al. 2019). In this study, we describe 4E-T, an essential P-body component and a 4E-BP, as a regulator of mRNA storage. 4E-T-bound mRNAs are translationally repressed, deadenylated, and protected from decapping-dependent decay. We show that regulation of deadenylation and decapping by 4E-T relies on specific protein partners. mRNA deadenylation is a consequence of the interaction of 4E-T's Mid region with the CCR4-NOT complex, whereas inhibition of decapping and subsequent degradation requires interaction with the cap-binding proteins eIF4E/4EHP. Our data also highlights that posttranscriptional regulation by 4E-T is of significance in the context of mRNAs targeted by the miRNA effector TNRC6B.

4E-T is a binding platform for multiple RNA-associated factors

The human 4E-T protein is a large disordered protein with multiple low-complexity regions that confer binding to translation, deadenylation, and decapping factors (Kamenska et al. 2016). Here, we reveal that in addition to the binding sites identified for eIF4E, UNR, DDX6, and LSM14A (Dostie et al. 2000; Ozgur et al. 2015; Kamenska et al. 2016; Brandmann et al. 2018), other short linear motifs (SLIMs) present in 4E-T convene independent binding to PatL1 and possibly to the CCR4-NOT complex as well. A conserved sequence motif in the C-term and previously known to be important but not essential for the localization of 4E-T to P-bodies (Kamenska et al. 2014) mediates the interaction with PatL1 (Fig. 2A; Supplemental Fig. S2). On the other hand, the interaction of 4E-T with the CCR4-NOT is confined to the Mid region of the protein (Fig. 2). Attempts to narrow down and identify the SLIMs involved in CCR4-NOT interaction within this region were unsuccessful, as multiple sequences seemed to be required (data not shown). Further work on the architecture of 4E-T complexes will be necessary to determine whether these protein interactions occur simultaneously or consecutively, and their role in cells.

One important finding in our studies is that the interaction with the CCR4-NOT complex induces deadenylation of the bound mRNA and accounts for one of the eIF4E-independent mechanisms involved in 4E-T mediated mRNA repression (Kamenska et al. 2014). As 4E-T participates in posttranscriptional events regulated by miRNAs and AU-rich element binding proteins (Ferraiuolo et al. 2005; Kamenska et al. 2014; Nishimura et al. 2015; Chapat et al. 2017), its interaction with the

deadenylase complex most likely contributes to and/or sustains the repressed state of the targeted transcript.

4E-T blocks decapping by binding eIF4E/4EHP

Another important observation in this work is that, similar to the fly-specific 4E-BP CUP (Igreja and Izaurralde 2011), interaction of 4E-T with eIF4E/4EHP protects the

deadenylated target mRNA from decapping-dependent decay. In the absence of eIF4E and 4EHP-binding, mRNA deadenylation promoted by the Mid region causes the decay of the 4E-T-bound mRNA (Fig. 4). Although the mechanism is still unclear, inhibition of decapping by 4E-T could be achieved by increasing eIF4E or 4EHP affinity for the cap structure. The direct interaction between 4E-T and 4EHP enhances binding to the cap structure and is a requisite for competition with the eIF4F complex during repression of translation initiation by miRNAs (Chapat et al. 2017). Similarly, binding of CUP to eIF4E increases the affinity of the latter to the cap (Kinkelin et al. 2012) and contributes to the translational regulation of localized mRNAs during early *Drosophila* development (Wilhelm et al. 2003; Nakamura et al. 2004; Zappavigna et al. 2004).

Additional mechanisms used to block decapping could involve the competition of 4E-T with unknown proteins that facilitate eIF4E or 4EHP dissociation from the cap structure. Similar to eIF4G, direct or indirect RNA-binding activity of 4E-T could also play a role in anchoring eIF4E or 4EHP to the mRNA and increase their association with the cap structure (Yanagiya et al. 2009).

Independent of the mechanism that prevents decapping, the interaction of 4E-T with eIF4E or 4EHP could be subject to regulation by posttranslational modifications or binding partners, so that 4E-T-bound mRNAs can be either stored in a repressed and deadenylated form in P-bodies or fully degraded depending on their sequence and binding proteins. For example, 4E-T-associated transcripts targeted by miRNAs and 4EHP (Chapat

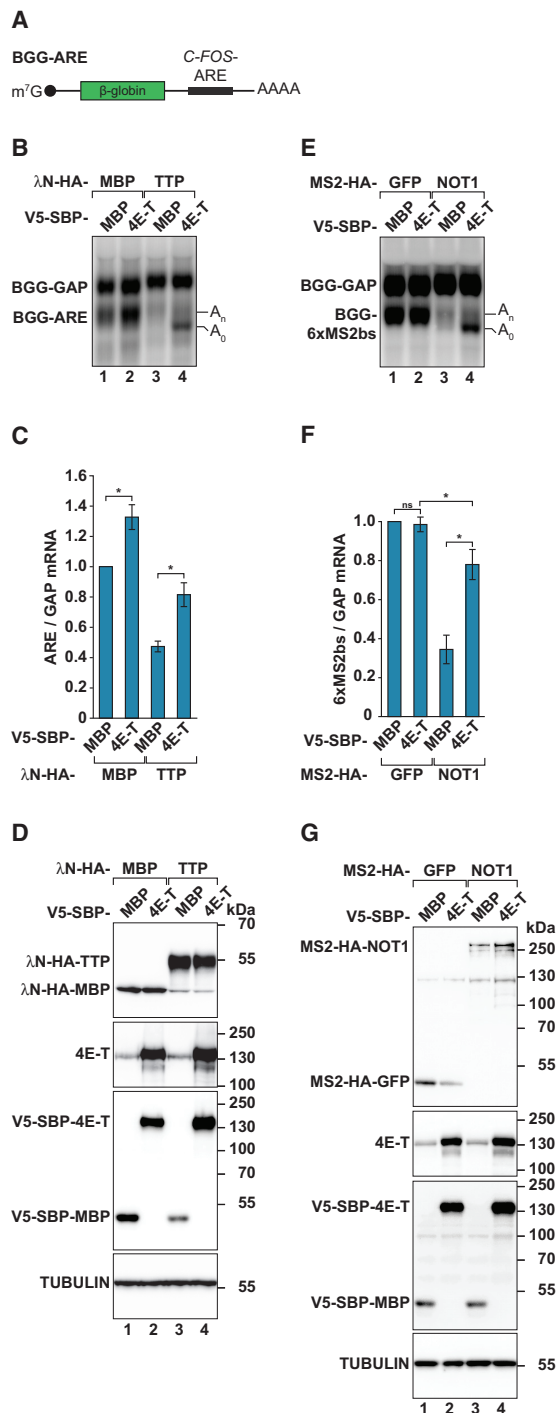


Figure 6. Overexpression of 4E-T blocks deadenylation-dependent decapping. (A) Schematic representation of the BGG-ARE reporter used in this study. A copy of the ARE sequence present in the 3' UTR of the *FOS* mRNA was cloned downstream from the β -*GLOBIN* ORF. The *FOS* ARE is recognized by tristetraprolin (TTP) to promote target mRNA decay upon recruitment of the CCR4-NOT complex (Fabian et al. 2013; Bulbrook et al. 2018). (B,C) HEK293T cells were transfected with the BGG-ARE reporter and plasmids expressing λ N-HA-MBP or λ N-HA-TTP, V5-SBP-MBP, or V5-SBP-4E-T. The BGG-GAP reporter served as a transfection and normalization control. A representative Northern blot is shown in B. (A₀) Deadenylated reporter mRNAs; (A_n) polyadenylated reporter mRNAs. (C) BGG-ARE mRNA levels were normalized to those of the BGG-GAP and set to 1 in cells expressing λ N-HA-MBP. Mean values \pm SD are shown ($n = 3$). (*) $P < 0.05$, paired t -test. (D) Expression levels of the proteins used in B and C analyzed by Western blotting. TUBULIN served as a loading control. (E,F) Tethering of MS2-HA-NOT1 or MS2-HA-GFP to the BGG-6xMS2bs reporter in cells overexpressing V5-SBP-4E-T or V5-SBP-MBP. BGG-GAP was used as a transfection control. A representative Northern blot analysis is shown in E. A₀, deadenylated and A_n, polyadenylated reporter mRNAs. (F) BGG-6xMS2bs mRNA levels were normalized to those of BGG-GAP and set to 1 in the experimental condition using MS2-HA-GFP and V5-SBP-MBP. Mean values \pm SD are shown ($n = 3$). (*) $P < 0.05$; (ns) not significant, paired t -test. (G) The expression levels of the proteins used in E and F were verified using Western blotting. TUBULIN served as a loading control. Proteins were detected using anti-HA, anti-4E-T, anti-V5, and anti-TUBULIN antibodies.

et al. 2017) or TNRC6B (this work) undergo translational repression while mRNAs targeted by 4E-T and the CCR4–NOT are degraded (Nishimura et al. 2015).

We also observed that cellular depletion of each cap-binding protein has distinct effects on the 4E-T-bound mRNA. Reduction of eIF4E expression appeared to sensitize the mRNA to further degradation. In contrast, 4EHP loss affected the initiation of deadenylation by 4E-T. The molecular details associated with these differences remain unclear but may be associated with distinct composition of the 4E-T mRNA–protein complexes.

4E-T as a coordinator of P-body-associated mRNA repression

The molecular mechanisms underlying selective translational regulation in P-bodies remain largely unknown. 4E-T is an essential P-body component (Andrei et al. 2005; Ferraiuolo et al. 2005) and thus emerges as an important regulator of the expression of transcripts present in these RNA granules. As a binding platform for various proteins, 4E-T coordinates the repression and protection of P-body-associated mRNAs. The interaction of 4E-T with eIF4E or 4EHP brings the cap binding proteins into P-bodies (Ferraiuolo et al. 2005; Kubacka et al. 2013), promotes translational repression (Ferraiuolo et al. 2005; Kamenska et al. 2014) and prevents decapping (this study). Moreover, 4E-T association with CCR4–NOT likely sustains the deadenylated and repressed state of the mRNA (this work and Waghray et al. 2015). Interestingly, P-bodies contain deadenylases, lack PABP, and associated mRNAs have been suggested to contain either a heterogeneous or no poly (A) tail (Cougot et al. 2004; Andrei et al. 2005; Kedersha et al. 2005; Aizer et al. 2014; Hubstenberger et al. 2017). Additionally, the interaction of 4E-T with DDX6 is also required for P-body assembly and translational repression (Kamenska et al. 2016).

4E-T localization to P-bodies is also subject to regulation. Our study highlights that binding to LSM14A is important for the recruitment of 4E-T, and consequently of eIF4E, 4EHP, and associated mRNAs, to P-bodies (Supplemental Fig. S3). Arginine methylation controls LSM14A recruitment to P-bodies (Matsumoto et al. 2012) and thus it may regulate the presence of 4E-T in these cytoplasmic RNA granules. 4E-T itself is posttranslationally modified by phosphorylation under arsenite-induced oxidative stress. In these conditions, P-body size increases (Cargnello et al. 2012). Interestingly, the majority of the phospho-regulated sites are in the Mid region of the protein that is responsible for the interaction with CCR4–NOT. The significance of these regulatory events to the function of 4E-T-containing mRNPs or to the dynamic nature of P-bodies remains uncharacterized.

4E-T driven mRNA storage in germinal and neuronal granules

The role of 4E-T in the specification of alternative fates for bound mRNAs (i.e., storage in a deadenylated, repressed form for later use, or complete degradation) has important

biological implications. Spatial and temporal control of mRNA translation is a common posttranscriptional mechanism operating in oocytes, eggs, and early embryos of many organisms and in neuronal cells (Martin and Ephrussi 2009; Jung et al. 2014; Formicola et al. 2019). Interestingly, 4E-T is a component of germinal and neuronal granules and regulates oocyte and neuronal development via poorly understood mechanisms (Villaescusa et al. 2006; Minshall et al. 2007; Kasippillai et al. 2013; Yang et al. 2014; Amadei et al. 2015; Pfender et al. 2015; Zahr et al. 2018; Zhao et al. 2019). In somatic cells, 4E-T has also documented roles in miRNA-mediated gene silencing and in the control of the expression of AU-rich mRNAs (Kamenska et al. 2014; Nishimura et al. 2015; Chapat et al. 2017). Thus, the identification of the target mRNAs and mechanisms used and governing 4E-T function in cells will advance our knowledge on the control of gene expression in fundamental developmental processes.

Furthermore, the current view that cytoplasmic granules such as P-bodies are reservoirs of repressed transcripts opens the possibility that, according to the cellular needs or developmental stage, specific mRNAs can be mobilized into the translating pool. Reactivation of silenced transcripts has been described during oocyte maturation, early embryonic development, mitotic cell cycle progression, in neurons, following stress relief or associated to the rhythmic expression of clock-controlled genes (Vassalli et al. 1989; Simon et al. 1992; Gebauer et al. 1994; Wu et al. 1998; Oh et al. 2000; Bhattacharyya et al. 2006; Novoa et al. 2010; Carbonaro et al. 2011; Kojima et al. 2012; Udagawa et al. 2012; Aizer et al. 2014). The mechanisms involved in translational activation following P-body storage most likely require remodeling and processing (e.g., polyadenylation) of the repressed mRNA. The repressor machinery must be replaced by factors that promote translation and polyadenylation of the stored transcripts. 4E-T, again, can play a crucial role in this mechanism, as regulation of the interactions with its protein partners might control the assembly and disassembly of the repressor complex, such as evidenced by the decay of the 4E-T-bound mRNA in the absence of interaction with eIF4E and 4EHP. This topic merits further investigation as multiple and redundant interactions (RNA–protein and protein–protein) operate in the control of gene expression in P-bodies.

Overall, our findings highlight 4E-T as a coordinator of mRNA turnover. As a binding platform for cap-binding proteins, the CCR4–NOT deadenylase complex and decapping factors, 4E-T guarantees that silenced mRNAs are protected from degradation in cytoplasmic granules associated with germline and neuronal development.

Materials and methods

DNA constructs

The DNA constructs used in this study are described in the Supplemental Material and listed in Supplemental Table S1. All constructs and mutations were confirmed by sequencing.

Tethering assays in human cells

All the conditions used in the tethering assays are described in the Supplemental Material.

Knockdown and complementation assays

HEK293T cells (0.8×10^6 cells per well) were transfected 24 h after seeding in six-well plates with 3 μ g of plasmid expressing scramble (control), 4E-T, or eIF4E shRNA using Lipofectamine 2000 (Invitrogen). Forty-eight hours after transfection, the cells were transfected a second time. In the TNRC6B tethering assay, the transfection mixtures contained 0.5 μ g of BGG-6xMS2bs, 0.5 μ g of BGG-GAP, 0.4 μ g of MS2-HA-TNRC6B, 0.15 μ g of V5-SBP-MBP or 0.3 μ g of V5-SBP-4E-T (shRNA resistant), and 1 μ g of vector expressing 4E-T shRNA. Following eIF4E depletion with 1 μ g of the respective shRNA, cells were transfected with 0.5 μ g of BGG-6xMS2bs, 0.5 μ g of BGG-GAP, 0.4 μ g of MS2-HA-4E-T or MS2-HA-GFP, and 1 μ g of eIF4E shRNA. Total RNA was isolated with TRIzol (Thermo Scientific) and analyzed as described above.

Half-life experiments

To determine reporter mRNA decay rates, cells were treated with actinomycin D (10 μ g/mL final concentration) 24 h after transfection and collected at the indicated time points. mRNA levels determined by Northern blotting were normalized to the levels of 18S rRNA. To determine the half-lives ($t_{1/2} = 50\%$ of remaining mRNA) indicated below the panels in the figures, the normalized BGG-6xMS2bs mRNA levels were set to 1 at time point zero and plotted against time.

RNase H digestion

Ten micrograms of RNA were incubated with 3 μ L of 5 U/ μ L RNase H (New England Biolabs) and 6 μ M oligo(dT) 15-mer in 100 μ L of H₂O for 1 h at 37°C. The RNase H-treated RNA was purified by phenol-chloroform extraction and analyzed by Northern blotting.

Terminator assay

Ten micrograms of RNA treated with 1 μ L of Terminator 5'-phosphate-dependent exonuclease 1 U/ μ L (Epicentre) in 20 μ L of H₂O for 1 h at 37°C was purified by phenol-chloroform extraction and analyzed via Northern blotting.

Coimmunoprecipitation (co-IP) and pull-down assays

The conditions used in the co-IP and pull-down assays are described in the Supplemental Material. All antibodies used in the co-IP and pull-down assays are listed in Supplemental Table S2.

Immunofluorescence

Immunofluorescence was performed as described in Lazzaretti et al. (2009). Details are included in the Supplemental Material.

Generation of the 4EHP-null cell line

Clonal cell lines were obtained and confirmed for gene editing as described previously (Peter et al. 2017). Details are described in the Supplemental Material.

Polysome profiling

Polysome profiles for HEK293T wild-type and 4EHP-null cells were performed as described before (Kuzuoğlu-Öztürk et al. 2016).

Statistics

Experiments were done in triplicates and all data is reported as the mean \pm the standard deviation (SD) represented as error bars. Statistical analyses were performed with a two-tailed paired Student's *t*-test. *P*-values < 0.05 were considered statistically significant.

Acknowledgments

We dedicate this manuscript to the memory of Elisa Izaurralde, who passed away before the conclusion of this work. All experiments were conceived and performed in her laboratory. We are thankful to Praveen Bawankar, Heike Budde, and Lara Wohlbold for cloning. We also thank Daniel Peter and Eugene Valkov for helpful suggestions on the manuscript. This work was supported by the Max Planck Society.

Author contributions: F.R. performed most of the experiments and generated several of the constructs. R.W. generated the 4EHP-null cell line and performed the polysome profiling experiment. E.I. was the principal investigator. C.I. coordinated the project. F.R. and C.I. wrote the manuscript.

References

- Aizer A, Kalo A, Kafri P, Shraga A, Ben-Yishay R, Jacob A, Kinor N, Shav-Tal Y. 2014. Quantifying mRNA targeting to P-bodies in living human cells reveals their dual role in mRNA decay and storage. *J Cell Sci* **127**: 4443–4456. doi:10.1242/jcs.152975
- Amadei G, Zander MA, Yang G, Dumelie JG, Vessey JP, Lipshitz HD, Smibert CA, Kaplan DR, Miller FD. 2015. A Smaug2-Based translational repression complex determines the balance between precursor maintenance versus differentiation during mammalian neurogenesis. *J Neurosci* **35**: 15666–15681. doi:10.1523/JNEUROSCI.2172-15.2015
- Andrei MA, Ingelfinger D, Heintzmann R, Achsel T, Rivera-Pomar R, Lührmann R. 2005. A role for eIF4E and eIF4E-transporter in targeting mRNPs to mammalian processing bodies. *RNA* **11**: 717–727. doi:10.1261/rna.2340405
- Bhaskar V, Roudko V, Basquin J, Sharma K, Urlaub H, Séraphin B, Conti E. 2013. Structure and RNA-binding properties of the Not1-Not2-Not5 module of the yeast CCR4-NOT complex. *Nat Struct Mol Biol* **20**: 1281–1288. doi:10.1038/nsmb.2686
- Bhattacharyya SN, Habermacher R, Martine U, Closs EI, Filipowicz W. 2006. Relief of microRNA-mediated translational repression in human cells subjected to stress. *Cell* **125**: 1111–1124. doi:10.1016/j.cell.2006.04.031
- Boland A, Chen Y, Raisch T, Jonas S, Kuzuoğlu-Öztürk D, Wohlbold L, Weichenrieder O, Izaurralde E. 2013. Structure and assembly of the NOT module of the human CCR4-NOT complex. *Nat Struct Mol Biol* **20**: 1289–1297. doi:10.1038/nsmb.2681
- Brandmann T, Fakim H, Padamsi Z, Youn JY, Gingras AC, Fabian MR, Jinek M. 2018. Molecular architecture of LSM14 interactions involved in the assembly of mRNA silencing complexes. *EMBO J* **37**: e97869. doi:10.15252/embj.201797869
- Braun JE, Truffault V, Boland A, Huntzinger E, Chang CT, Haas G, Weichenrieder O, Coles M, Izaurralde E. 2012. A direct

- interaction between DCP1 and XRN1 couples mRNA decapping to 5' exonucleolytic degradation. *Nat Struct Mol Biol* **19**: 1324–1331. doi:10.1038/nsmb.2413
- Bulbrook D, Brazier H, Mahajan P, Kliszczak M, Fedorov O, Marchese FP, Aubareda A, Chalk R, Picaud S, Strain-Damerell C, et al. 2018. Tryptophan-mediated interactions between tristetraprolin and the CNOT9 subunit are required for CCR4–NOT deadenylase complex recruitment. *J Mol Biol* **430**: 722–736. doi:10.1016/j.jmb.2017.12.018
- Carbonaro M, O'Brate A, Giannakakou P. 2011. Microtubule disruption targets HIF-1 α mRNA to cytoplasmic P-bodies for translational repression. *J Cell Biol* **192**: 83–99. doi:10.1083/jcb.201004145
- Carnello M, Tcherkezian J, Dorn JF, Huttlin EL, Maddox PS, Gygi SP, Roux PP. 2012. Phosphorylation of the eukaryotic translation initiation factor 4E-transporter (4E-T) by c-Jun N-terminal kinase promotes stress-dependent P-body assembly. *Mol Cell Biol* **32**: 4572–4584. doi:10.1128/MCB.00544-12
- Chang CT, Bercovich N, Loh B, Jonas S, Izaurralde E. 2014. The activation of the decapping enzyme DCP2 by DCP1 occurs on the EDC4 scaffold and involves a conserved loop in DCP1. *Nucleic Acids Res* **42**: 5217–5233. doi:10.1093/nar/gku129
- Chapat C, Jafarnejad SM, Matta-Camacho E, Hesketh GG, Gelbart IA, Attig J, Gkogkas CG, Alain T, Stern-Ginossar N, Fabian MR, et al. 2017. Cap-binding protein 4EHP effects translation silencing by microRNAs. *Proc Natl Acad Sci* **114**: 5425–5430. doi:10.1073/pnas.1701488114
- Cougot N, Babajko S, Séraphin B. 2004. Cytoplasmic foci are sites of mRNA decay in human cells. *J Cell Biol* **165**: 31–40. doi:10.1083/jcb.200309008
- Dostie J, Ferraiuolo M, Pause A, Adam SA, Sonenberg N. 2000. A novel shuttling protein, 4E-T, mediates the nuclear import of the mRNA 5' cap-binding protein, eIF4E. *EMBO J* **19**: 3142–3156. doi:10.1093/emboj/19.12.3142
- Fabian MR, Frank F, Rouya C, Siddiqui N, Lai WS, Karetnikov A, Blackshear PJ, Nagar B, Sonenberg N. 2013. Structural basis for the recruitment of the human CCR4–NOT deadenylase complex by tristetraprolin. *Nat Struct Mol Biol* **20**: 735–739. doi:10.1038/nsmb.2572
- Ferraiuolo MA, Basak S, Dostie J, Murray EL, Schoenberg DR, Sonenberg N. 2005. A role for the eIF4E-binding protein 4E-T in P-body formation and mRNA decay. *J Cell Biol* **170**: 913–924. doi:10.1083/jcb.200504039
- Formicola N, Vijayakumar J, Besse F. 2019. Neuronal ribonucleoprotein granules: dynamic sensors of localized signals. *Traffic* **20**: 639–649.
- Franks TM, Lykke-Andersen J. 2008. The control of mRNA decapping and P-body formation. *Mol Cell* **32**: 605–615. doi:10.1016/j.molcel.2008.11.001
- Gebauer F, Xu W, Cooper GM, Richter JD. 1994. Translational control by cytoplasmic polyadenylation of c-mos mRNA is necessary for oocyte maturation in the mouse. *EMBO J* **13**: 5712–5720. doi:10.1002/j.1460-2075.1994.tb06909.x
- Grüner S, Peter D, Weber R, Wohlbold L, Chung MY, Weichenrieder O, Valkov E, Igreja C, Izaurralde E. 2016. The structures of eIF4E–eIF4G complexes reveal an extended interface to regulate translation initiation. *Mol Cell* **64**: 467–479. doi:10.1016/j.molcel.2016.09.020
- Grüner S, Weber R, Peter D, Chung MY, Igreja C, Valkov E, Izaurralde E. 2018. Structural motifs in eIF4G and 4E-BPs modulate their binding to eIF4E to regulate translation initiation in yeast. *Nucleic Acids Res* **46**: 6893–6908. doi:10.1093/nar/gky542
- Haghighat A, Mader S, Pause A, Sonenberg N. 1995. Repression of cap-dependent translation by 4E-binding protein 1: competition with p220 for binding to eukaryotic initiation factor-4E. *EMBO J* **14**: 5701–5709. doi:10.1002/j.1460-2075.1995.tb00257.x
- Hanet A, Räsch F, Weber R, Ruscica V, Fauser M, Räsch T, Kuzuoglu-Öztürk D, Chang CT, Bhandari D, Igreja C, et al. 2019. HELZ directly interacts with CCR4–NOT and causes decay of bound mRNAs. *Life Sci Alliance* **2**: e201900405. doi:10.26508/lsa.201900405
- Hashem Y, Frank J. 2018. The jigsaw puzzle of mRNA translation initiation in eukaryotes: a decade of structures unraveling the mechanics of the process. *Annu Rev Biophys* **47**: 125–151. doi:10.1146/annurev-biophys-070816-034034
- Hubstenberger A, Courel M, Bénard M, Souquere S, Ernoult-Lange M, Chouaib R, Yi Z, Morlot JB, Munier A, Fradet M, et al. 2017. P-Body purification reveals the condensation of repressed mRNA regulons. *Mol Cell* **68**: 144–157.e5. doi:10.1016/j.molcel.2017.09.003
- Hutten S, Sharangdhara T, Kiebler M. 2014. Unmasking the messenger. *RNA Biol* **11**: 992–997. doi:10.4161/rna.32091
- Igreja C, Izaurralde E. 2011. CUP promotes deadenylation and inhibits decapping of mRNA targets. *Genes Dev* **25**: 1955–1967. doi:10.1101/gad.17136311
- Ivanov P, Kedersha N, Anderson P. 2019. Stress granules and processing bodies in translational control. *Cold Spring Harb Perspect Biol* **11**: a032813. doi:10.1101/cshperspect.a032813
- Jafarnejad SM, Chapat C, Matta-Camacho E, Gelbart IA, Hesketh GG, Arguello M, Garzia A, Kim SH, Attig J, Shapiro M, et al. 2018. Translational control of ERK signaling through miRNA/4EHP-directed silencing. *Elife* **7**: e35034. doi:10.7554/eLife.35034
- Jung H, Gkogkas CG, Sonenberg N, Holt CE. 2014. Remote control of gene function by local translation. *Cell* **157**: 26–40. doi:10.1016/j.cell.2014.03.005
- Kamenska A, Lu WT, Kubacka D, Broomhead H, Minshall N, Bushell M, Standart N. 2014. Human 4E-T represses translation of bound mRNAs and enhances microRNA-mediated silencing. *Nucleic Acids Res* **42**: 3298–3313. doi:10.1093/nar/gkt1265
- Kamenska A, Simpson C, Vindry C, Broomhead H, Bénard M, Ernoult-Lange M, Lee BP, Harries LW, Weil D, Standart N. 2016. The DDX6–4E-T interaction mediates translational repression and P-body assembly. *Nucleic Acids Res* **44**: 6318–6334. doi:10.1093/nar/gkw565
- Kasipillai T, MacArthur DG, Kirby A, Thomas B, Lambalk CB, Daly MJ, Welt CK. 2013. Mutations in eIF4ENIF1 are associated with primary ovarian insufficiency. *J Clin Endocrinol Metab* **98**: E1534–E1539. doi:10.1210/jc.2013-1102
- Kedersha N, Anderson P. 2007. Mammalian stress granules and processing bodies. *Methods Enzymol* **431**: 61–81. doi:10.1016/S0076-6879(07)31005-7
- Kedersha N, Stoecklin G, Ayodele M, Yacono P, Lykke-Andersen J, Fritzler MJ, Scheuner D, Kaufman RJ, Golan DE, Anderson P. 2005. Stress granules and processing bodies are dynamically linked sites of mRNP remodeling. *J Cell Biol* **169**: 871–884. doi:10.1083/jcb.200502088
- Kinkelin K, Veith K, Grunwald M, Bono F. 2012. Crystal structure of a minimal eIF4E–Cup complex reveals a general mechanism of eIF4E regulation in translational repression. *RNA* **18**: 1624–1634. doi:10.1261/rna.033639.112
- Kojima S, Sher-Chen EL, Green CB. 2012. Circadian control of mRNA polyadenylation dynamics regulates rhythmic protein expression. *Genes Dev* **26**: 2724–2736. doi:10.1101/gad.208306.112

- Kubacka D, Kamenska A, Broomhead H, Minshall N, Darzynkiewicz E, Standart N. 2013. Investigating the consequences of eIF4E2 (4EHP) interaction with 4E-transporter on its cellular distribution in HeLa cells. *PLoS One* **8**: e72761. doi:10.1371/journal.pone.0072761
- Kuzuoğlu-Öztürk D, Bhandari D, Huntzinger E, Fauser M, Helms S, Izaurralde E. 2016. miRISC and the CCR4–NOT complex silence mRNA targets independently of 43S ribosomal scanning. *EMBO J* **35**: 1186–1203. doi:10.15252/embj.201592901
- Lazzaretti D, Tournier I, Izaurralde E. 2009. The C-terminal domains of human TNRC6A, TNRC6B, and TNRC6C silence bound transcripts independently of Argonaute proteins. *RNA* **15**: 1059–1066. doi:10.1261/rna.1606309
- Lykke-Andersen J, Shu MD, Steitz JA. 2000. Human Upf proteins target an mRNA for nonsense-mediated decay when bound downstream of a termination codon. *Cell* **103**: 1121–1131. doi:10.1016/S0092-8674(00)00214-2
- Mader S, Lee H, Pause A, Sonenberg N. 1995. The translation initiation factor eIF-4E binds to a common motif shared by the translation factor eIF-4 gamma and the translational repressors 4E-binding proteins. *Mol Cell Biol* **15**: 4990–4997. doi:10.1128/MCB.15.9.4990
- Martin KC, Ephrussi A. 2009. mRNA localization: gene expression in the spatial dimension. *Cell* **136**: 719–730. doi:10.1016/j.cell.2009.01.044
- Matsumoto K, Nakayama H, Yoshimura M, Masuda A, Dohmae N, Matsumoto S, Tsujimoto M. 2012. PRMT1 is required for RAP55 to localize to processing bodies. *RNA Biol* **9**: 610–623. doi:10.4161/rna.19527
- Merrick WC, Pavitt GD. 2018. Protein synthesis initiation in eukaryotic cells. *Cold Spring Harb Perspect Biol* **10**: a033092. doi:10.1101/cshperspect.a033092
- Minshall N, Reiter MH, Weil D, Standart N. 2007. CPEB interacts with an ovary-specific eIF4E and 4E-T in early *Xenopus* oocytes. *J Biol Chem* **282**: 37389–37401. doi:10.1074/jbc.M704629200
- Nakamura A, Sato K, Hanyu-Nakamura K. 2004. *Drosophila* cup is an eIF4E binding protein that associates with Bruno and regulates *oskar* mRNA translation in oogenesis. *Dev Cell* **6**: 69–78. doi:10.1016/S1534-5807(03)00400-3
- Nishimura T, Padamsi Z, Fakim H, Milette S, Dunham WH, Gingras AC, Fabian MR. 2015. The eIF4E-Binding protein 4E-T is a component of the mRNA decay machinery that bridges the 5' and 3' Termini of Target mRNAs. *Cell Rep* **11**: 1425–1436. doi:10.1016/j.celrep.2015.04.065
- Novoa I, Gallego J, Ferreira PG, Mendez R. 2010. Mitotic cell-cycle progression is regulated by CPEB1 and CPEB4-dependent translational control. *Nat Cell Biol* **12**: 447–456. doi:10.1038/ncb2046
- Oh B, Hwang S, McLaughlin J, Solter D, Knowles BB. 2000. Time-ly translation during the mouse oocyte-to-embryo transition. *Development* **127**: 3795–3803.
- Ozgur S, Basquin J, Kamenska A, Filipowicz W, Standart N, Conti E. 2015. Structure of a human 4E-T/DDX6/CNOT1 complex reveals the different interplay of DDX6-binding proteins with the CCR4–NOT complex. *Cell Rep* **13**: 703–711. doi:10.1016/j.celrep.2015.09.033
- Peter D, Igreja C, Weber R, Wohlbold L, Weiler C, Ebertsch L, Weichenrieder O, Izaurralde E. 2015. Molecular architecture of 4E-BP translational inhibitors bound to eIF4E. *Mol Cell* **57**: 1074–1087. doi:10.1016/j.molcel.2015.01.017
- Peter D, Weber R, Sandmeir F, Wohlbold L, Helms S, Bawankar P, Valkov E, Igreja C, Izaurralde E. 2017. GIGYF1/2 proteins use auxiliary sequences to selectively bind to 4EHP and repress target mRNA expression. *Genes Dev* **31**: 1147–1161. doi:10.1101/gad.299420.117
- Pfender S, Kuznetsov V, Pasternak M, Tischer T, Santhanam B, Schuh M. 2015. Live imaging RNAi screen reveals genes essential for meiosis in mammalian oocytes. *Nature* **524**: 239–242. doi:10.1038/nature14568
- Piao X, Zhang X, Wu L, Belasco JG. 2010. CCR4–NOT deadenylates mRNA associated with RNA-induced silencing complexes in human cells. *Mol Cell Biol* **30**: 1486–1494. doi:10.1128/MCB.01481-09
- Pillai RS, Artus CG, Filipowicz W. 2004. Tethering of human Ago proteins to mRNA mimics the miRNA-mediated repression of protein synthesis. *RNA* **10**: 1518–1525. doi:10.1261/rna.7131604
- Raisch T, Chang CT, Levinsky Y, Muthukumar S, Raunser S, Valkov E. 2019. Reconstitution of recombinant human CCR4–NOT reveals molecular insights into regulated deadenylation. *Nat Commun* **10**: 3173. doi:10.1038/s41467-019-11094-z
- Schütz S, Nöldeke ER, Sprangers R. 2017. A synergistic network of interactions promotes the formation of in vitro processing bodies and protects mRNA against decapping. *Nucleic Acids Res* **45**: 6911–6922. doi:10.1093/nar/gkx353
- Schwartz DC, Parker R. 2000. mRNA decapping in yeast requires dissociation of the cap binding protein, eukaryotic translation initiation factor 4E. *Mol Cell Biol* **20**: 7933–7942. doi:10.1128/MCB.20.21.7933-7942.2000
- Simon R, Tassan JP, Richter JD. 1992. Translational control by poly(A) elongation during *Xenopus* development: differential repression and enhancement by a novel cytoplasmic polyadenylation element. *Genes Dev* **6**: 2580–2591. doi:10.1101/gad.6.12b.2580
- Standart N, Weil D. 2018. P-bodies: cytosolic droplets for coordinated mRNA storage. *Trends Genet* **34**: 612–626. doi:10.1016/j.tig.2018.05.005
- Topisirovic I, Svitkin YV, Sonenberg N, Shatkin AJ. 2011. Cap and cap-binding proteins in the control of gene expression. *Wiley Interdiscip Rev RNA* **2**: 277–298. doi:10.1002/wrna.52
- Udagawa T, Swanger SA, Takeuchi K, Kim JH, Nalavadi V, Shin J, Lorenz LJ, Zukin RS, Bassell GJ, Richter JD. 2012. Bidirectional control of mRNA translation and synaptic plasticity by the cytoplasmic polyadenylation complex. *Mol Cell* **47**: 253–266. doi:10.1016/j.molcel.2012.05.016
- Vassalli JD, Huarte J, Belin D, Gubler P, Vassalli A, O'Connell ML, Parton LA, Rickles RJ, Strickland S. 1989. Regulated polyadenylation controls mRNA translation during meiotic maturation of mouse oocytes. *Genes Dev* **3**: 2163–2171. doi:10.1101/gad.3.12b.2163
- Villaescusa JC, Allard P, Carminati E, Kontogianna M, Talarico D, Blasi F, Farookhi R, Verrotti AC. 2006. Clast4, the murine homologue of human eIF4E-Transporter, is highly expressed in developing oocytes and post-translationally modified at meiotic maturation. *Gene* **367**: 101–109. doi:10.1016/j.gene.2005.09.026
- Voronina E, Seydoux G, Sassone-Corsi P, Nagamori I. 2011. RNA granules in germ cells. *Cold Spring Harb Perspect Biol* **3**: a002774. doi:10.1101/cshperspect.a002774
- Waghray S, Williams C, Coon JJ, Wickens M. 2015. *Xenopus* CAF1 requires NOT1-mediated interaction with 4E-T to repress translation in vivo. *RNA* **21**: 1335–1345. doi:10.1261/rna.051565.115
- Wahle E, Winkler GS. 2013. RNA decay machines: deadenylation by the CCR4–NOT and Pan2–Pan3 complexes. *Biochim Biophys Acta* **1829**: 561–570. doi:10.1016/j.bbaggm.2013.01.003

Räsch et al.

- Wang Z, Jiao X, Carr-Schmid A, Kiledjian M. 2002. The hDcp2 protein is a mammalian mRNA decapping enzyme. *Proc Natl Acad Sci* **99**: 12663–12668. doi:10.1073/pnas.192445599
- Wilhelm JE, Hilton M, Amos Q, Henzel WJ. 2003. Cup is an eIF4E binding protein required for both the translational repression of *oskar* and the recruitment of Barentsz. *J Cell Biol* **163**: 1197–1204. doi:10.1083/jcb.200309088
- Wu L, Wells D, Tay J, Mendis D, Abbott MA, Barnitt A, Quinlan E, Heynen A, Fallon JR, Richter JD. 1998. CPEB-mediated cytoplasmic polyadenylation and the regulation of experience-dependent translation of α -CaMKII mRNA at synapses. *Neuron* **21**: 1129–1139. doi:10.1016/S0896-6273(00)80630-3
- Yanagiya A, Svitkin YV, Shibata S, Mikami S, Imataka H, Sonenberg N. 2009. Requirement of RNA binding of mammalian eukaryotic translation initiation factor 4GI (eIF4GI) for efficient interaction of eIF4E with the mRNA cap. *Mol Cell Biol* **29**: 1661–1669. doi:10.1128/MCB.01187-08
- Yang G, Smibert CA, Kaplan DR, Miller FD. 2014. An eIF4E1/4E-T complex determines the genesis of neurons from precursors by translationally repressing a proneurogenic transcription program. *Neuron* **84**: 723–739. doi:10.1016/j.neuron.2014.10.022
- Zahr SK, Yang G, Kazan H, Borrett MJ, Yuzwa SA, Voronova A, Kaplan DR, Miller FD. 2018. A Translational repression complex in developing mammalian neural stem cells that regulates neuronal specification. *Neuron* **97**: 520–537.e6. doi:10.1016/j.neuron.2017.12.045
- Zappavigna V, Piccioni F, Villaescusa JC, Verrotti AC. 2004. Cup is a nucleocytoplasmic shuttling protein that interacts with the eukaryotic translation initiation factor 4E to modulate *Drosophila* ovary development. *Proc Natl Acad Sci* **101**: 14800–14805. doi:10.1073/pnas.0406451101
- Zhao M, Feng F, Chu C, Yue W, Li L. 2019. A novel EIF4ENIF1 mutation associated with a diminished ovarian reserve and premature ovarian insufficiency identified by whole-exome sequencing. *J Ovarian Res* **12**: 119. doi:10.1186/s13048-019-0595-0

4E-T bound mRNAs are stored in a silenced and deadenylated form

Felix Räsch^a, Ramona Weber^a, Elisa Izaurralde^{a,†}, and Cátia Igreja^{a,*}

^aDepartment of Biochemistry, Max Planck Institute for Developmental Biology, Max-Planck-Ring 5, D-72076 Tübingen, Germany

*To whom correspondence should be addressed.

Tel: +49-7071-601-1360

Fax: +49-7071-601-1353

Email: catia.igreja@tuebingen.mpg.de

†Deceased April 30, 2018

Supplemental Information

Supplemental Material

DNA constructs

The β -*GLOBIN* (BGG)-6xMS2bs and BGG-GAPDH (GAP) reporters were described before (Lykke-Andersen *et al.* 2000). Briefly, the reporter contains six MS2 binding sites downstream of a portion of the β -*GLOBIN* gene. The BGG-ARE reporter was generated by inserting the AU-rich element present in the *FOS* gene (TTTTATTGTGTTTTTAATTTATTTATTTAAGATGGATTCTCAGATATTTATATTTTTTATTTATTTTTTTT) into the 3' UTR of the pcDNA3.1-BGG-6xMS2bs plasmid downstream of the NotI restriction site via site directed mutagenesis. The R-Luc-5xBoxB, R-Luc and firefly luciferase (F-Luc)-GFP reporters were described previously (Pillai *et al.* 2004; Lazzaretti *et al.* 2009). R-Luc-6xMS2bs was obtained by exchanging the 5xBoxB element in pCIneo-R-Luc-5xBoxB with 6xMS2bs using site directed mutagenesis. F-Luc-6xMS2bs was generated by replacing the R-Luc open reading frame (ORF) in pCIneo-R-Luc-6xMS2bs with F-Luc-GFP via mutagenesis.

MS2-HA-, λ N-HA-, V5-SBP- and GFP-tagged 4E-T (full length and fragments) constructs were generated via the insertion of the corresponding ORF into the HindIII and ApaI restriction sites of the pT7-MS2-HA-C1, pT7- λ N-HA-C1, pT7-V5-SBP-C1 and pEGFP-C1 (Clontech) vectors, respectively. The exact residue numbering of each construct can be found in Supplemental Table S1. The catalytically inactive DCP2 and NOT8 constructs, the GFP- or MS2-HA-NOT1, and the PatL1 expressing plasmids were previously described (Braun *et al.* 2010; Petit *et al.* 2012; Loh *et al.* 2013; Hanet *et al.* 2019). MS2-HA-UNR was obtained by inserting the corresponding cDNA into the BamHI and XhoI restriction sites of pcDNA3.1-MS2-HA. λ N-HA-TTP was generated by inserting the corresponding cDNA into the XhoI and EcoRI restriction sites of pT7- λ N-HA-C1. MS2-HA-TNRC6B was derived from the pCI-NHA-TNRC6B plasmid (Zipprich *et al.* 2009). The TNRC6B ORF

obtained by PCR amplification was inserted into the BamHI and Sall restriction sites of the pT7-MS2-HA vector.

The plasmids expressing short hairpin RNAs (shRNAs) used in the knockdown experiment were derived from the pSUPERpuro plasmid (kind gift from O. Mühlemann, University of Bern) containing the puromycin resistance gene for cell selection. The shRNA target sequences are as follows: scramble ATTCTCCGAACGTGTCACG, 4E-T GAACAAGATTATCGACCTA, and eIF4E GGACGATGGCTAATTACAT. The construct expressing the shRNA version of 4E-T contained synonymous mutations in the CDS motif targeted by the shRNA.

All mutants used in this study were generated by site-directed mutagenesis using the QuickChange Site-Directed Mutagenesis kit (Stratagene). All constructs and mutations were confirmed by sequencing and are listed in Supplemental Table S1.

Tethering assays in human cells

HEK293T cells were seeded in 6 well plates (0.8×10^6 cells per well) and transfected 24 hours later using Lipofectamine 2000 (Invitrogen). The reporters coding for β -GLOBIN and luciferase were described previously (Lykke-Andersen et al. 2000; Lazzaretti et al. 2009). These reporters contained either six MS2 (BGG-6xMS2bs, R-Luc-6xMS2bs or F-Luc-6xMS2bs) or five BoxB (R-Luc-5xboxB) binding sites in the 3' UTR. The transfection mixtures contained 0.5 μ g BGG-6xMS2bs, 0.5 μ g BGG-GAP and 0.4 μ g of MS2-HA-4E-T, MS2-HA-NOT1, MS2-HA-TNRC6B or MS2-HA-GFP. For the 4E-T mutants the following amounts were used: 0.2 μ g C, 0.35 μ g Δ UNR, 0.25 μ g Δ DDX6, 0.35 μ g Δ LSM14A, 0.35 μ g Δ PatL1, 0.3 μ g 4x Δ , 0.3 μ g N-term, 0.15 μ g Mid and 0.2 μ g C-term. In the tethering assay with the luciferase-based reporters, 0.2 μ g of MS2-HA-4E-T plasmid was transfected together with 0.25 μ g of the plasmids encoding R-Luc-6xMS2bs or R-Luc and F-Luc-GFP. Alternatively, 0.4 μ g of MS2-HA-4E-T plasmid were also co-expressed with 0.25 μ g F-Luc-

6xMS2bs and the R-Luc transfection control or 0.4 µg of λN-HA-4E-T with 0.25 µg R-Luc-5xboxB and F-Luc-GFP. mRNA deadenylation was blocked by overexpression of 0.5 µg of the NOT8 catalytic inactive mutant (HA-NOT8*) or 0.5 µg HA-MBP as control. To interfere with mRNA decapping, 1 µg of the plasmid expressing catalytic inactive DCP2 (GFP-DCP2*), or F-Luc-GFP as control, were expressed in HEK293T cells. For the assay with the ARE reporter the transfection mixture contained 1 µg of BGG-ARE and 0.1 µg BGG-GAP as well as 0.2 µg λN-HA-TTP or λN-HA-MBP and 0.5 µg V5-SBP-4E-T or 0.3 µg V5-SBP-MBP.

Firefly and *Renilla* luciferase activities were measured 48 hours post transfection using the Dual-Luciferase® Reporter Assay System (Promega). The cells transfected with the BGG reporters were collected 24 hours post transfection. Total RNA was isolated with TRIzol (Thermo Scientific) and analyzed via glyoxal based northern blot with ³²P-labeled cDNA probes complementary to the full open reading frames of the reporters. Band intensities were quantified with ImageQuant TL from non-saturated images obtained with Typhoon phosphorimager (GE Healthcare) and included always poly- (A_n) and deadenylated (A₀) reporter mRNA.

Coimmunoprecipitation (CoIP) assays, streptavidin pulldowns and western blot analysis

For coIP assays, HEK293T cells were grown for one day in 10 cm dishes (4.5x10⁶ cells) and transfected using TurboFect (Thermo Fisher Scientific) according to the manufacturer's instructions. In the GFP coIP assays the following amounts of plasmids were used: 1 µg GFP-F-Luc, 4 µg GFP-NOT1 N-term, 3 µg GFP-NOT1 Mid, 36 µg GFP-NOT1 C-term and 40 µg MS2-HA-4E-T. GFP- and HA-containing plasmids were transfected separately. Two days post transfection and prior to immunoprecipitation, the lysates of cells expressing the GFP-proteins were mixed in equal amounts with the lysates of cells expressing the HA-proteins.

The transfection mixtures for streptavidin-based pulldown assays contained 3 µg of V5-SBP-MBP or 10 µg of V5-SBP-4E-T. For the 4E-T mutants the following plasmid DNA amounts were transfected: 5 µg C, 4 µg ΔUNR, 12 µg ΔDDX6, 12 µg ΔLSM14A, 8 µg ΔPatL1, 10 µg N-term, 10 µg Mid and 20 µg C-term. In the assays described in Fig. 2, Supplemental Figs. S2 and S5, 5 µg of pT7-HA-UNR or 15 µg of pT7-HA-CNOT1 were transfected separately into cells. The cells were harvested 2 days post transfection and lysed for 15 min on ice in 1 ml NET buffer (50 mM Tris pH 7.5, 150 mM NaCl, 1 mM EDTA, 0.1% Triton X-100) supplemented with 1x cOmplete protease inhibitor (Sigma). Cell debris was pelleted at 20000 g for 15 min and the supernatant incubated with 0.2 µg/µl RNase A for 30 min. Prior to pulldown, the lysates of cells expressing the SBP-V5-proteins were mixed in equal amounts with the cell lysates containing the HA-proteins. 50 µl of Streptavidin Sepharose 50% slurry (GE Healthcare) on NET buffer was added directly after RNase A treatment to the cell lysate and incubated 1 h rotating at 4°C. In the GFP-coIP, 3 µl of anti-GFP antibody was added to the cell lysate and incubated for 1 h rotating at 4°C. Subsequently, 50 µl of GammaBind G Sepharose 50% slurry on NET buffer (GE Healthcare) was added to the cell lysate and incubated for one additional hour. Beads were washed three times with NET buffer and boiled in 2x Laemmli sample buffer.

Western blots were performed with 10 % polyacrylamide gels and developed using the ECL Western blotting detection system (GE Healthcare). Input samples were taken before addition of the antibodies or streptavidin beads and loaded at amounts adjusted to achieve detection levels similar to the IP/pulldown samples. All antibodies used in the western blots are described in Supplemental Table S2.

Immunofluorescence

Immunofluorescence was performed essentially as described in (Lazzaretti et al. 2009). HeLa cells were seeded 24 h before transfection in 24 well plates on sterilized cover slips

(90000 cells per well). 0.4 µg of plasmids encoding 4E-T (WT or mutants) were transfected using Lipofectamin 2000 (Invitrogen). Two days after transfection, cells were fixed with 4% para-formaldehyde in PBS for 10 min and permeabilized for 10 min with PBS containing 0.5% Triton X-100. The cells were incubated for 1 h with the primary antibody in PBS containing 0.1% Tween 20 and 10% FBS and then for another hour with the secondary antibody in PBS with 0.1% Tween 20. Nuclear staining was performed with Hoechst 33342 (Thermo Fisher Scientific) diluted 1:1000 in PBS for 5 min. The monoclonal p70 S6Kinase antibody was used to label P-bodies as it strongly cross reacts with EDC4 (Kedersha and Anderson 2007). Cells were mounted using Fluoromount-G (Invitrogen). Images were acquired on a Leica TCS SP8 microscope.

Generation of the 4EHP-null cell line

Two sgRNAs targeting 4EHP were designed using the CHOPCHOP (<http://chopchop.cbu.uib.no>) online tool and cloned into the pSpCas9(BB)-2A-Puro (PX459) vector [a gift from F. Zhang, Addgene plasmid 48139; (Ran et al., 2013)]. Clonal cell lines were obtained and confirmed for gene editing as described previously (Peter et al., 2017). Sanger sequencing of the targeted genomic regions confirmed two frameshift mutations in exon 4 (an 11 nucleotide and a 37 nucleotide deletion) targeted by sg4EHP-a. For sg4EHP-b we did not observe gene editing; the amplified sequence around the target site in exon 2 is wild type. The absence of detectable 4EHP protein was confirmed by western blotting (Figure S7D). The following guide sequences were used: sg4EHP-a: 5'-TATAGCCACATGGTACGTCC-3'; sg4EHP-b: 5'-TGTTTTCTTCATTCTGATCA-3'.

Supplemental Table S1. Mutants and constructs used in this study

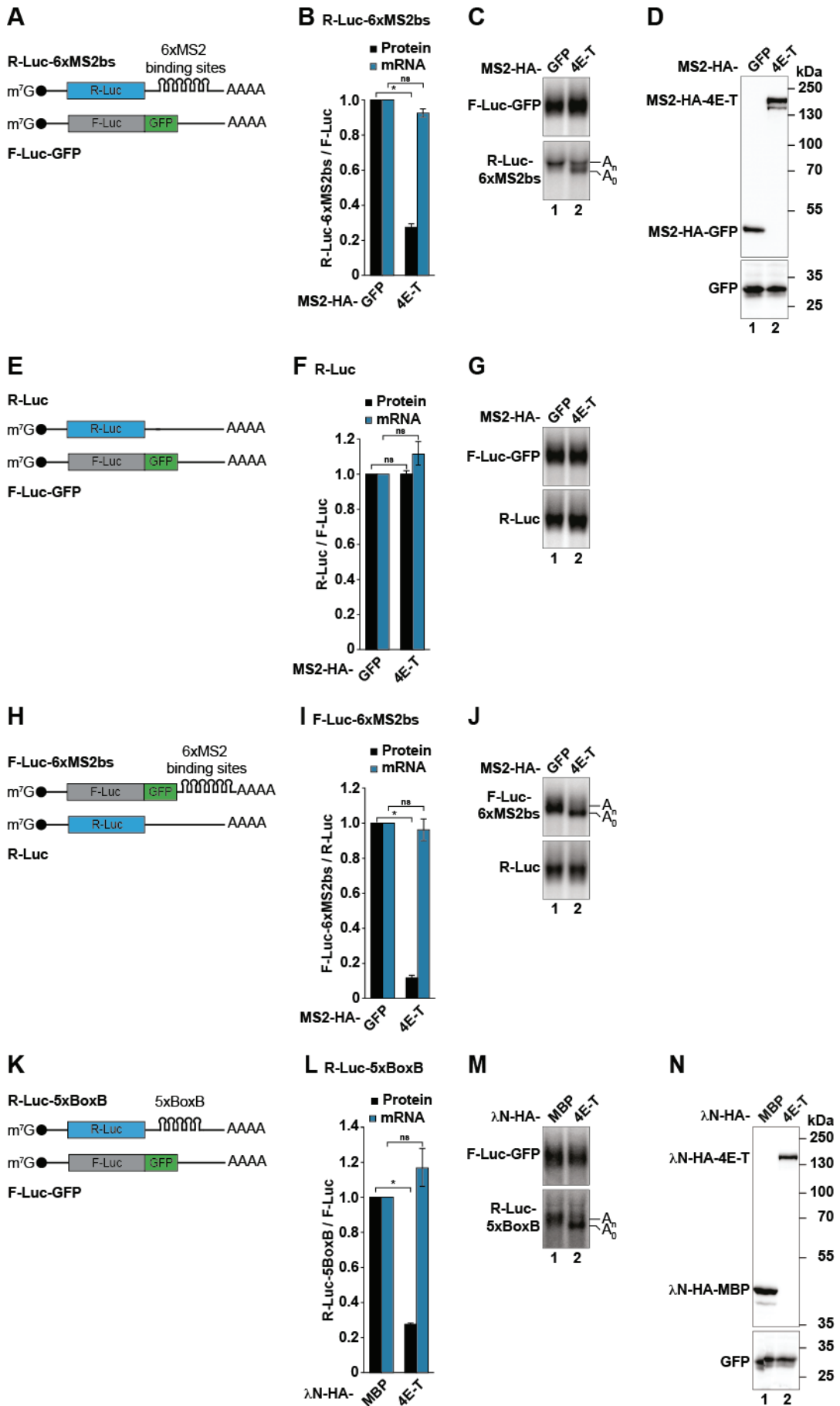
Name of construct	Fragment / mutations	Comments
<i>Hs</i> 4E-T (EIF4ENIF, Uniprot Q9NRA8)		
4E-T	Full length	
shRNA resistant	A2340G, A2343G, T2346C, T2349C, A2352T, T2355C	Nucleotides mutated in 4E-T CDS
C	Y30A, L35A	Mutated canonical eIF4E-binding motif
NC	W61D, W66D	Mutated non-canonical eIF4E-binding motif
Δ UNR	Δ V131-I161	
Δ DDX6	Δ P219-D240	Deletion of CHD (CUP homology domain)
Δ LSM14A	M1-S939, Δ D448-T490	
Δ PatL1	Δ S695-K713	
N-term	M1-F194	N-terminal fragment
Mid	D212-P612	Middle fragment
C-term	Q639-Q985	C-terminal fragment
4x Δ	M1-S939, Δ V131-I161, Δ P219-D240, Δ D448-T490, Δ S695-K713	Disruption of UNR, DDX6, LSM14A and PatL1 binding
Δ 335-490	Δ S335-T490	
Δ 448-490	Δ D448-T490	
1-939	M1-S939	
1-939 Δ 335-490	M1-S939, Δ S335-T490	
<i>Hs</i> NOT1 (CNOT1, Uniprot A5YKK6-1)		
NOT1 WT	Full length	
N-term	M1-V1089	N-terminal fragment
Central	T1085-T1605	Central fragment
C-term	L1595-S2376	C-terminal fragment
<i>Hs</i> UNR (CSDE1, Uniprot O75534)		
UNR	Full length	
<i>Hs</i> TTP (Uniprot P26651)		
TTP	Full length	
<i>Hs</i> DCP2 (Uniprot Q8IU60)		
DCP2*	E148Q	Catalytic inactive mutant
<i>Hs</i> NOT8 (POP2, Uniprot Q9UFF9)		
NOT8*	D40A, E42A	Catalytic inactive mutant
<i>Hs</i> TNRC6B (Uniprot Q9UPQ9-1)		
TNRC6B	Full length	

Supplemental Table S2: Antibodies used in this study

Antibody	Source	Cat. number	Dilution	Mono-/Polyclonal
Anti-HA-HRP	Roche	12013 819 001	1:5000	Monoclonal
Anti-GFP (for western blotting)	Roche	11 814 460 001	1:2000	Mouse Monoclonal
Anti-GFP (for immunoprecipitations)	In house			Rabbit Polyclonal
Anti-TUBULIN	Sigma Aldrich	T6199	1:5000	Monoclonal
Anti-DDX6	Bethyl	A300-461A	1:5000	Rabbit Polyclonal
Anti-PatL1	Bethyl	A303-482A		Rabbit Polyclonal
Anti-LSm14A	Abcam	ab123566	1:2000	Rabbit Polyclonal
Anti-V5	AbD Serotec	MCA1360GA	1:5000	Mouse Monoclonal
Anti-4E-T	Abcam	ab95030	1:2000	Rabbit Polyclonal
Anti-eIF4E	Bethyl	A301-154A-M	1:2000	Rabbit Polyclonal
Anti-NOT1	In house			Rabbit Polyclonal
Anti-NOT3	Abcam	ab55681	1:2000	Rabbit monoclonal
Anti-4EHP	In house		1:500	Rabbit Polyclonal
Anti-p70 S6 Kinase	Santa Cruz	sc-8418	1:1000	Mouse Monoclonal
Alexa Fluor ® 594 goat anti-mouse	Thermo Fisher Scientific	A-11005	1:1000	Polyclonal
Alexa Fluor ® 488 goat anti-rabbit	Thermo Fisher Scientific	A-11008	1:1000	Polyclonal

Supplemental Figures

Räsch336073_Supplemental Fig. S1

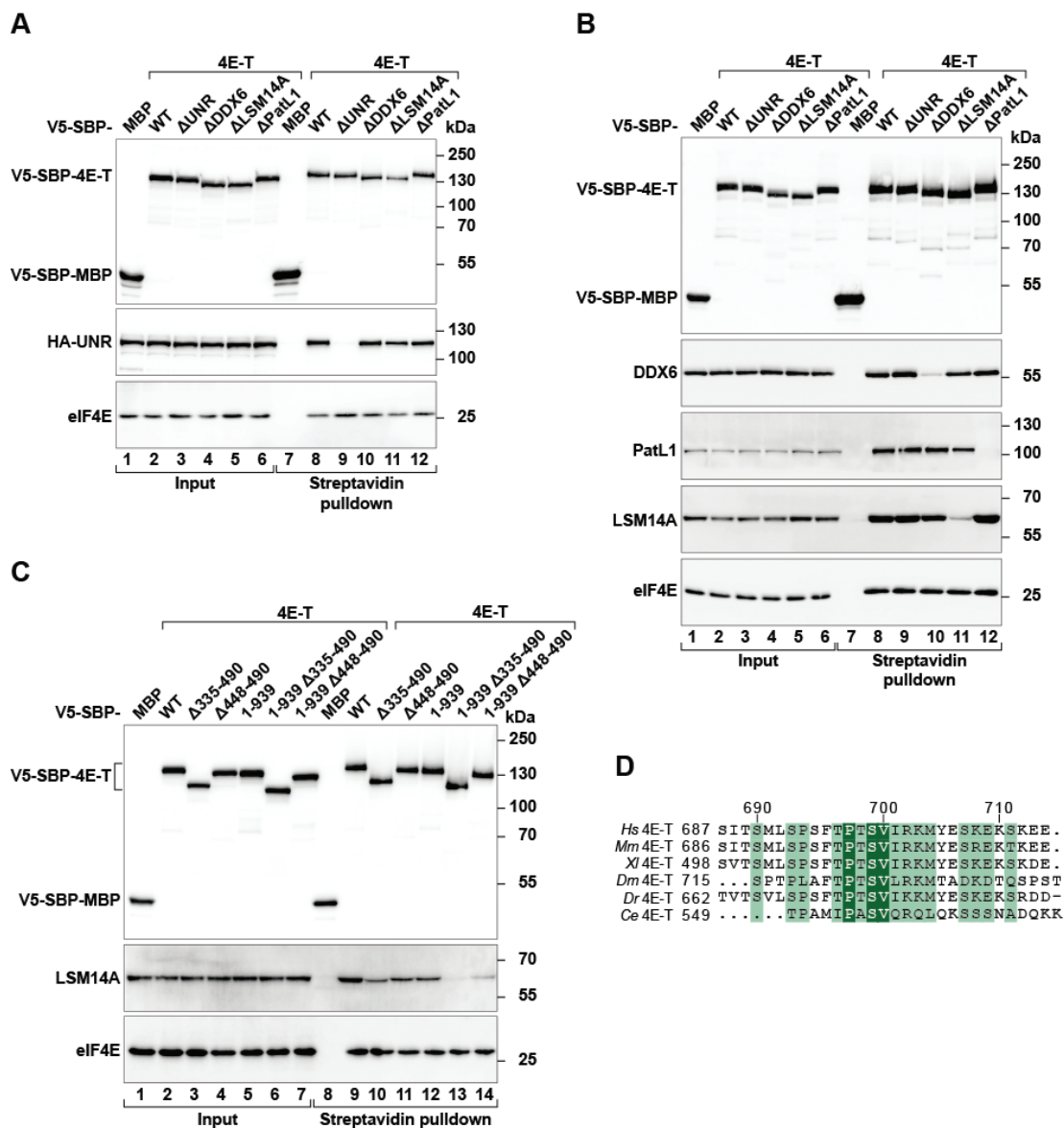


Supplemental Figure S1. 4E-T represses translation and induces mRNA deadenylation (related to Fig. 1)

(A, E, H, K) Schematic representations of the luciferase reporters used in this study. R-Luc: *Renilla* luciferase. F-Luc: firefly luciferase. GFP: Green fluorescent protein. The R-Luc-6xMS2bs and F-Luc-6xMS2bs reporters contain 6 MS2 binding sites in the 3' UTR. The R-Luc-5xBoxB contains 5 BoxB elements in the 3' UTR.

(B-D, F, G, I, J, L-N) Tethering of MS2-HA-4E-T or MS2-HA-GFP to the R-Luc-6xMS2bs (B), R-Luc (lacking the MS2 binding sites) (F), F-Luc-6xMS2bs (I) and R-Luc-5xBoxB (L) reporters in HEK293T cells. F-Luc-GFP (B, F and L) or R-Luc (I) were used as a transfection and normalization controls. R-Luc or F-Luc activity (protein: black bars) and mRNA levels (blue bars) were normalized to the transfection control and set to one in the experimental condition using MS2-HA-GFP. Mean values \pm SD are shown (n=3; *p<0.05; ns=not significant; paired t-test). Representative northern blot analyses are shown in (C), (G), (J) and (M). A₀, deadenylated and A_n, polyadenylated reporter mRNAs. The western blots showing the expression of the MS2-tagged and λ N-tagged proteins are shown in (D) and (N), respectively. GFP was used as a transfection control.

Räsch336073_Supplemental Fig. S2



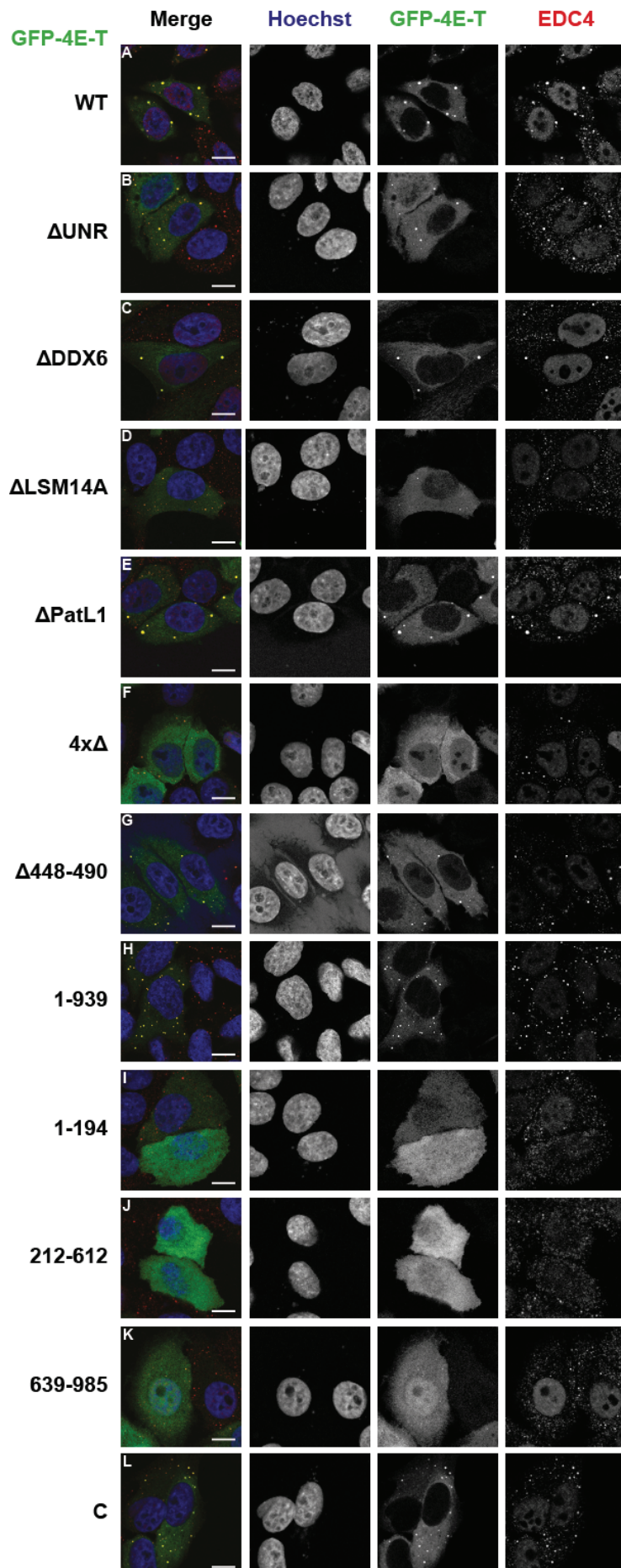
Supplemental Figure S2. 4E-T contains discrete UNR-, DDX6-, PatL1- and LSM14A-binding elements (related to Figs. 2 and 3)

(A-C) Analysis of the interaction of V5-SBP-4E-T wild type (WT), fragments or deletion mutants (Δ) with HA-UNR (A) or endogenous DDX6, PatL1 and LSM14A (B and C). SBP-tagged proteins were pulled down using streptavidin-coated beads. V5-SBP-MBP served as a negative control and eIF4E as a positive binding control. The inputs were 20 % for V5-SBP-proteins, 7.5 % for HA-UNR, 2.5 % for DDX6, 7.5 % for PatL1, 2 % for LSM14A and 20 % for eIF4E, whereas bound fractions corresponded to 10 % for V5-SBP-proteins, 30 % for HA-UNR, 40 % for DDX6, PatL1 and LSM14A, or 10 % for eIF4E. Samples were analyzed by

western blotting using anti-HA, anti-DDX6, anti-V5, anti-PatL1, anti-LSM14A and anti-eIF4E antibodies. In (C), the 4E-T 1-939 Δ 448-490 protein corresponds to Δ LSM14A. The lack of the NES in the proteins with deletion of residues 335-490 results in strong localization of 4E-T to the nucleus (data not shown) and therefore the 4E-T Δ 335-440 proteins were no longer used in this study.

(D) Sequence alignment of the motif required for PatL1 binding 4E-T proteins. Species are as follow: *Homo sapiens* (*Hs*), *Mus musculus* (*Mm*), *Xenopus laevis* (*Xl*), *Drosophila melanogaster* (*Dm*), *Danio rerio* (*Dr*) and *Caenorhabditis elegans* (*Ce*). Residues with >70% similarity are highlighted in light green. Conserved residues are shown with a dark green background and are printed in white.

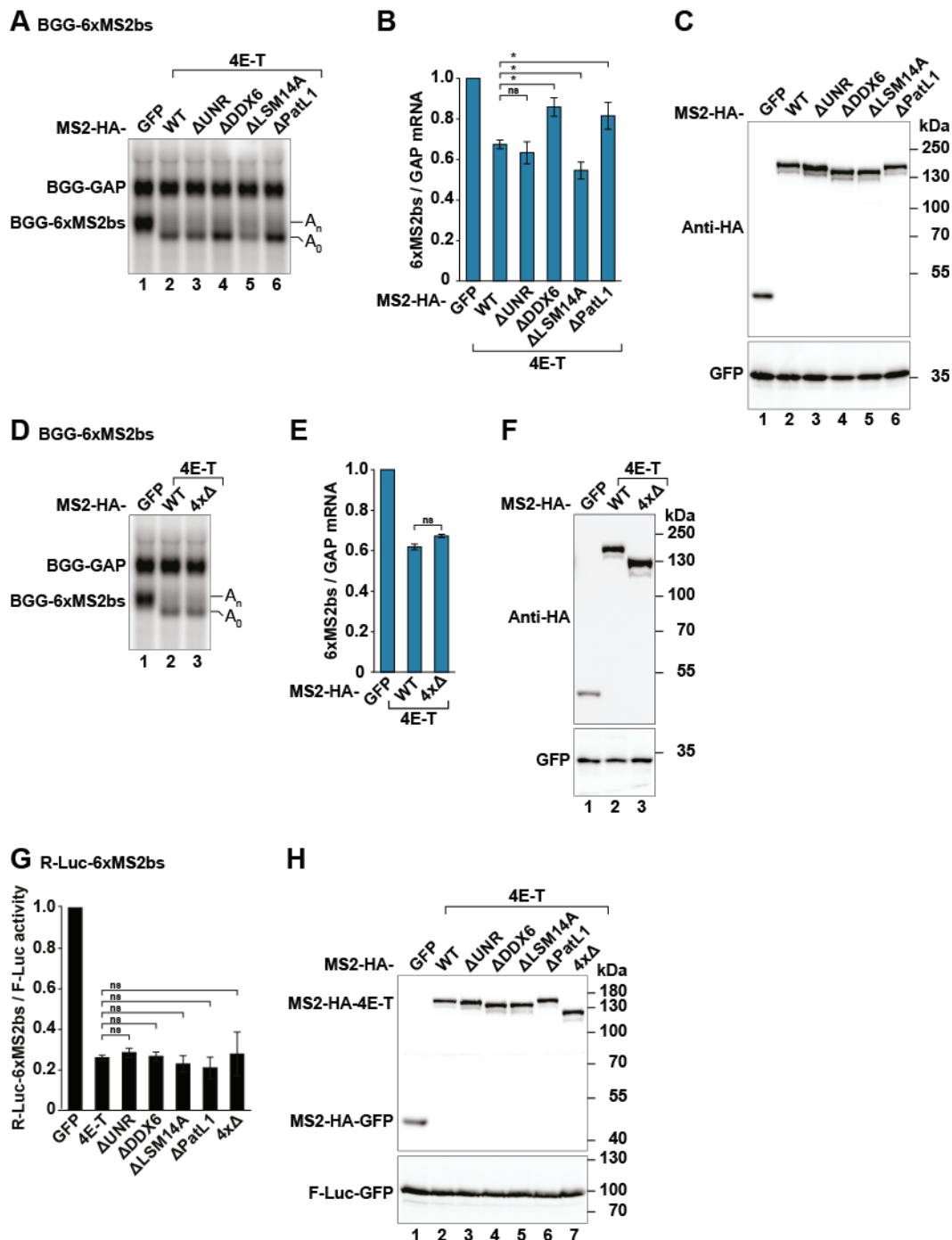
Räsch336073_Supplemental Fig. S3



Supplemental Figure S3. LSM14A regulates 4E-T accumulation in P-bodies (related to Figs. 2 and 3)

(A-L) Representative confocal fluorescent micrographs of fixed human HeLa cells expressing wild-type GFP-4E-T, the indicated mutants and fragments. Cells were stained with antibodies cross-reacting with EDC4 and a nuclear human antigen (Kedersha and Anderson 2007). The merged images show the GFP signal in green, the EDC4 signal in red and the nucleus in blue (Hoechst staining). Scale bar: 10 μ m. C: 4E-T canonical mutant, 4x Δ : combined deletions of the UNR, DDX6, LSM14A and PatL1 binding sites on 4E-T.

Räsch336073_Supplemental Fig. S4



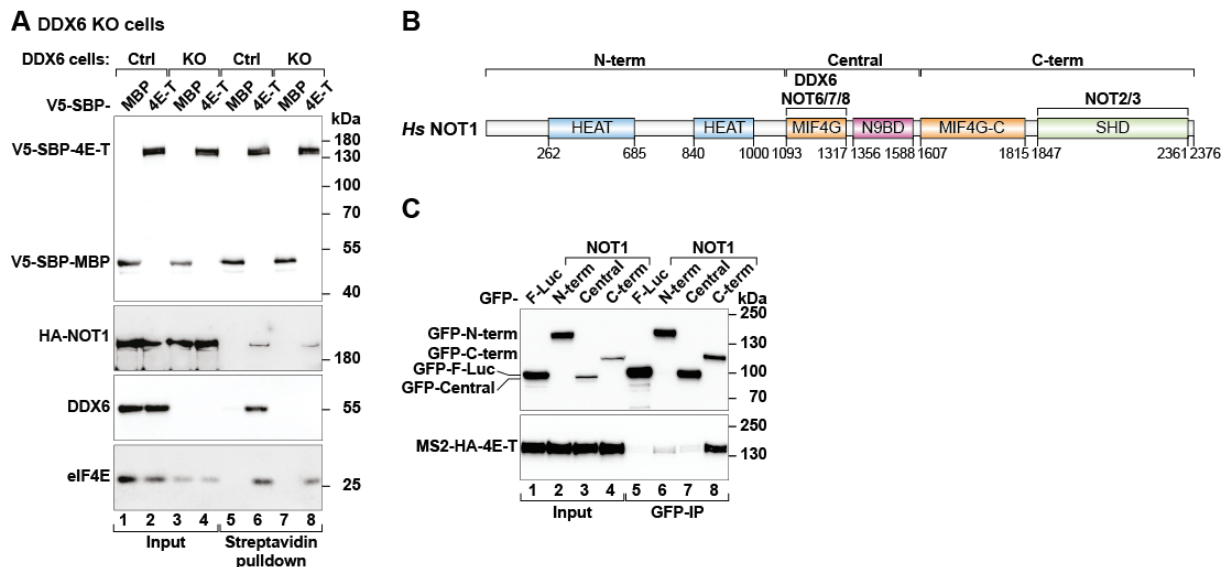
Supplemental Figure S4. 4E-T mediated mRNA deadenylation does not require UNR, DDX6, LSM14A and PatL1 (related to Fig. 3)

(A-F) HEK293T cells were co-transfected with plasmids expressing BGG-6xMS2bs, BGG-GAP and the indicated MS2-HA-tagged proteins. RNA samples were analyzed by northern blotting (A and D). A₀, deadenylated and A_n, polyadenylated reporter mRNAs. BGG-6xMS2bs mRNA levels were normalized to those of BGG-GAP and set to 1 in the presence

of MS2-HA-GFP. Mean values \pm SD are shown in (B) and (E) (n=3; *p<0.05; ns=not significant; paired t-test). Wild type and mutant 4E-T proteins were expressed at comparable levels as shown by western blotting in (C) and (F). GFP was used as a transfection control.

(G, H) Cells were transfected with plasmids expressing R-Luc-6xMS2bs, F-Luc-GFP and the indicated MS2-HA-tagged proteins. R-Luc activity was normalized to that of F-Luc and set to 1 in the presence of MS2-HA-GFP. Mean values \pm SD are shown in (G) (n=3; ns=not significant; paired t-test). Wild-type and mutant 4E-T proteins were expressed at comparable levels as shown by western blotting in (H).

Räsch336073_Supplemental Fig. S5



Supplemental Figure S5. The interactions of 4E-T with NOT1 (related to Fig. 3)

(A) Analysis of the interaction of V5-SBP-4E-T with HA-NOT1 in HEK293T control (Ctrl) and DDX6-null cells (KO). The proteins were pulled down using streptavidin beads. V5-SBP-MBP was used as a negative control. The inputs were 20 % for V5-SBP-proteins and eIF4E, and 5 % for HA-NOT1 and DDX6. Bound fractions corresponded to 10 % for V5-SBP-proteins and eIF4E, and 40 % for HA-NOT1 and DDX6. Samples were analyzed by western blotting using anti-HA, anti-V5, anti-DDX6 and anti-eIF4E antibodies.

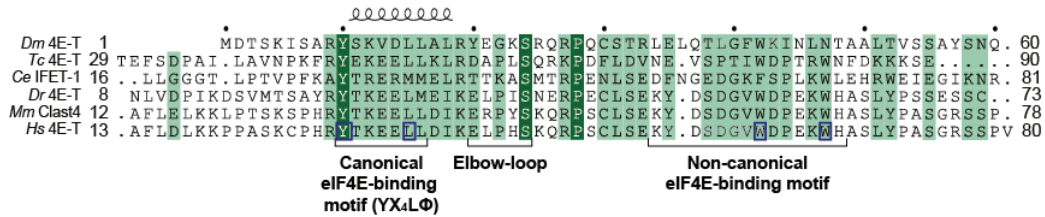
(B) Schematic overview of the domain architecture and binding regions of NOT1. NOT1 is divided into an N-term region containing two HEAT repeats, a Central region with the Middle domain of eukaryotic initiation factor 4G (MIF4G) that interacts with the deadenylases NOT6, NOT7 and NOT8 as well as DDX6, and the NOT9 binding domain which binds NOT9, and a C-term region comprising the C-terminal MIF4G domain (MIF4G-C) and the superfamily homology domain (SHD) which associates with NOT2 and NOT3. The amino acid positions at the domain/motif boundaries are indicated below the protein.

(C) Immunoprecipitation assay showing the interaction between the N-term, Central or C-term regions of NOT1 and HA-4E-T. The proteins were immunoprecipitated using anti-GFP antibodies. F-Luc-GFP served as a negative control. The input (10 % for GFP-tagged proteins

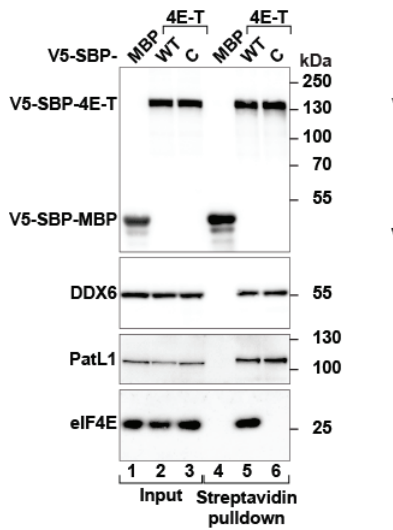
and 2.5 % for HA-4E-T) and bound fractions (20 % for GFP-tagged proteins and 40 % for HA-4E-T) were analyzed by western blotting using anti-GFP and anti-HA antibodies.

Räsch336073_Supplemental Fig. S6

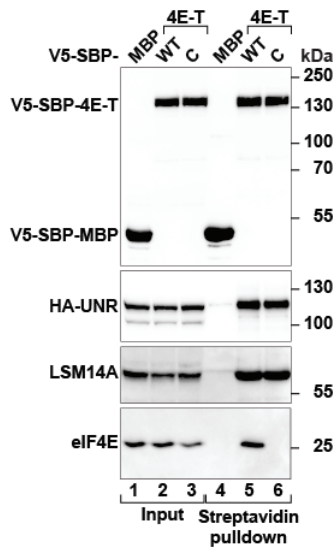
A



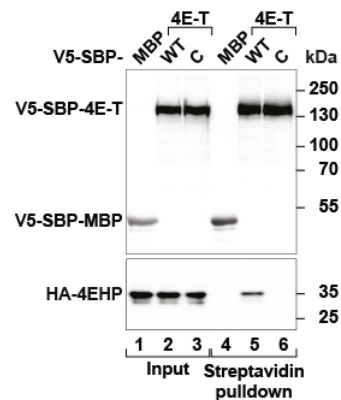
B



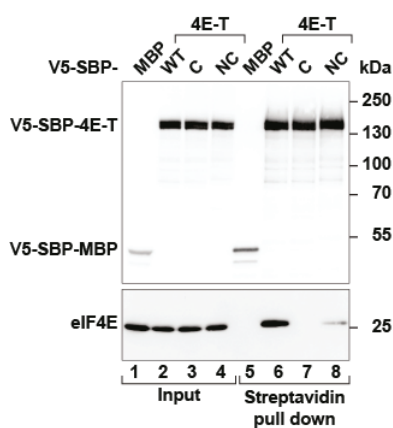
C



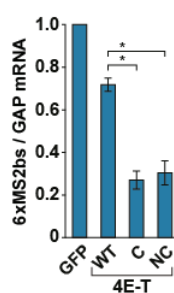
D



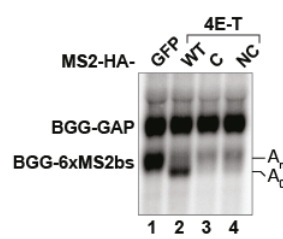
E



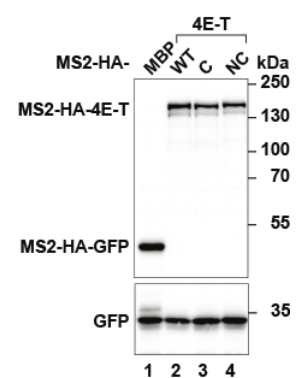
F



G



H



Supplemental Figure S6. The interactions of 4E-T with eIF4E and 4EHP (related to Fig.

4)

(A) Alignment of the eIF4E-binding region of 4E-T orthologues. The species are *Drosophila melanogaster* (Dm), *Tribolium castaneum* (Tc), *Caenorhabditis elegans* (Ce), *Danio rerio* (Dr), *Mus musculus* (Mm) and *Homo sapiens* (Hs). Conserved residues are highlighted with a dark green background and printed in white. Residues with >70% similarity are shown with a light green background and printed in white.

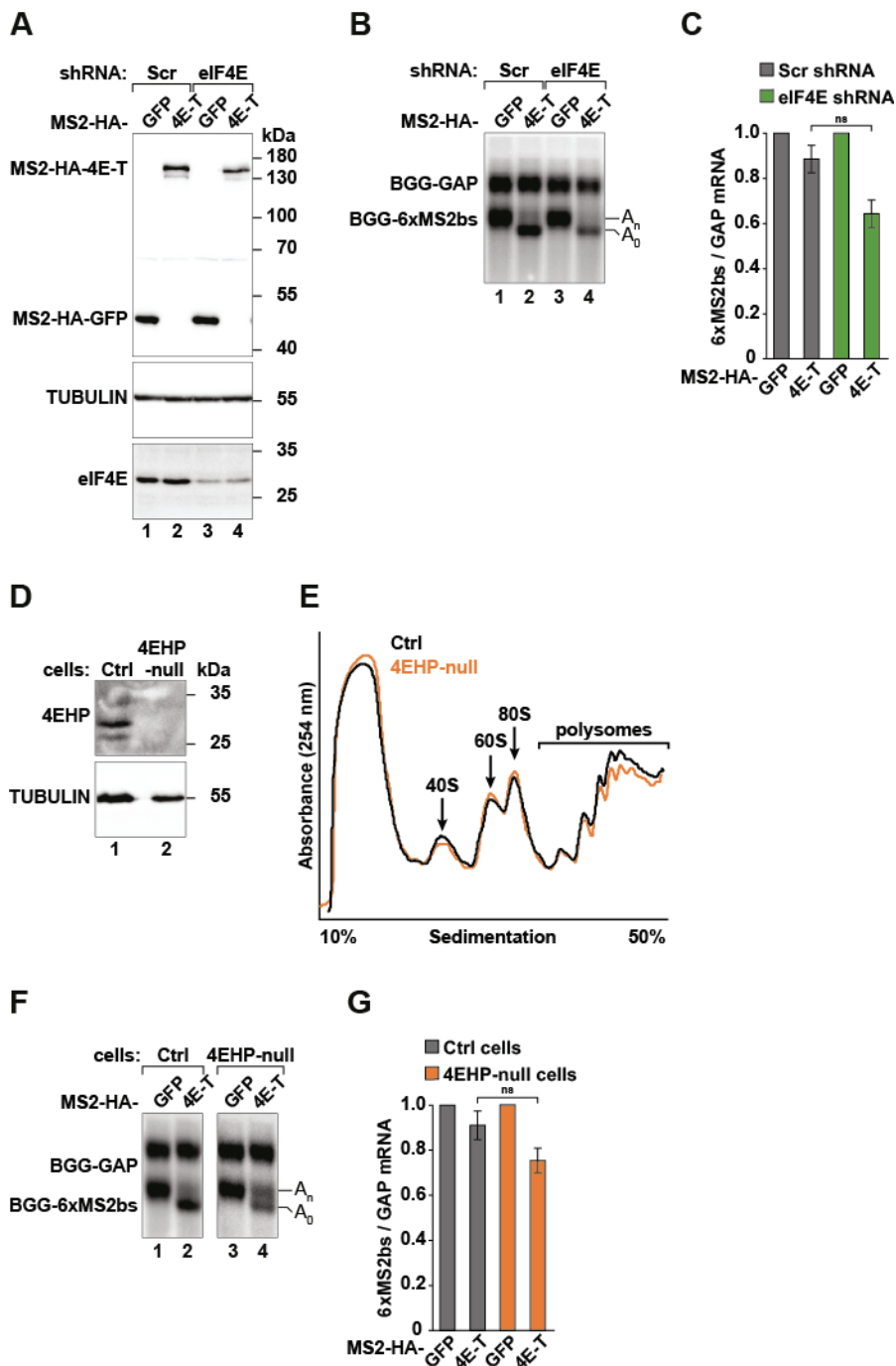
light green background. Secondary structural elements above the alignment are according to the structure of *Dm* 4E-T in complex with eIF4E (PDB ID: 4UE9; Peter et al., 2015). The eIF4E-binding region of 4E-BPs are characterized by a canonical motif (YX₄LΦ), an elbow-loop and a non-canonical motif. Residues mutated in this study are boxed in dark blue.

(B-D) Pulldown assays depicting the interaction of V5-SBP-4E-T WT or canonical mutant (C) with eIF4E, DDX6, PatL1, HA-UNR, LSM14A and 4EHP. The proteins were pulled down using streptavidin beads. V5-SBP-MBP was used as a negative control. The inputs were 20 % for V5-SBP-proteins, HA-4EHP and eIF4E, 7.5 % for HA-UNR, 2.5 % for DDX6, 7.5 % for PatL1 and 2 % for LSM14A. Bound fractions corresponded to 10 % for V5-SBP-proteins, HA-4EHP and eIF4E, 30 % for HA-UNR, 40 % for DDX6, PatL1 and LSM14A. Samples were analyzed by western blotting using anti-HA, anti-DDX6, anti-V5, anti-PatL1, anti-LSM14A and anti-eIF4E antibodies.

(E) Analysis of the interaction of V5-SBP-4E-T wild type (WT), canonical (C) and non-canonical (NC) eIF4E-binding mutants with eIF4E in HEK293T cells. The proteins were pulled down using streptavidin beads. V5-SBP-MBP was used as a negative control. The inputs were 40 % and the bound fractions 10 % of the total sample. Samples were analyzed by western blotting using anti-eIF4E and anti-V5 antibodies.

(F-H) Tethering assay with the BGG-6xMS2bs, BGG-GAP and MS2-HA-GFP or MS2-HA-4E-T wild type (WT), canonical (C) and non-canonical (NC) eIF4E-binding mutants. The graph in panel (F) depicts the relative quantification of the BGG-6xMS2bs mRNA levels, as described in Supplemental Fig. S4 (n=3; * = p < 0.05; paired t-test). Representative northern and western blots are depicted in panels (G) and (H), respectively. A₀, deadenylated and A_n, polyadenylated reporter mRNAs.

Räsch336073_Supplemental Fig. S7



Supplemental Figure S7. eIF4E and 4EHP have distinct roles in the regulation of deadenylation and decapping by 4E-T (related to Fig. 4)

(A) Immunoblot showing shRNA-mediated depletion of eIF4E in HEK293T cells. Transfected MS2-HA-GFP and MS2-HA-4E-T were expressed at comparable levels in scramble (Scr) shRNA or eIF4E shRNA-treated cells. TUBULIN served as a loading control. Samples were analyzed using anti-HA, anti-TUBULIN and anti-eIF4E antibodies.

(B, C) Tethering assay with the BGG-6xMS2bs, BGG-GAP and MS2-HA-GFP or MS2-HA-4E-T in Scr shRNA (gray) or eIF4E shRNA (green)-treated cells. A representative northern blot is shown in (B). A₀, deadenylated and A_n, polyadenylated reporter mRNAs. The graph in panel (C) depicts the relative quantification of the BGG-6xMS2bs mRNA levels, as described in Supplemental Fig. S4 (n=3; ns= not significant; paired t-test).

(D) Western blot demonstrating the loss of 4EHP expression in the null cells. TUBULIN served as a loading control. Samples were analyzed using anti-4EHP and anti-TUBULIN antibodies.

(E) UV absorbance profile at 254 nm of control (Ctrl) and 4EHP-null (orange) HEK293T cell extracts after polysome sedimentation in a sucrose gradient. Peaks representing free 40S and 60S subunits, 80S monosomes, and polysomes are indicated.

(F, G) Tethering assay in Ctrl (gray) and 4EHP-null (orange) cells with BGG-6xMS2bs, BGG-GAP and MS2-HA-GFP or MS2-HA-4E-T. A representative northern blot is shown in (F). A₀, deadenylated and A_n, polyadenylated reporter mRNAs. The graph in panel (G) depicts the relative quantification of the BGG-6xMS2bs mRNA levels, as described in Supplemental Fig. S4 (n=3; ns= not significant; paired t-test).

References

- Braun JE, Tritschler F, Haas G, Igreja C, Truffault V, Weichenrieder O, Izaurralde E. 2010. The C-terminal alpha-alpha superhelix of Pat is required for mRNA decapping in metazoa. *EMBO J* **29**: 2368-2380.
- Hanet A, Rasch F, Weber R, Ruscica V, Fauser M, Raisch T, Kuzuoglu-Ozturk D, Chang CT, Bhandari D, Igreja C et al. 2019. HELZ directly interacts with CCR4-NOT and causes decay of bound mRNAs. *Life Sci Alliance* **2**: e201900405.
- Lazzaretti D, Tournier I, Izaurralde E. 2009. The C-terminal domains of human TNRC6A, TNRC6B, and TNRC6C silence bound transcripts independently of Argonaute proteins. *RNA* **15**: 1059-1066.
- Loh B, Jonas S, Izaurralde E. 2013. The SMG5-SMG7 heterodimer directly recruits the CCR4-NOT deadenylase complex to mRNAs containing nonsense codons via interaction with POP2. *Genes Dev* **27**: 2125-2138.
- Lykke-Andersen J, Shu MD, Steitz JA. 2000. Human Upf proteins target an mRNA for nonsense-mediated decay when bound downstream of a termination codon. *Cell* **103**: 1121-1131.
- Peter D, Igreja C, Weber R, Wohlbold L, Weiler C, Ebertsch L, Weichenrieder O, Izaurralde E. 2015. Molecular Architecture of 4E-BP Translational Inhibitors Bound to eIF4E. *Mol Cell* **57**: 1074-1087.
- Peter D, Weber R, Sandmeir F, Wohlbold L, Helms S, Bawankar P, Valkov E, Igreja C, Izaurralde E. 2017. GIGYF1/2 proteins use auxiliary sequences to selectively bind to 4EHP and repress target mRNA expression. *Genes Dev* **31**: 1147-1161.
- Petit AP, Wohlbold L, Bawankar P, Huntzinger E, Schmidt S, Izaurralde E, Weichenrieder O. 2012. The structural basis for the interaction between the CAF1 nuclease and the NOT1 scaffold of the human CCR4-NOT deadenylase complex. *Nucleic Acids Res* **40**: 11058-11072.





Pillai RS, Artus CG, Filipowicz W. 2004. Tethering of human Ago proteins to mRNA mimics the miRNA-mediated repression of protein synthesis. *RNA* **10**: 1518-1525.

Ran FA, Hsu PD, Wright J, Agarwala V, Scott DA, Zhang F. 2013. Genome engineering using the CRISPR-Cas9 system. *Nat Protoc* **8**: 2281-2308.

Zipprich JT, Bhattacharyya S, Mathys H, Filipowicz W. 2009. Importance of the C-terminal domain of the human GW182 protein TNRC6C for translational repression. *RNA* **15**: 781-793.



HELZ directly interacts with CCR4–NOT and causes decay of bound mRNAs

Aoife Hanet¹, Felix Räsch¹ , Ramona Weber¹, Vincenzo Ruscica¹, Maria Fauser¹, Tobias Raisch^{1,2} , Duygu Kuzuoglu-Öztürk^{1,3} , Chung-Te Chang¹, Dipankar Bhandari¹, Cátia Igreja¹ , Lara Wohlbold¹

Eukaryotic superfamily (SF) 1 helicases have been implicated in various aspects of RNA metabolism, including transcription, processing, translation, and degradation. Nevertheless, until now, most human SF1 helicases remain poorly understood. Here, we have functionally and biochemically characterized the role of a putative SF1 helicase termed “helicase with zinc-finger,” or HELZ. We discovered that HELZ associates with various mRNA decay factors, including components of the carbon catabolite repressor 4-negative on TATA box (CCR4–NOT) deadenylase complex in human and *Drosophila melanogaster* cells. The interaction between HELZ and the CCR4–NOT complex is direct and mediated by extended low-complexity regions in the C-terminal part of the protein. We further reveal that HELZ requires the deadenylase complex to mediate translational repression and decapping-dependent mRNA decay. Finally, transcriptome-wide analysis of *Helz*-null cells suggests that HELZ has a role in the regulation of the expression of genes associated with the development of the nervous system.

DOI 10.26508/lsa.201900405 | Received 2 May 2019 | Revised 13 September 2019 | Accepted 13 September 2019 | Published online 30 September 2019

Introduction

RNA helicases are ubiquitous enzymes that mediate ATP-dependent unwinding of RNA duplexes and promote structural rearrangements of RNP complexes. They participate in all aspects of RNA metabolism such as transcription, processing, translation, ribosome assembly, and mRNA decay (Bleichert & Baserga, 2007). There are six helicase superfamilies (SFs) 1–6 defined by sequence, structure, and mechanism (Singleton et al, 2007). Eukaryotic helicases belong exclusively to either SF1 or SF2, which are characterized by a structural core composed of tandem RecA-like domains and as many as 12 conserved sequence motifs that mediate substrate binding, catalysis, and unwinding (Fairman-Williams et al, 2010). Approximately 70 RNA helicases are known to be expressed in human cells, most of which belong to the SF2 superfamily, such as the well characterized DEAD (Asp-Glu-Ala-Asp)-box family of helicases (Sloan & Bohnsack, 2018). To date, only 11

SF1 RNA helicases have been identified; among them is the highly conserved upstream frameshift 1 (UPF1) helicase, which has an important role in nonsense-mediated mRNA decay (Kim & Maquat, 2019). Few other eukaryotic UPF1-like SF1 helicases have been investigated in detail. Senataxin, the human orthologue of yeast Sen1p, has a role in transcriptional regulation (Ursic et al, 2004; Chen et al, 2006; Leonaite et al, 2017). Other examples are the mammalian moloney leukemia virus homolog 10 (MOV10), the fly Armitage and the silencing defective protein 3 (SDE3) in plants, which all function in post-transcriptional gene silencing (Dalmay et al, 2001; Cook et al, 2004; Burdick et al, 2010; Gregersen et al, 2014).

The putative RNA “Helicase with Zinc-finger” (HELZ) is conserved in Metazoa and belongs to the UPF1-like family of SF1 helicases (Fairman-Williams et al, 2010). The gene encoding HELZ was cloned from a human immature myeloid cell line cDNA library (KIA0054) over 20 years ago but its cellular function remains poorly studied (Nomura et al, 1994). HELZ helicases are large proteins that contain a Cys₃His (CCCH)-type zinc finger (ZnF) motif N-terminal to the helicase core, and a largely unstructured C-terminal half with a conserved polyadenosine (poly[A])-binding protein (PABP)-interacting motif 2 (PAM2) (Fig 1A). The C-terminal half of HELZ varies in size and sequence depending on the species. Two LxxLAP (Leu, x indicates any amino acid, Leu, Ala, Pro) motifs are also embedded within the HELZ C-terminal region; these motifs are found in hypoxia-inducible transcription factors and regulate their stability in response to oxygen depletion; HELZ abundance, however, does not appear to be associated with oxygen levels (Hasgall et al, 2011).

Murine HELZ has a widespread spatial and temporal expression throughout embryonic development (Wagner et al, 1999). Human HELZ is a component of complexes containing the RNA Polymerase II, as well as the histone methyltransferases Smyd2 or Smyd3, which indicates a target-specific role in transcription (Hamamoto et al, 2004; Diehl et al, 2010). HELZ stimulates translation when overexpressed in human cells and interacts with cytoplasmic polyadenylate-binding protein 1 (PABPC1) (Hasgall et al, 2011). PABPs represent a major class of mRNA-regulating proteins that interact with the poly(A) tail of mRNAs, thereby influencing their stability and translation efficiency (Goss & Kleiman, 2013; Nicholson & Pasquinelli, 2019). The shortening of the poly(A) tail

¹Department of Biochemistry, Max Planck Institute for Developmental Biology, Tübingen, Germany ²Department of Structural Biochemistry, Max Planck Institute of Molecular Physiology, Dortmund, Germany ³Helen Diller Family Cancer Research, University of California San Francisco, San Francisco, CA, USA

Correspondence: catia.igreja@tuebingen.mpg.de; lara.wohlbold@tuebingen.mpg.de

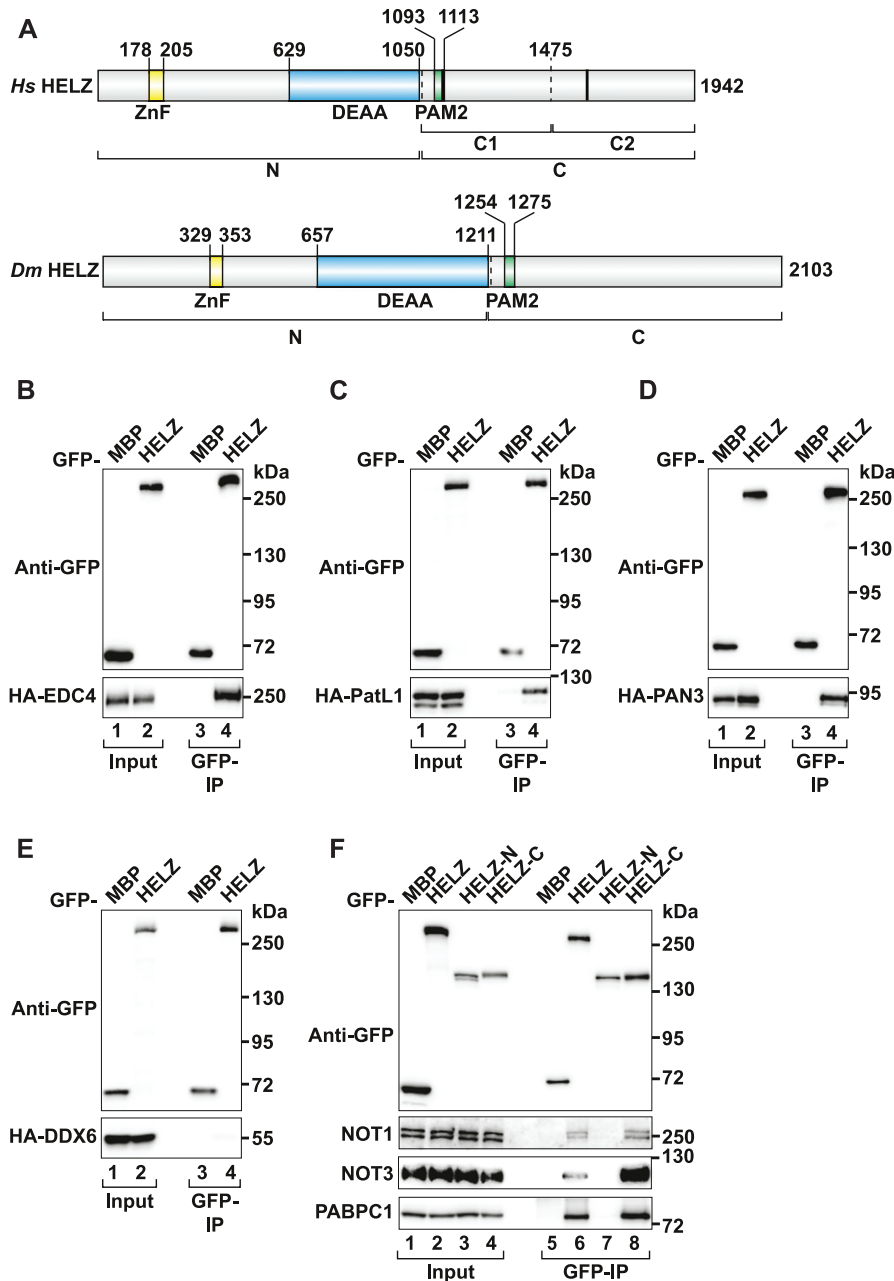


Figure 1. HELZ interacts with mRNA decay factors. (A) Schematic representation of *Hs* HELZ and *Dm* HELZ. The Zinc finger (ZnF), the putative helicase (DEAA, Asp, Glu, Ala, Ala), and the PABP interacting motif 2 (PAM2) are highlighted in yellow, blue, and green, respectively. Black bars indicate the position of the previously described LxxLAP motifs in *Hs* HELZ (Hasgall et al, 2011). HELZ N- and C-terminal fragments are indicated below the scheme. Border residue numbers are listed above the scheme. (B–E) Immunoprecipitation assay in HEK293T cells showing the interaction of GFP-HELZ with HA-tagged EDC4 (B), HA-tagged-PatL1 (C), HA-tagged-PAN3 (D), and HA-tagged-DDX6 (E). GFP-MBP served as negative control. Input (2% for GFP-tagged proteins and 1% for HA-tagged proteins) and bound fractions (20% for GFP-tagged proteins and 30% for HA-tagged proteins) were analysed by Western blotting. (F) Immunoprecipitation assay in HEK293T cells showing the interaction of GFP-tagged HELZ (full-length and indicated fragments) with endogenous NOT1, NOT3, and PABPC1. Input (1.2%) and bound fractions (20% for GFP-tagged proteins and 35% for endogenous proteins) were analysed by Western blotting. Source data are available for this figure.

and concomitant release of PABPC1, a process termed deadenylation, is a critical determinant of mRNA stability and translational efficiency (Inada & Makino, 2014; Webster et al, 2018). HELZ was detected in a screen for helicases that interact with the carbon catabolite repressor 4-negative on TATA box (CCR4–NOT) complex (Mathys et al, 2014), the major cytoplasmic deadenylase in eukaryotes (Yi et al, 2018). The association of HELZ with the deadenylase complex hints at an important but presently uncharacterized role of this helicase in regulating stability and translation of mRNA.

In this study, we show that human HELZ directly interacts with the NOT module of the CCR4–NOT complex via multiple motifs embedded within the low-complexity region of the protein. In tethering assays with reporter mRNAs, HELZ elicits deadenylation

followed by decapping and subsequent 5'-to-3' exonucleolytic decay. The ability of HELZ to induce decay of bound mRNAs is conserved in Metazoa and depends on the CCR4–NOT complex. We also provide evidence that tethered HELZ can repress translation independently of mRNA decay in a manner dependent on both the CCR4–NOT complex and the DEAD-box helicase DDX6. Finally, using transcriptome sequencing, we identified 3,512 transcripts differentially expressed (false discovery rate [FDR] < 0.005) in *Helz*-null cells. Interestingly, many of the up-regulated mRNAs are linked with the development of the nervous system.

Taken together, our data reveal an important function of HELZ in governing the expression of specific genes, possibly through both transcriptional and posttranscriptional regulatory mechanisms.

Results

HELZ interacts with mRNA decay factors

HELZ is a largely uncharacterized protein implicated in post-transcriptional gene regulation (Hasgall et al, 2011; Mathys et al, 2014). To identify novel HELZ-interacting partners, we performed co-immunoprecipitation (co-IP) assays using overexpressed GFP-tagged *Hs* HELZ as bait against different hemagglutinin (HA)-tagged proteins in human HEK293T cells. HELZ interacted with multiple mRNA decay factors, including the decapping enhancers EDC4 and PatL1 as well as the poly(A) specific ribonuclease subunit 3 (PAN3) subunit of the PAN2/PAN3 deadenylase complex (Fig 1B–D). However, under the co-IP conditions, we did not detect an interaction with DDX6, as previously identified by mass spectrometry (Ayache et al, 2015) (Fig 1E). GFP-HELZ readily immunoprecipitated the endogenous CCR4–NOT deadenylase complex proteins NOT1 and NOT3 (Fig 1F, lane 6), suggesting that HELZ associates with the fully assembled complex in cells. PABPC1, which binds to HELZ via its PAM2 motif (Hasgall et al, 2011), was used as a positive control.

To delineate the region of HELZ critical for the interaction with CCR4–NOT, we divided the HELZ protein into an N-terminal fragment encompassing the ZnF motif and the helicase domain (HELZ-N, Table S1) and a second fragment comprising the low-complexity C-terminal region of HELZ including the PAM2 motif (HELZ-C, Table S1 and Fig 1A). Both fragments were then tested separately for their ability to interact with NOT1 and NOT3. Interestingly, the HELZ-C fragment was sufficient to mediate binding to NOT1 and NOT3 as well as PABPC1. In contrast, HELZ-N did not interact with any of these proteins (Fig 1F, lanes 7 and 8).

HELZ directly binds CCR4–NOT via multiple C-terminal sites

The CCR4–NOT complex consists of several subunits arranged around the scaffold protein NOT1 (Collart & Panasenko, 2017). NOT10 and NOT11 bind to the N-terminal region of NOT1 (Lau et al, 2009; Bawankar et al, 2013; Mauxion et al, 2013). The catalytically active nucleases CAF1 (or its paralog POP2) and CCR4a (or its paralog CCR4b) bind to a central MIF4G (middle-domain of eIF4G)-like domain of NOT1 (Lau et al, 2009; Basquin et al, 2012; Petit et al, 2012) adjacent to the CAF40-binding domain (CC) of NOT1 (Chen et al, 2014; Mathys et al, 2014). The CC domain is followed by a short connector domain in NOT1, recently identified to be an additional MIF4G-like domain, termed MIF4G-C (Raisch et al, 2018). NOT2 and NOT3 assemble on the C-terminal part of NOT1 (Bhaskar et al, 2013; Boland et al, 2013).

To test whether the interaction of HELZ with the CCR4–NOT complex is direct, we performed pull-down assays with recombinant and purified proteins. Production of intact HELZ-C in bacteria was not possible as it was very susceptible to proteolytic degradation. Therefore, we divided HELZ-C into two non-overlapping fragments of roughly similar size: HELZ-C1 and HELZ-C2 (Table S1 and Fig 1A). These fragments, fused to an N-terminal maltose-binding protein (MBP) and a C-terminal B1 domain of immunoglobulin-binding protein G (GB1)-hexahistidine tag (Cheng & Patel, 2004), were more stable during bacterial production. Following capture by nickel affinity, the eluted HELZ fragments were incubated with different recombinant human

CCR4–NOT subcomplexes and pulled down via the MBP tag. In detail, we tested the interaction of HELZ with a pentameric subcomplex comprising a NOT1 fragment lacking the N-terminal region bound to CAF1, CAF40, and the C-terminal domains of NOT2 and NOT3 (Fig 2A) (Sgromo et al, 2017). HELZ-C1 and HELZ-C2 fragments both pulled down the pentameric subcomplex (Fig 2B and C, lanes 20). To elucidate which subunits of the pentameric subcomplex are involved in the interaction with HELZ, we also analysed binding to the CAF1/NOT1-MIF4G heterodimer, the CAF40 module (CAF40/NOT1-CC), the subsequent NOT1 MIF4G-C domain (CD), and the NOT module (NOT1/2/3) (Fig 2A) (Sgromo et al, 2017). HELZ-C1 and HELZ-C2 fragments both pulled down the NOT module of CCR4–NOT (Fig 2B and C, lane 24). Neither fragment interacted with the CAF1 module, the CAF40 module, or the MIF4G-C domain (Fig 2B and C, lanes 21–23). We conclude that human HELZ directly binds the NOT module using multiple sites in the low-complexity C-terminal region.

HELZ induces 5′-to-3′ decay of tethered reporter mRNAs

To address the role of HELZ in the regulation of mRNA stability, we performed MS2-based tethering assays in HEK293T cells. We used a β -globin mRNA reporter containing six MS2-binding sites in the 3′ UTR (β -globin-6xMS2bs) and co-expressed full-length HELZ with an MS2-HA-tag (Fig 3A–C) (Lykke-Andersen et al, 2000). Tethering of HELZ resulted in a threefold reduction in the β -globin-6xMS2bs mRNA levels compared with the control protein MS2-HA (Fig 3A and B). The levels of a control reporter mRNA lacking the 6xMS2bs (control) were unaffected (Fig 3B). Consistent with the ability to bind CCR4–NOT, the C-terminal region of HELZ was sufficient to trigger mRNA decay when tethered to the same reporter mRNA. In contrast, the N-terminal region of HELZ containing the ZnF and helicase core did not induce decay of the reporter mRNA (Fig 3A and B).

We then tested whether HELZ binding to PABPC1 is required to induce decay of the tethered reporter mRNA. We introduced a point mutation in the HELZ PAM2 motif (F1107V) that specifically disrupts the interaction with PABPC1 (Fig 3D, lane 6) (Kozlov et al, 2001; Berlanga et al, 2006). Interestingly, the F1107V mutation did not alter the ability of HELZ to reduce the abundance of the bound mRNA reporter (Fig 3E–G), indicating that binding to PABPC1 is not required for this function.

To determine if a functional CCR4–NOT complex was necessary for HELZ-mediated degradation of bound mRNAs in cells, we first impaired the deadenylation activity of the CCR4–NOT complex by overexpressing a catalytically inactive mutant of CAF1 (CAF1*; D40A/E42A), which replaces the endogenous enzyme in a dominant negative manner (Horiuchi et al, 2009; Huntzinger et al, 2013). In addition, we overexpressed the Mid-region of NOT1 (residues T1085–T1605) to compete with endogenous NOT1 and sequester CAF1/CCR4 deadenylases as well as CAF40 from the endogenous deadenylase complex, compromising its activity. Overexpression of CAF1*/NOT1-Mid, together with MS2-HA-HELZ, led to a marked stabilization of the β -globin-6xMS2bs mRNA (Fig 3H–J). This is consistent with a model in which mRNA decay triggered by HELZ requires CCR4–NOT-mediated deadenylation.

We then blocked mRNA decapping by overexpressing a catalytically inactive mutant of DCP2 (DCP2*; E148Q) (Wang et al, 2002; Chang et al, 2014). This resulted in the accumulation of a fast

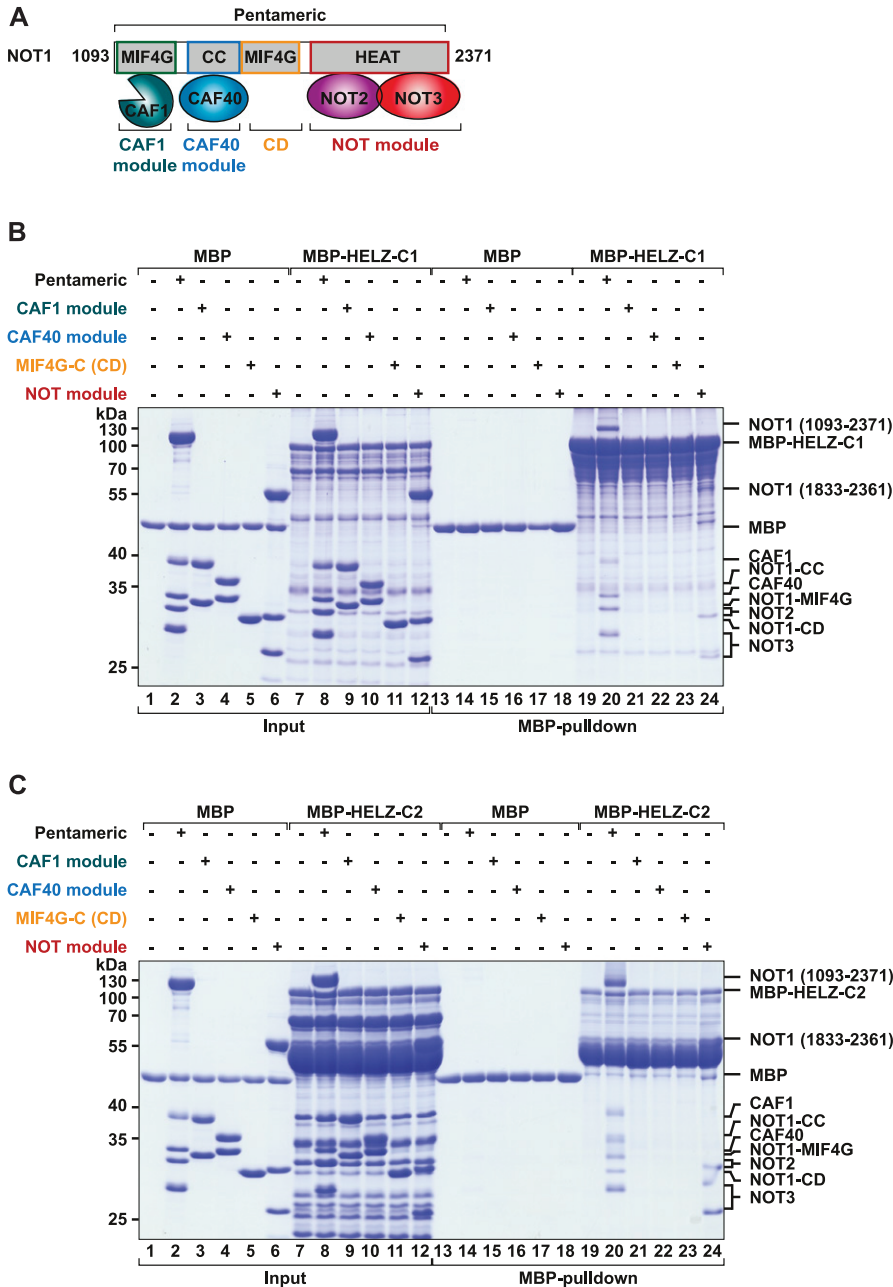


Figure 2. HELZ directly binds CCR4-NOT via multiple C-terminal sites.

(A) Schematic overview of the pentameric human CCR4-NOT complex used for in vitro interaction studies. The pentameric subcomplex is composed of NOT1 (residues E1093-E2371), CAF1, CAF40 (residues R19-E285), NOT2 (residues T344-F540), and NOT3 (residues L607-Q753). The CAF1 module contains the NOT1 MIF4G-like domain and CAF1 (green). The CAF40 module consists of CAF40 (blue; residues R19-E285) bound to the CAF40-binding coiled coil domain (CC; residues V1351-L1588). The adjacent NOT1 MIF4G-C (CD; residues D1607-S1815) is depicted in yellow. The NOT module consists of NOT1 (residues H1833-M2361), NOT2 (residues M350-F540; purple), and NOT3 (residues L607-E748; red). **(B, C)** In vitro MBP pull-down assay showing the interaction of recombinant MBP-Hs HELZ-C1-GB1-His (B) or MBP-Hs HELZ-C2-GB1-His (C) with distinct recombinant and purified CCR4-NOT modules (indicated on top of the respective gel). MBP served as a negative control. Input (33%) and eluted fractions (55%) were analysed by SDS-PAGE and Coomassie Blue staining. Source data are available for this figure.

migrating reporter mRNA intermediate that lacks a poly(A) tail upon tethering of MS2-HA-HELZ to the β -globin-6xMS2bs reporter. MS2-HA-NOT1 served as a positive control for deadenylation-dependent mRNA decapping (Fig 3K-M) (Kuzuoglu-Ozturk et al, 2016). To confirm that this mRNA intermediate is indeed deadenylated, we performed an oligo(dT)-directed ribonuclease H (RNase H) cleavage assay. Poly(A) tail cleavage by RNase H of the reporter mRNAs (control and β -globin-6xMS2bs) in cells expressing MS2-HA and DCP2* resulted in the accumulation of fast migrating bands (Fig S1A, lane 1 versus 3; A_n versus A_0). In contrast, in cells expressing MS2-HA-HELZ and DCP2*, the β -globin-6xMS2bs mRNA migrated as the deadenylated version of the reporter before and after the RNase H

treatment (Fig S1A, lane 2 versus 4). Based on these observations, we conclude that in human cells, HELZ promotes CCR4-NOT-dependent deadenylation followed by deadenylation-dependent degradation of the tethered mRNA.

The role of HELZ in inducing mRNA decay is conserved in Metazoa

Drosophila melanogaster (*Dm*) HELZ, denoted as CG9425 (FlyBase/DIOPT: DRSC integrative orthologue prediction tool [Hu et al, 2011; Gramates et al, 2017]), displays a domain organization similar to that of *Hs* HELZ (Fig 1A) and shares an overall sequence identity of 31.38% (17.65% for the nonconserved C-terminal sequences) (UniProt Clustal

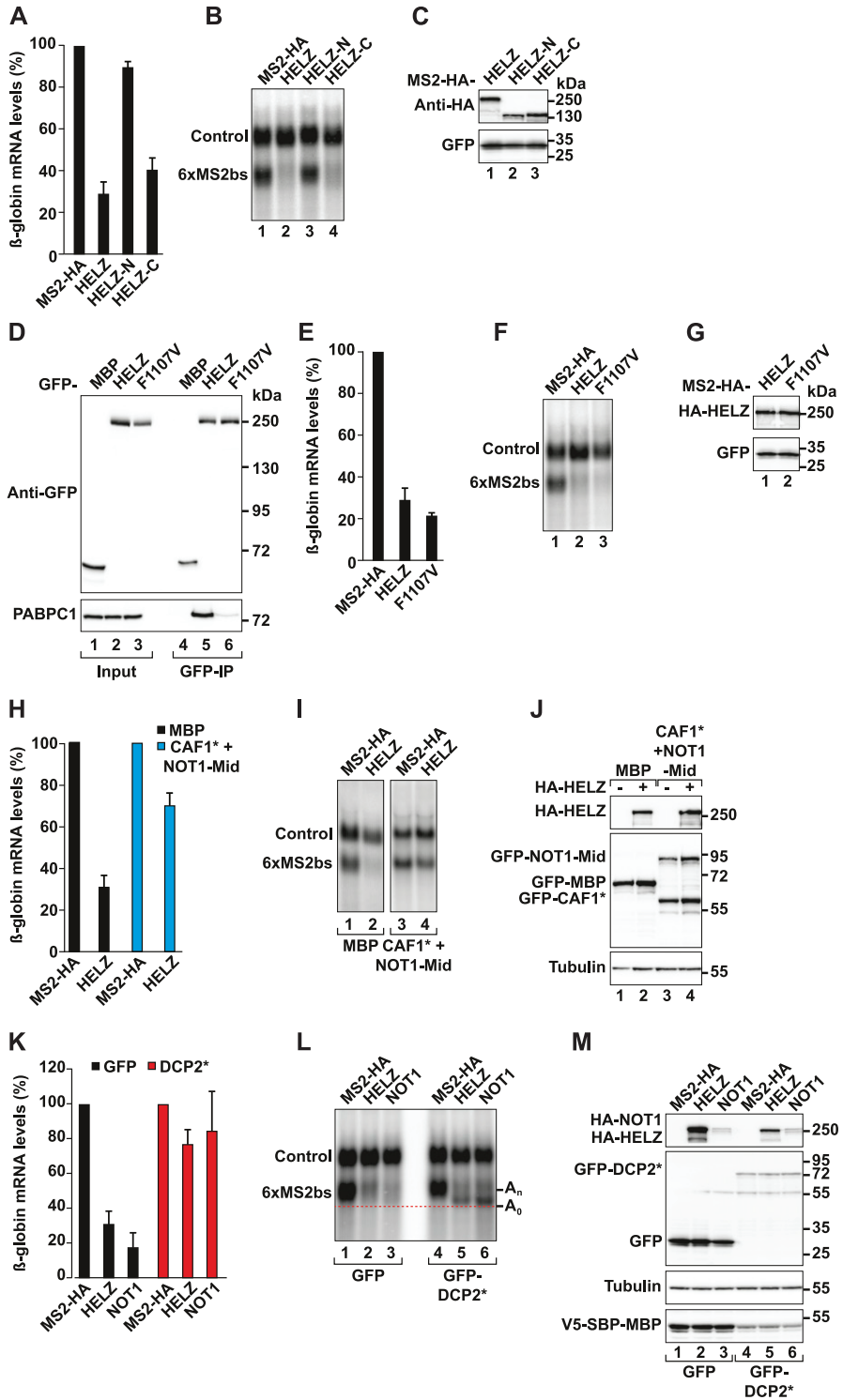


Figure 3. HELZ induces 5'-to-3' decay of tethered reporter mRNAs.

(A) Tethering assay in HEK293T cells using the β -globin-6xMS2bs reporter and MS2-HA-tagged HELZ (full-length or indicated fragments). The control reporter lacking the MS2bs (control) contains the β -globin gene fused to a fragment of the *gapdh* gene. The graph shows the quantification of mRNA levels of the β -globin-6xMS2bs reporter normalized to the levels of the control reporter and set to 100 for MS2-HA; the mean values \pm SD are shown for four independent experiments. (B) Representative Northern blot of samples shown in (A). (C) Representative Western blot depicting the equivalent expression of the MS2-HA-tagged proteins used in (A) and (B). GFP served as a transfection control. (D) Immunoprecipitation assay in HEK293T cells showing the interaction of GFP-tagged HELZ wild-type (WT) and F1107V mutant with endogenous PABPC1. GFP-MBP was used as a negative control. Input (1.2%) and bound fractions (20% for GFP-tagged proteins and 35% for endogenous PABPC1) were analysed by Western blotting. (E) Tethering assay as described in (A), in cells expressing MS2-HA-tagged HELZ WT and F1107V mutant as indicated. The mean values \pm SD are shown for four independent experiments. (F) Representative Northern blot of samples used in (E). (G) Western blot depicting the equivalent expression of the MS2-HA-HELZ WT and F1107V in (E) and (F). GFP served as a transfection control. (H) Tethering assay as described in (A), but the transfection mixture included additionally plasmids expressing GFP-CAF1* and GFP-NOT1-Mid to block deadenylation (blue bars). GFP-MBP was overexpressed in control samples (black bars). The mean values \pm SD are shown for three independent experiments. (I) Northern blot with representative RNA samples from the experiment depicted in (H). (J) Western blot showing the equivalent expression of HA-HELZ and the GFP-tagged proteins used in (H) and (I). Tubulin served as loading control. (K) Tethering assay as described in (A). The transfection mixture additionally included a plasmid expressing GFP-DCP2* catalytic mutant to block decapping (red bars). GFP was overexpressed in control samples (black bars). Tethering of MS2-HA-NOT1 served as positive control for deadenylation-dependent decapping (Kuzuoglu-Ozturk et al, 2016). The mean values \pm SD are shown for three independent experiments. (L) Northern blot of representative RNA samples corresponding to the experiment shown in (K). The position of the fast migrating deadenylated form of the reporter mRNA (A_0) is marked with a red dotted line, whereas the position of the reporter with an intact poly(A) is indicated as (A_n). (M) Western blot showing the expression of HA-HELZ, HA-NOT1, and the GFP-tagged proteins used in (K) and (L). Tubulin served as loading control and V5-SBP-MBP as a transfection control. Transfection efficiency and/or plasmid expression was decreased in cells expressing GFP-DCP2*. Source data are available for this figure.

Omega/Align [Pundir et al, 2016]). Similar to the human orthologue, GFP-tagged *Dm* HELZ immunoprecipitated various mRNA decay factors when expressed in *Dm* Schneider S2 cells, including *Dm* HPat (fly orthologue of mammalian PatL1) and *Dm* PAN3 (Fig 4A and B), but not *Dm* Ge-1 (fly orthologue of mammalian EDC4) or *Dm* Me31B (fly orthologue of mammalian DDX6) (Fig S1B and C). GFP-tagged *Dm* HELZ

also immunoprecipitated the *Dm* CCR4-NOT complex proteins NOT1 and NOT2 (Fig 4C and D), indicating that these interactions are a conserved feature of HELZ orthologues.

Next, we tested whether *Dm* HELZ can induce mRNA decay. We used a λ N-based tethering assay to recruit λ N-HA-tagged *Dm* HELZ full-length protein or fragments to a firefly luciferase reporter

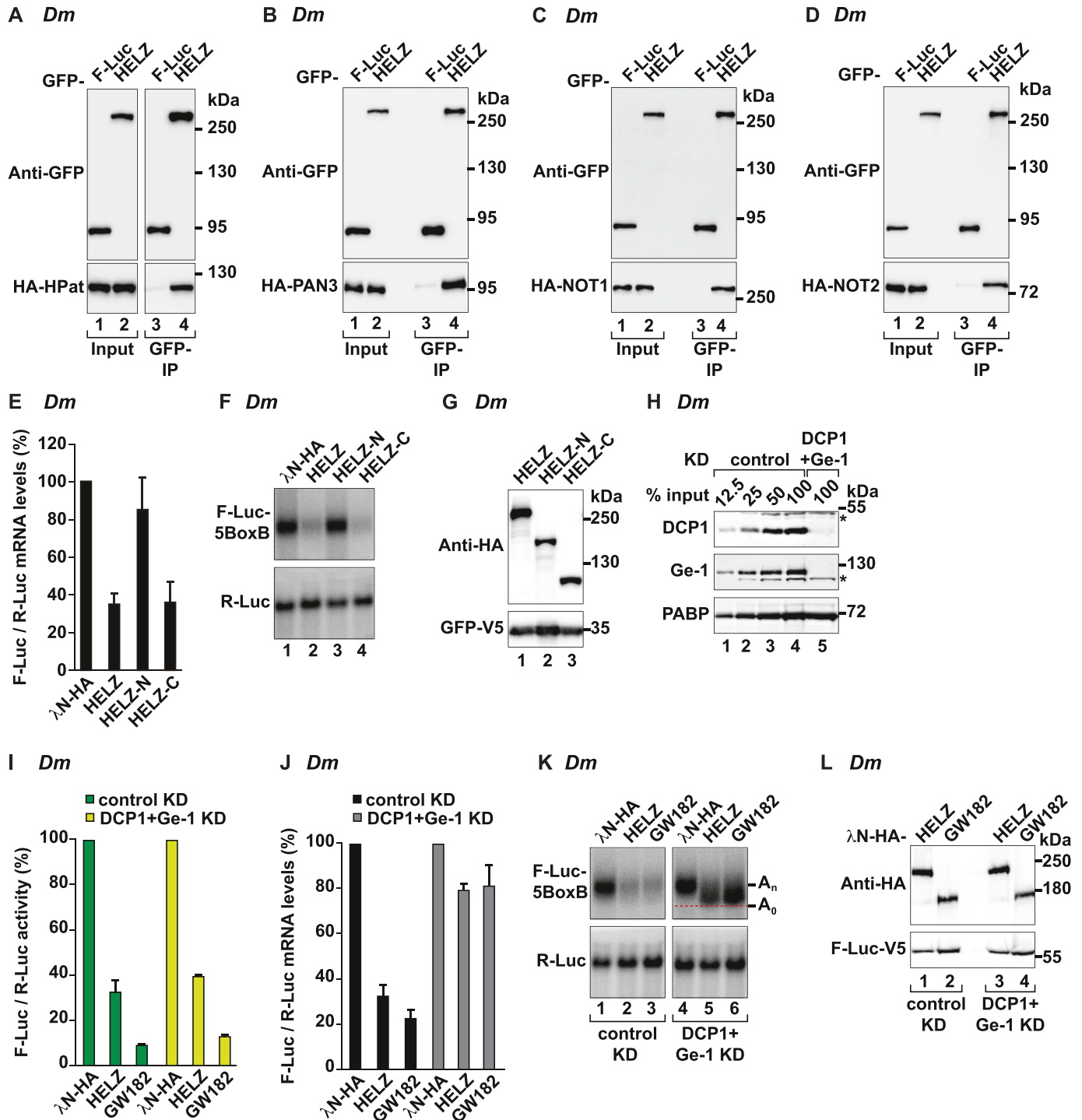


Figure 4. The role of HELZ in inducing mRNA decay is conserved in Metazoa.

(A–D) Immunoprecipitation assays in *Dm* S2 cells showing the interaction of GFP-*Dm* HELZ with HA-tagged-*Dm* HPat (A), HA-tagged-*Dm* PAN3 (B), HA-tagged-*Dm* NOT1 (C), and HA-tagged-*Dm* NOT2 (D). F-Luc-GFP served as negative control. Input (3.5% for GFP-tagged proteins and 0.5% for HA-tagged proteins) and bound fractions (10% for GFP-tagged proteins and 35% for HA-tagged proteins) were analysed by Western blotting. (E) Tethering assay in *Dm* S2 cells using the F-Luc-5BoxB reporter and λ N-HA-*Dm* HELZ (full-length and fragments). A plasmid expressing R-Luc served as transfection control. F-Luc mRNA levels were normalized to those of the R-Luc control and set to 100 in cells expressing λ N-HA. Graph shows the mean values \pm SD of four experiments. (F) Representative Northern blot of samples shown in (E). (G) Western blot showing the equivalent expression of the λ N-HA-tagged proteins used in (E). GFP-V5 was used as transfection control. (H) *Dm* S2 cells were treated with dsRNA targeting glutathione S-transferase (control) or DCP1 and Ge-1 mRNAs. The efficacy of the KD was estimated by Western blot with antibodies specifically recognizing endogenous DCP1 and Ge-1 proteins. PABP served as a loading control. Dilutions of control cell lysates were loaded in lanes 1–4 to estimate the efficacy of the depletion. The asterisks (*) mark unspecific bands recognized by the respective antibody. (I, J) *Dm* S2 cells treated with dsRNA targeting either glutathione S-transferase (control, green bars) or DCP1 and Ge-1 mRNAs (yellow bars) were transfected as described in (E). Tethering of λ N-HA-GW182 served as positive control for deadenylation-dependent decapping

harboring five λ N-binding sites (F-Luc-5xBoxB) in the 3' UTR (Gehring et al, 2005; Behm-Ansmant et al, 2006). A reporter mRNA encoding *Renilla* luciferase (R-Luc) served as a transfection control. Tethering of *Dm* HELZ caused strong repression of the firefly luciferase activity compared with the control λ N-HA protein (Fig S1D). Reporter mRNA levels were reduced in a similar manner (Fig 4E and F), indicating that the observed decrease in F-Luc activity was a consequence of mRNA decay. Interestingly, similar to the human orthologue, the C-terminal region of *Dm* HELZ (Table S1) was sufficient to elicit decay of the bound reporter. The *Dm* HELZ N-terminal fragment (Table S1) did not detectably impact on the stability of the F-Luc mRNA (Fig 4E–G) and instead stimulated F-Luc activity upon tethering (Fig S1D). The cause behind this observation is currently unclear.

To examine if *Dm* HELZ also induces deadenylation-dependent mRNA decapping, we performed tethering assays in *Dm* S2 cells depleted of two decapping activators DCP1 and Ge-1 to efficiently inhibit 5'-cap removal (Fig 4H–L; Eulalio et al, 2007b). In the absence of these decapping factors, tethering of HELZ to F-Luc-5BoxB resulted in a marked stabilization of the deadenylated variant of the reporter transcript (Fig 4J and K, lane 5). Similar results were obtained with tethered GW182 (Fig 4J and K, lane 6), which triggers deadenylation-dependent decapping and thus served as a positive control (Behm-Ansmant et al, 2006). The inhibition of decapping and the resulting stabilization of the deadenylated reporter did not lead to the restoration of F-Luc protein levels consistent with impaired translation of the reporter mRNA lacking a poly(A) tail (Fig 4I). We conclude that in *Dm*, as in human cells, HELZ interacts with components of the mRNA decay machinery and promotes decapping-dependent decay of a bound mRNA.

HELZ requires CCR4–NOT to repress translation of bound mRNAs

We then investigated if HELZ can repress translation in the absence of deadenylation. We used an R-Luc reporter mRNA that does not undergo deadenylation and subsequent decay (R-Luc-6xMS2bs-A₉₅-MALAT1) (Bhandari et al, 2014; Kuzuoglu-Ozturk et al, 2016). This reporter harbors a 95-nt internal poly(A) stretch followed by the 3'-terminal region of the metastasis associated lung adenocarcinoma transcript 1 (MALAT1) noncoding RNA, which is processed by RNaseP and thus lacks a poly(A) tail (Wilusz et al, 2012). An F-Luc-GFP reporter served as a transfection control. In the presence of HELZ, R-Luc activity was reduced to 40% relative to MS2-HA without changes in mRNA levels (Fig 5A–C, lane 2). This result indicates that deadenylation is not required for HELZ-mediated translational repression. Interestingly, the HELZ (F1107V) mutant, which cannot interact with PABPC1, was equally active to WT HELZ in eliciting deadenylation-independent translational repression (Fig 5A–D).

The CCR4–NOT complex not only mediates deadenylation but can also promote translational repression of target mRNAs (Cooke et al, 2010; Chekulaeva et al, 2011; Bawankar et al, 2013; Zekri et al, 2013). To address if HELZ-mediated translational repression depends

on the CCR4–NOT complex, we tethered HELZ to the R-Luc reporter in HeLa cells depleted of NOT1. shRNA-mediated knock-down (KD) resulted in a pronounced reduction of NOT1 protein levels without affecting MS2-HA-HELZ expression (Fig 5E, lanes 4 and 5). NOT1 depletion, however, severely compromised the ability of HELZ to repress the translation of the R-Luc-6xMS2bs-A₉₅-MALAT1 reporter (Fig 5F), consistent with the function of HELZ as a translational repressor being dependent on the CCR4–NOT complex.

Repression of translation by the CCR4–NOT complex is strongly associated with the DEAD-box helicase DDX6, a decapping activator and an inhibitor of translation (Maillet & Collart, 2002; Chu & Rana, 2006; Chen et al, 2014; Mathys et al, 2014; Freimer et al, 2018). To probe for this molecular connection in the context of translational repression by HELZ, we generated a HEK293T *Ddx6*-null cell line using CRISPR-Cas9 genome editing. Successful gene targeting was verified by the loss of DDX6 protein expression and genomic DNA sequencing of the targeted exon (Fig S2A and see the Materials and Methods section). Characterization of the *Ddx6*-null cells by polysome profiling indicated that DDX6 depletion does not induce major changes in general translation in HEK293T cells cultured under standard conditions (Fig S2B) relative to wild type (WT) cells. DDX6 depletion did, however, result in a drastic reduction of P-bodies as shown by the abnormal distribution of the P-body component EDC4 (Fig S2C and D) and as previously reported (Lumb et al, 2017; Freimer et al, 2018).

In the absence of DDX6, translational repression of the R-Luc-6xMS2bs-A₉₅-MALAT1 reporter by HELZ was impaired, albeit not completely abolished, as R-Luc activity recovered from 45% in WT cells to 70% in the *Ddx6*-null cells (Fig 5G). In contrast, loss of DDX6 did not change the ability of the silencing domain of TNRC6A (TNRC6A-SD; Lazzaretti et al, 2009) to repress the expression of the MALAT1 reporter (Fig S2E and F). Furthermore, exogenous expression of GFP-DDX6 restored HELZ repressive activity in *Ddx6*-null cells (Fig 5G and H). Comparable MS2-HA-HELZ protein levels in WT and DDX6-complemented cells were confirmed by Western blotting (Fig 5H). Thus, DDX6 is involved in HELZ-mediated translational repression.

HELZ is not required for CCR4–NOT-mediated translational repression and mRNA decay

To further address the role of HELZ in mRNA metabolism, we generated a *Helz*-null HEK293T cell line using CRISPR-Cas9 gene editing (Fig S2G). *Helz*-null cells proliferated at normal rates, and no changes were observed in general translation, as assessed by polysome profiling analysis (Fig S2H). Furthermore, in these cells, the protein levels of the CCR4–NOT components NOT2 and NOT3, PABPC1, as well as DDX6 were similar to WT cells (Fig S2G).

We then tested if NOT1-mediated posttranscriptional gene regulation is impaired in the absence of an interaction with HELZ.

(Behm-Ansmant et al, 2006). Panel (I) shows relative F-Luc activity in control and DCP1 + Ge-1 KD samples. Panel (J) depicts relative F-Luc mRNA levels in control and DCP1 + Ge-1 KD samples. The mean values \pm SD are shown for five independent experiments. (K) Representative Northern blot analysis of samples shown in (J). The position of the fast migrating deadenylated form of the reporter mRNA (A₀) is marked with a red dotted line, whereas the position of the reporter mRNA with intact poly(A) is indicated as (A_n). (L) Western blot showing the equivalent expression of the λ N-HA-tagged proteins used in (I). F-Luc-V5 was used as transfection control. Source data are available for this figure.

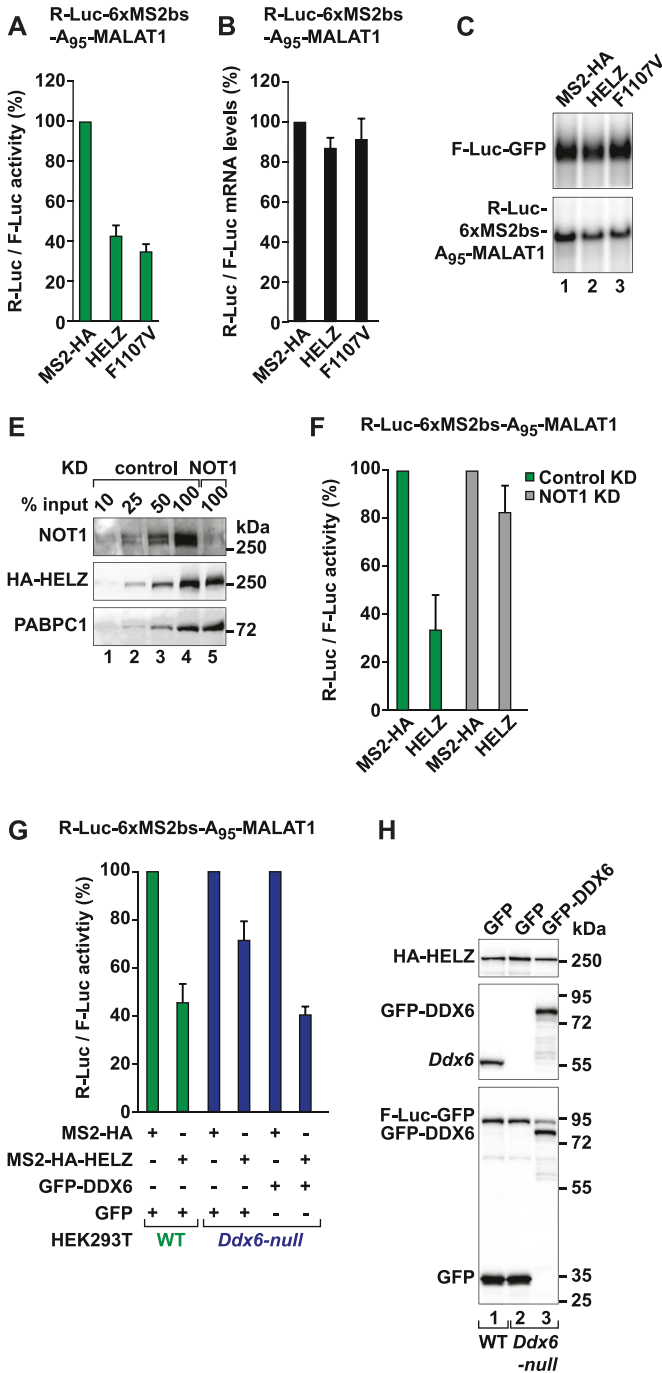


Figure 5. HELZ requires CCR4-NOT to repress translation of bound mRNAs.

(A, B) Tethering assay in HEK293T cells using the R-Luc-6xMS2bs-A₉₅-MALAT1 reporter with MS2-HA-HELZ WT and F1107V mutant. A plasmid coding for F-Luc-GFP served as control. Shown is the quantification of protein (A) and of mRNA levels (B) of the R-Luc-6xMS2bs-A₉₅-MALAT1 reporter normalized to the levels of the control reporter and set to 100 for MS2-HA. The mean values ± SD are shown for four independent experiments. (C) Representative Northern blots of samples shown in (B). (D) Western blot showing the equivalent expression of the MS2-HA tagged proteins used in (A). F-Luc-GFP was used as transfection control. (E) Western blot analysis of HeLa cells after NOT1 KD. Dilutions of control cell lysates were loaded in lanes 1–4 to estimate the efficacy of NOT1 depletion. Transfected MS2-HA-HELZ protein was expressed at comparable levels in WT and NOT1 KD cells. PABPC1 served as a loading control. (F) Tethering assay in HeLa cells using the R-Luc-6xMS2bs-A₉₅-MALAT1 reporter and MS2-HA-HELZ. HeLa cells were treated with scrambled shRNA (green bar) or shRNA targeting NOT1 mRNA (grey bar). The graph shows relative R-Luc activity in control and NOT1 KD samples. The mean values ± SD are shown for three independent experiments. (G) Tethering assay in HEK293T WT (green bars) and *Ddx6*-null cells (blue bars) with MS2-HA-HELZ and the R-Luc-6xMS2bs-A₉₅-MALAT1 reporter. For complementation studies, the cells were also transfected with either GFP or GFP-DDX6. A plasmid expressing F-Luc-GFP served as a transfection control. Shown is the quantification of R-Luc activity normalized to F-Luc activity and set to 100 for MS2-HA in WT or *Ddx6*-null cells. The mean values ± SD are shown for three independent experiments. (H) Western blot showing the levels of transfected MS2-HA-HELZ protein in the different cell lines used in (G). Loss of endogenous DDX6 protein expression in HEK293T *Ddx6*-null cells was confirmed using an anti-DDX6 antibody (lane 2, middle panel). The blot further illustrates that GFP-DDX6 was expressed at a level equivalent to endogenous DDX6 (lane 3 versus lane 1). F-Luc-GFP served as transfection control. Source data are available for this figure.

Therefore, we tethered NOT1 to the R-Luc-6xMS2bs or the R-Luc-6xMS2bs-A₉₅-MALAT1 reporters in *Helz*-null cells. These reporters are degraded or translationally repressed, respectively, when bound to NOT1 (Kuzuoglu-Ozturk et al, 2016). Tethered NOT1 reduced R-Luc activity of both mRNA reporters to 20% in WT and *Helz*-null cells (Fig S3A–E). These results are in agreement with HELZ acting upstream of the deadenylase complex (i.e., as a recruitment factor). The more likely scenario is that HELZ acts together with the CCR4-NOT to regulate the expression of a subset of mRNAs.

HELZ regulates the abundance of mRNAs encoding proteins involved in neurogenesis and nervous system development

To gain more insight into HELZ mRNA targets, we next investigated how the cellular transcriptome is affected in the absence of HELZ. Thus, we sequenced and analysed the transcriptome of the *Helz*-null and WT cells (Figs 6A and S4 and Table S2). The replicates of the RNA-Seq libraries of the two cell types clustered together as determined using multidimensional scaling analysis (Fig S4A). HELZ depletion induced major changes in the cellular transcriptome.

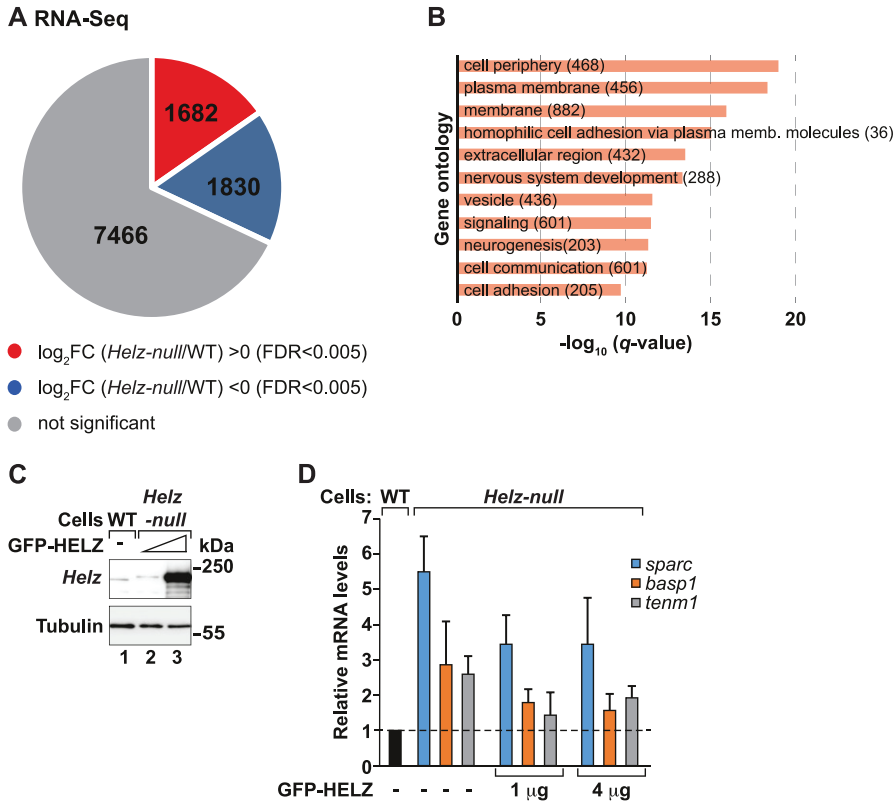


Figure 6. Transcriptome analysis of HEK293T *Helz*-null cells.
(A) Pie chart indicating the fractions and absolute numbers of differentially expressed genes derived from the analysis of the transcriptome of HEK293T wild-type (WT) and *Helz*-null cells by RNA-Seq. Two biological replicates of each cell line were analysed. The RNA-Seq analysis indicated that 7,466 (grey) of the total 10,978 genes selected using fragments per kilobase of transcript per million mapped reads >2 cut-off showed no significant differences between the two cell lines (FDR \geq 0.005). 1,682 genes were significantly up-regulated (red) whilst 1,830 genes were down-regulated (blue) using a fold change (FC) >0 on \log_2 scale with an FDR < 0.005 to determine abundance. **(B)** Gene ontology analysis of the biological processes overrepresented in the group of transcripts up-regulated in *Helz*-null cells ($\log_2FC > 0$, FDR < 0.005) versus all other expressed genes. Bar graph shows $-\log_{10}$ of q values for each category. Content of brackets indicates the number of genes within each category. **(C)** Western blot analysis depicting the levels of endogenous HELZ present in HEK293T WT cells (lane 1) compared with *Helz*-null cells transfected with either 1 or 4 μ g of GFP-HELZ (lanes 2 and 3, respectively). Tubulin served as loading control. **(D)** qPCR validation of three up-regulated ($\log_2FC > 0$, FDR < 0.005) transcripts identified in (A). Transcript levels of *sparc* (blue bars), *basp1* (orange bars) and *tenm1* (grey bars) were determined in HEK293T WT, *Helz*-null, and *Helz*-null cells complemented with either 1 or 4 μ g of GFP-HELZ. Transcript levels were normalized to *gapdh* mRNA. Shown are the normalized expression ratios \pm SD for three independent experiments.

In fact, differential gene expression analysis revealed 1,682 mRNAs to be significantly up-regulated ($\log_2FC > 0$ and FDR < 0.005) and 1,830 mRNAs to be down-regulated ($\log_2FC < 0$ and FDR < 0.005) in the *Helz*-null cells relative to WT cells (Figs 6A and S4B).

Functional annotation analysis using the goseq R-package (Young et al, 2010) for all up-regulated transcripts in *Helz*-null cells indicated a significant enrichment for genes encoding cell periphery (22%, $q < 9.19 \times 10^{-20}$), membrane-associated (17%, $q < 1.19 \times 10^{-16}$), cell adhesion (23%, $q < 2.05 \times 10^{-10}$), and signalling (19%, $q < 3.01 \times 10^{-12}$)-related proteins. Interestingly, many of the corresponding proteins have known functions in the biological processes of neurogenesis (25%, $q < 5.06 \times 10^{-12}$) and nervous system development (23%, $q < 4.5 \times 10^{-14}$). These include, for instance, GDNF (glial cell-line-derived neurotrophic factor) family receptor alpha-3 (GFRA3; Baloh et al, 1998; Naveilhan et al, 1998), brain acid soluble protein 1 (BASP1; Hartl & Schneider, 2019), teneurin (TENM1; Tucker, 2018), neurofilament medium polypeptide (NEFM; Coulombe et al, 2001) or the protocadherin G cluster (PCDHG; Keeler et al, 2015), among others (Table S3). After analysis of transcript length and nucleotide composition, we also observed that the mRNAs with increased abundance in the absence of HELZ have longer coding sequences (CDS; $P < 2.2 \times 10^{-16}$) and a higher guanine and cytosine (GC) content across the whole gene ($P = 6.1 \times 10^{-11}$ or $P < 2.2 \times 10^{-16}$) compared to all other genes expressed in these cells (down-regulated mRNAs and all mRNAs not significantly altered in *Helz*-null cells, Fig S5).

On the other hand, transcripts with decreased expression in *Helz*-null cells were related to translation (structural constituent of

ribosome [45%, $q < 2.64 \times 10^{-21}$], signal-recognition particle-dependent cotranslational protein targeting to membrane [59%, $q < 1.7 \times 10^{-20}$], ribosome biogenesis [36%, $q < 2.99 \times 10^{-17}$], translation [43%, $q < 3.66 \times 10^{-16}$], and rRNA processing [37%, $q < 7.08 \times 10^{-16}$). Other down-regulated and overrepresented GO terms included RNA metabolism and RNA-binding (RNP complex biogenesis [31%, $q < 1.08 \times 10^{-15}$], nonsense-mediated decay [47%, $q < 9.19 \times 10^{-20}$], non-coding RNA (ncRNA)-metabolic process [28%, $q < 6.96 \times 10^{-13}$], and RNA binding [23%, $q < 2.97 \times 10^{-11}$]) or organonitrogen compound metabolism (24%, $q < 3.15 \times 10^{-16}$; Fig S4C).

To validate that the differentially expressed mRNAs identified in this analysis are indeed regulated by HELZ, we measured the abundance of three significantly up-regulated (FC > twofold, FDR < 0.005) transcripts in *Helz*-null cells upon transient expression of increasing concentrations of GFP-tagged HELZ (Fig 6C). In *Helz*-null cells, *sparc*, *basp1*, and *tenm1* mRNA levels, determined by quantitative RT-PCR (RT-qPCR), were increased relative to WT cells (Fig 6D), as observed in the RNA-Seq analysis (Table S2). Transcript levels increased 2.5–5.5 fold, depending on the mRNA. Overexpression of GFP-HELZ decreased the abundance of these transcripts, partially restoring steady state mRNA levels (Fig 6D).

These results suggest that HELZ has an important role in the control of the expression of specific genes. Increased transcript abundance can be explained by the activity of HELZ as a transcriptional (Hamamoto et al, 2004) and/or posttranscriptional regulator via its interaction with the CCR4–NOT complex (this study and [Mathys et al, 2014]). Additional studies are required to identify the transcripts co-regulated by HELZ and the CCR4–NOT complex.

Discussion

The putative SF1 helicase HELZ has been associated with various steps in RNA metabolism, including transcription and translation. Here, we reveal that HELZ also regulates mRNA stability as it induces deadenylation and decapping of bound reporter mRNAs. This function is likely the result of HELZ interaction with various mRNA decay factors including components of the CCR4–NOT complex in human and *Drosophila* cells. In fact, human HELZ has multiple binding sites within its nonconserved and unstructured C-terminal region that directly interact with the NOT module of the CCR4–NOT complex (Fig 2). The NOT module, composed of NOT1/2/3 subunits is a known binding platform for various mRNA-associated proteins, including the posttranscriptional RNA regulator Nanos (Bhandari et al, 2014; Raisch et al, 2016) and the transcription factor E26-related gene (Rambout et al, 2016). Tethering of *Hs* and *Dm* HELZ to an mRNA reporter triggers decapping-dependent mRNA decay. In both species, the C-terminal region of HELZ was necessary and sufficient to elicit decay. The observation that the regulatory effect of HELZ on stability and translation of tethered mRNA requires the CCR4–NOT complex (Figs 3H–J and 5F) supports the functional connection between HELZ and CCR4–NOT in mRNA metabolism.

Recruitment of the CCR4–NOT complex to mRNA targets by short linear motifs (SLiMs) located in unstructured and poorly conserved regions of RNA-associated proteins is a common and widespread mechanism (Fabian et al, 2013; Bhandari et al, 2014; Raisch et al, 2016; Sgromo et al, 2017; Keskeny et al, 2019). The presence of multiple binding sites in the HELZ C-terminal region indicates a SLiM-mediated mode for interaction with the CCR4–NOT complex. The plastic evolutionary nature of SLiM-mediated protein binding (Davey et al, 2012; Tompa, 2012) readily explains how largely divergent and unstructured C-terminal regions of HELZ orthologues perform equivalent cellular functions.

Interestingly, HELZ is not the only SF1 helicase known to interact with the CCR4–NOT complex and promote mRNA decay. The UPF1 RNA helicase, through both direct and indirect interactions, binds to different mRNA decay factors, including the endoribonuclease SMG6 and the CAF1 deadenylase to induce target mRNA decay (Kim & Maquat, 2019). UPF1 contains a helicase core domain that is structurally highly similar to HELZ. UPF1 binds rather nonspecifically to accessible mRNAs (Zund & Muhlemann, 2013) but seems to be recruited through interaction with specific RNA-binding proteins to defined targets to participate in distinct mRNA decay pathways (Kim & Maquat, 2019). Whether HELZ function is subject to similar control is unknown.

Our study also highlights a potential role for HELZ as a translational repressor (Fig 5). HELZ-mediated translational repression of a reporter mRNA lacking a 3' poly(A) tail depends on the CCR4–NOT complex but does not require binding to PABPC1. Repression of translation by the CCR4–NOT complex is associated with the DEAD-box helicase DDX6 (Maillet & Collart, 2002; Chu & Rana, 2006; Chen et al, 2014; Mathys et al, 2014; Freimer et al, 2018), and we provide evidence that DDX6 contributes to HELZ-induced translational repression. However, in the absence of DDX6, the translational repressor function of HELZ was not completely abolished. Thus, other factors are involved in HELZ-mediated translational

repression. Another HELZ- and CCR4–NOT-interacting protein is the translational repressor PatL1 (Fig 1C) (Braun et al, 2010; Ozgur et al, 2010) and additional studies will determine the relevance of PatL1, or other factors, in the repression of translation by HELZ and the CCR4–NOT complex.

HELZ contains several sequence motifs that could confer RNA binding ability. Its PABPC1 binding property suggests that HELZ has a preference for polyadenylated mRNAs. Furthermore, HELZ contains a CCCH-type ZnF motif in the N terminus (Fig 1A) that may be critical for its biological role as it can promote protein–protein interactions or facilitate RNA recognition (Hall, 2005; Gamsjaeger et al, 2007). This specific type of ZnF is present in RNA-binding proteins such as tristetraprolin and Roquin, which also directly recruit the CCR4–NOT complex to mRNA targets, promoting their degradation (Fabian et al, 2013; Fu & Blackshear, 2017; Sgromo et al, 2017).

Although it remains unclear how HELZ is recruited to mRNA, transcriptome-wide analysis of *Helz*-null cells via RNA-Seq indicated that HELZ depletion has a substantial impact on gene expression (Figs 6 and S4). Interestingly, genes with up-regulated expression in the absence of HELZ code for membrane- and cell periphery-associated proteins, many of which participate in the development of the nervous system (Fig 6B and Table S3). An important goal for future studies is to investigate HELZ and its association with the CCR4–NOT complex in the posttranscriptional regulation of this biological process.

HELZ loss also resulted in decreased abundance of transcripts with gene products involved in translation. Even if global translation was not altered in *Helz*-null cells (Fig S2H), this observation is in line with the fact that HELZ overexpression results in increased translation and cellular proliferation (Hasgall et al, 2011). Moreover, similar to HELZ depletion, loss of the HELZ-interacting protein and transcriptional regulator *Smyd2* in cardiomyocytes leads to decreased expression of genes functionally associated with translation (Diehl et al, 2010).

In conclusion, our findings support a role of HELZ as a regulator of gene expression and highlight a potential development- or cell-specific function for this RNA helicase. Furthermore, the direct interaction of HELZ with the CCR4–NOT complex described in this study represents another molecular mechanism used by HELZ in the control of gene expression.

Materials and Methods

DNA constructs

All the mutants used in this study were generated by site-directed mutagenesis using the QuickChange mutagenesis kit (Stratagene). All the constructs and mutations were confirmed by sequencing and are listed in Table S1. To generate the pT7-EGFP-*Hs* CAF1* catalytic mutant, D40A and E42A point mutations were introduced into the pT7-EGFP-*Hs* CAF1 vector (Braun et al, 2011). *Hs* HELZ cDNA was amplified from the Kazusa clone KIAA0054 and inserted into the SacII and SalI restriction sites of the pT7-EGFP-C1 vector or the SacII and XbaI restriction sites of the pT7-MS2-HA vector. For MS2-HA-tagged *Hs* HELZ proteins, the pT7- λ N-HA-C1 vector was modified by

mutagenesis to replace the λ N-HA-tag with the MS2-HA-tag. The *Hs* HELZ-N and HELZ-C fragments (residues M1–D1050 and P1051–K1942, respectively) were amplified by PCR using specific primers (*Hs* HELZ-N: forward: ATACATCCGCGATATGGAAGACAGAAGAGCTGAAAAGT, reverse: ACATTCTAGATTAATCACCCACCACAGCAACCAGGGAT; *Hs* HELZ-C: forward: ATACATCCGCGATCCATTGCTGTGCTCTATTGGAA, reverse: ACATTCTAGATTATTTAAATATGAGTAAAAGCCA) and inserted between the restriction sites *Sac*II and *Xba*I of the pT7-EGFP-C1 and pT7-MS2-HA-C1 vectors. The *Hs* NOT1 ORF was amplified from cDNA and inserted into the *Xho*I and *Sac*II sites of the pT7-MS2-HA vector. The plasmid allowing the expression of HA-*Hs* DDX6 was generated by cloning the corresponding cDNA into the *Xho*I and *Not*I restriction sites of the pCneo- λ N-HA vector. To obtain the plasmid expressing the silencing domain of *Hs* TNRC6A (residues T1210–V1709), the corresponding cDNA amplified by PCR was cloned into the *Bam*HI and *Xho*I restriction sites of the pCNA3.1-MS2-HA vector. The plasmids for the expression of the HA-tagged versions of *Hs* EDC4, *Hs* PatL1, and *Hs* PAN3 or *Dm* HPat, *Dm* PAN3, *Dm* NOT1, *Dm* NOT2, *Dm* Ge-1, and *Dm* Me31B were previously described (Eulalio et al, 2007a; Tritschler et al, 2008, 2009; Braun et al, 2010, 2011; Bawankar et al, 2013).

Dm HELZ was amplified from cDNA derived from S2 cells and inserted into the pAc5.1B- λ N-HA and pAc5.1B-EGFP vectors between *Hind*III and *Xba*I restriction sites (Eulalio et al, 2007a). *Dm* HELZ-N and HELZ-C (residues M1–D1212 and P1213–Q2103, respectively) were amplified by PCR using specific primers (*Dm* HELZ-N: forward: ATACATAAGCTTCATGCGCCGAGAAAGGAGATGCAGGC, reverse: ACATTCTAGATTAATCACCAACCACTGCAACCAACGAC; *Dm* HELZ-C: forward: ATACATAAGCTTCCCCGTGGCTCTTTGTTCCATTGGTC, reverse: ACATTCTAGATTACTGAAAATAGTTGTAGAATCCG) and inserted between the restriction sites *Hind*III and *Xba*I of the pAc5.1B- λ N-HA plasmid.

For expression of recombinant *Hs* HELZ-C1 and HELZ-C2 in bacteria, the corresponding sequences were amplified by PCR and inserted between the *Bsp*TI and *Xba*I restriction sites of the pNEA-NvM plasmid (Diebold et al, 2011), resulting in HELZ fusion proteins carrying an N-terminal MBP tag cleavable by the tobacco etch virus protease. In addition, the DNA encoding the B1 domain of immunoglobulin-binding protein G (GB1) (Cheng & Patel, 2004), followed by a four-residue long (Met-Gly-Ser-Ser) linker sequence and a hexa histine (His₆)-tag were added to the end of the HELZ-C1 and HELZ-C2 coding sequences by site-directed mutagenesis.

Tethering assays

The reporter constructs used in the tethering assays performed in human and *Dm* cells were described previously (Lykke-Andersen et al, 2000; Behm-Ansmant et al, 2006; Kuzuoglu-Ozturk et al, 2016). In the case of tethering assays in HEK293T WT, *Helz*-null and *Ddx6*-null, and HeLa cell lines, cells were cultured in 6-well plates and transfected using Lipofectamine 2000 (Invitrogen) according to the manufacturer's recommendation. The transfection mixture used in Fig 3A and E contained the following plasmids: 0.5 μ g control β -globin, 0.5 μ g β -globin-6xMS2bs and the following amounts of the plasmids expressing the MS2-HA-tagged proteins: 1 μ g of *Hs* HELZ and *Hs* HELZ F1107V, 1.35 μ g of *Hs* HELZ-N, and 2.5 μ g of *Hs* HELZ-C. In Fig 3H, the transfection mixtures contained, in addition, plasmids expressing GFP-MBP (2 μ g) or GFP-*Hs* CAF1* (1 μ g) together with GFP-*Hs* NOT1-Mid region (residues M1085–T1605; 1 μ g) (Petit et al, 2012).

In Fig 3K, the transfection mixtures contained, in addition, plasmids expressing GFP (0.15 μ g) or GFP-*Hs* DCP2* (2 μ g) (Chang et al, 2014). In the tethering assays with luciferase (R-Luc and F-Luc) reporters depicted in Figs 5 and S3, the transfection mixtures contained 0.2 μ g F-Luc-GFP (transfection control), 0.2 μ g of R-Luc-6xMS2bs (or R-Luc), or 0.5 μ g R-Luc-6xMS2bs-A₉₅-MALAT1 (or R-Luc-A₉₅-MALAT1) and 1 μ g of MS2-HA-*Hs* HELZ or MS2-HA-*Hs* NOT1. The transfection mixture in the experiment described in Fig 5G additionally contained 0.2 μ g of the plasmid required for the expression of GFP-DDX6 in *Ddx6*-null cells. The cells were harvested 2 d after transfection for further analysis. shRNA-mediated KD of NOT1 in HeLa cells was performed as previously described (Chen et al, 2014). In the experiment described in Fig S2E, the transfection mixture contained 0.5 μ g of MS2-HA or MS2-HA-TNRC6A-SD, 0.5 μ g of R-Luc-6xMS2bs-MALAT1, and 0.5 μ g F-Luc-GFP (transfection control).

To perform tethering assays with *Dm* HELZ, S2 cells were seeded in 6-well plates and transfected with Effectene Transfection Reagent (QIAGEN) according to the manufacturer's recommendation. The transfection mixture contained 0.4 μ g of R-Luc, 0.1 μ g of F-Luc-V5, or F-Luc-5BoxB and 0.01 μ g of λ N-HA-GW182 or the following amounts of pAc5.1- λ N-HA plasmids expressing *Dm* HELZ proteins: 0.4 μ g HELZ, 0.2 μ g HELZ-N, and 0.2 μ g HELZ-C. RNAi-mediated KD of DCP1 and Ge-1 in *Dm* S2 cells was performed as described previously (Clemens et al, 2000; Zekri et al, 2013).

Total RNA was isolated using TriFast (Peqlab) and analysed by Northern blot as described previously (Behm-Ansmant et al, 2006). *Renilla* and firefly luciferase activities were measured using the Dual Luciferase Reporter Assay System (Promega).

RNase H digestion

For the experiment depicted in Fig S1A, 10 μ g of RNA was incubated with 3 μ l of RNase H 5 U/ μ l (New England BioLabs) and 6 μ M of oligo(dT) 15-mer in 100 μ l H₂O for 1 h at 37°C and subsequently purified by phenol-chloroform extraction. The RNase H-treated RNA was then analysed via Northern blotting.

Co-IP assays and Western blotting

Co-IP assays in human and *Dm* S2 cells were performed as previously described (Kuzuoglu-Ozturk et al, 2016). Briefly, for the human GFP-IP assays, 4 \times 10⁶ HEK293T cells were grown in 10-cm dishes and transfected the day after seeding using TurboFect transfection reagent (Thermo Fisher Scientific). The transfection mixtures in Fig 1B–E contained 15 μ g of GFP-*Hs* HELZ and 10 μ g of HA-EDC4, HA-PatL1, HA-PAN3, or HA-DDX6. The transfection mixtures in Fig 1F contained 20, 30, or 25 μ g of plasmids expressing GFP-tagged *Hs* HELZ, *Hs* HELZ-N, or *Hs* HELZ-C, respectively.

The co-IP assays in S2 cells required two wells of a six-well plate (seeded at 2.5 \times 10⁶ cells per well) per condition. The cells were harvested 3 d after transfection with Effectene Transfection Reagent (QIAGEN). The transfection mixture contained 1 μ g of GFP-*Dm* HELZ and 0.5 μ g of HA-*Dm* Me31B, 1 μ g of HA-*Dm* HPat, HA-*Dm* PAN3, HA-*Dm* NOT2, HA-*Dm* Ge-1, or 2 μ g of HA-*Dm* NOT1.

All lysates were treated with RNase A before IP. Western blots were developed with the ECL Western Blotting Detection System

(GE Healthcare) according to the manufacturer's recommendations. Antibodies used in this study are listed in Table S4.

Protein expression and purification

The purification of the human pentameric CCR4–NOT complex (CAF1/CAF40/NOT1/2/3) and the different modules was previously described (Sgromo et al, 2017). The pentameric CCR4–NOT complex comprises NOT1 (residues E1093–E2371), CAF1, CAF40 (residues R19–E285), NOT2 (residues T344–F540), and His₆–NOT3 (residues G607–Q753); the CAF1 module comprises NOT1 (residues E1093–S1317) and CAF1; the CAF40 module consists of NOT1 (residues V1351–L1588) and CAF40 (residues R19–E285); the MIF4G-C domain represents NOT1 residues Q1607–S1815; and the NOT module contains NOT1 (residues H1833–M2361), NOT2 (residues M350–F540), and NOT3 (residues L607–E748). *Hs* HELZ-C1 and *Hs* HELZ-C2 recombinant proteins were expressed with an N-terminal MBP- and a C-terminal GB1-His₆-tag in *Escherichia coli* BL21 (DE3) Star cells (Invitrogen) in Lysogeny broth (Luria broth) medium overnight at 20°C. The cells were sonicated in binding buffer containing 50 mM Hepes, pH 7, 200 mM NaCl, 20 mM imidazole, and 2 mM β-mercaptoethanol, supplemented with protease inhibitors, 1 mg/ml lysozyme, and 5 mg/ml DNase I. The cleared lysates were bound to an Ni²⁺ HiTrap IMAC HP (GE Healthcare) column and proteins were eluted by a step gradient to binding buffer supplemented with 500 mM imidazole using Äkta Pure (GE Healthcare). The fractions in the single peak were analysed on an SDS–PAGE, pooled, and used in MBP pull-downs.

In vitro MBP pull-down assays

Purified MBP (7.5 μg), MBP-*Hs* HELZ-C1-GB1-His or MBP-*Hs* HELZ-C2-GB1-His (500 μg each) were mixed with equimolar amounts of the purified CCR4–NOT subcomplexes in 1 ml of pull-down buffer (50 mM Hepes, pH 7, 200 mM NaCl, and 2 mM DTT) and incubated for 1 h at 4°C. After another hour of incubation at 4°C with 50 μl of amylose resin slurry (New England BioLabs), the beads were washed five times with pull-down buffer. The proteins were eluted with pull-down buffer supplemented with 25 mM D-(+)-maltose. The eluate was mixed 1:1 with 20% cold trichloroacetic acid (Roth) and incubated for 30 min on ice. The mix was then centrifuged at full speed at 4°C in a table-top centrifuge and the pellet was suspended in 35 μl of protein sample buffer (50 mM Tris–HCl, pH 6.8, 2% [wt/vol] SDS, 10% [vol/vol] glycerol, and 100 mM DTT). The eluted proteins were heated at 95°C for 5 min and analysed by SDS–PAGE. The gels were stained with Coomassie Blue overnight at room temperature and washed the next day.

Generation of the HEK293T *Helz*- and *Ddx6*-null cell lines

The generation of the HEK293T HELZ- and *Ddx6*-null cell lines was essentially performed as described previously (Sgromo et al, 2018). In the case of *ddx6*, a guide RNA targeting exon 2 (5'-GTCTTTTCCAGTCATCAC-3') was designed using DNA 2.0 (ATUM, www.atum.bio) online tool to minimize off-target effects. Genome targeting resulted in a 1-nt insertion in one allele and a 10-nt deletion in the other allele, both causing a frameshift of the ORF. To edit *helz* gene, a guide RNA targeting exon 8 (5'-GCAACTAGTAACGCCCTCTC-3') was used.

helz gene targeting produced a 7-nt deletion causing a frameshift of the ORF.

Transcriptome sequencing (RNA-Seq) and RT-qPCR validation

Total RNA was extracted from HEK293T WT or *Helz*-null cells using the RNeasy Mini Kit (QIAGEN) and a library prepared using the TruSeq RNA Sample Prep Kit (Illumina). Two biological replicates were analysed. RNA-Seq libraries were sequenced with the HiSeq 3000 sequencing system (Illumina) using paired-end sequencing. During data analysis, ribosomal RNA sequencing reads were filtered using Bowtie2 (Langmead & Salzberg, 2012). The remaining reads were then mapped on the hg19 (University of California, Santa Cruz) human genome with Tophat2 (Kim et al, 2013). 20.6–34.8 million reads (89.0–90.1%) were mapped. Read count analysis was performed with an R/Bioconductor package QuasR (Gaidatzis et al, 2015). A threshold of “fragments per kilobase of transcript per million mapped reads” (FPKM) greater than two was applied to select genes for subsequent differential gene expression analysis with an R/Bioconductor package edgeR (Robinson et al, 2010; McCarthy et al, 2012).

RT-qPCR was performed to determine transcript levels of selected transcripts in WT and *Helz*-null cells. Briefly, in the complementation assay described in Fig 6D, HEK293T *Helz*-null cells, plated in a six-well plate, were transfected with 1 and 4 μg of pT7-GFP-HELZ, as indicated. 48 h posttransfection, total RNA was extracted and reverse-transcribed using random hexamer primers. mRNA levels were subsequently determined by RT-qPCR using sequence-specific primers for the indicated transcripts and normalized to *gapdh* mRNA abundance in the same sample. qPCR primers were designed using Primer3 (Koressaar & Remm, 2007; Untergasser et al, 2012) or Primer-BLAST (Ye et al, 2012) and are listed in Table S5. Normalized expression ratios of the transcripts from three independent experiments were determined using the Livak method (Livak & Schmittgen, 2001).

Immunofluorescence

HEK293T WT and *Ddx6*-null cells were grown on poly-D-lysine (Sigma-Aldrich)-coated cover slips. Cells were fixed with 4% paraformaldehyde for 10 min and permeabilized with 0.1% Triton X-100 in PBS (10 min). Staining with anti-DDX6 or anti-p70S6K (EDC4) antibodies was performed in PBS containing 10% FBS and 0.1% Tween 20 for 1 h. Alexa Fluor 594-labeled secondary antibody (Thermo Fisher Scientific) was used at 1:1,000 dilution. Nuclei were stained with Hoechst stain solution (Sigma-Aldrich). Cells were mounted using Fluoromount-G (Southern Biotech). The images were acquired using a confocal laser scanning microscope (Leica TCS SP8).

Polysome profiling

Polysome profiles for HEK293T WT, *Helz*-null, and *Ddx6*-null cell lines were obtained as described before (Kuzuoglu-Ozturk et al, 2016).

Data availability

Raw sequencing reads and the processed data files corresponding to read counts and normalized abundance measurements generated

in this study were deposited in the GEO under the accession number [GSE135505](https://www.ncbi.nlm.nih.gov/geo/query/acc.cgi?acc=GSE135505).

Supplementary Information

Supplementary Information is available at <https://doi.org/10.26508/lsa.201900405>.

Acknowledgements

We dedicate this paper to the memory of Elisa Izaurralde who sadly passed away before the conclusion of this work. Elisa was instrumental in the design and supervision of the study and in the drafting and correction of early versions of the manuscript. Due to journal policy, Elisa is not listed as an author. We want to thank Eugene Valkov for extensive language editing, Heike Budde for support in the RT-qPCR experiments, and Sigrun Helms for excellent technical assistance. We are grateful to all current and former members of the Izaurralde laboratory, who provided insightful comments on the manuscript. This work was supported by the Max Planck Society.

Author Contribution

A Hanet: formal analysis, investigation, methodology, project administration, and writing—original draft, review, and editing.

F Räsch: investigation.

R Weber: formal analysis and investigation.

V Ruscica: investigation.

M Fauser: investigation.

T Raisch: resources.

D Kuzuoglu-Öztürk: investigation.

C-T Chang: resources.

D Bhandari: investigation.

C Igreja: formal analysis, methodology, project administration, and writing—review and editing.

L Wohlbold: formal analysis, methodology, project administration, and writing—review and editing.

Conflict of Interest Statement

The authors declare that they have no conflict of interest.

References

- Ayache J, Benard M, Ernoult-Lange M, Minshall N, Standart N, Kress M, Weil D (2015) P-body assembly requires DDX6 repression complexes rather than decay or Ataxin2/2L complexes. *Mol Biol Cell* 26: 2579–2595. doi:10.1091/mbc.e15-03-0136
- Baloh RH, Tansey MG, Lampe PA, Fahrner TJ, Enomoto H, Simburger KS, Leitner ML, Araki T, Johnson EM Jr, Milbrandt J (1998) Artemin, a novel member of the GDNF ligand family, supports peripheral and central neurons and signals through the GFRalpha3-RET receptor complex. *Neuron* 21: 1291–1302. doi:10.1016/s0896-6273(00)80649-2
- Basquin J, Roudko VV, Rode M, Basquin C, Seraphin B, Conti E (2012) Architecture of the nuclease module of the yeast Ccr4-not complex: The Not1-Caf1-Ccr4 interaction. *Mol Cell* 48: 207–218. doi:10.1016/j.molcel.2012.08.014
- Bawankar P, Loh B, Wohlbold L, Schmidt S, Izaurralde E (2013) NOT10 and C2orf29/NOT11 form a conserved module of the CCR4-NOT complex that docks onto the NOT1 N-terminal domain. *RNA Biol* 10: 228–244. doi:10.4161/rna.23018
- Behm-Ansmant I, Rehwinkel J, Doerks T, Stark A, Bork P, Izaurralde E (2006) mRNA degradation by miRNAs and GW182 requires both CCR4:NOT deadenylase and DCP1:DCP2 decapping complexes. *Genes Dev* 20: 1885–1898. doi:10.1101/gad.1424106
- Berlenga JJ, Baass A, Sonenberg N (2006) Regulation of poly(A) binding protein function in translation: Characterization of the Paip2 homolog, Paip2B. *RNA* 12: 1556–1568. doi:10.1261/rna.106506
- Bhandari D, Raisch T, Weichenrieder O, Jonas S, Izaurralde E (2014) Structural basis for the nanos-mediated recruitment of the CCR4-NOT complex and translational repression. *Genes Dev* 28: 888–901. doi:10.1101/gad.237289.113
- Bhaskar V, Roudko V, Basquin J, Sharma K, Urlaub H, Seraphin B, Conti E (2013) Structure and RNA-binding properties of the Not1-Not2-Not5 module of the yeast Ccr4-Not complex. *Nat Struct Mol Biol* 20: 1281–1288. doi:10.1038/nsmb.2686
- Bleichert F, Baserga SJ (2007) The long unwinding road of RNA helicases. *Mol Cell* 27: 339–352. doi:10.1016/j.molcel.2007.07.014
- Boland A, Chen Y, Raisch T, Jonas S, Kuzuoglu-Ozturk D, Wohlbold L, Weichenrieder O, Izaurralde E (2013) Structure and assembly of the NOT module of the human CCR4-NOT complex. *Nat Struct Mol Biol* 20: 1289–1297. doi:10.1038/nsmb.2681
- Braun JE, Huntzinger E, Fauser M, Izaurralde E (2011) GW182 proteins directly recruit cytoplasmic deadenylase complexes to miRNA targets. *Mol Cell* 44: 120–133. doi:10.1016/j.molcel.2011.09.007
- Braun JE, Tritschler F, Haas G, Igreja C, Truffault V, Weichenrieder O, Izaurralde E (2010) The C-terminal alpha-alpha superhelix of Pat is required for mRNA decapping in metazoa. *EMBO J* 29: 2368–2380. doi:10.1038/emboj.2010.124
- Burdick R, Smith JL, Chaipan C, Friew Y, Chen J, Venkatachari NJ, Delviks-Frankenberry KA, Hu WS, Pathak VK (2010) P body-associated protein Mov10 inhibits HIV-1 replication at multiple stages. *J Virol* 84: 10241–10253. doi:10.1128/jvi.00585-10
- Chang CT, Bercovich N, Loh B, Jonas S, Izaurralde E (2014) The activation of the decapping enzyme DCP2 by DCP1 occurs on the EDC4 scaffold and involves a conserved loop in DCP1. *Nucleic Acids Res* 42: 5217–5233. doi:10.1093/nar/gku129
- Chekulaeva M, Mathys H, Zipprich JT, Attig J, Colic M, Parker R, Filipowicz W (2011) miRNA repression involves GW182-mediated recruitment of CCR4-NOT through conserved W-containing motifs. *Nat Struct Mol Biol* 18: 1218–1226. doi:10.1038/nsmb.2166
- Chen Y, Boland A, Kuzuoglu-Ozturk D, Bawankar P, Loh B, Chang CT, Weichenrieder O, Izaurralde E (2014) A DDX6-CNOT1 complex and W-binding pockets in CNOT9 reveal direct links between miRNA target recognition and silencing. *Mol Cell* 54: 737–750. doi:10.1016/j.molcel.2014.03.034
- Chen YZ, Hashemi SH, Anderson SK, Huang Y, Moreira MC, Lynch DR, Glass IA, Chance PF, Bennett CL (2006) Senataxin, the yeast Sen1p orthologue: Characterization of a unique protein in which recessive mutations cause ataxia and dominant mutations cause motor neuron disease. *Neurobiol Dis* 23: 97–108. doi:10.1016/j.nbd.2006.02.007
- Cheng Y, Patel DJ (2004) An efficient system for small protein expression and refolding. *Biochem Biophys Res Commun* 317: 401–405. doi:10.1016/j.bbrc.2004.03.068
- Chu CY, Rana TM (2006) Translation repression in human cells by microRNA-induced gene silencing requires RCK/p54. *PLoS Biol* 4: e210. doi:10.1371/journal.pbio.0040210
- Clemens JC, Worthy CA, Simonson-Leff N, Muda M, Maehama T, Hemmings BA, Dixon JE (2000) Use of double-stranded RNA interference in

- Drosophila cell lines to dissect signal transduction pathways. *Proc Natl Acad Sci U S A* 97: 6499–6503. doi:10.1073/pnas.110149597
- Collart MA, Panasencko OO (2017) The Ccr4-Not complex: Architecture and structural insights. *Subcell Biochem* 83: 349–379. doi:10.1007/978-3-319-46503-6_13
- Cook HA, Koppetsch BS, Wu J, Theurkauf WE (2004) The Drosophila SDE3 homolog armitage is required for oskar mRNA silencing and embryonic axis specification. *Cell* 116: 817–829. doi:10.1016/j.s0092-8674(04)00250-8
- Cooke A, Prigge A, Wickens M (2010) Translational repression by deadenylases. *J Biol Chem* 285: 28506–28513. doi:10.1074/jbc.m110.150763
- Coulombe PA, Ma L, Yamada S, Wawersik M (2001) Intermediate filaments at a glance. *J Cell Sci* 114: 4345–4347.
- Dalmay T, Horsefield R, Braunstein TH, Baulcombe DC (2001) SDE3 encodes an RNA helicase required for post-transcriptional gene silencing in Arabidopsis. *EMBO J* 20: 2069–2078. doi:10.1093/emboj/20.8.2069
- Davey NE, Van Roey K, Weatheritt RJ, Toedt G, Uyar B, Altenberg B, Budd A, Diella F, Dinkel H, Gibson TJ (2012) Attributes of short linear motifs. *Mol Biosyst* 8: 268–281. doi:10.1039/c1mb05231d
- Diebold ML, Fribourg S, Koch M, Metzger T, Romier C (2011) Deciphering correct strategies for multiprotein complex assembly by co-expression: Application to complexes as large as the histone octamer. *J Struct Biol* 175: 178–188. doi:10.1016/j.jsb.2011.02.001
- Dieh I, Brown MA, van Amerongen MJ, Novoyatleva T, Wietelmann A, Harriss J, Ferrazzi F, Bottger T, Harvey RP, Tucker PW, et al (2010) Cardiac deletion of Smyd2 is dispensable for mouse heart development. *PLoS One* 5: e9748. doi:10.1371/journal.pone.0009748
- Eulalio A, Behm-Ansmant I, Schweizer D, Izaurralde E (2007a) P-body formation is a consequence, not the cause, of RNA-mediated gene silencing. *Mol Cell Biol* 27: 3970–3981. doi:10.1128/mcb.00128-07
- Eulalio A, Rehwinkel J, Stricker M, Huntzinger E, Yang SF, Doerks T, Dörner S, Bork P, Boutros M, Izaurralde E (2007b) Target-specific requirements for enhancers of decapping in miRNA-mediated gene silencing. *Genes Dev* 21: 2558–2570. doi:10.1101/gad.443107
- Fabian MR, Frank F, Rouya C, Siddiqui N, Lai WS, Karetnikov A, Blackshear PJ, Nagar B, Sonenberg N (2013) Structural basis for the recruitment of the human CCR4-NOT deadenylase complex by tristetraprolin. *Nat Struct Mol Biol* 20: 735–739. doi:10.1038/nsmb.2572
- Fairman-Williams ME, Guenther UP, Jankowsky E (2010) SF1 and SF2 helicases: Family matters. *Curr Opin Struct Biol* 20: 313–324. doi:10.1016/j.sbi.2010.03.011
- Freimer JW, Hu TJ, Blleloch R (2018) Decoupling the impact of microRNAs on translational repression versus RNA degradation in embryonic stem cells. *Elife* 7: e38014. doi:10.7554/elife.38014
- Fu M, Blackshear PJ (2017) RNA-binding proteins in immune regulation: A focus on CCCH zinc finger proteins. *Nat Rev Immunol* 17: 130–143. doi:10.1038/nri.2016.129
- Gaidatzis D, Lerch A, Hahne F, Stadler MB (2015) QuasR: Quantification and annotation of short reads in R. *Bioinformatics* 31: 1130–1132. doi:10.1093/bioinformatics/btu781
- Gamsjaeger R, Liew CK, Loughlin FE, Crossley M, Mackay JP (2007) Sticky fingers: Zinc-fingers as protein-recognition motifs. *Trends Biochem Sci* 32: 63–70. doi:10.1016/j.tibs.2006.12.007
- Gehring NH, Kunz JB, Neu-Yilik G, Breit S, Viegas MH, Hentze MW, Kulozik AE (2005) Exon-junction complex components specify distinct routes of nonsense-mediated mRNA decay with differential cofactor requirements. *Mol Cell* 20: 65–75. doi:10.1016/j.molcel.2005.08.012
- Goss DJ, Kleiman FE (2013) Poly(A) binding proteins: Are they all created equal? *Wiley Interdiscip Rev RNA* 4: 167–179. doi:10.1002/wrna.1151
- Gramates LS, Marygold SJ, Santos GD, Urbano JM, Antonazzo G, Matthews BB, Rey AJ, Tabone CJ, Crosby MA, Emmert DB, et al (2017) FlyBase at 25: Looking to the future. *Nucleic Acids Res* 45: D663–D671. doi:10.1093/nar/gkw1016
- Gregersen LH, Schueler M, Munschauer M, Mastrobuoni G, Chen W, Kempa S, Dieterich C, Landthaler M (2014) MOV10 Is a 5' to 3' RNA helicase contributing to UPF1 mRNA target degradation by translocation along 3' UTRs. *Mol Cell* 54: 573–585. doi:10.1016/j.molcel.2014.03.017
- Hall TM (2005) Multiple modes of RNA recognition by zinc finger proteins. *Curr Opin Struct Biol* 15: 367–373. doi:10.1016/j.sbi.2005.04.004
- Hamamoto R, Furukawa Y, Morita M, Iimura Y, Silva FP, Li M, Yagyu R, Nakamura Y (2004) SMYD3 encodes a histone methyltransferase involved in the proliferation of cancer cells. *Nat Cell Biol* 6: 731–740. doi:10.1038/ncb1151
- Hartl M, Schneider R (2019) A unique family of neuronal signaling proteins implicated in oncogenesis and tumor suppression. *Front Oncol* 9: 289. doi:10.3389/fonc.2019.00289
- Hasgall PA, Hoogewijs D, Faza MB, Panse VG, Wenger RH, Camenisch G (2011) The putative RNA helicase HELZ promotes cell proliferation, translation initiation and ribosomal protein S6 phosphorylation. *PLoS One* 6: e22107. doi:10.1371/journal.pone.0022107
- Horiuchi M, Takeuchi K, Noda N, Muroya N, Suzuki T, Nakamura T, Kawamura-Tsuzuku J, Takahashi K, Yamamoto T, Inagaki F (2009) Structural basis for the antiproliferative activity of the Tob-hCaf1 complex. *J Biol Chem* 284: 13244–13255. doi:10.1074/jbc.m809250200
- Hu Y, Flockhart I, Vinayagam A, Bergwitz C, Berger B, Perrimon N, Mohr SE (2011) An integrative approach to ortholog prediction for disease-focused and other functional studies. *BMC Bioinformatics* 12: 357. doi:10.1186/1471-2105-12-357
- Huntzinger E, Kuzuoglu-Ozturk D, Braun JE, Eulalio A, Wohlbold L, Izaurralde E (2013) The interactions of GW182 proteins with PABP and deadenylases are required for both translational repression and degradation of miRNA targets. *Nucleic Acids Res* 41: 978–994. doi:10.1093/nar/gks1078
- Inada T, Makino S (2014) Novel roles of the multi-functional CCR4-NOT complex in post-transcriptional regulation. *Front Genet* 5: 135. doi:10.3389/fgene.2014.00135
- Keeler AB, Molumbly MJ, Weiner JA (2015) Protocadherins branch out: Multiple roles in dendrite development. *Cell Adh Migr* 9: 214–226. doi:10.1080/19336918.2014.1000069
- Keskeny C, Raisch T, Sgromo A, Igreja C, Bhandari D, Weichenrieder O, Izaurralde E (2019) A conserved CAF40-binding motif in metazoan NOT4 mediates association with the CCR4-NOT complex. *Genes and Development* Feb 1: 236–252. doi:10.1101/gad.320952.118
- Kim D, Perteza G, Trapnell C, Pimentel H, Kelley R, Salzberg SL (2013) TopHat2: Accurate alignment of transcriptomes in the presence of insertions, deletions and gene fusions. *Genome Biol* 14: R36. doi:10.1186/gb-2013-14-4-r36
- Kim YK, Maquat LE (2019) UPFront and center in RNA decay: UPF1 in nonsense-mediated mRNA decay and beyond. *RNA* 25: 407–422. doi:10.1261/rna.070136.118
- Koressaar T, Remm M (2007) Enhancements and modifications of primer design program Primer3. *Bioinformatics* 23: 1289–1291. doi:10.1093/bioinformatics/btm091
- Kozlov G, Trempe JF, Khaleghpour K, Kahvejian A, Ekiel I, Gehring K (2001) Structure and function of the C-terminal PABC domain of human poly(A)-binding protein. *Proc Natl Acad Sci U S A* 98: 4409–4413. doi:10.1073/pnas.071024998
- Kuzuoglu-Ozturk D, Bhandari D, Huntzinger E, Fauser M, Helms S, Izaurralde E (2016) miRISC and the CCR4-NOT complex silence mRNA targets independently of 43S ribosomal scanning. *EMBO J* 35: 1186–1203. doi:10.15252/embj.201592901

- Langmead B, Salzberg SL (2012) Fast gapped-read alignment with Bowtie 2. *Nat Methods* 9: 357–359. doi:10.1038/nmeth.1923
- Lau NC, Kolkman A, van Schaik FM, Mulder KW, Pijnappel WW, Heck AJ, Timmers HT (2009) Human Ccr4-Not complexes contain variable deadenylase subunits. *Biochem J* 422: 443–453. doi:10.1042/bj20090500
- Lazzaretti D, Tournier I, Izaurralde E (2009) The C-terminal domains of human TNRC6A, TNRC6B, and TNRC6C silence bound transcripts independently of Argonaute proteins. *RNA* 15: 1059–1066. doi:10.1261/rna.1606309
- Leonaite B, Han Z, Basquin J, Bonneau F, Libri D, Porrua O, Conti E (2017) Sen1 has unique structural features grafted on the architecture of the Upf1-like helicase family. *EMBO J* 36: 1590–1604. doi:10.15252/embj.201696174
- Livak KJ, Schmittgen TD (2001) Analysis of relative gene expression data using real-time quantitative PCR and the 2^{-ΔΔC_T} Method. *Methods* 25: 402–408. doi:10.1006/meth.2001.1262
- Lumb JH, Li Q, Popov LM, Ding S, Keith MT, Merrill BD, Greenberg HB, Li JB, Carette JE (2017) DDX6 represses aberrant activation of interferon-stimulated genes. *Cell Rep* 20: 819–831. doi:10.1016/j.celrep.2017.06.085
- Lykke-Andersen J, Shu MD, Steitz JA (2000) Human Upf proteins target an mRNA for nonsense-mediated decay when bound downstream of a termination codon. *Cell* 103: 1121–1131. doi:10.1016/S0092-8674(00)00214-2
- Maillet L, Collart MA (2002) Interaction between Not1p, a component of the Ccr4-not complex, a global regulator of transcription, and Dh1p, a putative RNA helicase. *J Biol Chem* 277: 2835–2842. doi:10.1074/jbc.m107979200
- Mathys H, Basquin J, Ozgur S, Czarnocki-Cieciura M, Bonneau F, Aartse A, Dziembowski A, Nowotny M, Conti E, Filipowicz W (2014) Structural and biochemical insights to the role of the CCR4-NOT complex and DDX6 ATPase in microRNA repression. *Mol Cell* 54: 751–765. doi:10.1016/j.molcel.2014.03.036
- Mauxion F, Preve B, Seraphin B (2013) C2ORF29/CNOT11 and CNOT10 form a new module of the CCR4-NOT complex. *RNA Biol* 10: 267–276. doi:10.4161/rna.23065
- McCarthy DJ, Chen Y, Smyth GK (2012) Differential expression analysis of multifactor RNA-Seq experiments with respect to biological variation. *Nucleic Acids Res* 40: 4288–4297. doi:10.1093/nar/gks042
- Naveilhan P, Baudet C, Mikaelis A, Shen L, Westphal H, Ernfors P (1998) Expression and regulation of GFRA3, a glial cell line-derived neurotrophic factor family receptor. *Proc Natl Acad Sci U S A* 95: 1295–1300. doi:10.1073/pnas.95.3.1295
- Nicholson AL, Pasquinelli AE (2019) Tales of detailed poly(A) tails. *Trends Cell Biol* 29: 191–200. doi:10.1016/j.tcb.2018.11.002
- Nomura N, Nagase T, Miyajima N, Sazuka T, Tanaka A, Sato S, Seki N, Kawarabayashi Y, Ishikawa K, Tabata S (1994) Prediction of the coding sequences of unidentified human genes. II. The coding sequences of 40 new genes (K1AA0041-K1AA0080) deduced by analysis of cDNA clones from human cell line KG-1 (supplement). *DNA Res* 1: 251–262. doi:10.1093/dnares/1.5.251
- Ozgun S, Chekulaeva M, Stoecklin G (2010) Human Pat1b connects deadenylation with mRNA decapping and controls the assembly of processing bodies. *Mol Cell Biol* 30: 4308–4323. doi:10.1128/mcb.00429-10
- Petit AP, Wohlbold L, Bawankar P, Huntzinger E, Schmidt S, Izaurralde E, Weichenrieder O (2012) The structural basis for the interaction between the CAF1 nuclease and the NOT1 scaffold of the human CCR4-NOT deadenylase complex. *Nucleic Acids Res* 40: 11058–11072. doi:10.1093/nar/gks883
- Pundir S, Martin MJ, O'Donovan C, UniProt C (2016) UniProt tools. *Curr Protoc Bioinformatics* 53: 1.29.1–1.29.15. doi:10.1002/0471250953.bi0129s53
- Raisch T, Bhandari D, Sabath K, Helms S, Valkov E, Weichenrieder O, Izaurralde E (2016) Distinct modes of recruitment of the CCR4-NOT complex by Drosophila and vertebrate Nanos. *EMBO J* 35: 974–990. doi:10.15252/embj.201593634
- Raisch T, Sandmeier F, Weichenrieder O, Valkov E, Izaurralde E (2018) Structural and biochemical analysis of a NOT1 MIF4G-like domain of the CCR4-NOT complex. *J Struct Biol* 204: 388–395. doi:10.1016/j.jsb.2018.10.009
- Rambout X, Detiffe C, Bruyr J, Mariavelle E, Cherkaoui M, Brohee S, Demoitie P, Lebrun M, Soin R, Lesage B, et al (2016) The transcription factor ERG recruits CCR4-NOT to control mRNA decay and mitotic progression. *Nat Struct Mol Biol* 23: 663–672. doi:10.1038/nsmb.3243
- Robinson MD, McCarthy DJ, Smyth GK (2010) edgeR: A Bioconductor package for differential expression analysis of digital gene expression data. *Bioinformatics* 26: 139–140. doi:10.1093/bioinformatics/btp616
- Sgromo A, Raisch T, Backhaus C, Keskeny C, Alva V, Weichenrieder O, Izaurralde E (2018) Drosophila Bag-of-marbles directly interacts with the CAF40 subunit of the CCR4-NOT complex to elicit repression of mRNA targets. *RNA* 24: 381–395. doi:10.1261/rna.064584.117
- Sgromo A, Raisch T, Bawankar P, Bhandari D, Chen Y, Kuzuoglu-Ozturk D, Weichenrieder O, Izaurralde E (2017) A CAF40-binding motif facilitates recruitment of the CCR4-NOT complex to mRNAs targeted by Drosophila Roquin. *Nat Commun* 8: 14307. doi:10.1038/ncomms14307
- Singleton MR, Dillingham MS, Wigley DB (2007) Structure and mechanism of helicases and nucleic acid translocases. *Annu Rev Biochem* 76: 23–50. doi:10.1146/annurev.biochem.76.052305.115300
- Sloan KE, Bohnsack MT (2018) Unravelling the mechanisms of RNA helicase regulation. *Trends Biochem Sci* 43: 237–250. doi:10.1016/j.tibs.2018.02.001
- Tomba P (2012) Intrinsically disordered proteins: A 10-year recap. *Trends Biochem Sci* 37: 509–516. doi:10.1016/j.tibs.2012.08.004
- Tritschler F, Braun JE, Motz C, Igraja C, Haas G, Truffault V, Izaurralde E, Weichenrieder O (2009) DCP1 forms asymmetric trimers to assemble into active mRNA decapping complexes in metazoa. *Proc Natl Acad Sci U S A* 106: 21591–21596. doi:10.1073/pnas.0909871106
- Tritschler F, Eulalio A, Helms S, Schmidt S, Coles M, Weichenrieder O, Izaurralde E, Truffault V (2008) Similar modes of interaction enable Trailer Hitch and EDC3 to associate with DCP1 and Me31B in distinct protein complexes. *Mol Cell Biol* 28: 6695–6708. doi:10.1128/mcb.00759-08
- Tucker RP (2018) Teneurins: Domain architecture, evolutionary origins, and patterns of expression. *Front Neurosci* 12: 938. doi:10.3389/fnins.2018.00938
- Untergasser A, Cutcutache I, Koressaar T, Ye J, Faircloth BC, Remm M, Rozen SG (2012) Primer3: New capabilities and interfaces. *Nucleic Acids Res* 40: e115. doi:10.1093/nar/gks096
- Ursic D, Chinchilla K, Finkel JS, Culbertson MR (2004) Multiple protein/protein and protein/RNA interactions suggest roles for yeast DNA/RNA helicase Sen1p in transcription, transcription-coupled DNA repair and RNA processing. *Nucleic Acids Res* 32: 2441–2452. doi:10.1093/nar/gkh561
- Wagner DS, Gan L, Klein WH (1999) Identification of a differentially expressed RNA helicase by gene trapping. *Biochem Biophys Res Commun* 262: 677–684. doi:10.1006/bbrc.1999.1208
- Wang Z, Jiao X, Carr-Schmid A, Kiledjian M (2002) The hDcp2 protein is a mammalian mRNA decapping enzyme. *Proc Natl Acad Sci U S A* 99: 12663–12668. doi:10.1073/pnas.192445599
- Webster MW, Chen YH, Stowell JAW, Alhusaini N, Sweet T, Graveley BR, Collier J, Passmore LA (2018) mRNA deadenylation is coupled to translation rates by the differential activities of Ccr4-Not nucleases. *Mol Cell* 70: 1089–1100.e8. doi:10.1016/j.molcel.2018.05.033

- Wilusz JE, JnBaptiste CK, Lu LY, Kuhn CD, Joshua-Tor L, Sharp PA (2012) A triple helix stabilizes the 3' ends of long noncoding RNAs that lack poly(A) tails. *Genes Dev* 26: 2392–2407. doi:[10.1101/gad.204438.112](https://doi.org/10.1101/gad.204438.112)
- Ye J, Coulouris G, Zaretskaya I, Cutcutache I, Rozen S, Madden TL (2012) Primer-BLAST: A tool to design target-specific primers for polymerase chain reaction. *BMC Bioinformatics* 13: 134. doi:[10.1186/1471-2105-13-134](https://doi.org/10.1186/1471-2105-13-134)
- Yi H, Park J, Ha M, Lim J, Chang H, Kim VN (2018) PABP cooperates with the CCR4-NOT complex to promote mRNA deadenylation and block precocious decay. *Mol Cell* 70: 1081–1088.e5. doi:[10.1016/j.molcel.2018.05.009](https://doi.org/10.1016/j.molcel.2018.05.009)
- Young MD, Wakefield MJ, Smyth GK, Oshlack A (2010) Gene ontology analysis for RNA-seq: Accounting for selection bias. *Genome Biol* 11: R14. doi:[10.1186/gb-2010-11-2-r14](https://doi.org/10.1186/gb-2010-11-2-r14)
- Zekri L, Kuzuoglu-Ozturk D, Izaurralde E (2013) GW182 proteins cause PABP dissociation from silenced miRNA targets in the absence of deadenylation. *EMBO J* 32: 1052–1065. doi:[10.1038/emboj.2013.44](https://doi.org/10.1038/emboj.2013.44)
- Zund D, Muhlemann O (2013) Recent transcriptome-wide mapping of UPF1 binding sites reveals evidence for its recruitment to mRNA before translation. *Translation (Austin)* 1: e26977. doi:[10.4161/trla.26977](https://doi.org/10.4161/trla.26977)



License: This article is available under a Creative Commons License (Attribution 4.0 International, as described at <https://creativecommons.org/licenses/by/4.0/>).

HELZ directly interacts with CCR4-NOT and causes decay of bound mRNAs

Aoife Hanet¹, Felix Räsch¹, Ramona Weber¹, Vincenzo Ruscica¹, Maria Fauser¹, Tobias Raisch^{1,2}, Duygu Kuzuoğlu-Öztürk^{1,3}, Chung-Te Chang¹, Dipankar Bhandari¹, Cátia Igreja^{1,4}, Lara Wohlbold^{1,4}

¹ Department of Biochemistry, Max Planck Institute for Developmental Biology, Max-Planck-Ring 5, 72076 Tübingen, Germany

² Department of Structural Biochemistry, Max Planck Institute of Molecular Physiology, Otto-Hahn-Strasse 11, 44227 Dortmund, Germany

³ Helen Diller Family Cancer Research, University of California San Francisco, 1450 3rd Street, San Francisco, CA 94158, USA

⁴ Corresponding authors: catia.igreja@tuebingen.mpg.de; lara.wohlbold@tuebingen.mpg.de

Supplementary Material

Table S1. Constructs used in this study.

<i>Hs</i> HELZ (P42694)	
Full-length	pT7-MS2-HA-HELZ M1-K1942
	pT7-GFP-HELZ M1-K1942
HELZ-N	pT7-MS2-HA-HELZ M1-D1050
	pT7-GFP-HELZ M1-D1050
HELZ-C	pT7-MS2-HA-HELZ P1051-K1942
	pT7-GFP-HELZ P1051-K1942
	pnEA-NvM-MBP-HELZ P1051-I1474-GB1-6xHis
	pnEA-NvM-MBP-HELZ L1475-K1942-GB1-6xHis
F1107V (disrupts interaction with PABPC1)	pT7-MS2-HA-HELZ F1107V
	pT7-GFP-HELZ F1107V
<i>Dm</i> HELZ (CG9425)	
Full-length	pAc5.1B-GFP-HELZ M1-Q2103
	pAc5.1B- λ N-HA-HELZ M1-Q2103
HELZ-N	pAc5.1B- λ N-HA-HELZ M1-D1212
HELZ-C	pAc5.1- λ N-HA-HELZ P1213-Q2103
<i>Hs</i> mRNA decay factors	
	p λ N-HA-C1-NOT1
NOT1-Mid	pT7-GFP-C1-NOT1 M1085-T1605
Catalytically inactive	pT7-GFP-C1-CAF1 D40A E42A
Catalytically inactive	pT7-GFP-C1-DCP2 E148Q
	pCIneo- λ N-HA-EDC4
	p λ N-HA-C1-PatL1
	p λ N-HA-C1-PAN3
	pCIneo- λ N-HA-DDX6
	pT7-GFP-C1-DDX6
<i>Dm</i> mRNA decay factors	
	pAc5.1B- λ N-HA-HPat
	pAc5.1B- λ N-HA-PAN3
	pAc5.1B- λ N-HA-NOT1
	pAc5.1B- λ N-HA-NOT2
	pAc5.1B- λ N-HA-Ge-1
	pAc5.1B- λ N-HA-Me31B

Table S2. Transcriptome analysis of HELZ-null cells – Excel file. List of genes expressed and differentially expressed ($\log_2FC < 0$ or $\log_2FC > 0$ and $FDR < 0.005$) in HELZ-null cells compared to WT cells. FC: fold change; CPM: count per million; FDR: false discovery rate.

Table S3. Upregulated genes in HELZ-null cells belonging to the gene ontology (GO) categories neurogenesis (GO:0022008) and nervous system development (GO:0007399) – Excel file

Table S4. Antibodies used in this study.

Antibody	Source	Catalog number	Dilution	Monoclonal/polyclonal
Anti-HA-HRP	Roche	12013819001	1:5000	Monoclonal
Anti-GFP (for WB)	Roche	11814460001	1:3000	Mouse monoclonal
Anti-GFP (for IP)	In house	-	-	Rabbit polyclonal
Anti-Tubulin	Sigma Aldrich	T6199	1:10 000	Mouse Monoclonal
Anti-mouse IgG-HRP	GE Healthcare	NA931V	1:10 000	Sheep polyclonal
Anti-rabbit IgG-HRP	GE Healthcare	NA934V	1:10 000	Donkey polyclonal
Anti- <i>Hs</i> HELZ	Abnova	H00009931-M02	1:1000	Mouse monoclonal
Anti- <i>Hs</i> PABPC1	Abcam	Ab21060	1:5000	Rabbit polyclonal
Anti- <i>Hs</i> NOT1	In house	-	1:1000	Rabbit polyclonal
Anti- <i>Hs</i> NOT3	Abcam	Ab55681	1:1000	Mouse monoclonal
Anti- <i>Hs</i> DDX6	Bethyl Laboratories	A300-461Z	1:3000	Rabbit polyclonal
Anti- <i>Hs</i> p70S6K (EDC4)	Santa Cruz Biotechnology	sc-8418	1:1000	Mouse monoclonal
Anti- <i>Dm</i> DCP1	In house	-	1:1000	Rabbit polyclonal
Anti- <i>Dm</i> Gel1	In house	-	1:1000	Rat polyclonal
Anti- <i>Dm</i> PABP	In house	-	1:1000	Rabbit polyclonal

Table S5. Oligos used in the qPCR reactions.

Name	Sequence
<i>sparc_f</i>	CTAGAGGCTCAGTGGTGGGA
<i>sparc_r</i>	TCCCTAGAGCCCCTGAGAAG
<i>baspl_f</i>	TGGATTCCAAGATCCGCGT
<i>baspl_r</i>	TGGACAAGCTAAGTGGGCTC
<i>tenml_f</i>	TCGCCTGATGGAACCCTCTA
<i>tenml_r</i>	CCATTGCTGCTGGTAATCGC
<i>gapdh_f</i>	CTCTGCTCCTCCTGTTCGACAG
<i>gapdh_r</i>	TTCCTGTTCTCAGCCTTGACGG

SUPPLEMENTARY FIGURE LEGENDS**Figure S1. Probing the function of HELZ in mRNA decay.**

(A) RNA samples isolated from cells expressing GFP-DCP2*, MS2-HA or MS2-HA-HELZ, the β -globin-6xMS2bs and the control β -globin reporters (shown in **Fig 3L**) were treated with oligo(dT)₁₅ +/- RNase H and analysed by northern blot.

(B, C) Immunoprecipitation assays in *Dm* S2 cells investigating the interaction of GFP-*Dm* HELZ with HA-*Dm* Ge-1 (B) or HA-*Dm* Me31B (C). F-Luc-GFP served as control. Input (3.5% for GFP-tagged proteins and 0.5% for HA-tagged proteins) and bound fractions (10% for GFP-tagged proteins and 35% for HA-tagged proteins) were analysed by western blotting.

(D) Tethering assay in *Dm* S2 cells using the F-Luc-5BoxB reporter and λ N-HA-*Dm* HELZ (full-length and fragments). A plasmid expressing R-Luc served as transfection control. F-Luc activity was normalized to the R-Luc control and set to 100 in cells expressing λ N-HA. Graph shows the mean values +/- SD of five experiments.

Figure S2. Characterization of DDX6-null and HELZ-null cells

(A) Western blot demonstrating loss of endogenous DDX6 expression in HEK293T DDX6-null cells. Tubulin served as loading control.

(B) UV absorbance profile at 254 nm of HEK293T WT (green) and DDX6-null (blue) cell extracts after polysome sedimentation in a sucrose gradient. Absorbance peaks at 254 nm representing free 40S and 60S subunits, 80S monosomes, and polysomes are indicated.

(C) HEK293T WT and DDX6-null cells were fixed and analysed by indirect immunofluorescence for the presence of P-bodies using an anti-EDC4/p70S6K antibody. The

merged picture shows the EDC4/p70S6K signal in red and the Hoechst nuclear staining in blue.

Scale bar, 10 μ m.

(D) HEK293T WT and DDX6-null cells were fixed and analysed by indirect immunofluorescence for the presence of P-bodies using an anti-DDX6 antibody. The merged picture shows the DDX6 signal in red and the Hoechst nuclear staining in blue. Scale bar, 10 μ m.

(E) Tethering assay in HEK293T WT (green bars) and DDX6-null cells (blue bars) with MS2-HA-TNRC6A-SD and the R-Luc-6xMS2bs-A₉₅-MALAT1 reporter. A plasmid expressing F-Luc-GFP served as a transfection control. Shown is the quantification of protein levels of the R-Luc-6xMS2bs-A₉₅-MALAT1 reporter normalized to the levels of the F-Luc control reporter and set to 100 for MS2-HA. The mean values \pm SD are shown for three independent experiments.

(F) Western blot showing the levels of transfected MS2-HA-TNRC6A-SD in the different cell lines used in (E). Loss of endogenous DDX6 protein expression in HEK293T DDX6-null cells was confirmed using an anti-DDX6 antibody. GFP-F-Luc served as transfection control.

(G) Western blot demonstrating loss of endogenous HELZ in HEK293T HELZ-null cells. Dilutions of WT cell lysates were loaded in lanes 1-4 to estimate protein levels of HELZ, NOT2, NOT3 and DDX6 in HELZ-null cells compared to WT cells. PABPC1 served as loading control.

(H) UV absorbance profile at 254 nm of HEK293T WT (green) and HELZ-null (pink) cell extracts after polysome sedimentation in a sucrose gradient. Absorbance peaks at 254 nm representing free 40S and 60S subunits, 80S monosomes, and polysomes are indicated.

Figure S3. NOT1 repressor function is not impaired in HELZ-null cells

(A and B) Tethering assay in HEK293T WT and HELZ-null cells using the R-Luc-6xMS2bs (A) or the R-Luc control (lacking MS2 binding sites; B) reporters and MS2-HA or MS2-HA-tagged NOT1. The graphs show the relative R-Luc activity normalized to the levels of the control F-Luc reporter and set to 100 for MS2-HA; the mean values \pm SD are shown for three independent experiments.

(C and D) Tethering assay as described in (A) using the R-Luc-6xMS2bs-MALAT1 or the R-Luc-A₉₅-MALAT1 reporters. Data was analysed as described in (A).

(E) Representative western blot of cells used in (A-D) depicting the equivalent expression of the MS2-HA-tagged NOT1 in WT and HELZ-null cells. Tubulin served as loading control.

Figure S4. Transcriptome analysis of HEK293T HELZ-null cells

(A) Multidimensional scaling (MDS) analysis for RNA-Seq replicate libraries from HEK293T WT and HELZ-null cells.

(B) Scatterplot depicting the dependency of the logarithmic change in mRNA abundance (\log_2FC) on the gene expression level (\log_2CPM / logarithm of count per million) of differentially expressed transcripts in HELZ-null cells. The differentially expressed genes are highlighted as *red dots* (*upregulated*, $\log_2FC > 0$, $FDR < 0.005$) or *blue dots* (*downregulated*, $\log_2FC < 0$, $FDR < 0.005$).

(C) Gene ontology analysis of the biological processes overrepresented in the group of transcripts downregulated in HELZ-null cells ($\log_2FC < 0$, $FDR < 0.005$) versus all other expressed genes. Bar graph shows $-\log_{10}$ of q values for each category. Content of brackets indicates the number of genes within each category.

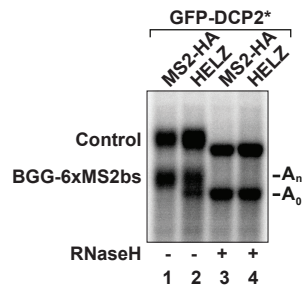
Figure S5. Analysis of GC-content and transcript length of all genes expressed in HELZ-null cells

(A-C) Histograms depicting the number of transcripts (Frequency) relative to the GC content of the 5' UTR (A), CDS (B) and 3' UTR (C) of upregulated transcripts [$\log_2FC > 0$, $FDR < 0.005$ (red)] and control group [downregulated ($\log_2FC < 0$, $FDR < 0.005$) and not significantly changed mRNAs (grey)]. Statistical significance was calculated using the Wilcoxon rank sum test.

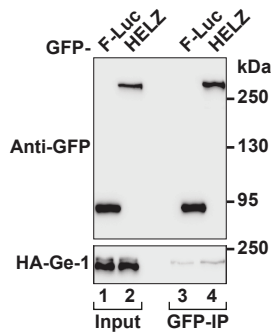
(D-F) Histograms of the number of transcripts (Frequency) relative to the 5' UTR (D), CDS (E) or 3' UTR (F) length of upregulated transcripts [$\log_2FC > 0$, $FDR < 0.005$ (red)] and control group [downregulated ($\log_2FC < 0$, $FDR < 0.005$) and not significantly changed mRNAs (grey)]. Statistical significance was calculated using the Wilcoxon rank sum test.

Hanet *et al.* Figure S1

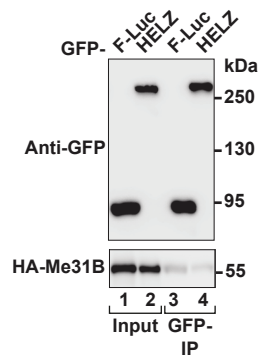
A RNase H



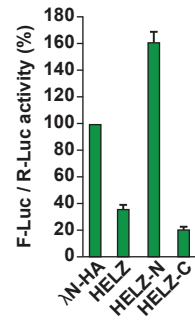
B *Dm*



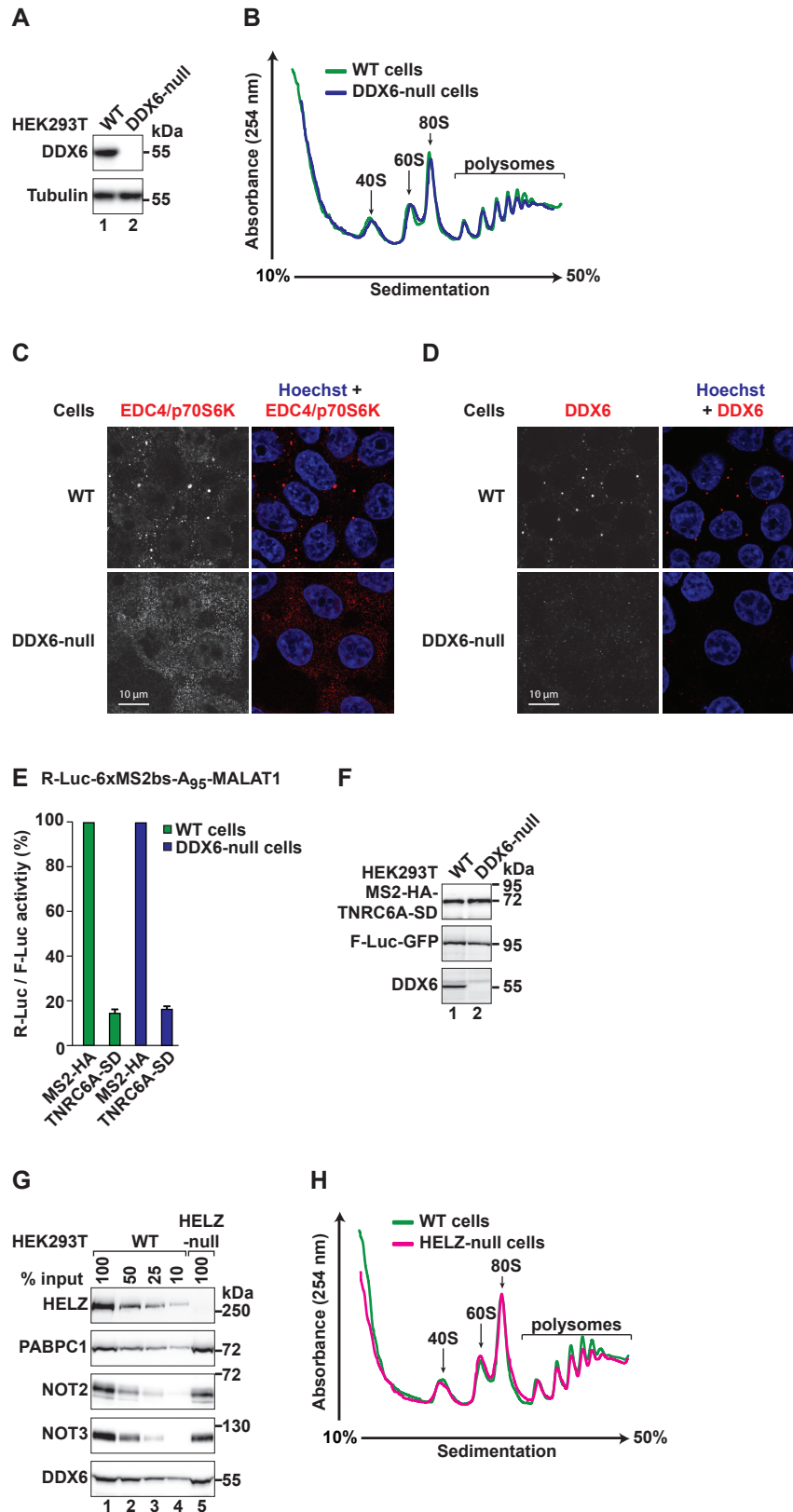
C *Dm*



D *Dm*

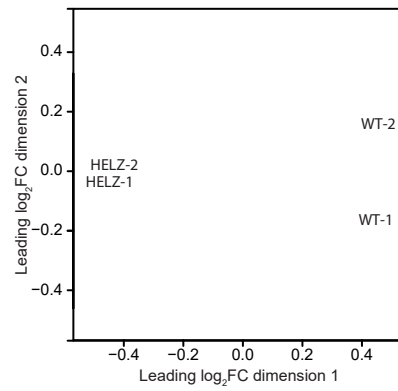


Hanet et al. Figure S2

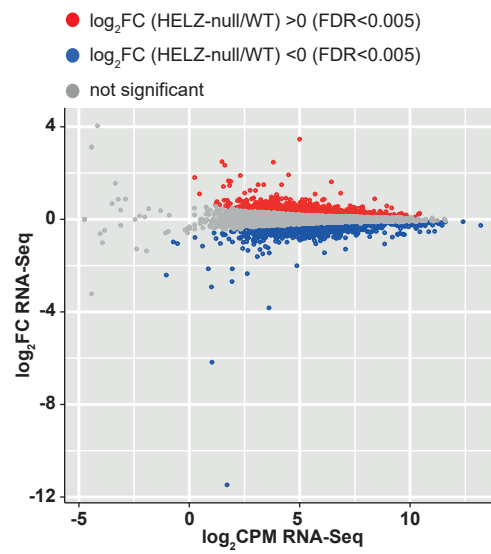


Hanet et al. Figure S4

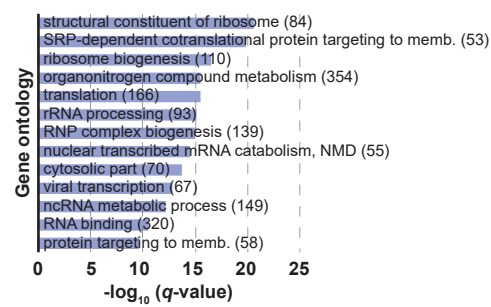
A



B

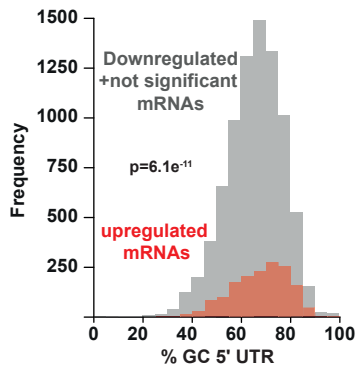


C

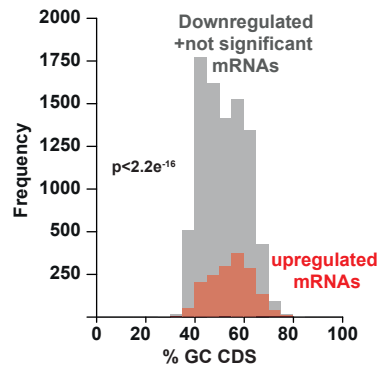


Hanet *et al.* Figure S5

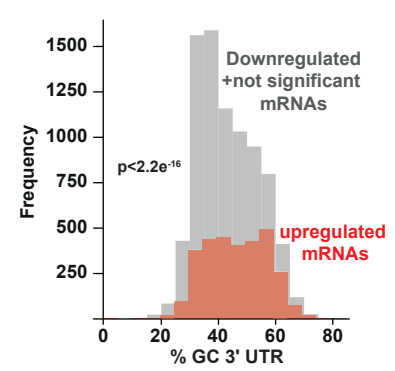
A 5' UTR



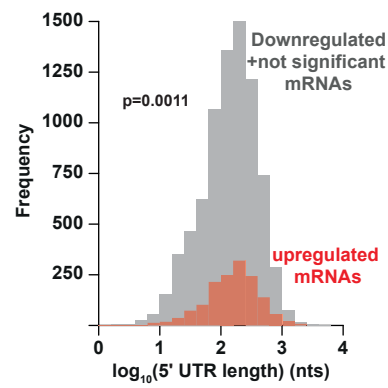
B CDS



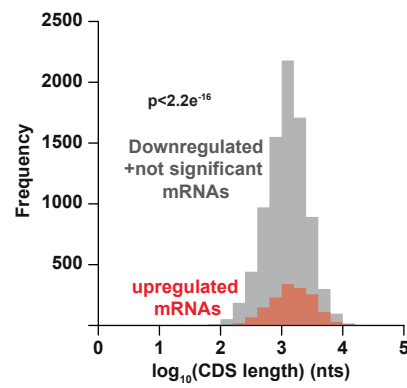
C 3' UTR



D 5' UTR



E CDS



F 3' UTR

